Characterisation of two developmentally important genes mutated by transgene insertion in the laboratory mouse

Bennett, William R.

Award date:
1999

Awarding institution:
University of Bath

CHARACTERISATION OF TWO DEVELOPMENTALLY IMPORTANT GENES MUTATED BY TRANSGENE INSERTION IN THE LABORATORY MOUSE.

Submitted by William R. Bennett

for the degree of PhD of the University of Bath

1999

ProQuest LLC
789 East Eisenhower Parkway
P.O. Box 1346
Ann Arbor, MI 48106-1346

Characterisation of two developmentally important genes mutated by transgene insertion in the laboratory mouse

William R. Bennett, PhD
University of Bath, 1999

ABSTRACT

A large number of transgenic mouse lines have been screened for post-natal mutant phenotypes by breeding to homozygosity, along with partial screening for pre- and peri-natal phenotypes during Caesarean re-derivation of the lines in Bath. Various developmental abnormalities were observed, some of which have been caused by disruption of somatic gene function by transgene insertion. Two lines were selected for further characterisation.

In the **Harry** transgenic line, the transgene has integrated close to the *Sox10* locus on chromosome 15. *Sox10* encodes a transcription factor which is expressed in a subset of neural crest cells during development and continues to be expressed in peripheral glia and oligodendrocytes during adult life. **Harry** homozygous mutants display a recessive phenotype which features limited skin pigmentation and toxic megacolon caused by a lack of enteric neurons. This is caused by transgene-induced disruption of correct function of the Sox10 gene product in neural crest cells. $Sox10^{Dom}$ (dominant megacolon) is a spontaneous mouse mutant which encodes a truncated form of the Sox10 protein. $Sox10^{Dom}/Sox10^{Dom}$ homozygotes are embryonic lethal by E13, but heterozygotes display essentially the same phenotype observed in **Harry** mice which are homozygous for the transgene. **Harry** mutants express wild-type levels of full-length *Sox10* mRNA in the CNS, however, and there is no disruption either within the Sox10 gene itself or within 2kb of the start or end of the transcribed region.

In the **Holly** transgenic line, homozygosity for the transgene causes acute angle-closure glaucoma to develop shortly after the eyes open around day 12 post-partum. Insertion of the transgene into proximal chromosome 1 appears to have disrupted the expression of *Col9a1* in a tissue-specific manner. *Col9a1* encodes the α1 chain of type IX collagen, a heterotrimeric protein thought to be important in mediating the interaction between structural collagen fibrils and the extracellular matrix in which they are embedded.

DEDICATION

This thesis is dedicated to Dr Deb Speden, for faithfully holding my ropes, both literally and metaphorically, and to "Pinky and the Brain", for inspiration.

"Both by virtue of its massiveness, and by the ubiquity and variety of tissues to which it gives rise, [the neural crest] would merit the status of a fourth germ layer were it not that it is above all from the study of its neural crest component that the limitations of the germ-layer concept in vertebrate embryology has been most strikingly demonstrated." (Newth, 1951)

18th century Japanese piebald mice (Chingan-sodategusa, author unknown)

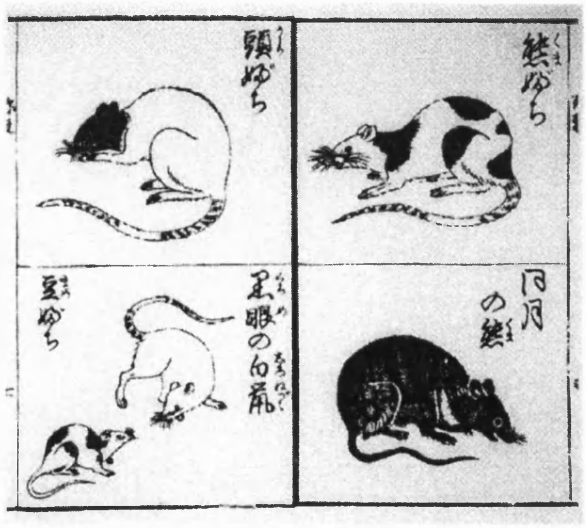

"Dear Mr Bennett,

I am responding to your letter dated 15th March 1999, requesting permission to use Warner Bros. materials, specifically a Pinky and the Brain GIF image from a Warner Bros website (the "Materials") in your PhD thesis. While we greatly appreciate your interest in using the Materials, Warner Bros. has a long standing policy against specifically granting anyone the rights that you seek. This is why I must deny your request for use.

We wish you the very best of luck with your academic career.

Kind Regards,
Rick Kent, Manager, Legal Affairs, Warner Bros. Online"

ACKNOWLEDGMENTS

I would like to thank Dr William J. Pavan (NHGRI, NIH, Bethesda, Maryland, USA) for helpful discussion and suggestions on the use of linkage mapping in transgenic insertional mutants. The mouse *Sox10* cDNA plasmids were a kind gift of Dr Michelle Southard-Smith (Pavan lab). I would also like to thank Dr Gerd Scherer (Institute of Human Genetics and Anthropology, Freiburg, Germany) for generously sharing unpublished data (the mouse *Sox10* gene structure and restriction map). Prof Michel Goosens and Dr Veronique Pingault (Hôpital Henri Mondor, Creteil, France) originally derived and provided me with the *Sox10* RT-PCR protocol and primer sequences. The *Dvl1* genomic clone was a gift of Dr Daniel Sussman (University of Maryland School of Medicine, Baltimore, USA), and the *Lifr* genomic clone was a gift of Dr Ian Chambers (MRC Human Genetics Unit, Western General Hospital, Edinburgh). The *Col9a1* probes pMCol9a1-1 and pMCol9a1-2 were provided by Prof Eero Vuorio (University of Turku, Turku, Finland). Transfer of the **Harry** line transgene onto different genetic backgrounds as congenic strains and subsequent breeding to homozygosity was carried out by Prof Chris Graham (Department of Zoology, University of Oxford), under whose aegis all transgenic lines in this study were originally derived and to whom I am deeply indebted. I am eternally grateful to Dr Muriel Lee (MRC Human Genetics Unit, Western General Hospital, Edinburgh) for teaching me how to perform FISH, and for giving me her expert "best guess" for chromosomal identities in the G-banding experiments. I would like to acknowledge the expert assistance and hard work of animal house technicians both in Bath and Oxford.

Finally, I would like to thank my supervisor, Dr. Andrew Ward, for giving me the freedom to pursue those avenues I thought most interesting, my fellow transgenic mutant investigator Derek Paisley for discussion and for mousing above and beyond the call and everyone else in lab 0.76 for providing a stimulating and fun environment to work in.

This work was funded by the School of Biology & Biochemistry at the University of Bath.

TABLE OF CONTENTS

LIST OF TABLES

LIST OF FIGURES

ABBREVIATIONS

ALDH3	aldehyde dehydrogenase class 3
BAC	bacterial artificial chromosome
BOR	branchio-oto-renal
bp	base pairs
BSA	bovine serum albumin, fraction V
CCD	centrally conserved domain (*Igf2/H19* intergenic region)
CCD	charge-coupled device (camera)
CDTA	cyclohexane diamine tetra-acetic acid
Chr	chromosome
cM	centimorgan(s)
CNS	central nervous system
cpm	counts per minute
DAB	diaminobenzidine
DBH	dopamine β-hydroxylase
DEPC	diethylpyrocarbonate
DMR	*Igf2* 5′ differentially methylated region
DTT	dithiothreitol
ECE	endothelin converting enzyme
ECM	extracellular matrix
EDTA	ethylene diamine tetra-acetic acid, sodium salt
ENS	enteric nervous system
ENU	ethylnitrosourea
ES cells	embryonic stem cells
FACIT	Fibril-Associated Collagen with Interrupted Triple helices
FACS	fluorescence-activated cell sorter
FITC	fluorescein isothiocyanate
GDNF	glial-derived neurotrophic factor
GFAP	glial fibrillary-associated protein
GRIP-1	glucocorticoid receptor interacting protein 1

H&E	haematoxylin and eosin
HNF-4	hepatocyte nuclear factor 4
HS	Hirschprung syndrome
IAP	intracisternal A particle
Igf-2	gene encoding insulin-like growth factor-II
IOP	intra-ocular pressure
kb	kilobase(s)
LIAG	light-induced avian glaucoma
Luc	luciferase coding region
Mb	megabase(s)
MODY	mature onset diabetes of young
MOPS	3-[N-Morpholino]propanesulfonic acid
MSA	migration staging area
NTD	neural tube defect
PAC	phage (P1) artificial chromosome
PAS	periodic acid-Schiff's reagent
PBS	phosphate buffered saline
PCNA	proliferating cell nuclear antigen
PDGF-A	platelet-derived growth factor A
PDGFRα	platelet-derived growth factor alpha-receptor
PNS	peripheral nervous system
PVP	polyvinylpyrollidine, MW 40,000
QTL	quantitative trait locus
RFLP	restriction fragment length polymorphism
RI	recombinant inbred
rpm	revolutions per minute
SCF	stem cell factor (Steel factor)
SDP	strain distribution pattern
SDS	sodium dodecyl sulfate
SRC-1	steroid receptor coactivator 1
SSC	150mM NaCl, 15mM Na citrate
SSCT	4xSSC containing 0.05% Tween-20

SSPE	20mM NaH_2PO_4, 0.3M NaCl, 2mM EDTA
TC	transiently catecholaminergic
TE	10mM Tris.HCl pH 8.0, 1mM EDTA
TGFβ1	transforming growth factor β1
TIGR	trabecular meshwork-inducible glucocorticoid receptor
TKT	transketolase
TNE	100mM NaCl, 10mM Tris.HCl, pH 7.5, 1mM EDTA
WS4	Waardenburg syndrome type IV (AKA Waardenburg-Shah syndrome)
YAC	yeast artificial chromosome

CHAPTER ONE:

INTRODUCTION

Background

The mouse as a model system

The mouse is widely used as a model for the study of mammalian genetics, growth and development. It is attractive as an experimental system, both for its rapid and prolific breeding cycle, and for the wealth of genetic data available, including high density genome maps which greatly simplify the task of positional cloning (Mouse Genome Database, 1999). Aside from these technical advantages, the divergence of mice and humans occurred relatively recently in evolutionary terms (around 60 million years ago), hence the mouse provides a reasonably good model for determing gene function in humans.

Alternative model systems

In the following discussion, it is important to draw a clear distinction between model organisms for the study of human genetic diseases and for the study of developmental genetics, although the line can be blurred.

When trying to dissect the genetics of clinical syndromes, a mammalian model is clearly essential, preferably as close to human as is practicable. Defined inbred strains (in which all animals are genetically homogenous and homozygous at all loci) are also essential to obviate the effects of modifer genes segregating in the genetic background. For experimental purposes, inbred strains are defined as deriving from at least 20 generations of strict brother-sister inbreeding at each generation. Many inbred strains of mice have been established since the pioneering work of Abbie Lathrop and William Ernest Castle early in the twentieth century (Morse, 1981), and this, coupled with the advantages of rapid generation time, detailed genetics and, crucially, the ability to manipulate the germline *in vitro* using recombinant DNA techniques (discussed below), have

ensured that mice have become the preeminent system for modelling human genetic defects and elucidating the function of mammalian genes.

Outwith the strict context of modelling clinical genetic syndromes, the major systems currently used in *developmental* molecular genetic studies and their key features can be summarised as follows:

1) *Drosophila*: easily and quickly bred; cheap; small genome; sequence-tagged mutagenesis by transposable elements possible; transgenesis possible; in vitro germline manipulation by homologous recombination not possible; not very closely related to humans; very good genetics data available.
2) *C. elegans*: easily and quickly bred; cheap; small genome; precisely defined cellular ontogeny which can be followed under the microscope; sequence-tagged mutagenesis by transposable elements not possible; transgenesis possible;in vitro germline manipulation by homologous recombination not possible; not closely related to humans; very good genetics data available.
3) Laboratory mouse: easily bred, fairly cheap provided facilities are available (animal house); fairly rapid breeding cycle; large genome, sequence-tagged mutagenesis by transposable elements not possible; transgenesis possible; in vitro germline manipulation by homologous recombination possible; closely related to humans; very good genetics data available.
4) Zebrafish: easily bred; fairly cheap once facilities are available (aquarium); fairly rapid breeding cycle; large genome; sequence-tagged mutagenesis by transposable elements not possible; transgenesis possible; in vitro germline manipulation by homologus recombination not possible; reasonably closely related to humans; poor but rapidly increasing genetics data available; transparent nature facilitates observation and manipulation during rapid development of the embryo.
5) Xenopus: very slow breeding cycle; tetraploid genome; practically no genetics data available. However, embryos are easily observed and manipulated and transgenesis is now possible. Recent investigations using a diploid species, *X. Tropicalis,* may herald the birth of Xenopus genetics (Amaya *et al.*, 1998).

6) Laboratory rat: easily bred; more expensive than mouse; fairly rapid breeding cycle; large genome; sequence-tagged mutagenesis by transposable elements not possible; transgenesis possible; in vitro germline manipulation by homologus recombination not possible (yet?); closely related to humans; poor but rapidly increasing genetics data available.

Rat genetics is in its infancy at the moment, but seems likely to explode over the next decade with the recent advent of detailed genetic maps of the rat genome along with accompanying polymorphic sequence-tagged site markers. The signal advantage of the rat over the mouse is the availability of various inbred or partially inbred strains which provide pharmacological and physiological models for various human conditions, such as epilepsy. This is of particular importance in the genetic dissection of multifactorial diseases such as spontaneous hypertension or obesity.

The other major system widely used for molecular genetics is Arabidopsis, but this is, of course, not strictly relevant for a discussion of animal genetics. It is, however, worth pointing out that Arabidopsis is cheap, easily bred, has fairly good genetics, sequence-tagged mutagenesis is possible, and is the system of choice for plant genomics. This can become relevant when studying highly conserved themes between plant and animal kingdoms e.g. homeotic genes.

Vertebrate genome evolution by duplication

Vertebrates are generally considered to have undergone two rounds of whole genome duplication early during their evolution, and this has led to considerable diversification of functions (Nadeau & Sankoff, 1997). Gene duplication is believed to buffer the effect of null mutations and allows greater opportunities for new functions to evolve (Spring, 1997). Indeed, genome duplication may be the mechanism underlying saltatory evolutionary jumps in organism complexity (Aparicio, 1998). To further complicate matters, tandem duplications of single genes or gene clusters have occurred. The overall effect of this, combined with >500 million years of normal evolutionary drift has created a situation where it can be extremely difficult to identify a direct functional

orthologue of any given human gene in Drosophila or *C. Elegans*, although an homologous "ancestral" gene can often be found.

From the list above, zebrafish would seem to satisfy many of the criteria for the perfect model organism with which to investigate vertebrate (although not mammalian) developmental genetics, and this may well be true. Although the overall breeding cycle is relatively slow, fertile fish can produce very large numbers of F_1 progeny every two weeks or so, the embryo is accessible and amenable to manipulation during development, it is transparent and embryogenesis can be observed and followed throughout, the fish are easily mutagenised and the genetic mapping data, as with the rat, is currently expanding at an exponential rate. Whilst not as closely related to humans as the mouse, zebrafish have been found to possess functional orthologues of most of the major genes looked for so far. However, what is of particular interest is that rather more homologous genes are being found in zebrafish than were expected from *a priori* considerations.

As an illustrative example: in *Drosophila*, there is one ancestral *hedgehog* gene. The mouse might reasonably be expected to have from one to four hedgehog genes (from 2 rounds of genome duplication) and three have been found so far. Of these, *Shh* (sonic hedgehog), has been extensively studied and found to be of critical importance during development. In due course, zebrafish geneticists looked for an *shh* orthologue and found *two*, rather than one (Schauerte *et al.*, 1998). This lends weight to the accumulation of recent evidence which strongly suggests that teleost fishes underwent a further genome duplication early in their evolution, perhaps quite soon after their divergence from the mammalian evolutionary line (Aparicio, 1998). Paradoxically, this abundance of homologues can both complicate and simplify the dissection of gene function during development. That is to say, while one might have to isolate and identify multiple genes to cover the functionality of one ancestral gene (from *Drosophila*, say), individual genes may be performing less functions. In the particular case of mouse knockouts, it may be necessary to knock out two or even three members of a related group to achieve the expected phenotype from fly mutant studies. However, individual knockouts can reveal the subtleties of

particular functions which the global mutant masks by virtue of its more severe effects.

The close relationship between mouse and human genomes

Thus, while *Drosophila* and *C. elegans* provide certain advantages to the geneticist, it can be crudely stated that humans and mice are ten times more closely related to each other than either species is to flies or nematodes. Indeed, so closely related are the two genomes that it has been estimated that only around 150 major rearrangements have occurred since the divergence of mouse and human from a common ancestor some 65 million years ago. To put it another way, one can construct an approximate replica of the human genome by breaking the mouse genome into ~150 pieces and reassembling them in the correct order (Copeland *et al.*, 1993).

With the twin advantages of conservation at the sequence level and large syntenic regions at the genomic, cloning of a new human gene almost invariably leads to the discovery of its murine counterpart, and the reciprocal generally holds true. Corresponding genes in mouse and human are often, although not always, direct functional orthologues, and this can be directly exploited in the mouse through the use of targeted mutagenesis and transgenesis experiments. The logical corollary of this is that exploring gene function in the mouse through the identification and characterisation of novel mutant alleles can shed light on what role the gene plays in humans.

Mouse mutants

Genome sequencing projects

The human genome project is on schedule to produce a complete sequence of the human genome by 2003, somewhat ahead of the original projections (Collins *et al.*, 1998)(http://www.ncbi.nlm.nih.gov/genemap/, 1999). The mouse genome project is proceeding along a similar course, although lagging a few years behind, but advances in sequencing technology, although inherently unpredictable, are projected to take place such that the mouse genome will have

been completely sequenced by 2005, with a "draft copy" ready by 2003, consisting of most or all cDNA sequences on a framework map.

The required technical advances in sequencing capacity are being aggressively pursued by academic and private concerns. For example, the Genome Science Laboratory at the Institute of Physical and Chemical Research (RIKEN) in Japan, recently announced details of an automated system for high-throughput preparation and sequencing of high-quality cDNA libraries using a number of cutting-edge innovative technologies. They claimed to be able to rapidly prepare cDNA libraries containing >90% full-length message using trehalose-stabilised high temperature reverse transcription (Carninci *et al.*, 1998), to mini-prep $4x10^4$ sequence-ready templates per 24 hours using an advanced robot, and to generate megabases of sequence per day using RNA polymerase-based fluorescent sequencing. If borne out, this technology represents a quantum leap in genome sequencing capacity compared to current high-throughput methodologies (Hayashizaki *et al.*, 1998). Similar advances can confidently be predicted to emerge over the next decade.

If the sequence of every gene and cDNA in mouse and human will be known in seven years or less, why expend any great effort now to identify novel genes via mutagenesis screens? The answer lies in the deficit in our current ability to predict gene function from gene sequence. This was recently highlighted in a fascinating report published on the Web by the steering group at the NIH coordinating the American mouse genome project. The report summarises the committee's reasoning and decisions on how much resources should be allocated over the next few years to which aspects of mouse genomics (http://www.nih.gov/welcome/director/reports/mgenome.htm, 1998). (A letter describing the outline of the report was recently also published (Battey *et al.*, 1999).) To quote from the report: "As the Human Genome Project progresses and the sequence of more human and mouse genes is determined, the function of a large number of these genes will not be predictable by sequence and expression alone. Phenotype-driven mutagenesis screens provide an important approach to understanding the function of genes."

Classical spontaneous mutants

In the 18th and 19th centuries, Asian breeders selected and bred lines of "fancy" mice with various coat and eye colouring. During the 19th century, British and American breeders joined in and a wide variety of lines of fancy mice were traded around the world. This was an attractive resource for early genetics researchers, since it offered visible genetic variation - rare in wild animals - and defined inbred strains carrying visible phenotypic markers could be more quickly derived from the fancy mice than from wild animals (Silver, 1995). Various naturally occurring alleles were mapped using these mice, including the recessive *s* locus, discussed extensively in this thesis, now known to contain the *Ednrb* gene which encodes the endothelin receptor B.

"Piebald" fancy mice are small with spotted white coats, and carry a recessive allele at the *s* locus which causes a dramatic reduction in the level of *Ednrb* mRNA (Hosoda *et al.*, 1994; Lyon *et al.*, 1996). The original Japanese fancy mice were described in "Chingan-sodategusa", an 18th century guide to mouse breeding (Tokuda, 1935), and the first known images of piebald mice are reproduced from this manuscript on the Dedications page of this thesis. This particular strain was believed to have become extinct sometime in the mid-19th century, but a pair of so-called "Japanese" fancy mice resembling classical piebalds were purchased in a market in Denmark in 1987 and introduced to a breeding centre for establishment of an inbred line. In a remarkable recent paper, the authors describe the resultant inbred JF1 strain, which carries the identical *s* allele at the *Ednrb* locus to that seen in classical piebald mice, but is otherwise genetically closely related to *M.m. molossinus*, the asiatic sub-species (Koide *et al.*, 1998). This strain is therefore considered to be a "resurrected" version of the original piebald Japanese fancy mouse, before this allele became bred onto the varied genetic backgrounds seen in modern laboratory strains. (The JF1 strain is of more than historical interest, however, as it shows a very high level of genetic polymorphism compared to most common laboratory inbred strains of mice, due to its *M.m.molossinus* heritage, and can be interbred with these, but is tame and tractable compared to other inbred strains derived from this sub-species.

Furthermore it carries a visible marker which does not compromise viability. This strain may therefore prove very useful in mapping studies.)

Early mutagenesis programmes

In addition to the array of classically-derived mutants from breeding studies, there exists a range of mutant strains derived from mutagenesis programmes using agents such as ethylnitrosourea or ionising radiation (Lyon *et al.*, 1996). ENU generally induces point mutations and X-rays generally give rise to large deletions. Prior to recombinant DNA technology, many such mutations were studied at the phenotypic level, and some were mapped using large-scale breeding programs, but this was very time-consuming and expensive. However, the recent advent of detailed genetic maps and genotyping based on microsatellite and other PCR-typable polymorphic loci has meant that any mutation - even a point mutation in a single base pair - can be rapidly mapped with high resolution. The Jackson Labs and other institutions such as Harwell in Britain and Neuherberg in Germany have maintained live or frozen stocks of many poorly-defined mutant alleles, and some of these are now beginning to be "resurrected" and investigated using the new technology.

Transgenic mutants

Transgenic mice - defined herein as mice carrying additional exogenous DNA sequences stably integrated into the host DNA - were originally derived by injection of DNA into the pronuclei of fertilised eggs (Gordon *et al.*, 1980) or by microinjection of retroviral DNA into the blastocoel cavity of blastocyst stage embryos (Jaenisch & Mintz, 1974). Early on, it was found that the random insertion of transgene DNA can cause the disruption of normal somatic gene function and a mutant phenotype (Gridley *et al.*, 1987), albeit at fairly low frequency. This is discussed in more detail below. The explosion in transgenic technology has led to the generation of thousands of transgenic mouse lines and a number of such transgenic insertional mouse mutants.

ES cell mutagenesis

An added level of sophistication was brought to this approach to mutant generation with the establishment of murine embryonic stem (ES) cell lines (Evans & Kaufman, 1981; Martin, 1981), and the subsequent discovery that when ES cells are injected into the blastocoel cavity of pre-implantation blastocysts, they can integrate with the inner cell mass, and go on to form a part of the normal somatic tissues of the resultant chimeric mouse (Bradley *et al.*, 1984). A great deal of cell mixing occurs during early post-implantation development (Rossant, 1985; Beddington *et al.*, 1989), and consequently, the ES cell-derived tissues in the chimeric mouse will quite often include the germline. As a consequence of this, mice can be bred which are clonally derived from the injected ES cells. Prior to the establishment of ES cells, embryonal carcinoma (EC) cells derived from murine teratocarcinomas were employed in this fashion, but it was found that although they could contribute to normal somatic tissues to form chimeric mice quite successfully, they rarely contributed to the germline, presumably due to karyotypic abnormality. The early experiments with EC cells acted as "proof of concept", however, and paved the way for the success of ES cell-derived germlines in mice (Brinster, 1974).

The genomes of cells in culture are readily amenable to manipulation and, unlike injected eggs, can be selected for successful integration events, clonally amplified for storage and for multiple rounds of injection. It also appears that homologous recombination occurs at very low frequencies when targeting constructs are injected directly into the pronuclei of fertilised eggs compared to transfecting the same construct into ES cells. Manipulations most commonly performed in ES cells can be broadly divided into two categories: Gene targeting and gene trapping.

Gene targeting

Gene targeting by homologous recombination in ES cells has been used to generate specific mutations in genes of interest (Capecchi, 1989). The injection of modified ES cells into pre-implantation blastocysts can then introduce the mutant alleles into the mouse germ-line at a reasonable frequency. Alternatively, the

more sophisticated technique of ES cell aggregation with tetraploid embryos can be employed, which results in entirely ES-cell derived animals without the need for subsequent breeding to screen for germline transmission (Nagy *et al.*, 1993). These strategies are now widely used with particular emphasis placed on gene "knockouts" in which the target gene is rendered completely non-functional, and mice transmitting the null allele in the germline are bred to homozygosity to generate animals in which the gene function is entirely absent.

Gene trapping

While homologous recombination can be used to perform targeted mutagenesis to alter known genes, this does not address the question of developmentally important genes or gene families which have not yet been characterised. The need for efficient random screening led to the development of gene trapping experiments in ES cells to generate transgenic mutant mice (Gossler *et al.*, 1989). This usually involves insertion of a reporter gene, commonly the β-galactosidase *lacZ* gene, into the ES cell genome in such a way that expression of the reporter is dependent upon integration into a functional genomic region. This can be used to randomly screen for active coding sequences (Gossler *et al.*, 1989), promoters (Friedrich & Soriano, 1991), enhancers (Skarnes *et al.*, 1992) and secreted and membrane-spanning proteins (Skarnes *et al.*, 1995). The reporter gene can be used to map the expression patterns of the trapped genes and to clone and sequence the flanking regions of interest (Skarnes *et al.*, 1995; Wurst *et al.*, 1995).

Insertional mutagenesis

The insertion of linear DNA into the genome following micro-injection into single-cell embryos is thought to occur randomly, although it has been suggested from the statistical analysis of a number of transgene integration sites that there are structural requirements, or "hot spots" for the integration of transgene DNA. The integration events may involve the presence of nearby inverted repeats (Wilkie & Palmiter, 1987), and possibly the conserved family of T1 dispersed repeats (Makarova *et al.*, 1988). If true, this pseudo-random insertion would

probably affect the frequency with which transgenes disrupt somatic gene function. This has been estimated to be around 5-10% in the past although the accumulation of more data from transgenic screens - such as the one discussed herein - may alter this figure (Palmiter & Brinster, 1986; Jaenisch, 1988). In particular, the figure of 5-10% given refers mainly to visible, post-natal phenotypes. Screening for pre-natal phenotypes is likely to increase this figure significantly.

Transgene integration

It was found early on that DNA micro-injected into the pronucleus of fertilised eggs tended to integrate more frequently if it was linear. It was also thought possible that sticky ends rather than blunt ends enhanced integration frequency, as did injection into the male, rather than the female, pronucleus (Brinster *et al.*, 1985).

A number of studies have confirmed that injected linear transgene DNA tends to integrate into the genome as a multiple head-to-tail array at a single chromosomal site. Multiple, independently segregating integration sites have also been observed, and can be readily detected through breeding, but these occur at low frequency. Single copy integrations are possible, but somewhat less frequent than multi-copy. In addition, it is not uncommon for some copies of the transgene to be inserted in the reverse orientation within a multi-copy array, but this seems to be a less stable configuration (Wilkie & Palmiter, 1987). If long inverted repeats are unstable in the mammalian genome (as they are in bacteria and yeast), this offers a ready explanation for the instability of head-to-head and tail-to-tail transgenes within an array. In support of this, Collick and co-workers have shown that long inverted repeats *within* a transgene are inherently unstable following integration into the mouse genome (Collick *et al.*, 1996).

In addition to the tendency towards multi-copy integration of the injected transgene construct, the chromosomal sequence flanking the integration site frequently undergoes rearrangements, deletions, translocations or duplications (Mark *et al.*, 1985; Covarrubias *et al.*, 1986). It has been suggested, based on the detailed analysis of several integration sites, that the initial product of transgene

integration is highly unstable, and that the DNA subsequently undergoes a number of rearrangements, possibly involving the insert as well as the host DNA, until it achieves a stable configuration. This can result in duplicated host sequence being inserted between copies of the transgene inside a multi-copy array (Covarrubias *et al.*, 1986). The sequence of the injected DNA seems to influence the process of transgene integration and aberration in the flanking genomic sequence (Chen *et al.*, 1995).

It has been postulated, with the support of experiments performed in transfected cells by Bishop and others, that prior to integration with the host genome, the injected DNA circularises and is then randomly cleaved by cellular nucleases. This generates a set of overlapping linear fragments which have been "circularly permuted". These could then form extrachromosomal concatemers by rounds of homologous recombination events between overlapping fragments. This model would account for the intact nature of many of the *internal* copies of the transgene construct in a multi-copy array (despite the disruptive nature of the integration event) and their propensity to be aligned head-to-tail (since end-to-end concatemerisation would result in random orientations) (Bishop, 1996).

The actual integration probably takes place by illegitimate recombination with genomic DNA, possibly during DNA replication during mitosis, since founder transgenic mice are generally mosaic in composition. The precise mechanism of integration remains unknown, but it has been suggested that the free ends of the injected DNA molecules may induce repair enzymes, which can cause random chromosome breaks, these acting as integration sites for the transgenic DNA (Brinster *et al.*, 1985). It has also been observed that the chromosomal rearrangements associated with transgene integration are similar to those induced by ionizing radiation, which is known to cause double-stranded breaks in DNA. It has been postulated that the microinjection and handling of the zygotes during the procedure might induce double-stranded breaks in the host DNA (Woychik & Alagramam, 1998). It is certainly true that deliberate induction of double-stranded breaks at a target site in chromosomal DNA using transient expression of I-SceI endonuclease greatly enhances the frequency of homologous recombination events at this locus in ES cells (Smih *et al.*, 1995), the implication

being that the presence of naked double-stranded ends enhances recruitment of the cellular recombinogenic machinery. It is also known that the formation of double-stranded chromosome breaks is an essential early step during meiotic recombination of sister chromatids (Shinohara & Ogawa, 1995), although whether any of this this can be extrapolated to transgene integration is a moot point.

Identification of disrupted genes

Although mutations in mice can be readily induced with chemical agents or ionising radiation, traditionally it has required a huge breeding programme to map the mutant alleles. This has now changed with the advent of polymorphic DNA loci which can be typed by PCR, and the mouse genome now has complete coverage (>98%) with 3000 such markers in 1cM "bins" (Dietrich *et al.*, 1996). The upshot of this is that any mutation can be rapidly mapped to within ~1cM provided that the laboratory concerned has the facilities to handle large numbers of PCRs and subsequent detection on high resolution agarose or polyacrylamide gels. The initial cost of buying large numbers of PCR primers to give genome-wide coverage is also high.

However, the presence of a known sequence nearby to act as a tag, such as a gene trap construct or an injected transgene, can greatly facilitate the mapping, cloning and characterisation of a disrupted gene. The transgene can be treated as a dominant allele and incorporated into PCR-based linkage mapping protocols as a marker which is very tightly linked to the mutant locus, eliminating the need for high resolution genetic crosses. More directly, the foreign nature of the DNA sequence of many transgenes can be usefully employed to directly map the transgene using fluorescent *in situ* hybridisation (FISH) on metaphase chromosome spreads. These twin approaches can be combined (see chapters 6 and 11), with significant advantages for small laboratories which are not set up for genome-wide linkage scans.

The chromosomal rearrangements associated with transgene integration can make identification and cloning of the disrupted gene quite difficult. Typically, however, flanking deletions are no larger than 10-100Kb (Zhou *et al.*, 1995), and mapping a mutant allele to within 100Kb can be considered to be

extremely high resolution mapping by conventional genetic standards. Modern chromosome walking techniques can readily be applied to sub-megabase regions of interest, making mapping, cloning and sequencing of genomic DNA flanking a transgene feasible, and considerably easier than conventional mapping of mutant loci and identification of the altered genes. This task is made even easier if large genomic clones (PACs, YACs or BACs) of the region of interest are available, and one of the stated priorities of the NIH working group report mentioned previously is to provide complete two-fold BAC coverage of the mouse genome (to "close the gaps" in molecular genetics parlance), to place all BACs on a framework map and and to make them available to the mouse genomics community (Dove & Cox, 1998). Gridded BACs which span most or all of the mouse genome are already available at low cost from Research Genetics, but most have not been placed on the map (Research Genetics Inc., 1999). Gridded YACs have been available for some time, but their utility has now been greatly enhanced by the publication of a YAC-based physical map covering 92% of the mouse genome (Nusbaum *et al.*, 1999).

Broadly speaking, compared to conventional positional cloning, armed with the map position of a transgene insertion site and having cloned some flanking sequence, gene identification can be confined to a genomic region containing perhaps only 1 or 2 genes compared to 10 or 20 (Meisler *et al.*, 1997).

Alternative approaches to mutagenesis in the mouse

Conventional mutagenesis

The contrast between the transgenic approach and the conventional genetic approach is exemplified by the *ld* (limb deformity) locus, comprising several alleles causing severe lower limb deformity and renal aplasia (Lyon *et al.*, 1996). This had previously been studied extensively and mapped to Chr 2 by classical means. Once disrupted serendipitously by a transgenic insertion, it was quickly cloned and turned out to be a large gene encoding a number of protein isoforms, termed formins, which are involved in the morphogenesis and patterning of the limb and kidney (Woychik *et al.*, 1985; Vogt *et al.*, 1992; Vogt *et al.*, 1993).

Another previously known locus now characterised at the molecular level through insertional transgene mutagenesis is the *pigmy* locus, which had been defined classically as a dwarf phenotype which was, uniquely, not associated with the growth hormone deficiency pathways characteristic of dwarf mice. Transgenic insertional mutagenesis has now revealed this phenotype to be associated with the loss of function of the *hmgi-c* gene, a member of a family of nuclear proteins which function as architectural factors during the assembly of stereospecific transcriptional complexes (Zhou *et al.*, 1995).

A final, and more recent example, underscores the power of transgene insertions to uncover previously unknown types of developmentally important gene. The *inv* mouse (inversion of embryo turning) is the only known mouse mutant in which visceral left-right asymmetry is consistently inverted. The phenotype resulted from a complex transgene insertional event which deleted a small region of chromosome 4 and duplicated another small region. Recent work convincingly showed that the transgene integration had partly deleted the *inv* gene, and transgenic rescue experiments showed that this was indeed responsible for the phenotype (Morgan *et al.*, 1998). The *inv* gene codes for a completely novel protein containing no recognisable motifs other than 16 ankyrin-like tandem repeats and nuclear localisation signals. However, it is clear that the *inv* gene product plays a critical role in the determination of left-right asymmetry and lies upstream of all other known genes in this pathway with the possible exception of *iv* (inversus viscerum).

ES cells

In comparing strategies for disrupting and characterising genes involved in mouse development, it is a perhaps obvious, but important, point that homologous recombination techniques can only be used on previously characterised genes and related genes within homology groups, and cannot be used to identify unknown genes. It has been estimated that targeted mutations currently sample less than 1% of the genes in the mouse genome (Evans *et al.*, 1997).

On the other hand, random strategies such as gene trapping and transgenic insertional mutagenesis have the potential to reveal novel gene functions, but it is important to recognise that gene trapping experiments are optimised for the detection of genes expressed in undifferentiated ES cell lines. Thus, for example, *En-2* and *Hox1.3*(*Hox-A5*) are expressed, whereas others such as *wnt-1* and *En-1* , whilst of equal developmental interest, are not, and a gene trap vector integration event in these latter genes in ES cells would not be selected during screening (Joyner *et al.*, 1985; Joyner & Martin, 1987; McMahon & Bradley, 1990; Jeannotte *et al.*, 1991). (All four genes have, however, been knocked out by homologus recombination and the phenotypic effects studied.) However, it must be pointed out that it is possible to assess the pattern of expression of gene trap constructs in ES cells differentiated *in vitro*, although the extent to which this reflects the pattern of gene expression in the developing mouse embryo, particularly at later stages, is perhaps questionable. Furthermore, the range of somatic cell types which can be derived from ES cells in culture is not particularly comprehensive at present.

Perhaps more usefully, recent work offers the exciting possibility of being able to pre-select ES cell clones which express the gene trap construct only in specific lineages after differentiation. After sequencing to gain some knowledge of the trapped gene, these ES cells can then be injected into blastocysts with some assurance of tissue-specific loss-of-function (Baker *et al.*, 1997).

A further caveat is that while gene trapping experiments and, to a lesser extent, transgenic insertional mutagenesis, have proved to be highly efficient at generating mutants, they provide no control over phenotype, concomitant with their random nature. That is to say, they do not allow you to select for mutations in any particular loci of interest, and furthermore, they simply act as insertional loss-of-function mutations, as opposed to the more subtle targeted mutagenesis experiments which can be performed by homologous recombination in ES cells.

One final consideration is that, thus far, it has only proved possible to derive ES cells which can contribute to the germline with high efficiency from one particular strain of mouse, namely 129. Unfortunately, the canonical "129 strain" has a highly chequered genetic history with a great deal of accidental outcrossing. As a consequence, there is considerable genetic variability between 129 substrains

and ES cells derived from them, and this can further confuse the results of experiments performed in ES-cell derived mice. The Jackson Labs have recently published an excellent investigation of this problem (Simpson *et al.*, 1997).

Summary

Overall, while some of the alternative strategies mentioned above are undoubtedly more *efficient* for the identification and cloning of genes of developmental interest, somatic gene disruption by transgene insertion can be viewed as an interesting by-product of mouse transgenic experiments. it also has the potential to reveal genes of developmental importance which might otherwise be missed. Once a mutant phenotype has been identified in a transgenic line, the presence of the transgene as a molecular tag can enormously facilitate the mapping and cloning of the disrupted gene.

The future?

Retrovirus

One aspect of transgenic technology conspicuous by its absence in the preceding discussion is the use of retroviral vectors to make transgenic mice and/or to generate insertional mutants. Early retroviral vectors were found to integrate randomly, or perhaps pseudo-randomly, into the genome and acted as efficent mutagenic agents. Retroviral integration tends to be much "cleaner" than integration of micro-injected DNA, reflecting the virus' nature, and there is much less disruption to the surrounding chromosomal DNA. Retroviral transfer into cells tends also to be much more efficient than the transfer of gene-trap constructs by electroporation (Evans *et al.*, 1997). Technical difficulties with the earlier retroviral vectors resulted in their being overshadowed by homologous recombination and gene-trapping experiments, but the new generation of retroviral vectors have overcome the procedural drawbacks and this may become the methodology of choice in the future for large-scale mutagenesis (Bradley *et al.*, 1998). Retroviral mutagenesis shares the key advantage of transgenic insertional mutation - the presence of a molecular tag - and the new generation of retroviral

vectors can be readily identified, can be selected for integration into an actively transcribed gene and integrate at high efficiency into the host genome. In theory, any locus of interest could be mutagenised in a tagged fashion with minimal effort. This approach has been validated in zebrafish (Gaiano *et al.*, 1996), and has recently been applied to the mouse with retroviral mutagenesis performed on a large scale by Lexicon Genetics with the stated intention of knocking out every gene in the mouse genome (Omnibank, Lexicon Genetics Inc. 1999).

One "feature" of retroviral integration, at least in mice, is that many retroviruses have preferred, or at least consensus, integration sites and the mutagenesis is not entirely random. For example, several studies have shown that the provirus will often integrate within several hundred base pairs of a DNAse I-hypersensitive site, diagnostic of a region of active transcription. Hence proviral integrations are often found at the 5′ end of a gene (Rijkers *et al.*, 1994). This may not be disadvantageous, but it does perhaps limit the types of mutation induced by retrovirus. Furthermore, a recent pilot study sequenced some 400 retroviral gene-trap events in ES cells, and found that two particular genes were each disrupted three times in the sample of 400 (Hicks *et al.*, 1997), a much higher frequency than predicted. This suggests that retroviral mutagenesis can be skewed in favour of certain genes, but that the bias may be quite small. Futhermore, if there are "hot-spots" for integration, there may well be "cold-spots", hence some genes might never be mutated by these methods.

Large-scale ENU mutagenesis screens

The power of ENU lies in its mutagenic efficiency - with careful dosage, one can generate one mutation in *any* locus of interest within a cohort of 700 F_1 progeny (Hitotsumachi *et al.*, 1985). Given an efficient screen for mutant phenotypes, PCR-based linkage mapping can rapidly map mutant alleles and provide a systematic mutant screen for genes involved in particular pathways. While this approach is only really practicable for a large laboratory or institution, a recent pilot study in Kathryn Anderson's laboratory proved its validity in screening for genes affecting early embryogenesis (Kasarskis *et al.*, 1998), and again, the NIH working group report earmarks this as a priority area of research

(Dove & Cox, 1998). Large-scale ENU mutagenesis screens are currently underway in both Britain and Germany (http://www.gsf.de/isg/groups/enu-mouse.html; http://www.mgu.har.mrc.ac.uk/mutabase/, 1999)

Other ES cells and EG cells

One exciting area of research to emerge recently is the establishment of pluripotent stem cell lines from the gonadal primordial germ cells of post-implantation embryos. These embryonic germ (EG) cells have been derived from several species, including human (Shamblott *et al.*, 1998).

Traditionally, ES cell lines have been derived from the inner cell mass of pre-implantation embryos. ES cell lines have been generated from several species, and have been shown in many cases to be pluripotent and to contribute to somatic tissues in chimeric animals, but one reason for the mouse's dominance in mammalian genetic research has been the impossibility of deriving ES cell lines from any other species which are capable of contributing to the germline. Indeed, as discussed previously, even mouse ES cells from strains other than 129 have been found to colonise the germline at very low frequency (Gardner & Brook, 1997).

Culture conditions have now been established for the successful propagation of pluripotent embryonic stem cells derived from primordial germ cells from multiple species, including humans. These have not as yet been shown to colonise the germline, however, except in the case of mouse EG cells. Nevertheless, the tantalising possibility of *in vitro* manipulation of the germline in species other than the mouse may soon become a reality.

Amongst more obvious direct clinical applications, such as *in vitro* organ cultures for tissue transplants, human pluripotent stem cells offer the intriguing possibility of being able to first test genetic models of disease in an *in vitro* culture system which more faithfully mimics the human condition, before trying to extend this to a whole animal model such as the mouse (Lewis, 1997; Trounson & Pera, 1998). This may help overcome some of the problems attendant in trying to extrapolate from the rodent to the human condition.

ES cell deletion banks

To reiterate: targeted homologous recombination is limited to genes of known sequence, current alternatives for mutagenesis are entirely random, with little or no control over phenotype or location. An attractive alternative has recently become feasible with the publication of two independent methods for generating and selecting ES cell clones with specific deletions on one chromosome (Ramirez-Solis *et al.*, 1995; You *et al.*, 1997). Armed with a mouse which possesses only one copy of a gene in a region of interest, it then becomes possible to use conventional random mutagenesis e.g. ENU, to saturate a target area, rapidly screen for recessive mutations (since they will manifest as "dominant" due to the opposing deletion on the sister chromosome) and to generate an allelic series of mutations in a specific region.

Radiation hybrid mapping panels

Radiation hybrid mapping panels can almost be viewed as the complement to the small chromosomal deletions discussed in the preceding section, as they comprise segments of mouse chromosomal DNA generated by X-irradiation of ES cells and transferred into hamster cells by fusion. Due to the high level of genetic polymorphism between mouse and hamster, mapping is relatively straightforward in these panels, but they have the signal disadvantage that large-scale linkage studies are made difficult by the nature of panel generation, with X-irradiation leading to frequent breaks in chromosomes and non-contiguous linkage groups. Backcross or recombinant inbred (RI) mapping remain the protocols of choice for initial establishment of linkage (discussed more fully in chapter 6). However, the numerous random breaks in each chromosome mean that radiation hybrid panels can be used for very fine genetic mapping. To attain the same degree of resolution from the alternatives mentioned above would require a very large backcross or set of RI strains, particularly in cases where the locus of interest lies within a recombination-poor region, such as close to the centromere (Flaherty & Herron, 1998).

A new radiation hybrid panel, T31, has recently been produced and made available to the mouse community and promises to allow fine genetic mapping of

loci of interest (McCarthy *et al.*, 1997). The first detailed characterisation of the panel has recently been completed and published, encompassing 2483 loci distributed across the 93 cell lines in the panel (Van Etten *et al.*, 1999).

Excisable targeting constructs

Referring back to the list of developmental model organisms given earlier, one of the most desirable features is the ability to perform sequence-tagged mutagenesis via transposable elements, such as the P element widely used in Drosophila. After a phenotype has been observed, and a disrupted gene identified, if one can then rescue the phenotype by excising the foreign element, this categorically proves that the mutation was due to the disruption of that gene. Up until now, this has not been possible in mice, but recent work suggests the exciting possibility of an "exchangeable gene trap" vector being used in an even more sophisticated way (Yamamura *et al.*, 1998). Briefly, this involves a fairly standard gene-trapping protocol in ES cells using a vector which includes two compromised flanking Cre-LoxP *lox* sites. After an interesting gene has been trapped and identified by the usual methods, Cre recombinase can be used to excise the integrated gene-trap vector and optionally replace it with new sequence. Due to the nature of the mutant *lox* sites used, the *lox* sites which re-form after successful excision/exchange are insensitive to Cre recombinase, resulting in stable exchange and integration of the new exogenous DNA.

Since gene-trapping of this kind usually generates loss-of-function mutations in the first instance, this exchangeable gene trap vector can be used to identify developmentally important genes via loss-of-function, to map their patterns of expression via a lacZ reporter and then to *reconstitute gene function* to rescue the phenotype, with the option of introducing deliberate mutations (e.g. novel enhancer elements) to further probe the gene's role.

Mouse balancer chromosomes

One of the most powerful genetic aids to mutation analysis has only been available to *Drosophila* geneticists until now. Balancer chromosomes, as with non-lethal defined chromosomal deletions, allow one to rapidly screen for recessive

mutations in a region of interest (as part of an ENU mutagenesis screen, for example). This is achieved by having some readily assayed phenotypic characteristic present as a dominant allele, since the absence of this trait is diagnostic for progeny lacking the balancer i.e. homozygous for the wild-type chromosome.

They also perform the useful function of maintaining stocks of a recessive lethal mutation without the need for selection. Balancer chromosomes contain a chromosomal inversion, with the inverted region containing a single recessive lethal allele. In a heterozygote, the inversion suppresses recombination between balancer chromosome and a wild-type sister chromosome, since meiotic recombination generates di- or acentric chromatids, leading to inviable progeny. Crossing a balancer onto another recessive mutation in the same region generates a double heterozygote, which, when in-crossed, will only generate viable progeny with the same genotype as the parents i.e. the doubly heterozygous balancer/mutant stock is maintained. This is because homozygosity for either the new mutation or the balancer is lethal, and the suppression of recombination by the balancer region means that the lethal alleles cannot be removed during meosis.

In order to generate a balancer for a genomic region of interest, therefore, one has to have a recessive lethal allele present in the region, and one has to be able to engineer a sizeable (viable) chromosomal inversion with the said allele contained within it. It is also desirable to have a visible trait to mark the presence of the balancer, such as coat or eye colour.

Recent advances in engineering mouse chromosomes using *Cre-LoxP* recombination have led to the generation of a bona fide balancer chromosome, consisting of an inversion spanning some 24cM between *Trp53* and *Wnt3* on Chr 11 (Ramirez-Solis *et al.*, 1995; Zheng *et al.*, 1999). During the process of generating the targeted *loxP* sites, both the delimiting genes were inactivated, so that balancer homozygotes were embryonic lethal due to the absence of *Wnt3*. In addition, a dominant allele of *Agouti* was introduced (as a transgene targeted into the inactivated *Wnt3* gene) to provide a visible coat colour marker diagnostic for the presence of the balancer.

As a proof of concept experiment, the balancer line was crossed onto a mutant strain carrying a recessive lethal mutation in *Hoxb4*, which lies within the inversion region. This resulted in viable double heterozygotes, carrying the inversion on one chromosome and the *Hoxb4* mutation on the other. Inbreeding of these stocks generates 25% *Hoxb4-/-* homozygotes, which are lethal, 50% heterozygotes (bearing parental genotypes), and 25% balancer homozygotes, also lethal due to their *Wnt3-/-* genotype.

Although the process of generating balancer stocks is laborious, once achieved for any region of interest they are self-perpetuating, and would greatly assist in the generation and maintenance of mouse mutant stocks. *Drosophila* geneticists have been trading useful balancers for most regions of the fly genome for many years now, and it is to be hoped that the mouse genetics community might also reach this happy state of affairs

Improved transgene integration

Research into the exact nature of the integration mechanism pertaining to micro-injected transgene DNA remains somewhat sparse. However, one interesting paper described a detailed investigation of a highly unusual transgene integration event (McFarlane & Wilson, 1996). The transgene had integrated very cleanly, as two head-to-tail copies with virtually no disruption of the flanking sequence or the transgene itself. The investigators postulate that the nearby presence of several motifs implicated in recombination events in the host DNA, coupled with short regions of homology at the ends of the transgene construct combined to favour a very clean integration. As well as shedding some light on the mechanism of transgene integration, the nature of the transgene sequence itself allowed the investigators to go on to speculate and make some suggestions towards designing transgene constructs which might integrate more cleanly into the host genome e.g. incorporating a recombination-associated sequence, such as the "Chi-like motif", (the mammalian homologue of the yeast Chi sequence, believed to be an initiation site for meiotic crossover) into the transgene construct near its ends. This might promote precise integration by recruiting the natural cellular recombination machinery.

Clearly, the above is speculative at present, but as more transgene integration events are characterised at the sequence level and our understanding of the precise mechanisms involved increases, it may become possible to design transgene constructs to favour clean integrations.

At a more practical level, a new and highly efficient method of generating transgenic mice has recently been described which differs significantly from the traditional pronuclear micro-injection route. The new technique involves incubating the transgene DNA briefly with sperm before injecting a single sperm head into the cytoplasm of an *unfertilised* egg (Perry *et al.*, 1999). The authors claim that between 64% and 94% of embryos developing from injected eggs expressed the transgene construct, figures considerably higher than those associated with pronuclear microinjection, generally <20% (Hogan *et al.*, 1994). Intracytoplasmic sperm injection (ICSI) has been tried in the past as a vehicle for the introduction of transgene constructs, but the results were disappointing, with very low rates of transgene integration (Lavitrano *et al.*, 1989a; Lavitrano *et al.*, 1989b). The critical differences between the original experiments and the more recent successes achieved by Perry and co-workers hinge upon pre-treatment of the sperm heads to partially disrupt the membrane and upon the use of a piezo-electric injector to introduce the sperm head to the oocyte. Given access to the interior of the sperm, transgene DNA has been shown to rapidly and reversibly associate with internal membrane structures and to "decorate" the sperm head. This appears to greatly enhance the likelihood of the transgene integrating with the host genome.

Although these experiments are unrepeated as yet, should the initial promise of this technique be borne out, it could well supplant pronuclear microinjection as the method of choice for generation of transgenic mice.

Aims of the project

Rationale

Some 92 independent transgenic lines had been derived in our laboratory during the course of research into the nature of the imprinted *Igf2/H19* loci (Ward

et al., 1997). 78 of these lines were shown to transmit the transgene construct through the germline, with most of these lines expressing the luciferase reporter at detectable levels in a tail biopsy, facilitating ready detection of the transgene. With some research conclusions already drawn from the expression levels and patterns of the various constructs, a number of the transgenic lines were now considered surplus to requirements and could be extinguished. However, given the availability of 78 transgenic lines which already existed as part of a separate study, it seemed wasteful to extinguish lines at the end of the experiments without first ascertaining whether a transgenic insertion had generated a serendipitous mutation. Two putative insertional mutations had already been observed during routine breeding. Given this, combined with the ease with which the transgene could be tracked during breeding, it was felt that the 78 lines represented a valuable opportunity to do a more comprehensive, relatively large-scale screen for insertional mutations.

Objective

It was hoped that at least one transgenic insertion had generated a classical, recessive loss-of-function mutation with a readily discernible phenotype, and that this could be mapped and characterised at a molecular and phenotypic level by the end of the project. Further mutants could be characterised to a lesser degree, given enough time.

The major drawback in a screen of this nature, discussed in more detail in Chapter 3, is that roughly half of all transgene insertional mutations to date have been found to be allelic with classical mutant loci. The danger in a project of this kind is therefore that a great deal of effort could be expended characterising an already well-studied locus.

With published frequencies of 5-10% of transgene insertions causing a visible phenotype, it seemed reasonable to expect several mutants to emerge from the primary screen (Meisler, 1992). It was therefore felt that, following preliminary investigations, judicious choice of which phenotype(s) to investigate could reasonably be expected to yield genuinely novel results.

CHAPTER TWO:
MATERIALS AND METHODS

Mice

Generation of transgenic mice

All transgenic mice were originally generated by the micro-injection of linear construct DNA into one pronucleus of an F_1 zygote resulting from a cross between a C57BL/6J♂ and a CBACa♀cross (hereafter abreviated as C57/CBA) (Ward *et al.*, 1997). As well as having the advantages of hybrid vigour, including large litter sizes, this combination has been found empirically to respond well to superovulation and has been widely used in the production of transgenic mice (McLaren & Michie, 1954; Hogan *et al.*, 1994).

Animal husbandry

Transgenic lines were maintained by both incrossing of randomly selected wild-type transgenic mice and outcrossing to C57/CBA F_1 non-transgenics as required. This resulted in maintenance of hybrid vigour (McLaren & Michie, 1954), but as a consequence the transgene was transmitted through various combinations of the C57 and CBA genomes.

Caesarean re-derivation

The protocol for Caesarean re-derivation during transfer of transgenic lines from Oxford to Bath, was designed to minimise the possibility of contact between sectioned neonates and maternal blood, which was assumed to be contaminated with virus (it was further assumed that any viruses present did not cross the placental barrier during gestation). Caesarean re-derivation was performed by setting up matings in Oxford between homozygous animals, where such were known to exist, or hemizygotes with either transgenic or non-transgenic C57/CBA F_1 partners. The mothers were transported to Bath and sacrificed by cervical dislocation on day 18.5 of gestation. The bodies were then dipped in 70% ethanol at 37°C, and the uterus dissected out and rinsed in sterile phosphate

buffered saline (PBS) (Oxoid) at 37°C to remove traces of maternal blood. A second person was then required to dissect out the foetuses, which were then passed to a third person for revival and fostering to a host mother. Host mothers were usually MF1 mice which had given birth the same day (or in non-ideal circumstances, the day before) and whose own litter had been removed up to four hours previously.

Luciferase assay

This was performed essentially according to Ward *et al.* (1997). Animals were tested for the presence of the transgene by taking a tail biopsy on or around day 4 post-partum and freezing this at -20°C. The thawed tail was then vortexed in 100µl luciferase assay cell lysis buffer (25mM Tris.H_3PO_4, 2mM DTT, 2mM CDTA, 10% glycerol, 1% Triton X-100, pH 7.8), and re-frozen at -20°C to assist cell lysis. 10µl aliquots of the re-thawed lysate were then assayed in duplicate for luciferase activity, using 50µl luciferase assay substrate (Promega) in an E.G. & G. Berthold AutoLumat LB953 luminometer, or 50µl Genglow-1000 luciferase assay substrate (LabTech) in an Anthos Lucy 1 luminometer (LabTech). Light emission was counted for 10s in each case. Lines which expressed low levels of luciferase required homogenisation of tail samples in lysis buffer to release additional enzyme, and this was performed using the 0.1-5ml dispersing tool of an IKA-Labortechnik Ultra-Turrax T8 homogeniser (about 10 s at medium speed).

Genomic DNA preparation

This was performed according to Hogan *et al.* (1994) with modifications. Mice were euthanased by intra-peritoneal injection of 50-100µl 200mg/ml sodium pentobarbital (Rhone Mérieux), or anaesthetised by inhalation of Halothane BP (Rhone Mérieux). Following euthanasia or recovery anaesthesia, a 5-15mm tail biopsy was obtained and placed in 525µl tail buffer (50mM Tris.HCl pH 8.0, 100mM EDTA, 100mM NaCl, 1% SDS) containing 285µg/ml proteinase K (Boeringher Mannheim). This was digested overnight at 55°C, and then treated with 0.7µg/ml RNase A for 1 hr at 37°C. NaCl was added to 1.25M, and then an equal volume of chloroform/isoamylalcohol 24:1 (vol/vol) was added and gentle mixing allowed to occur for 2 hr at room temperature. The solution was spun in a

micro-centrifuge at 15000rpm for 10 min, and the upper, aqueous layer removed to a fresh tube. To this was added an equal volume of propan-2-ol, and mixed gently to precipitate the DNA. This was then spun down at 15000rpm for 10 min, and the supernatant aspirated off. The pellet was washed for 1 hr at 4°C with 300µl ice-cold 70% ethanol, spun down, and the ethanol aspirated off. The genomic DNA pellet was then dissolved in 100µl TE (10mM Tris.HCl pH 8.0, 1mM EDTA) by mixing on a roller overnight at room temperature or leaving at 4°C for several days.

Transgene genotyping by PCR

Some lines failed to express luciferase in sufficient quantities to be reliably detected using the assay above, and these litters were tested for the presence of the transgene using PCR. Following a luciferase assay in which it was impossible to distinguish samples positive for the transgene from background, the remaining 80µl of lysate containing the tail fragment was diluted into 525µl tail buffer and genomic DNA prepared as in the section above.

0.1µl genomic DNA solution (about 0.05µg) was added to 24.9µl PCR reaction master mix to give final PCR reaction conditions (optimised for Mg^{2+} concentration) of: 75mM Tris.HCl pH 9.0, 20mM $(NH_4)_2SO_4$, 0.01% Tween-20 (Advanced Biosciences reaction buffer IV), 3mM $MgCl_2$(Advanced Biosciences), 250µM dATP (Promega), 250µM dCTP, 250µM dGTP, 250µM dTTP , 0.5 units "Red Hot" *Taq* DNA polymerase (Advanced Biosciences Inc.) and 0.2µM each of four primers:

IGF2-03 (5'-CAGTTTGTCTGTTCGGACCGCGGC)
(bp160-183 of *Igf-2* exon 4)

IGF2IN-89 (5'-TCACTGCCTTCTGTGAGCAGTGAG)
(from *Igf-2* intron between exons 4 and 5)

LUCIF-41 (5'-GTGTTGGGCGCGTTATTTATCGGA)
(bp 668-691 of P3-*luc*)

LUCIF-42 (5'-GGGTTGGTACTAGCAACGCACTTT)
(bp 1341-1364 of P3-*luc*)

PCR reactions were denatured for 5 min at 94°C, then cycled at 94°C for 1 min, 62°C for 1 min, 74°C for 1 min for 36 cycles, followed by 10 min final

extension at 74°C. 10µl of each reaction was run on 2% agarose gels, stained with ethidium bromide and examined.

Primers IGF2-03+IGF2IN-89 give a 420bp product from the endogenous *Igf-2* gene, which should be present in samples from all mice.

Primers LUCIF-42 and LUCIF-42 give a 696bp product from the luciferase coding region, which should only be present in samples from transgenic mice.

Probes used in Southern and Northern blots

Probes derived from the transgene construct are illustrated digrammatically in **Figure 1** on page 69 (the constructs have been described previously in Ward *et. al.* (1997)). A **Luc** probe based on the 5′ end of the luciferase coding region was cut out from construct vector P3MM (used to make **M** construct transgenic mouse lines) with HindIII/BstEII and the appropriate 743bp band purified from the gel using the Qiagen gel extraction kit (Qiagen) according to the manufacturer's instructions. A **P3** probe specific to the *Igf2* P3 promoter region (and the endogenous *Igf2* gene) was prepared by digestion with BamHI and HindIII and purifying the appropriate 265bp band. A **CCD** probe, specific to the 3' end of the transgene construct (and the endogenous *Igf2/H19* intergenic region) was cut out from plasmid p180.49A containing the H construct by digestion with EcoRI and BstEII and the appropriate 1144bp band was gel purified as above. A **DMR** probe based on the 5′ differentially methylated region of the *Igf2* gene was prepared from construct vector p176a.14 (used to make **G** construct transgenic mouse lines). The plasmid was digested with Bam HI and PvuI to give a 2.8kb fragment which spans the DMR, and this was gel purified for use as a probe.

Probes representing the 5' and 3' end of the *Sox10* cDNA which excluded the highly conserved HMG box were obtained cloned into the Bluescript Sk(-) vector (Stratagene) (Southard-Smith *et al.*, 1998). Both probes were cut out by digesting their respective vectors with EcoRI and KpnI and gel purifying the appropriate bands. The 5' probe contained 606bp of the *Sox10* sequence upstream of the XmnI site at position 676 relative to the transcription start site. The 3' probe contained 1294bp of *Sox10* sequence commencing at the PvuII site just downstream of the HMG box.

Col9a1 probes COL9A1-1 (corresponding to the 3' end of the mRNA and recognising both isoforms) and COL9A1-2 (corresponding to the 5' end of the long isoform) were as described by Savontaus *et al* (1998). The COL9A1-1 probe was prepared by digesting the plasmid pMCOL9A1-1 with KpnI and EcoRI and purifying the 444bp band from a gel as described above. The COL9A1-2 probe was prepared in a similar manner using an EcoRV digest to liberate the 792bp probe fragment from plasmid pMCOL9A1-2.

Southern blotting and hybridisation

24µl (representing 5-15µg) of genomic DNA samples were digested with restriction enzymes overnight and run on 1% agarose gels. Following staining with ethidium bromide and photography of the markers, the gels were capillary transferred onto Hybond-N (Amersham) membranes under high salt denaturating conditions according to standard procedures (Sambrook *et al.*, 1989). DNA was cross-linked to the membrane either by UV cross-linking or by baking at 80°C for 2hr.

10-50ng of purified probe was labelled to high specific activity with Redivue α^{32}P-dCTP (Amersham) using the High-Prime labelling kit (Boeringher Mannheim), according to the manufacturers instructions, with nucleotide incorporation allowed to proceed for 1hr at 37°C. Unincorporated nucleotide was removed using G-50 spin columns, as follows: The reaction was stopped by the addition of 5µl of stop solution (5% SDS, 50mM EDTA, 0.25% bromophenol blue) and made up to 100µl by the addition of 75µl TNE buffer (100mM NaCl, 10mM Tris.HCl, pH 7.5, 1mM EDTA). This was then applied to a 0.9ml column of Sephadex G-50 Superfine beads (Pharmacia) prepared in a 1ml syringe barrel with a glass wool frit and packed and pre-equilibrated in TNE. The column was then spun for 5min at 250g and the eluate collected. A further 100µl of TNE was applied to the column, the column spun and the eluate collected and pooled with the first aliquot. The resultant 200µl of labelled probe solution was denatured before use by boiling at 100°C for 10min, chilled on ice and added to the hybridisation mixture.

The cross-linked filter was pre-hybridized at 65°C for 2hr in 30ml "Church & Gilbert" hybridisation buffer (500mM Na_2HPO_4 pH 7.2, 1mM EDTA, 7% SDS, 1% BSA, 100µg/ml sonicated salmon sperm DNA) (Church & Gilbert, 1984) or in 30ml "FBI buffer" (10% PEG 8000; 7% SDS; 1.5x SSPE) (K. Foley, Zymogenetics Inc., pers. comm.). The use of FBI hybridisation buffer (used in FBI crime labs) was found to give enhanced sensitivity at the expense of increased background. The filters were then hybridized for 12hr at 65°C in 15-30ml fresh hybridisation buffer containg >10^6cpm/ml denatured probe , then washed twice for 15 min at 65°C in 40mM Na_2HPO_4 pH 7.2, 1mM EDTA, 5% SDS, 0.5% BSA, followed by two washes for 1hr at 65°C in 40mM Na_2HPO_4 pH 7.2, 1mM EDTA, 1% SDS. The filters were then briefly rinsed at room temperature in 40mM Na_2HPO_4 pH 7.2, 1mM EDTA, wrapped in SaranWrap and put down for autoradiography with blue sensitive X-ray film (Genetic Research Instrumentation) or with Kodak X-Omat AR film (Sigma) or with Kodak BIO-Max film (Sigma) at -80°C with intensifying screens.

Image scanning and densitometry

X-ray films of Southern blots were scanned on a UMAX S6E flat-bed scanner using Vista-Scan software to generate 256 greyscale TIFF images. Contrast and gamma were adjusted using Adobe Photoshop V4.0 and the scans were analyzed quantitatively using NIH Image Win95 Beta V3 (Scion Corporation) and its "Gelplot 2" macro, to give numerical values representing the integrated density of each band by measuring the area under the peak.

Alizarin red/alcian blue skeletal preparations

This was performed according to Hogan *et al.* (1994) with modifications. Mice were euthanased by intra-peritoneal injection of 50-100µl 200mg/ml sodium pentobarbital (Euthatal, Rhone Mérieux), skinned, eviscerated and muscle tissue trimmed off. The carcasses were then fixed in ethanol for 5 days, rinsed in water for a few minutes, and transferred to staining solution for 4 days: 1 volume 0.3% alcian blue (Gurr) dissolved in 70% ethanol, 1 volume 0.1% alizarin red (Raymond Lamb) dissolved in 95% ethanol, 1 volume glacial acetic acid, 17 volumes 70% ethanol. The stained preparations were washed in distilled water for a few

minutes, then cleared in 20% glycerol, 1% KOH until the bones were visible (several weeks), then dehydrated through a 70%, 80%, 90%, 100% ethanol series and stored and photographed in methyl salicylate (BDH).

FISH

Metaphase chromosome spreads from splenocytes

This protocol was based upon that used in the MRC Human Genetics Unit, Edinburgh (M. Lee, pers. comm.) with modifications. Splenocytes were found to proliferate more readily and yield more metaphase chromosome spreads when spleens from two or more animals were pooled together.

Following sacrifice by cervical dislocation or intra-peritoneal injection of Euthatal, spleens were dissected out into PBS and then transferred into roome temperature RPMI1640 medium (Glutamax II variant, Gibco-BRL) in a 5cm petri dish. Spleens were then pricked all over with a 26G syringe needle, and using one needle to hold the spleen steady, a second needle was used to inject 5-10ml of medium into the body of the spleen to flush out cells into the surrounding medium. The spleen was then discarded and the cells pelleted by spinning the medium down for 6min at 400*g*. The supernatant was removed, and the cells resuspended in 5ml of pre-warmed splenocyte culture medium (RPMI1640 containing 15% fetal calf serum(Gibco-BRL) and 0.1mg/ml gentamicin sulfate (Sigma). Various volumes of cell suspension ranging from 0.2 to 2ml were added to 5ml total volume of splenocyte culture medium in a 15ml snap-cap round-bottomed polystyrene tissue culture tube and lipopolysaccharide (from *Salmonella enteriditis,* Sigma #L-6011) was added to each tube to a final concentration of 50μg/ml (stored at -20°C as a 5mg/ml stock in H_2O). Cells were cultured with lids left on loosely in 5% CO_2 at 37°C for 44 and 46hrs (independent cultures). They were then optionally treated with demecolcine (Sigma) added to 0.1μg/ml for 30min. This can give more spreads, but the chromosomes are more condensed and G-banding is impaired. Cells were spun down for 6min at 400*g*, supernatant removed, and cells were resuspended in 1ml freshly made room temperature 0.56% w/v KCl (75mM). Cells were resuspended by adding this hypotonic solution dropwise and flicking the tube vigorously between additions. After the

first 1ml had been added, the suspension was carefully overlaid with 9ml hypotonic solution and left for 10min at room temperature. The swollen cells were then spun down for 6min at 400*g*, the supernatant carefully aspirated off, and the cells were fixed by the addition of 1ml freshly made methanol:glacial acetic acid (3:1). As before, this was added dropwise, with vigorous flicking of the tube between additions to resuspend the cells and prevent clumping during fixation. After the first ml had been added, the suspension was carefully overlaid with 9ml of fixative and left overnight at 4°C. The next day, the cells were spun down for 6min at 400*g*, fixative removed, and the cells were resuspended in 10ml fixative, spun down and supernatant removed. This was repeated, followed by final resuspension of cells in 0.1-0.5ml fixative.

Glass slides which had been previously cleaned overnight in absolute alcohol/concentrated HCl 1:1 (vol/vol), washed extensively in deionized H_2O, and stored in absolute alcohol were placed in deionized water for 5min before use. They were removed from the water and given a single wipe with a piece of tissue moistened in deionized H_2O. If this did not result in a uniform thin film of water on the slide (i.e. if any beading was observed), the slide was discarded. 10µl of cell suspension was applied directly to the wet slide using the tip of a Gilson pipette. The resulting spreads were allowed to air-dry at room temperature for several hours, then placed under vacuum with no desiccant for 72hr at room temperature. They were then ready for use in FISH experiments, but optimal G-banding was obtained if the slides were subsequently left at room temperature (without vacuum) for around 14 days. This accords with the recommendations given by E.P. Evans (Hogan *et al.*, 1994).

Metaphase chromosome spreads from embryonic fibroblasts

This was performed essentially according to Hogan *et. al.* (1994). E12-E15 embryos were dissected from the uterus and placed in a small petri dish in Medium 199 (Sigma) containing 25mM HEPES (Sigma) with Earles salts (Sigma), 2mM L-glutamine (Sigma) and 10% foetal calf serum (Gibco-BRL). The yolk sacs were assayed for luciferase to determine which embryos were transgenic. The livers were removed from the embryos. The embryos were then teased apart using forceps to release cells. The cell suspension was transferred to a second dish

and incubated in 5% CO_2 at 37°C to generate embryonic fibroblasts. Once the cells were judged to be growing in log phase (24-36 hr), they were treated with 0.05μg/ml demecolcine (Sigma) for 2 hr to induce mitotic arrest. The cells were trypsinised and pipetted up and down to generate a single-cell suspension. The suspension was removed, serum-containing medium added to neutralise the trypsin, and the cells were pelleted by centrifugation at 500*g* for 5min. The supernatant was discarded and the cells resuspended in hypotonic KCl solution and thereafter treated exactly as in the preceding method.

Metaphase chromosome spreads from peripheral lymphocytes

Lymphocyte culture was performed essentially according to McFee *et al.* 1997) and was found to be successful for human blood, but not for mouse. Adult mice were sacrificed by intraperitoneal injection of Euthatal and exsanguinated into heparinised syringes. For human experiments, 10ml was removed from the median cubital vein of the arm into a heparinised syringe. Whole blood (1-2ml from each mouse) was carefully layered onto 0.5 volumes density gradient centrifugation medium Histopaque 1077 (Sigma) and centrifuged at 1000*g* for 15min. Most of the upper yellow (plasma) layer was then discarded and the middle white monocyte layer (enriched for small lymphocytes) was carefully removed, leaving behind the bottom red layer containing the erythrocytes. The cell suspension was then mixed with 10ml PBS and centrifuged at 1000*g* for 10min to pellet the cells. The cell pellet was washed with 10ml PBS and resuspended in 2ml mitogenic culture medium: Medium 199 (HEPES modification, Sigma), 15% foetal calf serum (Gibco-BRL), 2mM L-glutamine (Sigma), 0.1mg/ml gentamicin sulfate (Sigma), 6μg/ml phytohemagglutinin (PHA-P lectin, Sigma), 3.3μg/ml lipopolysaccharide (E. Coli serotype 0111.B4, Sigma). Cells were cultured at 37°C with 5% CO_2 for 48hr then democolcine added to 0.05μg/ml and left for 2hr to induce mitotic arrest and chromosome spreads prepared exactly as in the preceding methods.

Probe template purification

Transgene probes were prepared from vector Bluescript 2 SK(+) (Stratagene) containing the **H** construct, consisting of the *Igf-2* P3 promoter, *Luc*

coding region and the conserved central domain (CCD) lying between the *Igf-2* and the *H19* loci (**Figure 1**). The construct was purified away from the vector backbone by performing a triple restriction digest with SalI, NheI and PvuI, then running the restriction fragments out on a 1% agarose gel and purifying the 3kb band corresponding to the transgene construct using a Geneclean II gel extraction kit (Anachem), according to the manufacturer's instructions. Purified construct was re-dissolved in H_2O to a concentration of ~100ng/µl and 0.5µg aliquots labelled with either biotin or digoxigen by nick translation.

The *Dvl* probe, corresponding to 17kb of genomic sequence from the *Dvl* locus on Chr 4 contained in a phage lambda cloning vector, was obtained (D. Sussman, University of Maryland School of Medicine, Baltimore, USA) as purified DNA and labelled directly by nick translation.

Probe labelling

This was performed according to Wilkinson *et. al* (1992) with modifications. For biotinylated probe, 5µl (corresponding to 500ng) of purified DNA was added to the nick translation mix, which was assembled on ice, and also contained: 2µl 10x nick translation salts (0.5M Tris.HCl pH 7.5; 0.1M $MgSO_4$; 1mM dithiothreitol; 500µg/ml BSA fraction V (all from Sigma)); 2.5µl 0.5mM dATP (Pharmacia), 2.5µl 0.5mM dCTP (Pharmacia), 2.5µl 0.5mM dGTP (Pharmacia), 2.5µl 0.5mM bio-16-dUTP (Boeringher Mannheim) and 1µl of RNAse-free DNAse I (Pharmacia) which had been freshly diluted 1:500 in ice-cold H_2O. This totalled a reaction volume of 19µl, which was mixed and spun down briefly to collect. To this was added 1µl of E. Coli DNA polymerase I (Sigma) to give final reaction conditions of 50mM Tris.HCl pH 7.5, 10mM $MgSO_4$, 0.1mM DTT, 50µg/ml BSA, 62.5mM dATP, 62.5mM dCTP, 62.5mM dGTP and 62.5mM bio-16-dUTP. The reaction was incubated at 15°C for 90min and then stopped by the addition of 2µl 0.2M EDTA and 1µl 5% SDS followed by incubation at 65°C for 10min. The reaction was then made up to 100µl by the addition of TNE and unincorporated nucleotide was separated from the labelled probe using G-50 spin columns as described previously under 'Southern blotting'. 5µl of 10mg/ml sheared salmon sperm DNA (Sigma), 50µl of 3M NH_4 acetate pH4.6 and 500µl of ice-cold absolute

ethanol were then added to the probe mixture and the DNA allowed to precipitate overnight at -20°C. The precipitated DNA was pelleted by spinning at 12000*g* for 10min, the supernatant removed, the pellet washed with 1ml 70% EtOH, dried and re-dissolved in 50µl of TE for use in the hybridisation cocktail.

For digoxigenin labelling of probe, an identical procedure was followed, except that the biotinylated nucleotide was replaced with 1.5µl 0.5M dTTP and 1µl 0.5M dig-11-dUTP (Boeringher Mannheim).

G-banding

This was based upon standard protocols, with modifications (Franke & Oliver, 1978; Wilkinson, 1992; Hogan *et al.*, 1994). Giemsa stain stock was prepared by dissolving 7.63g Giemsa powder (BDH) in 500ml glycerol by leaving it for 30min in a 50°C water-bath with periodic mixing. This was allowed to cool and 500ml methanol added. This stock solution was filtered and stored at room temperature.

After aging as described above, slides bearing chromosome spreads were equilibrated in 2xSSC (1xSSC = 15mM Na citrate, 150mM NaCl pH 7.0) for 5min at room temperature, then incubated in 2xSSC at 60°C for 1hr in glass coplin jars. The jars were removed from the water bath and allowed to cool for 5min then cooled to room temperature by placing them (with lids) under a running cold tap. The slides were then equilibrated in PBS. Trypsin solution was made fresh by diluting 0.25ml Difco Bacto-trypsin stock (dissolved in H_2O and stored at -20°C) (Difco Labs #0153-60-2) in 50ml PBS. Slides were then dipped in trypsin solution for varying times ranging from 5-30s (this required optimisation for each batch of slides) and then briefly rinsed in 10mM sodium phosphate buffer pH 6.8 followed by staining for 15-20min in 50ml freshly prepared Giemsa stain (1ml Giemsa stock in 50ml 10mM sodium phosphate buffer pH 6.8). Slides were then rinsed in deionized H_2O and air dried.

Following staining, the resultant G-banding was documented (without mounting) the same day and the immersion oil removed by 2 x 1min incubation in xylene:ethanol (1:1) in a fume hood. Giemsa stain was then removed by 2x5min washes in methanol:acetic acid (3:1). the destained chromosome spreads were then re-fixed in 4% paraformaldehyde in PBS for 10min, followed by 4x5min

washes in PBS, then briefly rinsed in deionized H_2O and air-dried. Slides were taken through to FISH within 24hr.

Hybridisation

This was performed according to the protocol used in the MRC Human Genetics Unit, Edinburgh, with modifications. If slides had not been G-banded, pre-treatment with RNase was necessary. Slides were equilibrated in 2xSSC at room temperature for 5min, then incubated in 0.1mg/ml RNase (Sigma) for 1hr at 37°C. Slides were then washed briefly in 2xSSC then dehydrated by taking them sequentially through 70%, 90% and 100% EtOH (2min in each) and air-dried under vacuum for 10min. Slides which had been G-banded the previous day were simply equilibrated in 2xSSC and dehydrated without the RNAse treatment.

During RNAse treatment, the probe cocktail was prepared. For each slide, a tube was prepared containing 5µl labelled probe DNA (~50ng), 2µl mouse genomic C_0t-1 DNA (Gibco-BRL) and 2 volumes of absolute EtOH. The DNA was precipitated and the pellet dried by evaporating the 21µl of liquid in a speedivac. The dried pellet was resuspended in 15µl hybridisation mix (stored at -20°C) consisting of 50% formamide (Ultra grade, Sigma), 2xSSC, 1% Tween-20 (Sigma) and 10% dextran sulfate (Sigma) by incubation for at least 15min at 37°C during slide treatment. The DNA was denatured by incubating the hybridisation cocktail at 70°C for 5min, then left at 37°C for around 30min to pre-anneal the C_0t-1 DNA to any repetitive sequence elements of the probe. It is considered desirable to synchronise probe preparation with slide preparation, but longer pre-annealing times did not seem to affect results.

Dried slides were placed in an oven at 70°C for 5min to pre-warm then placed in pre-warmed denaturing solution at 70°C for exactly 2min. This consisted of 50ml 70% formamide, 2xSSC in a coplin jar, and this step was performed in a fume hood. Following denaturation, slides were immediately plunged into ice-cold 70% EtOH and left for 2min, followed by dehydration through 70&, 80% and 100% EtOH at room temperature as before, then dried under vacuum.

Slides were pre-warmed on a 37°C hotplate for no more than 2min, then used to pick up the 15µl of pre-annealed hybridisation cocktail which had been placed on a 22x22mm coverslip on the hotplate. The edge of the coverslip was sealed with Tip-Top rubber cement (Cat #5059128, Rema Tip-Top UK, Westland Square, Leeds LS11 5X5), and slides hybridised overnight at 37°C without the need for a humidity chamber.

Following overnight hybridisation, the rubber cement was carefully peeled off, and the coverslips allowed to fall off by leaving the slides in 2xSSC for 10min. Slides were then washed by incubation in a 45°C water-bath in pre-warmed 2xSSC, 50% formamide (4x3min), 2xSSC (4x3min), followed by high-stringency washes in 0.1xSSC at 60°C (4x3min). Slides were then equilibrated in SSCT (4xSSC 0.1% Tween-20) at room temperature for 10min prior to detection.

Detection

All antibodies were diluted in SSCTM, prepared by dissolving 5% non-fat milk (Sainsburys) in SSCT, and spinning this solution for 10min at 3000g to clarify it. The diluted antibodies were further clarified to remove particulate matter by spinning at 15000g for 10min. All antibody incubations were carried out at 37°C in a humidity chamber, applying 50µl per slide under a coverslip. Washes in between antibody incubations consisted of 3x2min washes in SSCT at 37°C.

For green detection of biotinylated probe, slides were blocked in SSCTM for 30min, then incubated in avidin-FITC (Vector) diluted 1:500 for 30min, biotinylated anti-avidin (Vector) diluted 1:100 for 30min, followed by another round of 1:500 avidin-FITC for 30min. For red detection, avidin-Texas Red (Vector) was substituted for avidin-FITC. For detection of digoxigen-labelled probe, slides were incubated in sheep anti-digoxigenin-FITC (Boeringher Mannheim) diluted 1:15, followed by anti-sheep FITC (Vector) diluted 1:200.

Following antibody incubation and final washes, slides were incubated in the dark for 5min in PBS containing 0.25µg/ml 4,6-diamidino-2-phenylindole (DAPI)(Sigma), followed by 2x5min washes in PBS. Slides were then mounted in anti-fade mountant (Vectashield, Vector) and the coverslips sealed with nail varnish (Boots).

Documentation

Slides were examined on a Leica DMRB microscope equipped with epifluorescence illumination and appropriate filter blocks. Spreads were located at low power, then examined and photographed at x1000 magnification using a 100x oil immersion objective and a cooled CCD camera (Hamamatsu) linked to an IBM-compatible PC equipped with a frame grabber card. Images were captured and processed for contrast and brightness using Image Pro Plus V3.0 software (Media Cybernetics), and were then transferred into Adobe Photoshop V5.0 for false colouring and merging of fluorescent images from multiple channels.

For G-banding, it was found empirically that the best images (those showing the greatest fine banding detail) were obtained by first setting up Kohler brightfield illumination, then using phase ring 1 rather than the brightfield setting in the condenser turret (it should be noted that the x100 objective was not rated for phase contrast). This was believed to be caused by a decrease in numerical aperture, leading to an increase in both contrast and depth of field, but a decrease in resolution (V. de las Casas, pers. comm.). Much the same effect could be achieved by stopping down the aperture diaphragm under normal brightfield illumination, but this was found to be slightly inferior to the first method.

Multiple G-banded spreads were documented and their locations noted using the X-Y stage ruler on each slide prior to destaining and FISH hybridisation. The same spreads could then be located following FISH.

Histology

Fixation, embedding and sectioning

Tissue blocks were fixed in Zamboni's fixative overnight at 4°C, prepared by mixing 200ml 0.2M Na phospate buffer pH 7.3 with 200ml 2% paraformaldehyde and 70ml saturated picric acid (Culling, 1974). The fixed blocks were then dehydrated through 70%, 80%, 90%, 95%, 95%, 100% and 100% EtOH (10minutes - 1 hour in each, depending on tissue block size), cleared in xylene or Histoclear (National Diagnostics), and then imbedded in paraffin wax.

Tissue sections were cut at between 5 and 10μm, floated on a water-bath and dried onto slides which had been previously subbed with TESPA (3-

aminopropyltriethoxysilane)(Sigma), as per standard procedures (Wilkinson, 1992).

Haematoxylin & Eosin (H & E) staining

This was performed according to standard procedures (Bancroft & Stevens, 1977). Ehrlich's haematoxylin was either purchased pre-prepared (Raymond Lamb) or made by dissolving 2g haematoxylin (BDH) in 100ml absolute EtOH, then adding 100ml glycerol, 100ml deionised H_2O, 10ml glacial acetic acid and 15g potassium alum ($AlKSO_4.12H_2O$)(BDH), mixing and allowing to ripen for 2 months before use.

Slides were dewaxed in Histoclear 2 x 3min, then rehydrated through 100%, 100%, 95%, 90%,70% and 50% EtOH (2min in each), followed by 1min in deionized H_2O and 10min in Ehrlich's haematoxylin. Slides were washed in running cold tap water for 1min to turn the stain blue, rinsed in deionised H2O then differentiated by dipping in acid alcohol (1% conc. HCl in EtOH) for 15s followed by 30s in 1% NH_3 in 70% EtOH. Slides were then left in 70% EtOH for 1 min and stained for 1min in Eosin Yellow (BDH)(0.1% in 70% EtOH). Slides were then dehydrated through an ethanol series: 1min each in 70%, 90%, 95%, 100%, 100% EtOH, 2 x 2min in Histoclear and mounted under coverslips in DPX mountant (BDH).

Periodic acid-Schiff reaction (PAS) staining

This reagent reacts with tissue carbohydrates and stains mucopolysaccharides and other glycoproteins magenta, emphasizing certain basement membranes in particular. PAS staining was performed essentially according to standard procedures (Culling, 1974; Bancroft & Stevens, 1977), except that in some cases the Schiff's reagent (Feulgen stain) was purchased pre-prepared (Raymond Lamb). Otherwise, Schiff's reagent was prepared by dissolving 1g basic fuchsin (BDH) in 200ml boiling deionised H_2O, removing the flask from the heat just before the addition of the dye. Once the solution had cooled to 50°C, 2g of potassium metabisulfite (BDH) was added and dissolved by mixing. Once the solution had cooled to room temperature, 2ml conc. HCl was added and the mixture allowed to stand overnight in the dark. The following

day, 0.2g activated charcoal (BDH) was added and the mixture shaken for 2min. This was then filtered through No. 1 Whatman paper and stored in a dark bottle at 4°C for no more than two months.

For staining, slides were dewaxed in Histoclear 2 x 3min, then rehydrated through 100%, 100%, 95%, 90%,70% and 50% EtOH (2min in each), followed by 1min in deionized H_2O. They were then incubated in freshly-prepared 1% w/v periodic acid (BDH) in distilled H_2O for 6min, followed by 3min wash in running tap water and 1min in distilled H_2O. They were then incubated for 15min in Schiff's reagent which was stored at 4°C and had been allowed to warm to room temperature before use. Slides were then washed for 5min in running tap water, then counterstained in haematoxylin, dehydrated and mounted as described for H&E staining, with the exception that the time in haematoxylin was reduced to 1-2min only, since PAS accentuates the nuclear staining seen with haematoxylin.

Immunofluorescence

Following dewaxing and rehydration, 7μm sections of mutant and wild-type colons from **Harry** mice were blocked by incubation in SSCTM for 30min at 37°C. Following washes in SSCT (3x2min at 37°C in all cases), the slides were incubated with either SSCTM (control) or 50μl rabbit anti-neurofilament (Sigma) diluted 1:100 overnight at 4°C. The next day, the slides were washed and incubated with biotinylated anti-rabbit diluted 1:200 for 30min at 37°C, washed again and incubated with streptavidin-Texas red (Vector) diluted 1:200 for 30min at 37°C. Slides were then equilibrated in PBS, counter-stained with DAPI and mounted in Vectashield as described previously for FISH detection.

α-PCNA immunohistochemistry

Following dewaxing and rehydration, antigen retrieval was performed: Slides were pressure cooked for 1min in 10mM citrate buffer pH 6.0 (the pressure cooker was filled with sufficient buffer to cover the slides, brought to the boil, the slides were placed in it and the lid sealed. Timing began once the pressure indicator rose to visibility), then washed for 3 x 5min in PBS + 0.1% Tween-20 + 0.01% sodium azide (PBST) at room temperature. Endogenous peroxidase activity was then quenched by incubating slides for 5min in 3% hydrogen peroxide

(Sigma) in tap water, followed by 30min in 0.5% hydrogen peroxide in methanol. Slides were then washed 3 x 10min in PBST. Slides were immunostained using the MOM (Mouse on Mouse) kit (Vector), designed to allow the use of mouse monoclonals on mouse tissue sections without incurring undue background. This is achieved using proprietary blocking reagent, the nature of which was not disclosed, and kit-specific biotinylated anti-mouse IgG. Slides were blocked for 1hr at room temperature in the blocking reagent supplied with the kit diluted as per the manufacturer's instructions. They were then incubated at 37°C for 30min in monoclonal α-PCNA clone PC10 (Dako) diluted 1:200 in the diluent supplied with the MOM kit. Slides were then washed 3 x 10min in PBST, followed by incubation in biotinylated anti-mouse-IgG (supplied with MOM kit) diluted 1:250 in kit diluent. Slides were incubated in this secondary antibody layer for 10min at room temperature, then washed 3 x 10min in PBST. Slides were then incubated for 5min at room temperature in ABC kit streptavidin-horseradish peroxidase complex (Vector), prepared according to the manufacturer's instructions 30min previously. Following the final 3 x 5min washes in PBT, the slides were stained in diaminobenzidine (DAB) substrate prepared from the ABC kit according to the manufacturer's instructions, with the nickel compound added to give a blue-black coloured substrate. The substrate reaction was allowed to proceed for 5-10min, with staining monitored under the dissecting microscope, and stopped by placing the slides in distilled H_2O at the appropriate time and incubating for 10min. Slides were then lightly counterstained in methyl green (0.1% in distilled H_2O) for 30s, followed by rapid dehydration and mounting in DEPX. This was found to give optimal contrast to the antibody staining.

Documentation

H & E or PAS stained slides were photographed on a Leica DMRB or a Nikon Eclipse E800 microscope using brightfield illumination and Kodak Ektachrome 64 film. Images were digitised using a Nikon Coolscan 35mm slide scanner and colour balance and contrast adjusted using Adobe Photoshop V5.0.

Immunofluorescent staining was documented as described previously for FISH detection.

RT-PCR and Northerns

Isolation of total RNA

This was performed according to the manufacturer's instructions using TRI reagent (acid guanidinium thiocyanate phenol chloroform extraction) (Chomczynski & Sacchi, 1987).

50-100mg of tissue (brain, kidney, hindlimb or eye) was removed from animals immediately after sacrifice and placed in 1ml TRI reagent (Sigma) on ice. This was homogenised using the 0.1-5ml dispersing tool of an Ultra-Turrax T8 homogeniser (IKA-Labortechnik), and the homogenate clarified by spinning at 12000g for 10min at 4°C. The supernatant was removed (avoiding fatty scum at the surface) and allowed to stand for 10min at room temperature, then 0.2ml chloroform was added and the tube shaken vigorously to mix the phases and left to stand for 15min at room temperature. The mixture was spun at 12000g for 15min at 4°C and the upper, aqueous phase removed to a fresh tube. 1/10 volume propan-2-ol was added to this and following mixing, this was allowed to stand at room temperature for 5min, then spun down at 12000g for 10min at 4°C. The supernatant was removed and RNA precipitated by the addition of an equal volume of propan-2-ol. This was mixed and allowed to stand for 10min at room temperature, then the RNA pelleted by spinning at 12000g for 10min at 4°C. The supernatant was removed and the pellet washed with 1ml 75% EtOH. The pellet was spun down again, the supernatant removed, and the pellet was allowed to air-dry for 10min at room temperature, then re-dissolved in DEPC-treated H_2O (for RT-PCR and Northerns)or in formamide (for Northerns only) by incubating it at 55°C for 15min with occasional vigorous pipetting using a Gilson. 1µl recombinant RNAse inhibitor (Promega) was added in some cases.

***Sox10* RT-PCR**

For diagnostic *Sox10* RT-PCR, two pairs of nested primers were used whose positions and orientations are illustrated diagrammatically on **Figure 18** in chapter 7. The sequences of these primers were as follows:

```
Sox10-98   5'-CTGTCCAGCCAGGGTGTTTG-3'
Sox10-99   5'-TCTCAGGTCCTGGGATAGAG-3'
```

Sox10-96 5'-AGGTCAAGAAGGAACAGCAGGACG-3'

Sox10-97 5'-GCAGGTATTGGTCCAGCTCAGTCA-3'

The first PCR was performed using the Access RT-PCR kit (Promega) which allows first strand reverse transcription and amplification using a pair of PCR primers to occur in a single reaction. This kit has the added advantage that the reverse transcriptase used (Avian Myeloblastosis Virus (AMV) reverse transcriptase) can operate at 48°C. This higher working temperature obviates some of the RNA secondary structure formation which can cause premature termination of reverse transcription with enzymes which operate at lower temperatures (Promega Corporation, 1995).

0.5µg total RNA was placed on ice and the other reaction components added: 10µl 5x reaction buffer (proprietary reaction buffer supplied with Access RT-PCR kit, composition unknown), 1µl dNTP mixture (10mM each nucleotide), 3.25µl 15µM Sox10-98 primer, 3.25µl 15µM Sox10-99 primer, 2µl 25mM $MgSO_4$ and nuclease-free H_2O to a total volume of 48µl. To this was added 1µl (5U)AMV reverse transcriptase and 1µl (5U) *Tfl* DNA polymerase.The reaction was mixed, spun down and incubated at 48°C for 45min to produce reverse transcribed first strand product. It was then denatured at 94°C for 2min, then 40 cycles were performed, with each cycle comprising 40s at 94°C, 30s at 55°C and 2min at 68°C, followed by final extension for 7min at 68°C, and cooling to 4°C.

1µl of the primary RT-PCR reaction was used as a template in a nested PCR using primers 96 and 97. 25µl PCR reactions were set up containing 75mM Tris.HCl pH 9.0, 20mM $(NH_4)_2SO_4$, 0.01% Tween-20 (Advanced Biosciences reaction buffer IV), 2mM $MgCl_2$(Promega), 250µM dATP, 250µM dCTP, 250µM dGTP, 250µM dTTP , 1U "Red*Taq*" DNA polymerase (Sigma) and 150nM each primer. Reactions were denatured for 5min at 95°C, then 40 cycles performed, with each cycle consisting of 45s at 95°C, 30s at 60°C and 2min at 72°C, followed by final extension for 10min at 72°C and cooling to 4°C.

10µl of the nested PCR was run out on a 2% agarose gel, stained with ethidium bromide and photographed on a UV transilluminator using a black and

white video camera (UVP) equipped with an appropriate filter and documented using a video graphic thermal printer (Sony).

***Eya1* RT-PCR**

An *Eya1* probe was generated for use in Northern blotting using RT-PCR. The published cDNA sequences of *Eya1*, *Eya2* and *Eya3* were aligned against each other using the **Pileup** function of the GCG software package, and regions of the *Eya1* message which were not conserved or not present in the other two family members (the sequence of *Eya4* was not available in the databases at the time of experimental design) were used to design RT-PCR primers which would specifically amplify the *Eya1* message (Xu *et al.*, 1997b).

```
Eya1F-110 5'-CCTCCTATGGTGCATTGTGG-3'
Eya1R-111 5'-GGCTGGTGTTACTGCTCGTC-3'
```

0.5μg of brain total RNA from a non-transgenic animal was used as a template for RT-PCR using the Access system, with reaction conditions exactly as described above for *Sox10* RT-PCR. This was followed by nested amplification using the same primer pair, using 0.1μl of the primary RT-PCR as a template. 25μl PCR reactions were set up containing 75mM Tris.HCl pH 9.0, 20mM $(NH_4)_2SO_4$, 0.01% Tween-20 (Advanced Biosciences reaction buffer IV), 1.5mM $MgCl_2$(Promega), 250μM dATP, 250μM dCTP, 250μM dGTP, 250μM dTTP , 1U "Red*Taq*" DNA polymerase (Sigma) and 150nM each primer. Reactions were denatured for 5min at 95°C, then 40 cycles performed, with each cycle consisting of 45s at 95°C, 30s at 58°C and 1min at 72°C, followed by final extension for 10min at 72°C and cooling to 4°C.

Upon analysis of the PCR products on a 2% agarose gel, a single strong band of the predicted size of 320bp was observed. This band was cut out of the gel, purified using a Quiagen gel extraction kit (Qiagen) according to the manufacturer's instructions, and aliquots of the purified fragment were restriction digested with enzymes calculated to give a diagnostic pattern unique to the *Eya1* cDNA (utilising the presence of KnpI and XmnI sites which are not present in either *Eya2* or *Eya3*). The restriction digests gave the predicted fragments (data

not shown), and it was concluded that the amplified fragment represented a 320bp central fragment of the *Eya1* cDNA.

Northern blotting and hybridisation

Northern blots were performed according to standard protocols (Sambrook *et al.*, 1989) with modifications. RNA samples were analysed using 1.2% gels: 4.2g agarose was dissolved in 304ml nuclease-free H_2O and cooled to 65°C in a water-bath. To this was added 35ml 10x MOPS running buffer (10x MOPS buffer = 200mM MOPS (3-[N-Morpholino]propanesulfonic acid)(Sigma) pH 7.0, 50mM Na acetate, 10mM EDTA) and 10.5ml 37% formaldehyde (Sigma), and the gel was immediately poured. RNA samples were prepared for loading by mixing up to 11.25µl RNA solution with 5µl 10xMOPS buffer, 8.75µl formaldehyde, 25µl formamide and bringing the total volume to 50µl. This was denatured for 15min at 55°C, 5µl 10x Ficoll loading buffer (Sambrook *et al.*, 1989) added and the samples loaded onto the gel and run in 1x MOPS buffer for 18hr at 50V. The gel was then capillary blotted (without pre-treatment) onto Hybond-N membrane and subsequent hybridisations with labelled probes were carried out exactly as described earlier under Southern blotting.

Linkage mapping

Microsatellite PCR

All primers were purchased as pairs (MapPairs, Research Genetics). Each primer pair used required optimisation of the Mg^{2+} concentration and annealing temperature. Following the recommended protocol from the Whitehead Institute (http://www.genome.wi.mit.edu, 1999), primer pairs were tested at annealing temperatures of 54°C and 57°C using concentrations of 1.5mM and 3mM Mg^{2+}.

All PCR reactions were carried out using 5µl of genomic DNA (prepared from tail biopsies exactly as detailed above) which had been diluted 1:150 in H_2O, corresponding to ~25ng of template DNA per PCR reaction. Reactions were carried out in a final volume of 20µl containing 75mM Tris.HCl pH 9.0, 20mM $(NH_4)_2SO_4$, 0.01% Tween-20 (Reaction Buffer IV, Advanced Biosciences), 1.5mM

or 3mM $MgCl_2$(Promega), 200μM dATP, 200μM dCTP, 200μM dGTP, 200μM dTTP (Pharmacia), 1U "Red*Taq*" DNA polymerase (Sigma) and 133nM each primer. The results from experiments to determine optimal reaction conditions for each primer pair are summarised in Table 1:

Table 1. PCR conditions and results for microsatellite PCR primer pairs

Marker	Linked to locus	C57 size	C3H size	C57/CBA Polymorphic?	1.5mM Mg^{2+} 57°C	3mM Mg^{2+} 57°C	1.5mM Mg^{2+} 54°C	3mM Mg^{2+} 54°C
D15Mit2	*Sox10*	93	84	YES	OK	GOOD	u/t	u/t
D15Mit238	*Sox10*	122	134	u/n	NO	NO	NO	NO
D15Mit1	*Sox10*	184	188	YES	NO	YES	u/t	u/t
D15Mit71	*Sox10*	118	132	YES	GOOD	u/t	u/t	u/t
	Ednrb	136	121	u/n	C57 ONLY	NO	u/t	u/t
D14Mit197	*Ednrb*	94	90	YES	GOOD	u/t	u/t	u/t
D2Mit148	*Edn3*	117	121	YES	FAINT	GOOD	u/t	u/t
D2Mit265	*Edn3*	103	146	YES	C57 ONLY	GOOD	u/t	u/t
D4Mit263	*Tcm*	110	104	YES	NO	OK	u/t	u/t
D4Mit101	*Tcm*	102	96	YES	NO	GOOD	u/t	u/t
D1Mit64	Proximal Chr 1	110	104	u/n	NO	NO	NO	NO
D1Mit66	Proximal Chr 1	158	170	YES	GOOD	u/t	u/t	u/t

u/n = unknown; u/t = untested; GOOD = strong bands; OK = satisfactory (distinguishable) bands; NO = no specific products observed

Subsequent to this, with the exception of D1Mit64, D14Mit165, D4Mit263 and D15Mit238, which could not be successfully amplified, PCRs were performed using the best conditions obtained from the results above.

Non-denaturing polyacrylamide mini-gels

Those PCR products with sizeable differences (>10bp) between C57 and CBA alleles could be analyzed on 10cm polyacrylamide minigels for test purposes, although it was found more convenient to run large numbers of samples simultaneously on the larger sequencing gels detailed below.

Mini-gels were cast and run using the Mini-Protean II rig (Bio-Rad), according to the manufacturer's instructions. 12.5ml of 8% non-denaturing gel

mix was prepared by mixing together 7.75ml H_2O, 3.3ml 30% acrylamide:bis-acrylamide (19:1) (Bio-Rad) and 1.25ml 10xTBE buffer (1xTBE = 90mM Tris base, 90mM boric acid, 2mM EDTA). Polymerisation was initiated by the addition of 125µl freshly made 10% ammonium persulfate (BDH) and 15µl TEMED (N,N,N',N'-Tetramethylethylenediamine) (Sigma), the gel was poured and left to set for 30-60min at room temperature. The gel rig was then assembled, and the PCR reaction samples prepared by addition of 10x Ficoll loading buffer. 5µl of each PCR reaction was electrophoresed on the gels at 100V for 1hr. Gels were then fixed in clean glass troughs in 200ml 40% methanol for at least 30min prior to silver staining.

Denaturing polyacrylamide sequencing gels

These were cast in sequencing gel rigs (Flowgen) assembled essentially according to the manufacturers instructions. Both glass plates were scrupulously cleaned with hot soapy water, cold deionized water, acetone and 70% EtOH. The notched plate was treated before every fourth run with repel silane (Sigmacote SL-2, Sigma), while the un-notched plate was treated every run with 3µl of bind silane (Silane A-174, Electran grade, BDH) dissolved in 1ml of 70% EtOH containing 0.05% glacial acetic acid. In either case, silane was wiped over the surface of the plate, left for 5min, then the plate was cleaned 4 times with 70% EtOH. Following this, the plates and spacers were assembled, sealed with pressure-sensitive tape (Gibco-BRL) and the gel mix prepared.

Denaturing 6% urea polyacrylamide gels were prepared by dissolving 21g urea in 20ml Milli-Q H_2O, 10ml 30% acrylamide:bis-acrylamide (19:1) and 5ml 10x TBE. When this solution had warmed to room temperature, it was filtered through a 0.22µm syringe filter (Gelman) and polymerisation initiated by the addition of 400µl freshly prepared 10% ammonium persulfate and 37µl TEMED. The gel was allowed to set for 2hr to overnight, then pre-run until it had warmed to 50°C using a temperature probe linked to the power-pack (PowerPac 3000, Bio-Rad) to automatically vary the voltage to maintain this temperature throughout electrophoresis. Alternatively, electrophoresis was performed at 45W constant power.

Samples were prepared by adding 3x STR loading buffer (10mM NaOH, 95% formamide, 0.05% bromophenol blue, 0.05% xylene cyanol) and incubating at 95°C for 2min, then placed on ice before loading 5µl onto the gel. A 24-well sharks-tooth sequencing comb was used to load sets of 24 samples at 10min intervals, with the reactions being loaded in order of size, smallest first. 4 sets of PCR reactions could be loaded, resulting in visualisation of up 96 reactions on one gel.

The bind silane retained the gel firmly on the un-notched plate throughout silver staining, and the gel could only be removed at the end of staining by incubating it in 10% NaOH for 2 hours. An eccentric rotary shaker was used to incubate the sequencing gel and plate with 500ml of solution contained in a large plastic tray (purchased from a gardening centre).

Silver staining

This was performed essentially according to the manufacturers instructions included with a commercial silver stain kit (Bio-Rad) based on the method of Merril *et. al* 1981). Further modifications to this protocol were derived from the manufacturers instructions included with a second commercial silver stain kit designed to detect microsatellite PCR products on sequencing gels (http://www.promega.com/tbs/tmd005/tmd005.html, 1993). Staining was performed identically for both gel types, the only difference being that solution volumes were 100ml for mini-gels and 500ml for sequencing gels. Following fixation, the gels were washed 2x15min in 10% EtOH, then oxidised for 5min in dichromate oxidiser solution, purchased commercially as a 10x stock (Bio-Rad). The gel was then rinsed for 15min in several changes of deionized H_2O until all hint of yellow colouring was gone. It was then incubated for 20min in freshly made 0.1% silver nitrate (Sigma), rinsed for 1min in deionized H_2O and developed in several changes of freshly-made developer solution, consisting of 2% sodium carbonate (Sigma) containing 0.005% formaldehyde. Developer solution was discarded and replaced after it started to turn "smoky-brown" due to the presence of silver precipitate. 3-4 changes were usually required to develop good staining.

Documentation

Silver-stained gels were scanned using the same set-up described previously under Densitometry. It was found that the use of a dampened sheet of white paper applied directly to the gel surface removed bright bubble artifacts in the scanned image.

CHAPTER THREE:
PRIMARY SCREENING

Introduction

Origin of transgenic lines used in this study

A series of some 78 lines of transgenic mice had been generated in our laboratory by micro-injection of linear construct DNA into the pronuclei of fertilised eggs. Eight different constructs were used, in which regulatory elements from the murine insulin-like growth factor II (*Igf-2)* locus and the associated *H19* locus (**Figure 1**) drove expression of the firefly luciferase reporter enzyme (Ward *et al.*, 1997). Each transgenic line represented an independent integration event of one or more copies of the transgene construct at a single position in the genome, as determined by Southern blotting and breeding analysis. Most lines could readily be tested for the presence or absence, but not the copy number, of the transgene by performing a simple luciferase assay on a tail biopsy from one to five day old mice (at which time expression from the P3 promoter driving the luciferase gene was maximal). Those few lines which did not express luciferase at detectable levels in this assay could be genotyped by PCR or Southern blotting.

Nature of the transgene constructs

All eight transgene constructs contained an *Igf-2* P3 promoter region of 153bp attached to the *luc* construct. This consisted of the firefly (*Photinus pyralis*) luciferase-encoding sequence followed by the SV40 small t intron/polyadenylation signal to ensure stability of the mRNA and proper expression of the gene product in mammalian cells (Caricasole & Ward, 1993). While this basic construct displayed minimal levels of expression in transgenic mice, seven of the constructs contained additional sequences from the *Igf-2/H19* region (**Figure 2**) which included enhancers and other regulatory elements which might have a role in the regulation of both genes through genomic imprinting.

Figure 1. The *Igf2* and *H19* loci and surrounding genomic regions

A 100kb region of distal Chr 7 containing the *Igf2* and *H19* gene, with the relevant regions used to make transgene constructs illustrated diagrammatically, along with transcription start sites and CpG dinucleotides which are known to be differentially methylated.

Figure 2. Transgene constructs used in this study

All transgene constructs contain the P3 promoter of *Ifg2* linked to a luciferase reporter gene and a polyadenylation signal derived from SV40 (not shown). With the exception of the minimal construct **M**, all constructs contain various combinations of regulatory regions derived from the *Igf2/H19* gene complex shown in **Figure 1**.

Fig.1

The *Igf2* and *H19* loci and regions used to make transgene constructs

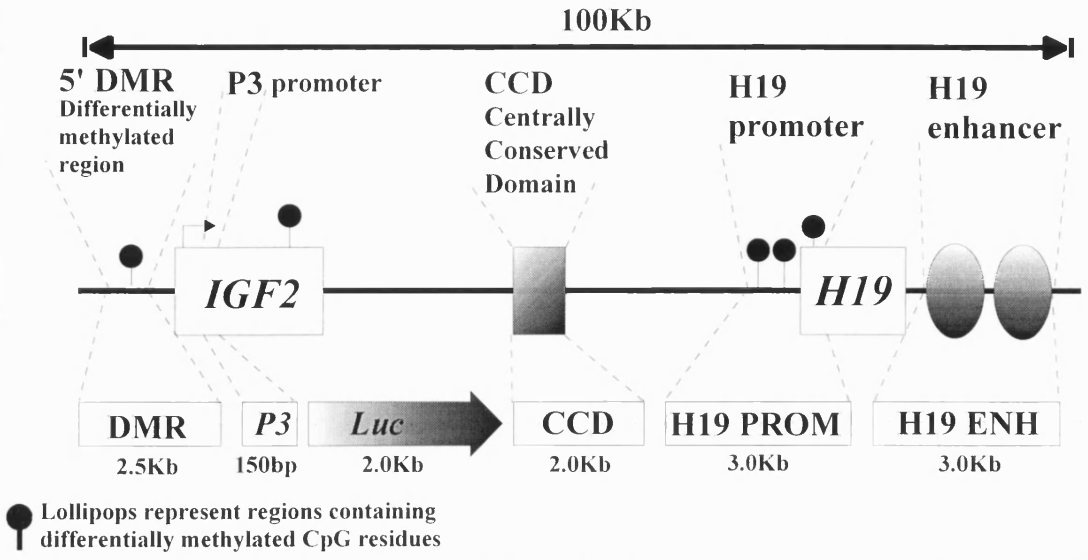

Fig. 2

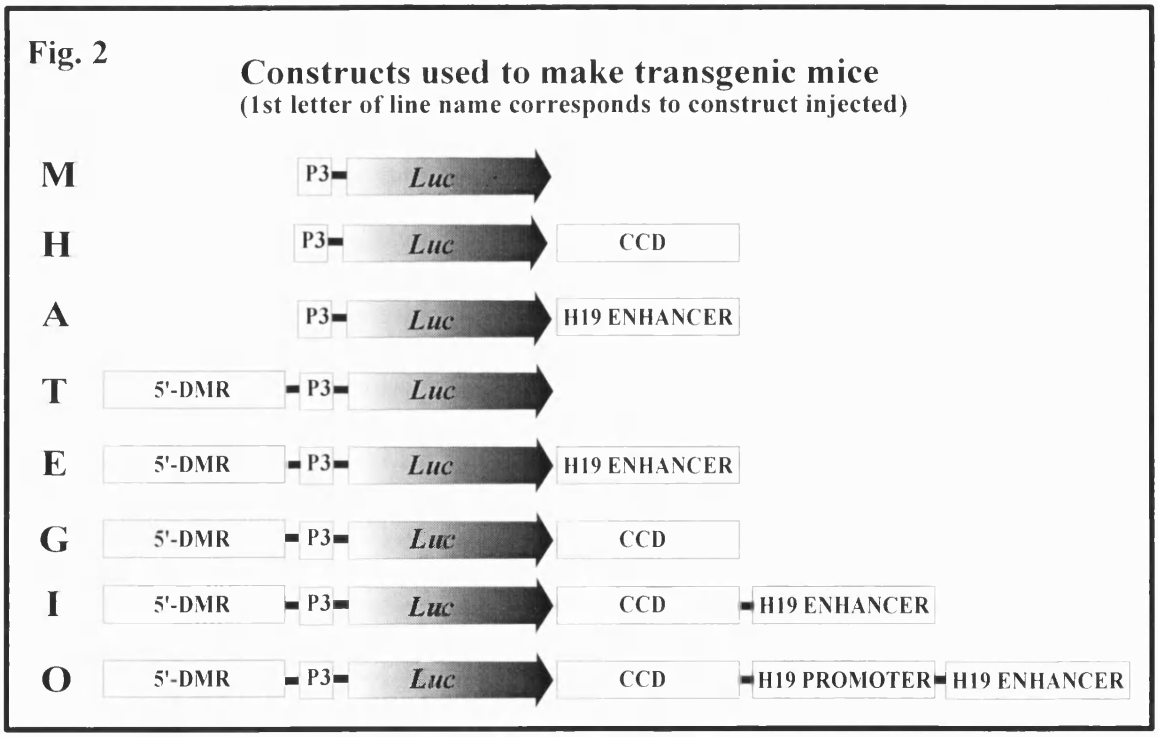

Transgenic line names

The naming convention for transgenic lines was as follows: the construct letter gave the first letter of the line name and the sex of the transgenic founder mouse determines the sex of the name. Thus, **Alicia** is derived from a female founder carrying the '**A**' construct and **Harry** is derived from a male founder carrying the '**H**' construct. Although this scheme did not adhere to the conventions laid down for naming transgenic mice (Lyon *et al.*, 1996), it proved to be highly useful as a mnemonic aid during the course of these studies.

Research aims involving the transgene constructs

The transgene expression analyses form part of ongoing studies in Oxford and Bath, which are not strictly relevant to this project (Ward *et al.*, 1997). Briefly, however, the closely linked *Igf-2/H19* loci are imprinted in mice, with differential allelic expression depending upon paternal or maternal inheritance. The constructs were designed to determine the function of four elements of the *Igf-2/H19* region in isolation from their normal genomic environment. Some of the functions of these elements may depend on *cis* interactions, and it is important to dissect out these regions in order to elucidate their precise behaviour. This is easier to do with injection transgenesis and comparison of multiple transgenic lines carrying different constructs, than with directed mutagenic experiments on the regulatory elements *in situ* in their normal environment. A consequence of these studies has therefore been the generation of a large number of independent transgenic lines.

Screening strategy

During the first stage of the screen a breeding programme was instigated to breed all lines to homozygosity and this is still an ongoing process. This simple screen was designed to detect mutant phenotypes, either by obvious physical or behavioural abnormalities amongst the litters, or by small litter size and absence of homozygotes, as assayed by breeding and Southern blots, which would suggest impairment of development in homozygous embryos. A number of possible mutants were detected by this means.

The screen involved two phases for each line tested: Crossing hemizygous males against hemizygous females to test for homozygous embryonic or peri-natal lethality among their offspring, or for other developmental effects on homozygous pups; and crossing transgenic animals against non-transgenic F1 animals to test for homozygosity in both sexes without obvious phenotype, thus eliminating this line from enquiries and permitting extinction of the line if appropriate. Hemizygous intercrosses are self-explanatory, since 25% of pups should be homozygous for the transgene, allowing for a simple screen for readily detectable phenotypes. The rationale behind the homozygous testing perhaps requires some clarification, however.

In the absence of a simple direct test for hemi- or homozygosity for the transgene (see the introduction to chapter 4 for a more detailed discussion of this problem) a breeding approach was adopted. Clearly, when crossing a transgenic animal against a non-transgenic, a hemizygote should generate equal numers of transgenic and non-transgenic offspring, while a homozygote should generate only transgenics. The question therefore becomes, how many transgenic offspring need be scored without observing any non-transgenic siblings before the parent can be designated homozygous for the transgene? Taking the null hypothesis to be that the (transgenic) parent is hemizygous, for a χ^2 test to have significance, the expected numbers in each class must be at least 5 (Appendix A). At least 10 offspring need to be scored therefore. In fact, if 11 offspring are tested, and all carry the transgene, the likelihood of the transgenic parent being hemizygous is less than one in a thousand (i.e. $P<0.001$), and this was chosen as a cut-off.

Caesarean rederivation

All lines used in this study were originally derived in Oxford. At the time of commencement of this project, it was planned to transfer all or most of the transgenic lines from Oxford to Bath. Unfortunately, stocks in Oxford proved to have been exposed to a variety of common mouse viruses, and it was decided that each line would have to be re-derived by Caesarean section before transfer to the animal house in Bath. Since the viruses do not cross the placental barrier, careful handling procedures during the re-derivation should have resulted in non-

infected litters, which were raised by foster mothers. During this process, a number of developmental abnormalities came to light that might not otherwise have been observed, since still-born or abnormal pups are frequently consumed by the mother, leaving only an apparently healthy litter.

Caveats

It must be pointed out that the screening strategy, whilst having the advantage of simplicity, could easily have missed more subtle phenotypes, or those with variable penetrance or expressivity, particularly with regard to strain-dependent variable expression of mutant genes. A further pitfall was the possibility of spontaneous mutations and their reinforcement in the gene pool by the in-breeding necessitated by this strategy. The possibility of transgene-associated phenotypes appearing in hemizygous animals cannot be ignored, but the wealth of data on knockout mice and transgene insertions support the premise, as a first approximation, that mutations in many genes of developmental importance will only produce a phenotype in a homozygous environment (Copp, 1995). That is to say, a single wild-type allele of the gene can, in most cases, give rise to normal development.

Results

General breeding data

Of the 78 original transgenic lines derived, 16 were bred to homozygosity in both sexes and in sufficient numbers with no observable phenotype (one homozygote of each sex was considered sufficient, unless the ratio of observed homozygotes deviated significantly from the expected 25%). These lines were therefore eliminated (data not shown for 14 of these lines), and 9 lines failed to breed and became extinct (**Andrew, Edmond, Elton, Gloria, Heidi, Irk, Tessa, Theresa** and **Tutu**).

Caesarean re-derivation was performed for the remaining 55 lines, but failed in a number of cases due to the mothers rejecting the fostered litters. A number of abnormalities came to light during Caesarean sectioning, and these,

together with the results of the breeding programme are tabulated below. All homozygous animals were so designated on the basis that they produced at least 11 transgenic offspring (and no non-transgenics) when crossed against non-transgenic animals.

Table 2. Overall results of breeding programme

Transgenic line	Number of animals surviving re-derivation in Bath	Visible mutants observed during Caesarean sections?	Visible mutants observed during breeding to homozygosity?	Viable animals genotyped by breeding against non-transgenic C57/CBA F_1			
				tg/+ ♂	tg/+ ♀	tg/tg ♂	tg/tg ♀
Alicia	2♂ 3♀	NO	NO	8	6	3	1
Amanda	5♂ 2♀	NO	NO	2	4	1	1
Annabella	5♂ 5♀	NO	NO	1	2		
Ann	1♂ 6♀	NO	YES	3			
Antonio	7♂ 4♀	NO	NO	1	4		
Archy	2♂	NO	NO	1	2	1	4
Axe	6♂ 4♀	YES	NO	10	1		1
Ayah	5♂ 7♀	NO	NO	2	6		
Azure	2♂ 3♀	NO	NO	5	2		
Eleanor		NO	NO				
Elvis	4♂ 2♀	NO	NO	5	7		1
Ethel	13♂ 11♀	NO	NO	3	6		1
Eva	10♂ 8♀	YES	NO	7	5	1	2
George	2♂ 4♀	NO	NO	2	13	2	2
Gertrude	14♂ 8♀	NO	YES				
Grace	6♂ 2♀	NO	NO	6	10		1
Graham	3♂ 2♀	NO	NO	2	8	2	1
Gentian	16♂ 18♀	NO	NO	3	11	1	
Hamish	4♂ 6♀	YES	NO	5	3	2	2
Harold	3♂ 7♀	YES	NO	3	4	3	7
Harry	2♂ 3♀	NO	YES				
Helen	5♂ 10♀	NO	NO				
Helga	3♂ 3♀	NO	NO	10	7	1	1
Holly	2♂ 5♀	NO	YES				
Ian	2♂ 11♀	YES	NO	2			
Ibadan	12♂ 11♀	NO	NO	2	4	1	1
Ice	8♂ 6♀	YES	NO				
Id	8♂ 6♀	YES	NO				
If	10♂ 4♀	NO	NO	3	5	1	4
Ill	8♂ 2♀	NO	NO	4			1
In	6♂ 9♀	YES	NO	2	3	1	
Ingrid	8♂ 20♀	YES	NO	2	9		
Isac	7♂ 9♀	NO	NO				
May	8♂ 12♀	NO	NO				
Marcus	7♂ 7♀	NO	NO	1			

Transgenic line	Number of animals surviving re-derivation in Bath	Visible mutants observed during Caesarean sections?	Visible mutants observed during breeding to homozygosity?	Viable animals genotyped by breeding against non-transgenic C57/CBA F_1			
				tg/+ ♂	tg/+ ♀	tg/tg ♂	tg/tg ♀
Oat							
Ob	9♂ 8♀	NO	YES	5			
Oc	5♂ 8♀	YES	NO	4	3		1
Odd	2♂ 5♀	YES	NO		1		1
Of							
Oh							
Oil	17♂ 27♀	YES	NO		7	1	1
Ok	8♂ 11♀	NO	NO				
On	4♂ 4♀	YES	NO				
Open	2♂ 5♀	NO	NO				
Ost	6♂ 10♀	YES	NO				
Oui	5♂ 10♀	NO	NO				
Ovid	11♂ 4♀	NO	NO	3		2	
Owl	5♂ 3♀	YES	NO	3		1	1
Tarquin	13♂ 8♀	NO	NO			1	
Tiberius	0	NO	YES				
Tilly	4♂ 4♀	NO	NO	3	1	2	
Tim	8♂ 16♀	NO	NO				
Titus	9♂ 9♀	NO	NO	8	2		2
Tracy	8♂ 3♀	NO	NO		3	2	2

Table 3. Defects observed in embryos during Caesarean sectioning

Line	Defect
Hamish	2 exencephalies
Harold	1 exencephaly
Ian	1 exencephaly, 2 omphalocoel, 1 "puffer" - fluid-filled thoracic region and pale appearance
Ice	1 "thalidomide" - stunted limbs
Id	1 thalidomide
In	1 hindleg deformity
Ingrid	1 thalidomide
Oc	1 hindlimb deformity - "paddle limb"
Odd	1 hindlimb deformity - "flipper foot"
Oil	1 hunchback - poss. lumbo-sacral spina bifida
On	1 "puffer"
Owl	1 "puffer"

Table 4. Mutants observed during breeding

Line	Defect
Ann	Poss. neurological defect - progressive paralysis and death by 3-6 weeks
Axe	1 craniofacial defect - lower jaw severely affected
Eva	2 "big-skulls" - grossly expanded crania
Hamish	poss. sex ratio distortion - low numbers of females
Harry	"piebald" runts
Holly	blind mice - opaque corneas
Ob	male sterile
Owl	poss. sex ratio distortion - low numbers of females
Tiberius	very poor breeder - poss. hemizygous phenotype, all transgenics "less robust"

Harry

During early hemizygous intercrosses in Oxford (to raise stock for Caesarean re-derivation), **Harry** produced a litter of nine still-borns, seven of which appeared normal and may have been abandoned. The remaining two showed extreme ventral curvature, small size and highly abnormal skin texture and colour (**Figure 3**). Luciferase assays on the dead litter (**Table 5**) showed that both the abnormal pups were transgenic, although they showed extremely low luciferase activity compared to their transgenic littermates. This could be because the mutants had been dead for considerably longer than their siblings and the enzyme activity had started to degrade.

Table 5. Luciferase assays on still-born Harry litter born 5/12/95

Line	Parents	Date of birth	Animal number	Luciferase counts (RLU)	Genotype + = transgenic - = non-transgenic	Phenotype
Harry	8864♂ x 8♀	5/12/95	1	114 124	+	mut
			2	2940 2801	+	mut
			3	24661 22825	+	wt
			4	73 65	-	wt
			5	42851 43527	+	wt
			6	28663 33833	+	wt
			7	27075 27233	+	wt
			8	89 72	-	wt
			9	13556 13992	+	wt
			background	72 70		wt

Holly

During breeding in Oxford (again, to raise stocks for re-derivation), it was observed that **Holly** consistently gave small litters, which were frequently consumed shortly after birth, or occasionally found dead in the cage. Whether neonatal death occurred through phenotypic abnormality or through being abandoned by the mother was indeterminate. All the transgenic pups derived by

Figure 3. Still-born Harry mutants

Two presumptive mutant animals (centre and right) from a litter of nine, all found dead on the day of birth. A wild-type littermate is shown for comparison (left). Both mutants were transgenic, and showed extreme ventral curvature and highly abnormal skin texture.

Figure 4. Wild-type and Eva mutant skulls

a) Alizarin red/alcian blue preparation of a 4-week old skull from a wild-type mouse. In this preparation, bone is red, cartilage is blue.
b) Skull from a 4-week old transgenic animal from a hemizygous Eva intercross, showing marked cranial expansion. This is a composite of two photographs, due to the size of the specimen.

Figure 3

Figure 4a

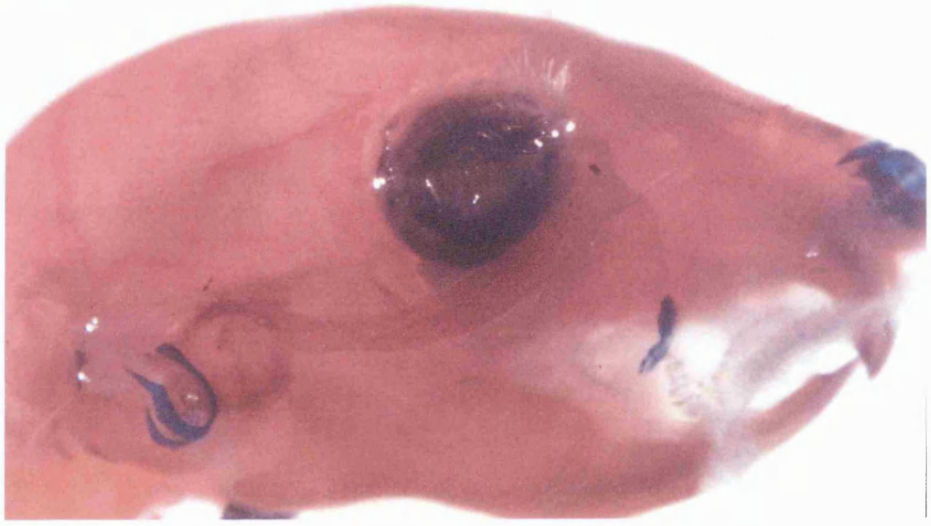

Figure 4b

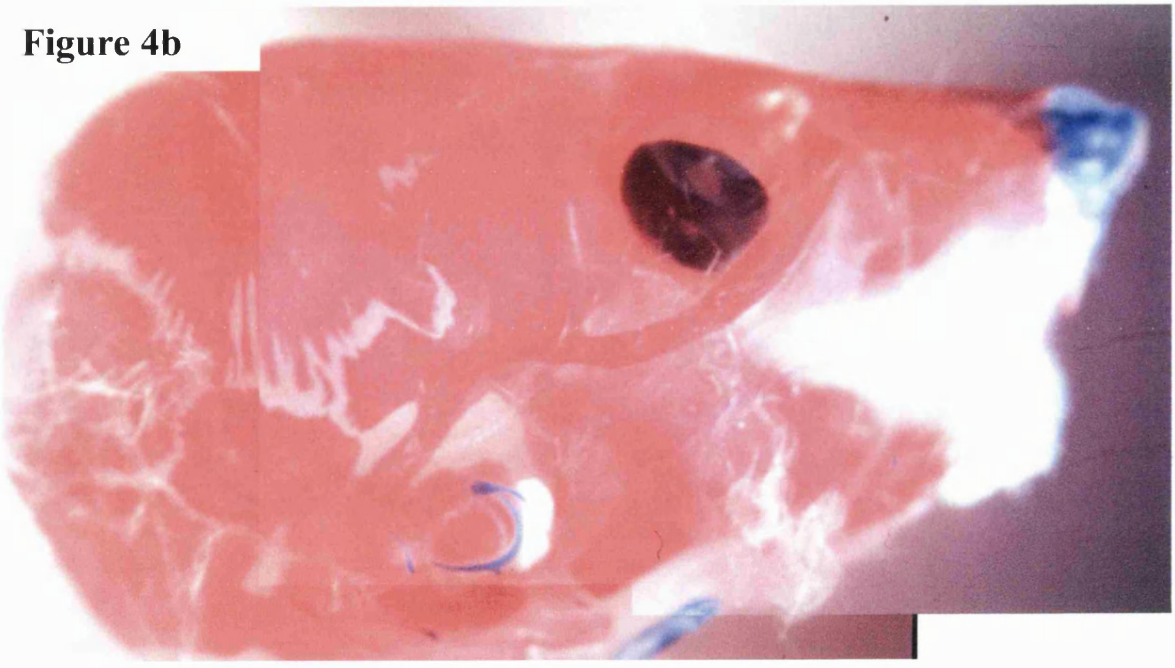

Caesarean from a single hemizygous intercross of the **Holly** line appeared normal at the time of birth. By about two weeks of age, three of the transgenic animals displayed distinct opacity of the corneas, which worsened with age.

Other possible insertional mutants observed

All hemizygous animals appeared phenotypically normal, with the possible exception of **Tiberius,** which showed consistently small litter sizes even when bred against non-transgenic animals, (and which subsequently failed to breed and became extinct) and **Archy**, which produced a large number of runts during breeding against non-transgenic animals.

2 lines had previously been found to display an abnormal recessive phenotype: **Gertrude** and **Ann**.

Ann mutant mice were relatively inactive, and when resting, lie on their sides rather than their bellies. They showed weight loss from around twelve days post-partum, together with tremors and kyphosis (hunched spinal posture). Paralysis increased until the mice died at 3-6 weeks of age.

Gertrude mutant mice appeared normal at birth but typically died 7-10 days after birth (although one or two survived for some weeks), at which time they weighed 30-40% less than their siblings. They appeared to feed normally, since their stomachs contain milk whenever this has been examined.

Both of these mutations have formed the focus of parallel investigation in our laboratory.

The **Hamish** line gave rise to one "wobbler" mouse, which showed a markedly awkward gait. This could have resulted from careless handling during sectioning, but may also reflect a skeletal or neurological defect.

An **Eva** hemizygous intercross gave rise to two pups with markedly enlarged crania, which were both transgenic. These were killed at about four weeks of age, and alizarin/alcian red skeletal preparations made, with calcified bone stained red and cartilage blue. **Figure 4** shows one of these skulls with a normal skull for comparison. The highly visible cranial sutures (white) perhaps suggest intracranial pressure as a causal factor, rather than overproliferation of

the skull plates. No further such mutants were observed during subsequent breeding of this line, however.

Possible Neural tube defects

Many of the sporadic abnormalities observed during Caesarean sectioning appeared to fall into distinct classes which are observed across multiple lines. These are tabulated in more detail in Table 3, but can be summarised as follows:

Limb deformity (fused digits, stunted or absent fore-limbs): **In, Ice, Ingrid, Id, Oc** and **Odd**.

Fluid-filled thoracic cavity ("Puffer" mutants): **Owl, Ian, On**.

Exencephaly: **Ian, Harold, Hamish**

It is notable that all of these defects, and the omphalocoele and sacro-lumbar defects observed in **Ian, Oil** and **Ost** could be considered to fall within the gamut of neural tube defects (NTD), caused by failure of the neural tube to close at various sites along its length. While there is clear precedent for failure of neural tube closure as a cause of exencephaly, limb defects, omphalocoele and lower spinal defects, the thoracic oedema observed in some animals is perhaps worth discussing in more detail: Neural crest cells which migrate along the sixth aortic arch colonise the cardiac outflow tract. If this were to be disrupted by failure of the neural tube to close in the region of origin of this group of neural crest cells, this might lead to defects in cardiac outflow septation (truncus arteriosus) and oedema into the thoracic cavity. This would also help to explain the pale appearance of these mice, which had presumably lost most of their blood supply into the thoracic cavity. A similar oedematous phenotype is known to occur with variable penetrance in a mouse model for neural tube defects, the *sp* (Splotch) mutant which is deficient for the transcription factor Pax3 (Conway *et al.*, 1997a; Conway *et al.*, 1997b). However, in the sixth branchial arch, the Pax3 deficiency affects the migration of neural crest cells (via modulation of the extracellular matrix) rather than neural tube closure (Henderson *et al.*, 1997). It is highly questionable whether failure to close the neural tube would affect the migration of trunk neural crest cells in this fashion.

Discussion

Further lines of investigation

The mutant phenotype observed in some Harry animals was highly visible and characteristic, and this line was selected for further investigation. Chapters 4-8 cover this work in more detail.

However, the very visibility of a mutant phenotype can be a drawback, as this might prove to be a mutant allele of an already well-characterised locus. In a 1992 review of 23 visible, viable insertional mutations in transgenic mice, it was notable that 13 of them proved to be at known loci (Meisler, 1992).

It was decided that, rather than focus entirely on one line, which might well prove to harbour an uninformative mutation in a known gene, a second mutant line would be at least partially characterised. The phenotype observed in Holly suggested itself as an interesting line to pursue, and Chapters 9-13 detail the results of this parallel investigation.

Gertrude and Ann

The recessive phenotype displayed in **Ann**, while not forming part of this work, have been shown during the course of parallel investigations in our laboratory to be associated with the transgene and fully penetrant (D. Paisley, personal communication) and therefore can be considered as bona fide transgene insertional mutations. The phenotype observed in **Gertrude**, on the other hand was found not to be reproducible during subsequent breeding.

Other possible mutants

A number of lines showed small litter sizes in hemizygous intercrosses, with some giving birth to runts or transgenic still-borns, and these are being actively pursued through breeding to homozygosity (**Annabella, Archy, Eleanor, Ill, Oui, On**). It is possible that some of these lines have insertional events which cause foetal death in early or mid-gestation, giving rise to small litters, and this could be investigated by sacrificing mothers from hemizygous intercrosses and examining embryos *in utero* at earlier stages,

In addition, two lines showed possible sex ratio distortion throughout multiple litters, with **Owl** lacking males, and **Hamish** lacking females. This might represent conditional male or female lethality.

Ob, whilst not showing any sex ratio distortion, appears to harbour a transgene-associated recessive trait causing male sterility - homozygous males plug females but have consistently failed to impregnate them. This is now being investigated in our laboratory, and may be a defect in spermatogenesis.

Tiberius failed to produce any litters from hemizygous intercrosses, and even crosses between transgenic animals and F_1 non-transgenics produced small litters. It had been previously observed that the **Tiberius** line had been a generally poor breeder, with physically less robust animals, since its inception some years ago (L.Richardson, personal communication). This may reflect an insertional event which produced a phenotype in hemizygous animals. **Tiberius** was not established in Bath and subsequently became extinct in Oxford through poor breeding.

Neural tube defects

Since some of the defects appeared remarkably similar in different transgenic lines, with presumptive different integration sites for the same construct, it is tempting to speculate that the phenotypic effects were caused by the transgene construct itself, rather than by an insertional effect on the host genome. Within this context, it is of interest to note that the constructs used to make the lines (**H, I** and **O**) in which these NTDs were observed all contain the centrally conserved domain (CCD), which has been proposed as the putative mesoderm-specific enhancer for the *Igf2* locus (Koide *et al.*, 1994; Ward *et al.*, 1997). Given that the notochord and somites are of mesodermal origin, it is possible that the constructs containing the CCD are highly expressed during development in these regions, and that this might, in some cases, perturb neural tube formation. The mechanisms of neural tube closure are very poorly understood, but it is clear that it is a multifactorial process which is exquisitely sensitive to perturbation (Copp, 1994).

A further intriguing possibility is that, although the original investigators found no evidence for any transcripts deriving from the CCD, work in our laboratory has recently located a putative open reading frame (M. Charalambous, personal communication) at the 3′ end. The CCD, and by implication those transgene constructs containing it, might therefore encode a functional RNA or protein. Multiple exogenous copies of such a molecule might conceivably have a dose-dependent effect upon tissues in which the endogenous gene acts.

A final putative mechanism by which CCD-bearing transgene constructs might exert an effect upon tissues of mesodermal origin lies in the CCD's suggested enhancer function: The CCD was originally identified as a DNAseI-hypersensitive region, which implies exposed chromatin, and possibly bound transcription factors and other ancillary proteins. It is possible that multiple exogenous copies of the CCD might also bind such transcription factors and "mop them up", thus perturbing normal gene expression in certain tissues.

While these phenotypic effects are likely to be independent of the insertional mutagenic events which are the focus of this project, the mechanism by which a putative *cis*-acting regulatory element linked to a luciferase reporter gene construct could produce neural tube defects is of considerable interest, and may be worth pursuing at some point in the future. One starting point might be to study the expression patterns of the various constructs in the mouse embryo at the time of neural tube closure, paying particular attention to differences in expression between constructs with and without the CCD. It might also prove interesting to look for correlations between the lines most affected and the copy-number of the transgene or its expression levels in these lines.

CHAPTER FOUR:
HARRY - INITIAL CHARACTERISATION OF THE PHENOTYPE

Introduction

As discussed in the previous chapter, during primary screening an initial hemizygous intercross using **Harry** mice generated two abnormal pups in a single litter of nine - a frequency consistent with a recessive mutant phenotype. Following Caesarean re-derivation and establishment of the **Harry** line in Bath, further hemizygous intercrosses were therefore set up with three initial aims: Firstly, to see if the phenotype was reproducible, recessive and fully penetrant. Secondly, to characterise the phenotype itself at a gross level with a view towards assigning candidate loci, should such exist. Thirdly, and vitally, to ensure that the phenotype truly was associated with the transgene i.e. that the transgene insertion site was genetically linked to the phenotype.

The first two objectives are self-evident - was the initial observation merely a fluke event, or was there a consistent recessive mutant trait present in the **Harry** transgenic line? If so, what was the nature of this trait?

The last objective is a little more subtle - due to space considerations when keeping 78 lines of transgenic mice, many of the lines in Oxford were propagated and maintained by inbreeding a very small population of mice. Referring back to Table 2, it should be noted that all **Harry** mice established in Bath are descended from only 2 males and 3 females which survived Caesarean re-derivation. All of the transgenic lines in this study could be considered to have been through at least one population bottleneck (not to mention the bottleneck necessarily incurred when deriving a transgenic line from a single founder mouse). Clearly, spontaneous mutations do occur at normal frequencies, and subsequent inbreeding can easily reinforce a mutant trait in a transgenic line. If the five **Harry** animals re-derived in Bath came from a single cross, 50% (or more) of them could conceivably have been heterozygous carriers of a mutant allele which had nothing to do with the transgene insertion.

Determining linkage between transgene and phenotype

There can be said to be two basic approaches to determining whether a mutant trait is associated with the transgene, one direct and one statistical. Both are predicated on the assumption that the mutant trait is fully recessive. The direct approach relies on being able to unambiguously detect animals homozygous for the transgene - if this is possible, then it becomes simply a matter of asking whether all observed mutants are homozygotes (linkage) and whether all homozygotes display the phenotype (penetrance).

Direct identification of homozygotes

There were a number of possible approaches to this problem:

Reporter specific activity: The luciferase reporter gene activity in the transgene constructs could be quantitatively measured in a luminometric assay, and such measurements could be converted into specific enzyme activity by measuring protein levels in the sample and dividing luciferase counts by protein concentration. In theory, comparison of specific activity levels within a litter from a hemizygous intercross would allow identification of homozygotes. This method has been successfully used in E13 embryos in transgenic mice expressing a different luciferase reporter construct (Depierreux *et al.*, 1997). During pilot studies in our laboratory however, it was found, at least in our hands, that the specific activities obtained by this method varied too widely to permit such identification (data not shown).

Breeding: If the mutant animals were viable and fertile, they could be crossed with non-transgenic animals. Clearly, if no non-transgenic offspring are observed among a statistically significant number of transgenics, the mutant parent is likely to be homozygous for the transgene. This approach was successfully used in many lines during primary screening to determine homozygosity in the absence of a phenotype (see Table 2). Unfortunately, all **Harry** mutants died before reaching breeding age (see Results).

Southern blotting: Using a transgene-specific fragment to probe a Southern blot of genomic DNA from a full hemizygous intercross litter (containing mutants and wild-type transgenics), densitometric measurements could be made from the X-ray film. Such measurements need to be divided by

parallel results obtained from a probe which hybridises to an endogenous gene, to control for variation in the amount of genomic DNA loaded in each lane. The ratio of these two measurements gives a "specific activity" for the amount of transgene present - homozygotes should be double the level of hemizygotes.

FISH: If metaphase chromosome spreads were made from all transgenic animals in a hemizygous intercross litter, these could then be probed with a transgene-specific probe. Homozygotes should give a signal on two separate chromosomes, hemizygotes on only one. This approach was viewed as a "last resort", as it was deemed to be very labour intensive and technically demanding. If a single animal in the litter failed to give chromosome spreads, then the experiment became partially invalid, since one could not then be absolutely sure of full linkage or penetrance. Alternatives were therefore explored initially.

It is also possible to perform FISH on interphase nuclei,usually on the white blood cells from a simple blood smear (Paris *et al.*, 1996). This was attractive because it is much less labour intensive than splenocyte culture and making metaphase spreads. Furthermore, only a drop of blood from each animal is required, so multiple attempts at genotyping can be undertaken.

Unfortunately, pilot experiments were not encouraging, due to high background and absence of convincing signals from the interphase nuclei (data not shown) and this approach was abandoned.

In the presence of high background, FISH on metaphase chromosome spreads has the advantage of being unambiguous - a "true" hybridisation signal can be distinguished from non-specific fluorescent spots by the presence of pairs of twin spots on replicated sister chromatids.

An intermediate approach which offers the advantages of both of the methods discussed above is to make metaphase spreads from lymphocytes cultured from blood. A published protocol used only 35-75μl of blood from a tail bleed to culture enough peripheral lymphocytes to make good metaphase spreads (Shi *et al.*, 1994). This offers the resolution and discrimination of FISH performed on chromosome spreads, combined with the fact that the test animal stays alive and the experiment can be repeated. However, during pilot studies (see

Methods), the lymphocytes failed to proliferate in culture and this method was abandoned (data not shown).

A modified protocol was attempted, in which the mouse was sacrificed, completely exsanguinated to extract 2-4ml of blood and lymphocytes were partially purified by density centrifugation on a Ficoll gradient (McFee *et al.*, 1997). This method, too, failed to yield any chromosome spreads from mouse, although it was found to work very well with human blood. This reflects the experience of others (M. Lee, pers. comm.) in that culture conditions optimised for human lymphocytes or particular strains of mouse do not necessarily work well with all mice.

Another approach to making metaphase chromosome spreads utilised embryonic fibroblasts (Evans, 1987; Evans, 1994). These were derived from E12-E14 embryos (see Methods) and had the advantage that the cells could be frozen down and stored in liquid nitrogen for repeat experiments, but the distinct disadvantage that no obvious mutant phenotype could be discerned at this time, hence no correlation could be made between homozygosity for the transgene and phenotype. This method was found to yield good metaphase spreads, albeit at low frequency, but was abandoned in favour of the splenocyte culture method.

Overall, the splenocyte culture method for making metaphase chromosome spreads was found to be the most reliable and this was used to generate spreads for all FISH experiments shown in this work.

Linkage by statistical analysis

The null hypothesis was taken to be that there was no association between the transgene and mutants i.e. that the two traits were independently segregating alleles. The transgene is a "dominant" trait (since hemizygotes and homozygotes cannot be distinguished and are merely 'transgenic') and the mutant trait was assumed to be recessive. A hemizygous intercross therefore has a genotype of (Tg/+, M/m) x (Tg/+, M/m) where Tg represents the transgene and 'M' and 'm' are wild-type and mutant alleles of some independent locus. By Mendelian genetics, and assuming no linkage, this gives expected frequencies of:

9/16 wild-type transgenic	(Tg/Tg, M/M; Tg/Tg, M/m; Tg/+, M/M; Tg/+, M/m)
3/16 mutant transgenic	(Tg/+, m/m)
3/16 wild-type non-transgenic	(+/+, M/M)
1/16 mutant non-transgenic.	(+/+,m/m)

Providing sufficient animals from hemizygous intercrosses are genotyped, a simple χ^2 test (see Appendix A) can be applied to see whether the null hypothesis can be rejected or not. Expected numbers for each class in a χ^2 test must be 5 or greater. Since the smallest class (mutant non-transgenics) represents only $1/16^{th}$ of the population, this approach required that at least 80 animals from hemizygous intercrosses were bred and genotyped for the transgene.

During the time required to breed and collect this amount of data, the more direct molecular approaches discussed above were also attempted.

Results

Gross phenotype

Following Caesarean re-derivation in Bath, hemizygous intercrosses were set up and throughout four subsequent generations to date, mutant animals have emerged from these at frequencies consistent with a recessive trait. Although appearing normal at the time of birth, the mutants showed significant retardation in both growth and the onset of fur growth, hence the mutant shown in **Figure 5** was completely nude at a time when its sibling possessed a full coat of fur. They frequently had a thin, malnourished appearance and distended abdomens.

The mutants also displayed limited skin pigmentation with occasional well-demarcated patches at the head and rear quarters of the animal, and when the fur did eventually grow, this pattern of pigmentation was reflected therein. **Figure 6** shows a full intercross litter with an unusually large number of mutants, displaying variegated patterns of coat spotting. Animal #5 has a clear patch of pigmentation in the mid dorsal region and this was found to occur at lower frequency than spotting at the head and rump. Ventral pigmentation was always entirely absent. Coat pigmentation in all mutants to date has been black i.e.

Figure 5. 10-day old Harry littermates

One mutant and one wild-type animal at 10 days post-partum, derived from an early hemizygous intercross. The smaller animal entirely lacked pigmentation, had very little fur and was clearly debilitated in appearance and movement.

Figure 6. Full Harry intercross litter

A full litter from a hemizygous intercross, culled at 8 days of age, with an unusually large number of mutants. Non-transgenics are indicated by a "-" symbol after the animal's number, transgenics by a "+" symbol.

Figure 5

Figure 6

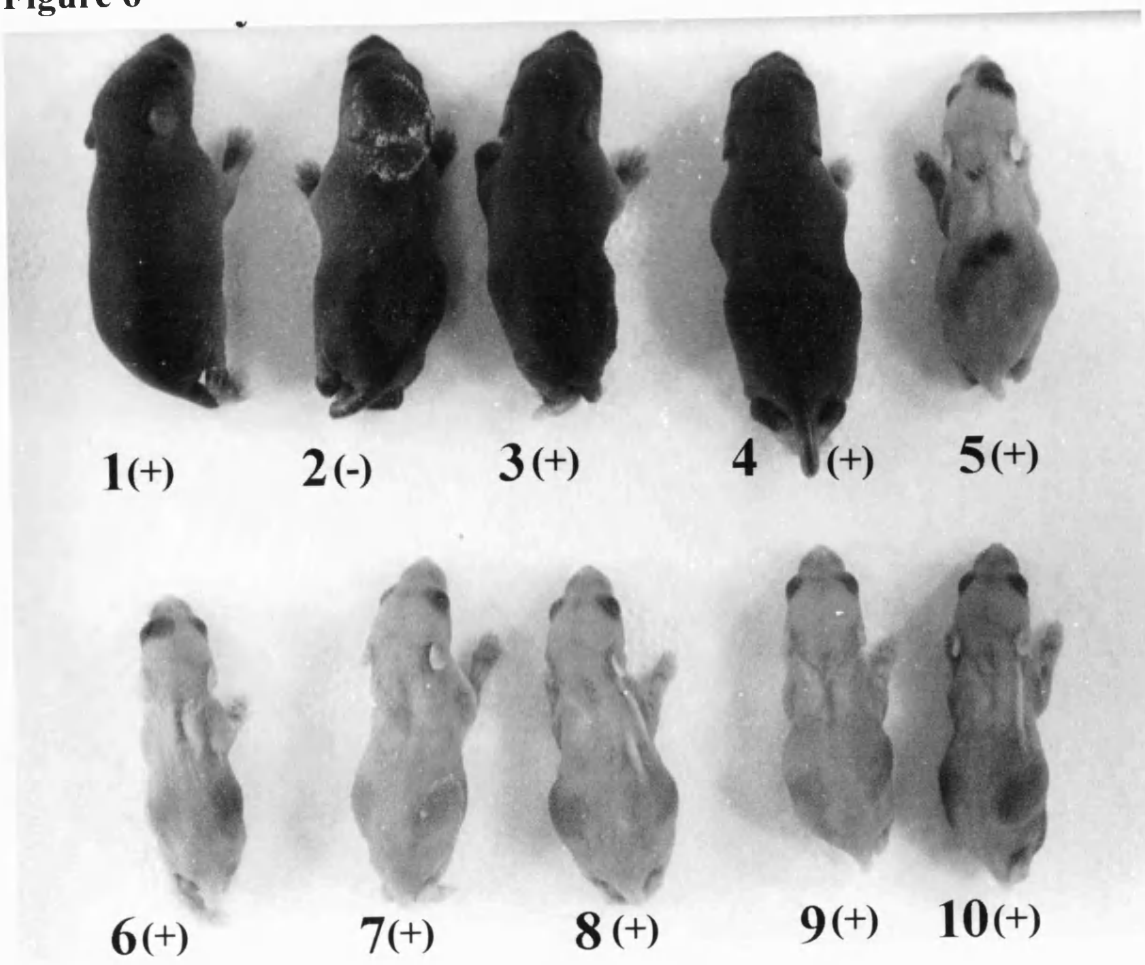

C57BL/6 in nature, rather than the dominant brown (agouti) colour of the CBA background present in these crosses..

Most mutants either died or were killed before day 14, but all those allowed to live have so far died within four weeks with grossly distended abdomens. On dissection, the entire intestinal tract, apart from a small variable region of the colon, was usually found to be distended and full of liquid faecal material. This was suggestive of a blockage in the distal colon.

During subsequent intercrosses, it was observed that the degree of coat spotting was loosely correlated to growth retardation and time of death: Smaller animals tended to have less fur growth and skin pigmentation, more distended abdomens, and tended to die sooner, some by as early as day 6 post-partum. Larger animals lasted longer and tended to have more coat colouring. **Figure 7** shows two age-matched mutants from separate crosses (i.e. different parents) each with a respective wild-type sibling for size comparison (the wild-type animals were all roughly the same size within each litter). The lateral and dorsal views show the different degrees of coat spotting. It will be noted that the larger mutant has more coat spotting. Wild-type animals could be black or brown in coat colour, with brown the dominant colour, as predicted. Mutant animals were invariably black in colour when pigmented patches were present.

A single intercross litter produced 6 pups, two of which were fully wild-type, two mutants with very limited skin pigmentation and two apparently wild-type animals, which upon closer inspection both had small white belly spots. They were otherwise fully normal, and both were transgenic (presumed hemizygote). These were the only such animals observed in more than 200 "wild-type" transgenic animals from hemizygous intercrosses.

Association between transgene and phenotype

As mentioned in the introduction, a number of possible approaches to this problem were attempted, with statistical breeding analysis, densitometric analysis of Southern blots and FISH analysis of metapase chromosome spreads from splenocyte cultures being the avenues pursued in most detail.

Figure 7. Variation in coat spotting in Harry mutants

a) 10-day old **Harry** mutant with wild-type sibling for comparison

b) 11-day old **Harry** mutant with wild-type sibling for comparison

c) Dorsal view of both mutants. The older mutant is considerably smaller and shows much less coat spotting.

d) Lateral view of both mutants.

Figure 8. Transgene genotyping by Southern blotting and densitometry

a) Scanned autoradiogram showing digested genomic DNA from a full **Harry** hemizygous intercross litter which has been Southern blotted and simultaneously hybridised with two probes, generating an endogenous band (DMR probe) and a transgene-specific band (Luc probe). Transgenic status (by luciferase assay) is shown above each sample. #1 was a mutant animal, and the remaining 6 were wild-type.

b) Profile plots of the intensities of the endogenous and transgene-specific bands, showing numerical values derived by integrating the area under each peak.

Figure 7

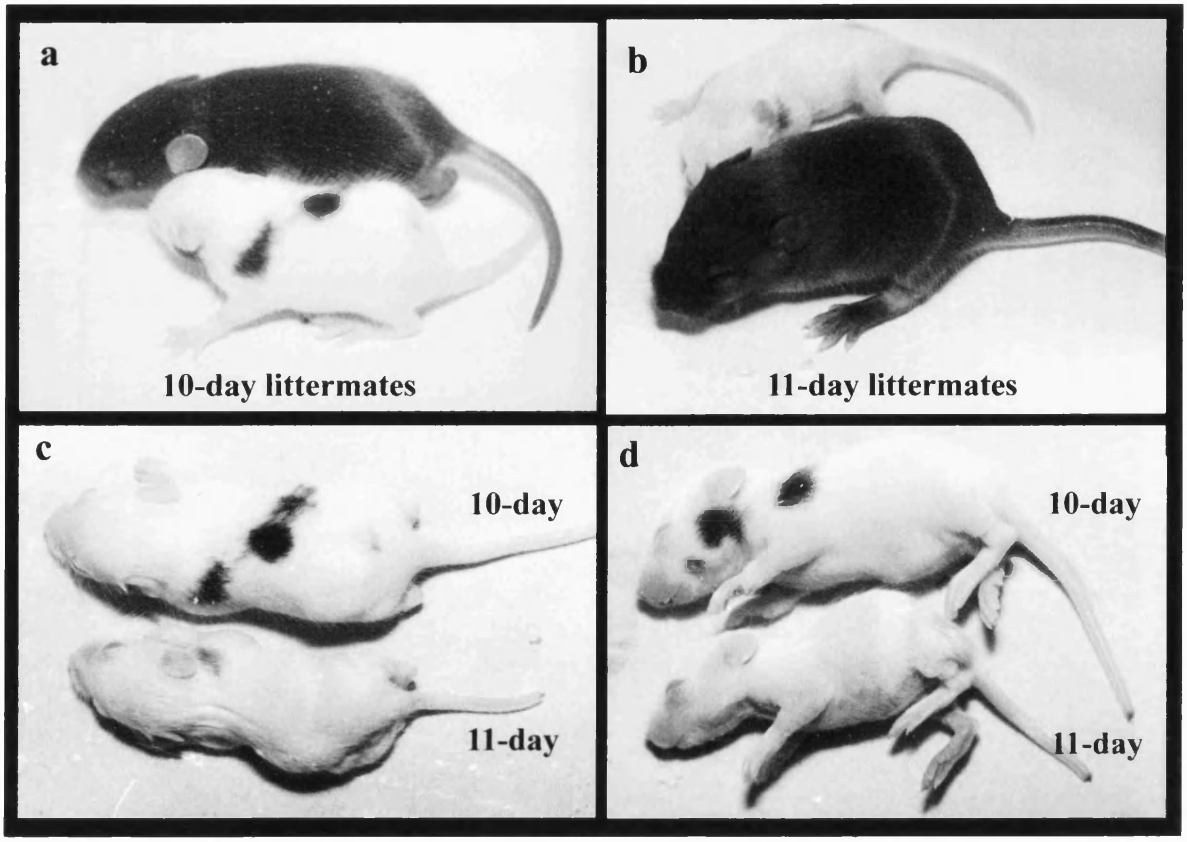

Figure 8 a

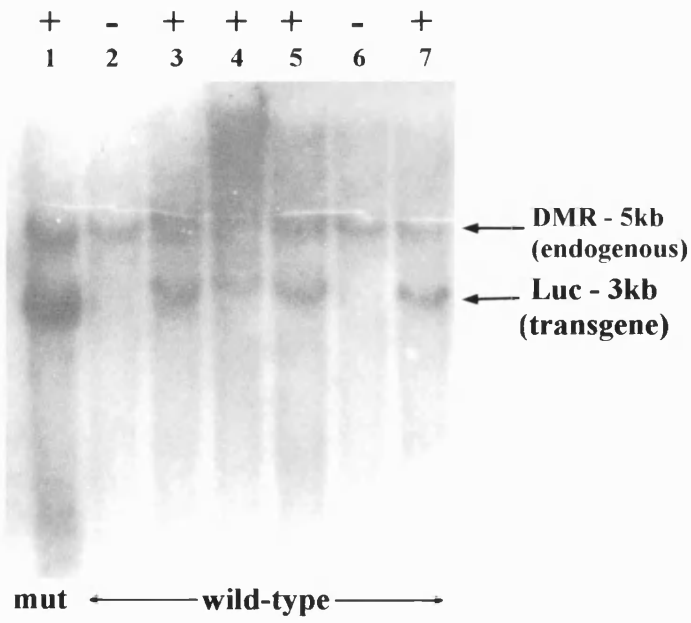

b

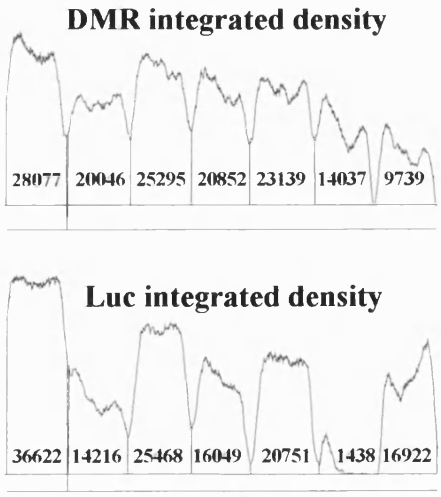

Association by statistical analysis

Taking the null hypothesis to be that the transgene and the fully recessive mutant trait are at independently segregating loci, in a doubly heterozygous intercross, this gives a predicted Mendelian distribution of 9/16 transgenic wild-type, 3/16 transgenic mutant, 3/16 non-transgenic wild-type and 1/16 non-transgenic mutant. Data for 223 **Harry** pups from hemizygous intercrosses can be summarised into a 2x2 contingency table:

Table 6 Collated breeding data from multiple Harry intercrosses

	wild-type	**mutant**	Σ
transgenic	124 (125.4)	52 (41.8)	176
non-transgenic	47 (41.8)	0 (13.9)	47
Σ	171	52	
Overall Σ = 223			

Expected values are given in brackets below each observed value. Using the formula given in Appendix A, this gives

$\chi^2 = 16.5$

and for 1 degree of freedom this gives $P < 0.0001$

This means that the null hypothesis can be rejected with a 99.9% confidence limit, or to put it another way: that the data obtained would be expected to occur at a frequency of less than 0.01% if the transgene and mutant locus were not linked.

Association by Southern blotting analysis

Figure 8 shows a scanned autoradiogram of a Southern blot probed with a transgene-specific and an endogenous probe (the probes corresponded to the regions marked DMR and Luc indicated on **Figure 1**) and the densitometric values obtained from the scanned image by integrating the area under each peak. **Table 7** below shows the numerical values obtained from the scanned film, together with subsequent numerical analysis and correlation with genotype.

Table 7. Densitometric analysis of Southern blotted DNA from a single Harry hemizygous intercross litter.

Animal	Phenotype	Transgene (from luciferase assay)	Luc integrated density	DMR integrated density	Luc/DMR ratio	Possible genotype
1	Mut	+	36622	28077	1.30	+/+ ?
2	Wt	-	14216	20046	0.71	-/-
3	Wt	+	25468	25295	1.00	+/-
4	Wt	+	16049	20852	0.77	+/-
5	Wt	+	20751	23139	0.90	+/-
6	Wt	-	1438	14037	0.10	-/-
7	Wt	+	16922	9739	1.74	+/+?

To casual inspection, the transgene signal in lane 1 appears to be strongest, and since this was the only mutant in the litter, this might support the conclusion that it was also the only homozygote. Indeed, taking the Luc/DMR value (the ratio of the respective integrated density measurements) as a measure of the copy number of the transgene, lane 1 (the mutant) has a higher Luc/DMR than lanes 3,4, and 5, suggesting that it is a homozygote. However, lane 7 has the highest value of all, and this animal was wild-type. Furthermore, lane 2 has a value of 0.71, which is close to the value for lane 4 (0.77), a wild-type transgenic. Since lane 2 is clearly non-transgenic, this quantitative analysis has to be treated with a degree of suspicion. Lane 6 is also non-transgenic and has a Luc/DMR ratio of 0.10, some seven times lower than that seen in lane 2. The variation in background levels makes it impossible to subtract background and normalise the ratios. Analyses of other Southern blots have proved equally ambiguous.

Association by FISH analysis

A full litter consisting of 7 pups from a hemizygous intercross was tested for the transgene by luciferase assay (data not shown). There were no non-transgenics in this litter. 3 of the pups showed a clear mutant phenotype at 6 days of age, and all were culled and chromosome spreads prepared from each individual. These therefore comprised 3 mutants and 4 wild-types. The spreads

were then hybridised with the "H" construct - a probe specific for the transgene. FISH analysis clearly showed that all 3 mutants were homozygous, and all 4 wild-type transgenics were hemizygous (**Figure 9**).

Discussion

Harry transgenic mice carry a transgene-associated mutant trait

The **Harry** transgenic line showed a clear, reproducible mutant phenotype manifest in the progeny of hemizygous intercrosses at a frequency consistent with a recessive trait. The statistical analysis clearly showed tight genetic linkage between this mutant locus and the transgene.

The FISH analysis confirmed this linkage, and suggested full penetrance of the recessive phenotype in that all 3 homozygotes displayed a mutant phenotype.

While FISH analysis alone provided good evidence for linkage in this case, it should be borne in mind that the protocol proved to be technically demanding and that FISH genotyping was not working reliably during the early phases of this project. (With reference to the methods detailed in chapter 2, it will be noted that for efficient proliferation of splenocytes in culture, spleens from multiple animals needed to be pooled. This was clearly impossible in the genotyping of single animals, and the number and quality of spreads from some of the animals in the genotyped litter were very low.) Pending a working direct molecular approach, statistical analysis of breeding data was opted for because it offered a time-consuming but reliable method of establishing linkage.

Densitometric analysis of Southern blots proved an unreliable measure of transgene copy number. Two factors might have had a bearing upon this:

Firstly, the loading of genomic DNA in the tracks was uneven. Although spectrophotometric assay of the DNA samples was impossible due to the presence of varying amounts of contaminating protein, if a fluorimeter had been available, it might have been possible to accurately measure DNA concentration in these samples and hence achieve equal loadings on the Southerns.

Figure 9. Harry genotyping by FISH analysis

Metaphase chromosome spreads from all 7 transgenic animals from a **Harry** hemizygous intercross. Spreads were hybridised with a transgene-specific probe (red) and counterstained with DAPI (cyan).

a), b) and c) Mutant animals. Two transgene signals can be discerned for each (arrows), and these are all therefore homozygous (+/+)

d), e), f) and g). Wild-type animals. One transgene signal can be discerned for each (arrows), and these are all therefore hemizygous (+/-)

Figure 9

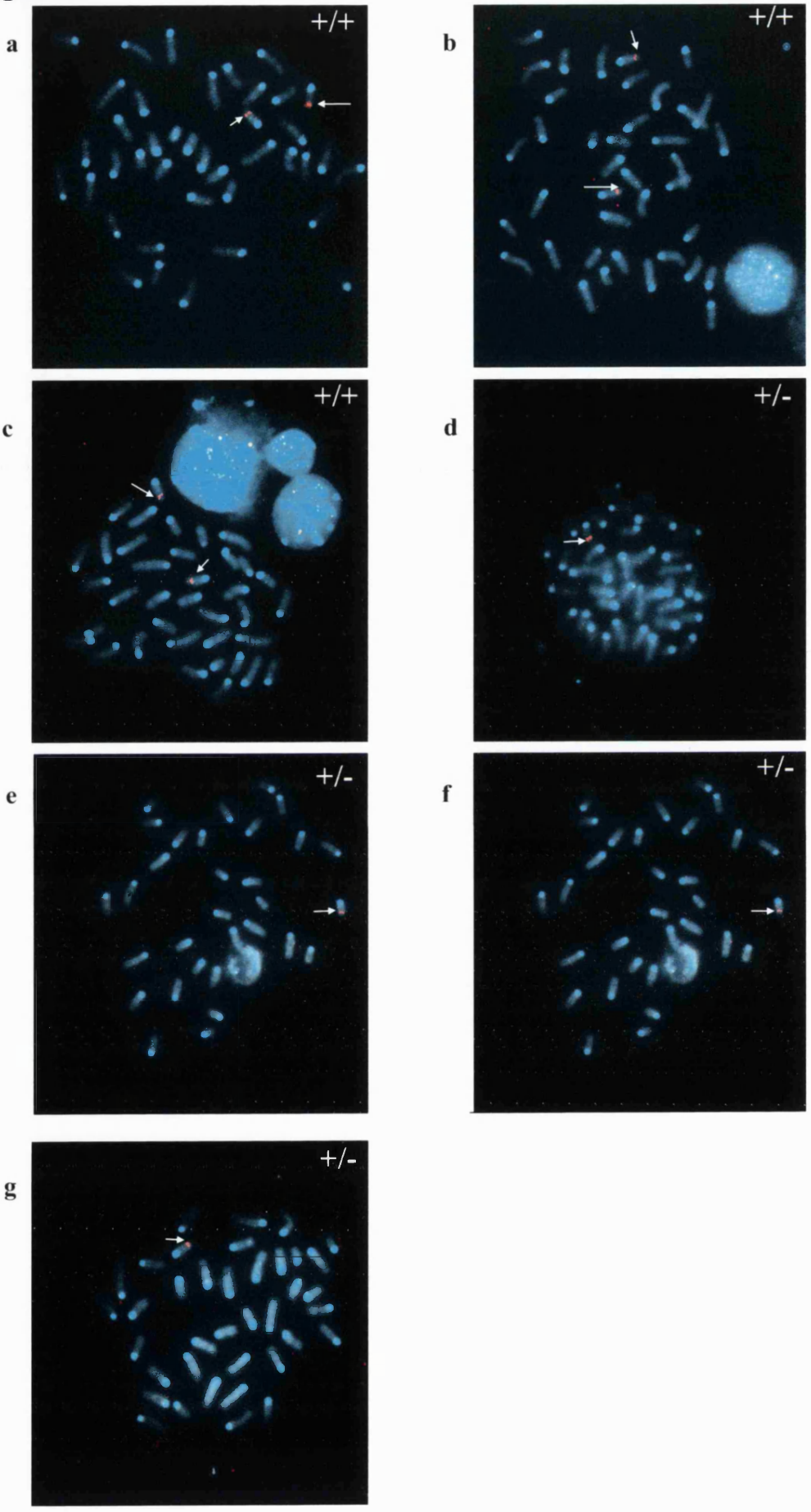

Secondly, the autoradiograms were quantitated using a simple 256-level grayscale flatbed scanner. With the use of a laser-scanning densitometer, it might have been possible to obtain more accurate values for the bands seen on the films, or for the background, which would have allowed normalisation of the signal ratios. This might have facilitated unambiguous genotyping.

Candidate loci for disruption by the transgene insertion

The mutant phenotype observed closely resembled that associated with the s^l (Piebald lethal) allele of the *s* locus with pigmentation restricted to the head and rear quarters, growth retardation and death at around 3 weeks of age (Lane, 1966; Lyon *et al*, 1996). As well as the *s* locus, mutations at two other loci are known to produce precisely this phenotype, and it is associated in all three cases with defects in the migration and colonisation of specific groups of neural crest cells.

Neural crest cells arise from the interaction between surface ectoderm and the neural tube shortly after the neural tube closes (around E8.5 in mouse). They then migrate away along the entire length of the neural tube following two major pathways initially (see **Figure 10** below). The majority of crest cells follow the ventro-medial route, which lies along the anterior portion of the somites through clefts between the dermamyotome and the sclerotome. These then migrate to and colonise a wide variety of areas around the developing embryo, contributing to a very diverse range of structures (Le Douarin & Teillet, 1973). Neural crest derivatives form the bulk of the peripheral nervous system, with crest cells aggregating in clusters near the neural tube and forming the dorsal root ganglia of the spinal cord. Others form peripheral glia and myelinating Schwann cells, and a group of neuroblasts derived from neural crest migrate along the entire length of the gut wall, colonising it and giving rise to the enteric nervous system (Gershon *et al.*, 1993). This comprises both enteric ganglia controlling gut motility and a complex set of neuroendocrine cells of the gut. Neural crest give rise to a large and complex panoply of connective tissue structures, perhaps the most critical of these being the neural crest-derived cardiac septa discussed in the context of truncus arteriosus in chapter 3 (Conway *et al.*, 1997a). Neural crest cells also form

the cartilaginous elements of the lower jaw and related bones of the inner ear. In addition to this, neural crest cells of restricted fate arising from the anterior region of the neural tube (cephalic crest cells) contribute substantially to the bones of the skull and face.

Following ventro-medial migration of neural crest, after a short delay, a smaller number of neural crest cells migrate away from the neural tube along the dorso-lateral route, moving away from the posterior region of the somites in between the dermatome and the ectoderm (Erickson *et al.*, 1992). These preferentially colonise the developing skin and differentiate into melanocytes. A few melanoblast-related neural crest cells migrate to the inner ear and make a highly specialised contribution to the cochlea. The only non-crest derived melanocytes are those found in the retinal pigmented epithelium, discussed below.

Figure 10. Neural crest cell migration pathways and derivatives (Reprinted from "Principles of Development, by Lewis Wolpert *et. al.* Copyright (©) 1998, with kind permission from Elsevier Science Ltd.)

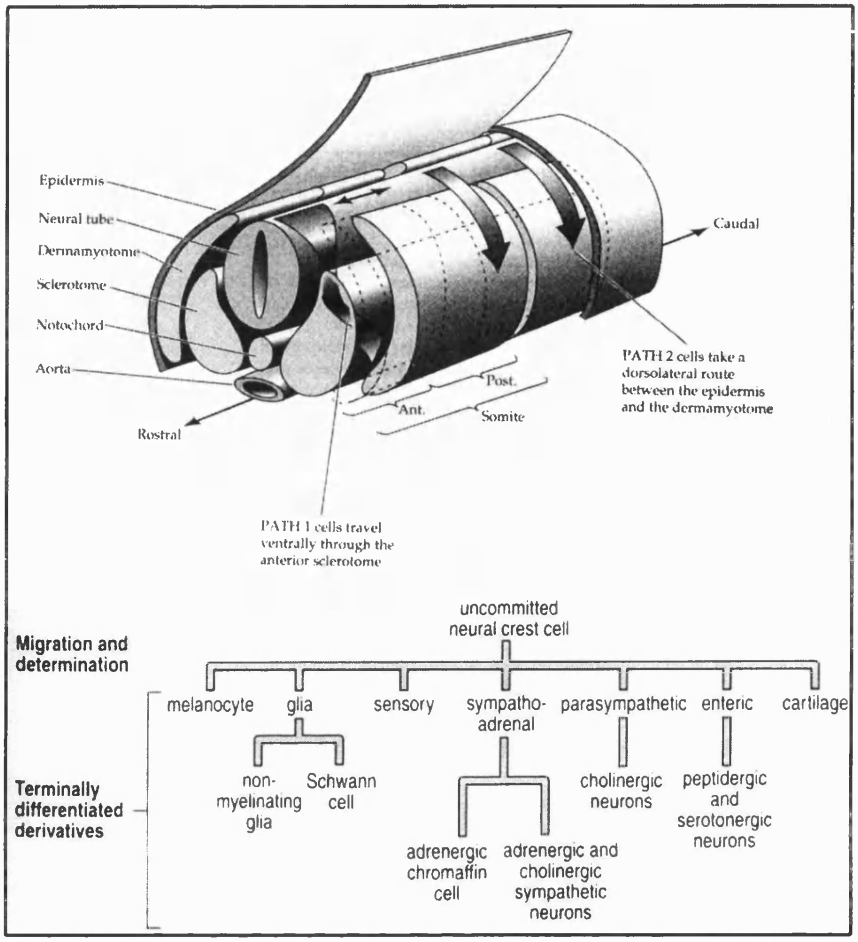

In the piebald lethal phenotype mentioned above, there are primarily three classes of neural crest cell derivatives which are known to be affected:-

Firstly, the neural crest-derived melanocytes which give rise to skin pigmentation are reduced or absent and these were clearly defective in **Harry**, giving rise to the patchy skin colouring. The exact mechanism by which melanocytes colonise the skin and hair follicles in the mouse is uncertain, and the mechanism by which these large patches of unpigmented skin and hair are generated is controversial. However, it is thought that defects in neural crest cells which act early upon melanoblasts, as opposed to defects in differentiating melanocytes, tend to give rise to large patches of unpigmented skin, since removal

of a single melanoblast can cause complete absence of melanocytes over a wide area.

Secondly, there are two classes of melanocyte forming the pigmented layer behind the retina. The thin layer of pigmented retinal epithelium immediately adjacent to the rods and cones is neuroectodermally-derived and is normal in piebald mice, but the layer of choroidal melanocytes embedded in the sclera outside and apposed to the pigmented retinal epithelium is neural crest-derived and absent. This led to an early description of piebald mice as "black-eyed whites", since they have white (or nearly so) coats, but unlike albino mice, possess dark eyes.

Thirdly, enteric neurons are depleted or absent in the colon due to defective migration and colonisation of the neural crest cells which populate the gut wall, and this aganglionosis leads to the condition of toxic megacolon (Webster, 1974; Bolande, 1975). **Harry** showed the gross signs of this, with the characteristic distended abdomen, and gut dissections revealed a severely constricted colon with faecal impaction and consequent distension.

The *s* locus gene product is now known to be the endothelin-B receptor (*Ednrb*), and a number of alleles exist. These have variable phenotypes dependent on the severity of their effects on the migration and differentiation of neural crest cells upon reaching their targets in the gut wall and the epidermis, leading to pigmentation defects and, in the case of piebald-lethal (which is a null allele of the *Ednrb* gene), failure to properly innervate the colon (Hosoda *et al.*, 1994). In the absence of enteric ganglia, the resultant toxic megacolon (grossly enlarged colonic membranes and structures and lack of colonic peristalsis, with attendant blockage of the lumen) can cause systemic sepsis leading to growth retardation and death.

Death in piebald mice is actually normally caused by systemic sepsis, rather than enteric infection, and this is thought to be an effect of the severely depressed immune system relating to the general debilitation caused by the colonic obstruction (Caniano *et al.*, 1989), rather than any more subtle aspect of the mutant phenotype, since the same result can be observed in surgically-induced megacolon (Brann *et al.*, 1977).

It is interesting to note that no **Harry** mutants survived beyond 4 weeks, whereas in a study of classical piebald lethal (s^l) mice it was found that two distinct patterns of mortality were evident: some 64% of mice died at 3 to 4 weeks of age with severe enterocolitis, while the remainder died at 9 to 11 weeks with abdominal distension and megacolon (Fujimoto, 1988). This represents a less severe phenotype than that observed for **Harry** but this could be accounted for by allele or strain background differences. It may also be accounted for by an insertional event at the other recessive locus known to cause piebaldism - the lethal spotted (*ls*) locus which encodes the cognate ligand for the endothelin receptor B, endothelin-3 (*Edn3*) (Baynash *et al.*, 1994). The *ls* null phenotype is almost identical to piebald-lethal (Lane, 1966), but shows subtle differences in the coat spotting, the aganglionosis and the timing of death, with *Edn3* -/- mice showing an appreciably milder phenotype than that seen in *Ednrb* -/- mice.

A third locus, *Dom* (dominant megacolon), is known to cause the piebald lethal phenotype but this acts as an autosomal semidominant (Lane & Liu, 1984; Kapur *et al.*, 1996). *Dom* arose in 1984 as a spontaneous mutation in hybrid stocks (C3HeB/FeJLe-*a/a*♂ x C57Bl/6JLe♀) maintained at the Jackson Labs. Following characterisation and fine-scale mapping studies over the last 13 years, the gene product of the *Dom* locus was recently identified by two independent groups as the SRY-related transcription factor Sox10 (Herbarth *et al.*, 1998; Southard-Smith *et al.*, 1998).

Homologous loci for *Ednrb*, *Edn3* and *Sox10* have all been identified in humans, and mutations at these loci are known to cause megacolon in new-born babies (Hofstra *et al.*, 1996; Kusafuka & Puri, 1997; Kuhlbrodt *et al.*, 1998c). This is known clinically as Hirschprung disease (HD), and has an incidence of 1 in 5000 live births. It can also manifest in later life, but is usually found as a congenital defect and diagnosed within 3 months of birth (Robertson *et al.*, 1997).

Hirschprung disease presents as an heterogenous condition and a higher incidence is associated with other genetic disorders such as Down's syndrome and Waardenburg-Shah syndrome (discussed below). It is generally divided into three classes: The most common form, representing some 74% of patients is short-segment HD, in which aganglionosis extends as far as the rectosigmoidal junction.

The second class is long-segment HD, where aganglionosis extends beyond the rectosigmoidal junction, but does not involve the small intestine. The last class, representing some 12-14% of patients, are the most severely affected group, in which aganglionosis extends beyond the ileo-cecal junction into the ileum, sometimes as far as the stomach (Martucciello, 1996; Robertson *et al.*, 1997). Since HD is caused by incorrect enteric innervation, and since the enteric nervous system is derived from the neural crest, HD can be referred to clinically as a neurocristopathy, one of several (Martucciello, 1996).

HD provides a classic example of a multigenic congenital syndrome: as well as the three loci already cited, mutations affecting the *c-ret* proto-oncogene and its cognate ligands, glial-derived neurotrophic factor (GDNF) and neurturin have also been implicated in human cases of Hirschprung disease (Lyonnet *et al.*, 1994; Angrist *et al.*, 1996).

Applying "reverse genetics" to extrapolate from human genetic syndromes to mice, c-*ret* and its ligands should also be considered as candidate loci for the Harry mutation. *c-ret* is a tyrosine kinase cell surface receptor, and GDNF and neurturin have recently been identified as two of its ligands.

The c-*ret* protooncogene has been knocked out in mice, but can probably be excluded as a candidate locus for the **Harry** phenotype on the grounds that *ret* -/- mice die shortly after birth due to bilateral renal agenesis (Schuchardt *et al.*, 1994), and also display total intestinal aganglionosis. GDNF-null mice exhibit a similar phenotype to *ret* -/- mice, with renal agenesis and a complete lack of enteric neurons (Sanchez *et al.*, 1996). Mutations in the GDNF/*ret* system can therefore have a more severe effect on enteric neurogenesis than mutations in the endothelin system. Mutations at the RET locus are known to be a major cause of Hirschprung disease in humans (Martucciello, 1996). Interestingly, GDNF appears to be only a minor susceptibility locus for Hirschprung disease in humans, perhaps suggesting a degree of compensation by other neurotrophic factors which do not exist in the mouse (Angrist *et al.*, 1996). This highlights the dangers of extrapolating from rodent models to the human disease condition. Neurturin has also been implicated in familial Hirschprung disease (Doray *et al.*, 1998).

Hirschprung disease in humans is frequently found in combination with Waardenburg syndrome (WS). A Dutch eye doctor, P. J. Waardenburg, was the first to notice that some people with two different colored eyes frequently had hearing problems. Dr. Waardenburg went on to study other characteristics of the syndrome which is now named after him (Online Mendelian Inheritance in Man, http://www.ncbi.nlm.nih.gov/omim/, 1999).

These auditory-pigmentary syndromes are caused by physical absence of melanocytes from the skin, hair, eyes, or the stria vascularis of the cochlea, where neural crest-derived melanocytes of an unusual nature are found interspersed with neurectodermally-derived tissue and play a critical role in the formation and maintenance of the acoustic ganglion (Deol, 1967). There are 4 main classes of WS, with all featuring skin and eye pigmentary disturbances, along with cochlear deafness in some cases. WS1 and 2 are distinguished by the presence in WS1 of dystopia canthus (a subtle facial defect with a widened bridge of the nose due to aberrant development of the neural crest-derived facial cartilage, widely used as a pathognomonic indicator of this syndrome). WS3, also known as Klein-Waardenburg syndrome, features upper limb abnormalities including hypoplasia of the musculoskeletal system, flexion contractures, fusion of the carpal bones, and syndactyly, as well as the more usual facial and pigmentary disturbances. WS4, commonly referred to as Waardenburg-Shah syndrome, consists of WS combined with Hirschprung disease, and is the only member of this group of congenital disorders to consistently display an enteric phenotype (short-segment Hirschprung is occasionally seen in classic WS) .

All these syndromes affect neural crest derivatives in various ways, and WS1 and 3 have now been associated with a range of mutations in the *Pax3* gene, with WS3 representing more severe mutations, (sometimes to homozygosity) in this gene (Read & Newton, 1997). *Pax3* is a 'paired box' domain transcription factor with important functions in the specification and migration of neural crest cells. The upper limb abnormalities observed in WS3 are a result of defects in the migration of muscle pioneer cells, which, like neural crest, arise close to the neural tube and migrate to their sites of action. Whilst it is clear that Pax3 is expressed in neural crest cells, its mode of action in inhibiting their migration is not always

cell-autonomous. Recent work has shown that Pax3 expression in tissues lying in the pathways of crest migration may serve to down-regulate expression of extra-cellular matrix molecules which block such migration, and thus Pax3 could be considered to also be "clearing a path"for neural crest cells (Henderson *et al.*, 1997). There are a large number of mutant alleles of Pax3 in the mouse, the most widely known being the "Splotch" mouse, a useful model for neural tube defects (Copp, 1994). As the name suggests, Splotch, and several other alleles of Pax3, feature coat spotting in the mouse, but to date there has been no report of any mutation in Pax3 affecting crest-derived enteric neurons. It could perhaps be considered a weak candidate gene for the mutation seen in **Harry**.

In an interesting study using interspecific hybrids between *Spretus* and Splotch (Sp^d) mice, two modifer loci were mapped which strongly influenced the craniofacial phenotype seen in Splotch mice, reminiscent both of the heterogeneity seen across the spectrum of WS1 and WS3 patients and of the variation in coat spotting seen in **Harry** mutants (Asher *et al.*, 1996).

In contrast to WS1 and 3, WS2 is a more heterogenous condition, with several distinct loci implicated. Some 15% of cases have been found to involve mutations at the *Mitf* (micropthalmia-associated transcription factor) locus. This encodes a basic helix-loop-helix leucine zipper transcription factor, and again, there are a plethora of alleles at this locus in the mouse. Mutations at the *Mitf* locus affect one or more of three different traits: eye size, pigmentation, and capacity for secondary bone resorption. However, although *Mitf* is known to play a crucial role in the specification and differentiation of neural crest cells, in this regard it is thought to be specific for melanoblasts and terminally differentiating melanocytes (Opdecamp *et al.*, 1997). None of the 20 alleles of this gene in mouse or human mutations in *Mitf* have been shown to have an effect upon enteric neurons. This gene can probably therefore be discounted as a candidate locus for the mutation seen in **Harry**.

WS4 presents a more interesting case: Again, this is an heterogenous syndrome with multiple causative and susceptibility loci. Given its similarity to mutants such as piebald lethal and lethal spotting in the mouse, it is hardly surprising that mutations in the human homologues of *Ednrb, Edn3* and *Sox10*

have all been implicated in this condition. Interestingly, heterozygous mutations in the human EDNRB and EDN3 genes can cause Hirschprung disease alone, whilst homozygosity gives the full clinical picture of WS4. On the other hand, heterozygosity for mutations at the SOX10 locus can give the more severe Waardenburg-Shah condition. This parallels the situation in mouse, where mutations at *Ednrb* and *Edn3* are recessive, whilst the only known mutaion in *Sox10* is semi-dominant, with homozygosity being embryonic lethal. The situation is complicated in humans by the presence of susceptibility loci such as mutations in the GDNF gene, which by themselves may not show a phenotype, but which can modulate the severity of the phenotype seen with a heterozygous mutation at other loci such as RET (Angrist *et al.*, 1996).

WS4 does not feature dystopia canthus, hence the neural crest cells which give rise to cranio-facial structures appear unaffected despite a report that, in contrast to the situation in rodents, SOX10 is expressed in crest-derived facial mesenchyme during human embryonic development (Bondurand *et al.*, 1998).

Clearly, combined Waardenburg-Hirschprung phenotypes bear many similiarities to piebald lethal phenotypes in the mouse, as seen in **Harry** mutants (Martucciello, 1996). To date, the mouse homologues of the only known loci implicated in WS4 are the ones already discussed and considered above: *Ednrb, Edn3, Sox10* and *Ret* and its ligands. This still leaves some 15% of human cases of WS4 unaccounted for however.

Modifer genes

It is curious that the extreme phenotype observed early during **Harry** breeding in Oxford (and shown in **Figure 3**) has never reappeared. However, strain background effects must be considered. In a recent analysis using piebald (*s*) mice inbred onto two different genetic backgrounds, six genetic modifiers were mapped which act as quantitative trait loci (QTLs) to modify coat spotting in these mice (Pavan *et al.*, 1995). By implication, these loci interact with pathways involving the *Ednrb* gene, and could perhaps also modify the degree and extent of aganglionosis in piebald-lethal (s^l) mice. In this context, it is interesting to note that the allele of the *Ednrb* gene used in these mapping experiments (the classical

piebald mouse, *s*) is known to express the mRNA at levels of around 28% of wild-type but that this is sufficient to completely abrogate the aganglionic phenotype, although the mice still show coat colour spotting (Hosoda *et al.*, 1994).

Extending the argument, similar (or indeed the same) QTLs might act to modify the phenotype observed in **Harry** piebald mice. This argument, whilst speculative, gains weight from the observation that the level of coat colour spotting and the growth retardation (and by implication, the severity of the toxic megacolon) was seen to vary widely between different crosses, with a loose inverse correlation between coat spotting and growth retardation. This strongly suggests that modifer genes are segregating independently of the transgene, probably differentially derived from the mixed C57Bl and CBA backgrounds used to propagate the strains.

Although the phenotype was considered to be fully recessive, two animals from the same litter (out of several hundred wild-type transgenics bred to date) showed a white belly-spot, but no other phenotype. Again, this can probably be explained with reference to modifier genes, with this cross containing a particularly "severe" combination which led to a very mild coat colour phenotype, even in presumptive hemizygotes with one mutant and one wild-type allele of the gene affected by transgene integration. Although these animals were killed, they could have been tested for homozygosity by FISH analysis. Given the severe nature of the mutation in homozygotes, however, it was considered unlikely that the very mild phenotype seen in these animals could have resulted from modulation of the phenotype in a homozygous animal.

Summary

Overall, at this stage of the investigation there could be said to be three strong candidate loci for the recessive mutant piebald lethal phenotype observed in **Harry** transgenic homozygotes. These are *Ednrb*, *Edn3* and *Sox10*. *ret* and its ligands were considered weak candidates, firstly due to the lack of any renal phenotype and secondly, due to the restricted nature of the gut phenotype.

The only evidence which might favour the *Edn3* locus over the others is the observation that the coat colour of **Harry** mutants was always black. The black

colour derives from the recessive *a* (non-agouti) allele derived from the C57 background, and lies close to *Edn3* on distal Chr 2. If the mutation seen in **Harry** mice was caused by transgene insertion into the C57 chromosome of the original injected C57/CBA F_1 zygote, and if it were close to the *Edn3* locus, it would be predicted to be linked to the recessive black coat colouration phenotype seen in these mice.

Clearly, the mutation seen in **Harry** does not necessarily have to be at a known locus. As for novel loci, it has been suggested that there is a second endothelin B receptor gene, since activation of the receptor with the specific agonist sarafotoxin S6c can mediate opposite effects, specifically vasodilation and vasoconstriction. However, two separate studies seem to indicate that this is not the case, at least in mice, since in s^l/s^l (piebald-lethal) animals, which entirely lack the *Ednrb* gene, no ligand-binding activity (endothelin 1) was present, and sarafotoxin failed to elicit either vasodilation or vasoconstriction in the relevant tissues from these mice (Giller *et al.*, 1997; Mizuguchi *et al.*, 1997). Another group have done the same in rats - this study suggests that the endothelial ETB receptor mediating dilation and the smooth muscle cell ETB receptor mediating constriction may not represent two different subtypes (Clozel & Gray, 1995).

An alternative might simply be a mutation in a gene directly upstream of either *Ednrb* or *Edn3* such as the endothelin converting enzymes (ECE) which convert preproendothelins into the active form of the ligand by cleavage. A defect in ECE-1 has been shown to cause Hirschprung disease and cardiac defects in a human patient (Hofstra *et al.*, 1998). A similar defect in the ECE responsible for activation of endothelin 3 in the mouse might be predicted to replicate the lethal spotting phenotype seen in *Edn3*-null mice. (Xu *et al.*, 1994)

CHAPTER FIVE:
HARRY - DETAILED CHARACTERISATION OF THE PHENOTYPE

Introduction

With a clear mutant phenotype associated with the transgene and given the three strong candidate loci mentioned in the previous chapter, a bipartite approach was adopted and performed in parallel. The mapping of the transgene integration site, to eliminate or reinforce a candidate gene is discussed in the next chapter. Alongside this, a detailed characterisation of the phenotype was undertaken, with special attention paid to the presence or absence of features from known mutant phenotypes associated with the candidate loci.

The investigations included the status of melanocytes via studies of coat colouration, covered in the previous chapter, and further to this, retinal histology was performed to determine the status of the neural crest-derived choroidal melanocytes. Gut dissection and histology was performed in order to determine whether the megacolon observed was truly associated with a reduction in enteric neurons, and to assess the extent of such hypo- or aganglionosis. Finally, the transgene was introgressed onto a different genetic background by breeding to congenicity to assess strain-dependent variation in the phenotype.

Results

Coat spotting

Coat colouration was discussed in the previous chapter, but it is worth re-iterating that to date, a single litter has shown evidence of a mild coat colour phenotype in 2 presumptive *hemizygous* animals. These were the only such animals observed out of some 200 transgenic offspring from hemizygous intercrosses.

Retinal histology

The choroid layer forms a dark brown vascular sheet which separates the outer, fibrous sclera from the retina (**Figure 11a**). It gains its colour from

Figure 11. Retinal histology in Harry mutants

a) Diagrammatic representation of layered structure of the wall of posterior eye, showing retina, choroid and sclera. (Taken from "Principles of Anatomy & Physiology, 6th Edition, by Gerald J. Tortora and Nicholas P. Anagnostakos; Copyright (©) 1990 by HARPERCOLLINS. Reprinted by permission of Addison-Wesley, Educational Publishers.)

b) Whole eyes from wild-type (left) and mutant (right) **Harry** mice, dissected at day 10 post-partum. The mutant eye can be seen to have a lighter, brownish colour.

c) wild-type retina x 200 (H&E staining)

d) mutant retina x 200

e) wild-type retina x 400

f) mutant retina x 400 (ret = retina; rpe = retinal pigmented epithelium; chor = choroid; cm = choroidal melanocytes)

Figure 11

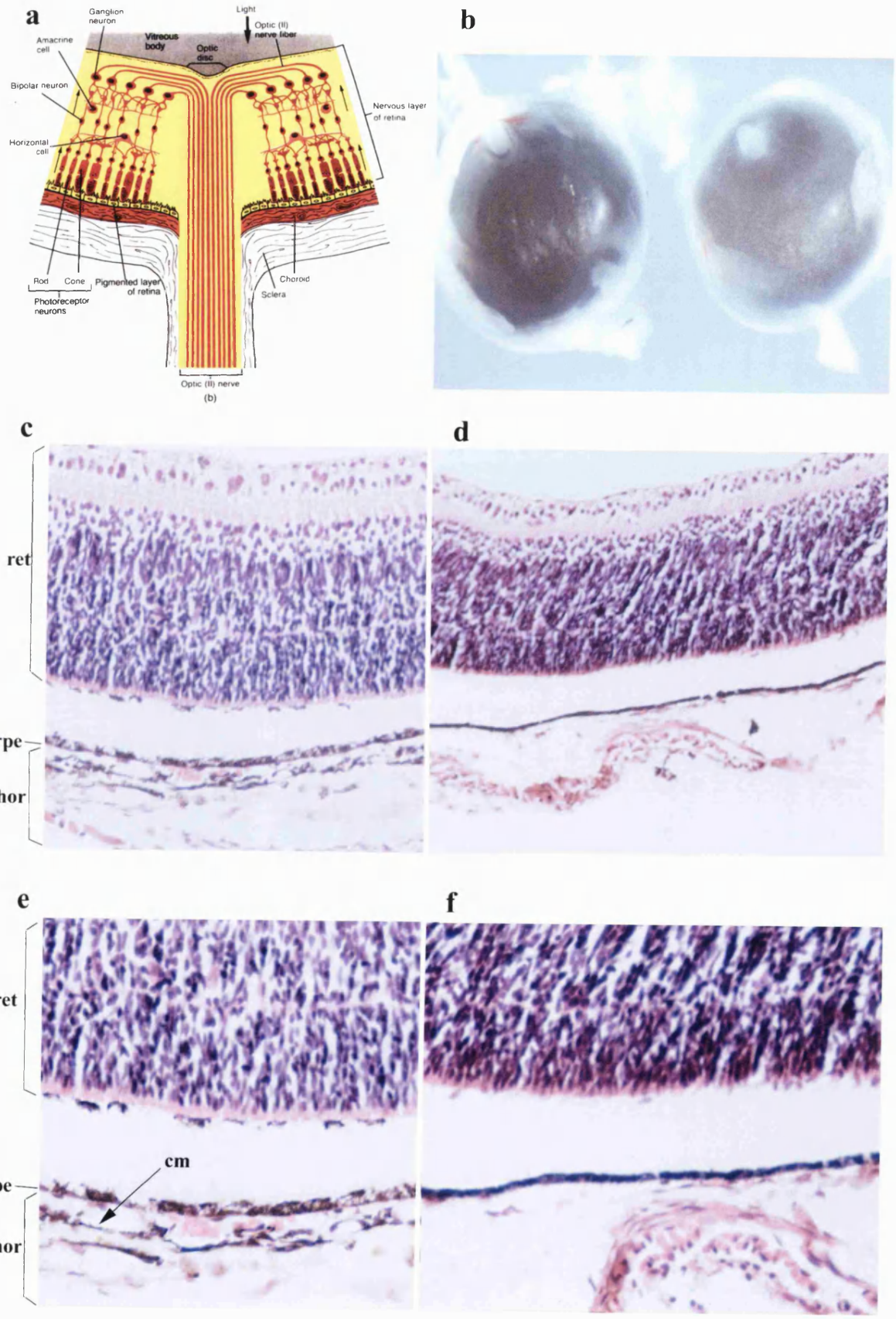
a
Ganglion neuron
Light
Optic (II) nerve fiber
Vitreous body
Optic disc
Amacrine cell
Bipolar neuron
Nervous layer of retina
Horizontal cell
Rod
Cone
Photoreceptor neurons
Pigmented layer of retina
Choroid
Sclera
Optic (II) nerve
(b)
b
c
ret
rpe
chor
d
e
ret
cm
rpe
chor
f

numerous melanin deposits laid down by choroidal melanocytes, which derive from the neural crest. The choroid is immediately apposed to the outermost layer of the retina, which consists of the neuroectodermally-derived retinal pigmented epithelium, however the innermost section of the choroid comprises the largely unpigmented choriocapillary layer, the major blood supply to the retina. The choriocapillary layer is separated from the retina proper by the *lamina vitrea*, a thin, complex structure mostly composed of basal lamina-type extracellular matrix (Ross *et al.*, 1989). During histological preparation, the retinal pigmented epithelium very often separates from the inner layers of the retina.

Harry mutants lacked, or had a severe reduction, in the neural crest-derived choroidal melanocytes, while the neuroectodermally-derived retinal pigmented epithelium remained unaffected. This could actually be seen without the aid of microscopic sections simply by examining whole eyeballs from wild-type and mutant mice under a dissecting microscope. The mutant eyeball could clearly be seen to have a reduced level of pigment, manifest as a lighter, slightly speckled, dark brown appearance, compared to the solid purplish-black colour of the wild-type (**Figure 11b**). At the histological level, the choroidal melanocytes were absent or severely reduced while the retinal pigmented epithelium was unaffected (**Figure 11c-f**).

Megacolon

Intestinal tracts were examined from around 30 wild-type and mutant animals. The particular mutant shown in **Figure 12** was atypical in that the obvious constriction point lay above the ileo-cecal junction. This was observed only twice out of around 30 such dissections, with the constriction point more commonly lying somewhere in the colon, most often in the region distal to the ileo-cecal junction i.e.closer to the anus.

The relevant features of gut anatomy are illustrated diagrammatically in **Figure 12b**, with the outer muscularis consisting of an outer layer of longitudinal and an inner layer of circular smooth muscle. Contractions of these orthogonally opposed layers generate peristaltis and propel food through the gut. Sandwiched in between these layers of muscle are found the neural crest-derived myenteric

Figure 12. Gut histology in Harry mutants

a) Dissected whole intestinal tracts from wild-type (left) and mutant (right) **Harry** littermates culled at 19 days of age. The constriction point (arrowed) appears to lie above the ileo-cecal junction in this particular mutant.

b) Composite diagram of the layers and structures found in the gut wall at various levels throughout the intestinal tract. (Taken from "Principles of Anatomy & Physiology, 6th Edition, by Gerald J. Tortora and Nicholas P. Anagnostakos; Copyright (©) 1990 by HARPERCOLLINS. Reprinted by permission of Addison-Wesley, Educational Publishers.)

Longitudinal sections through the wall of the colon, stained with H & E, x 400 magnification. The various layers aredemarcated on the right. From top to bottom: MU = mucosae; SM = sub-mucosae; CM = circular smooth muscle; MG = putative myenteric ganglia; LM = longitudinal smooth muscle.

c) Wild-type **Harry** colon.

d) Mutant **Harry** colon.

e) The wild-type **Harry** colon shown immunostained in **Figure 13.**

f) The mutant **Harry** colon shown immunostained in **Figure 13**.

Figure 12

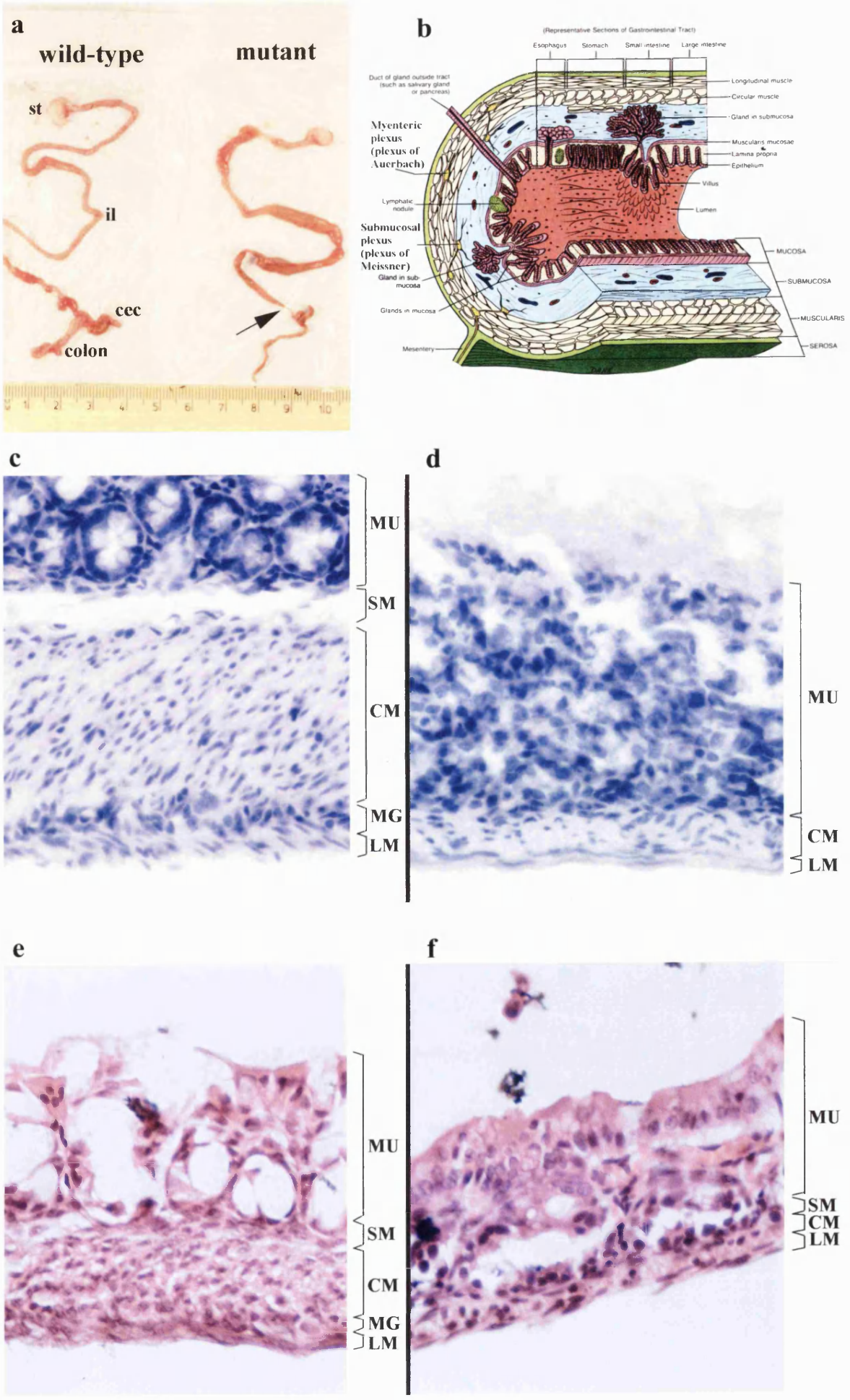
a
wild-type
mutant
st
il
cec
colon
b
(Representative Sections of Gastrointestinal Tract)
Esophagus
Stomach
Small intestine
Large intestine
Duct of gland outside tract (such as salivary gland or pancreas)
Myenteric plexus (plexus of Auerbach)
Lymphatic nodule
Submucosal plexus (plexus of Meissner)
Gland in submucosa
Glands in mucosa
Mesentery
Longitudinal muscle
Circular muscle
Gland in submucosa
Muscularis mucosae
Lamina propria
Epithelium
Villus
Lumen
MUCOSA
SUBMUCOSA
MUSCULARIS
SEROSA
c
MU
SM
CM
MG
LM
d
MU
CM
LM
e
MU
SM
CM
MG
LM
f
MU
SM
CM
LM

ganglia (neurons and glia) which collectively comprise the plexus of Auerbach. This plexus mostly controls peristalsis (Tortora & Anagnostakos, 1990). The inner submucosa consists of dense connective tissue which binds the inner mucosa to the outer muscle layer. It is highly vascular and contains the other component of the neural crest-derived enteric nervous system - the less abundant ganglia which make up the plexus of Meissner. This forms part of the autonomic nerve supply to the muscularis mucosae (which maintains the inner epithelium in folds to increase surface area for absorption) and is also important in controlling secretions to the gastrointestinal tract. This plexus contains a large number of different neuroendocrine and neuronal cell types and is less well-characterised than the plexus of Auerbach. A subset of these cells stain with chromium or silver salts, as do the neuroendocrine chromaffin cells of the adrenal medulla, and are therefore sometimes referred to as enterochromaffin cells (Pearse, 1973).

Histological sections through wild-type and constricted regions of mutant colons were stained with haematoxylin and eosin and examined for obvious morphological differences. The eosin staining shown in **Figure 12c** and **d** is quite weak, but these sections show the difference in morphology between wild-type and affected mutant colon, with a dramatic reduction in the thickness of the muscle layers and severely disorganised mucosae. Sections **12e** and **f** are sections from the same tissue blocks used in the immunofluorescence experiments shown in **Figure 13**. These mice were killed at an earlier stage than those in **12c** and **d**, hence the pathology is not as advanced, but clear differences in the muscle layer thicknesses can still be observed.

Numerous clustered cells with large oval nuclei - putative myenteric ganglion cells - are apparent in **12c** and **e** (wild-type) between the muscle layers, and these are almost entirely absent in **12d** and **f** (mutant).

Sections through wild-type and mutant colons were immunostained for α-neurofilament, a general neuronal marker. In these sections, these only distinguished myenteric neurons of the external Auerbach's plexus, as cells of the inner plexus of Meissner are not as numerous, and this plexus does not contain as many neurofilamentous fibres (Burns & LeDouarin, 1998). Furthermore, non-

Figure 13. Myenteric ganglia in Harry mice revealed by α-neurofilament staining

Longitudinal sections through the wall of wild-type (a) and mutant (b and c) **Harry** colons. The lumenal aspect is at the top of each picture. α-neurofilament is stained red and nuclei are counterstained with DAPI (cyan).

a) Wild-type. Significant continuous staining can be seen between the longitudinal (LM) and circular (CM) smooth muscle layers, presumably corresponding to the myenteric plexus. The sub-mucosae (SM) also show staining, but it is difficult to unambiguously discern the plexus of Meissner, due to the high level of background.

b) Mutant. The muscle layers are much thinner, and α-neurofilament staining is restricted to bright patches (arrowed) with lower levels of continuous staining present.

c) Control (no α-neurofilament Ab). Note the high level of non-specific background, particularly at the lumenal border and in the sub-mucosae.

Figure 13

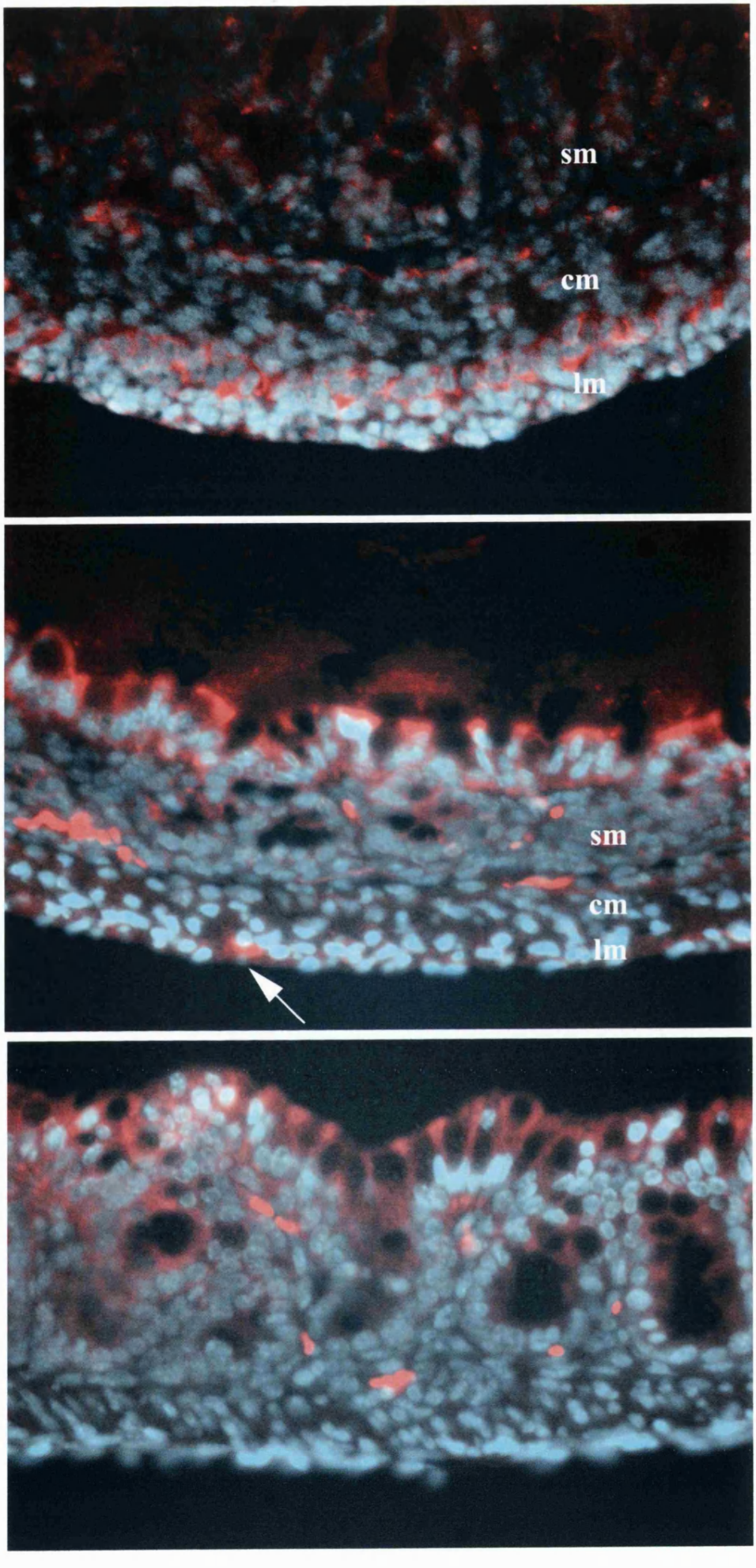

specific fluorescent signal in the inner submucosal layers made it impossible to identify submucosal ganglia by this method. In the wild-type colon, immunofluorescence showed an almost continuous layer of bright neurofilament staining between the two layers of smooth muscle, corresponding to the myenteric ganglia (**Figure 13**). Fibres could be seen penetrating into the circular smooth muscle layer. **Harry** mutants showed limited bright staining clustered in small patches, with fainter background staining visible suggesting a significant reduction in myenteric neurons, hence hypoganglionosis and megacolon.

Introgression onto other genetic backgrounds

This was not performed rigorously, but rather, data became available as a spin-off from work being carried out in another laboratory: Many of the transgenic lines used in this work, including **Harry** and **Holly**, are still maintained at their point of origin in Oxford. Parallel studies carried out there involved the introgression of the various transgene constructs onto different genetic backgrounds in order to assess the effects of strain background on regulatory regions of the *Igf2/H19* loci (via monitoring comparative levels of expression of the luciferase reporter). During the course of this work, the **Harry** line was backcrossed onto the 129J/Sv strain for at least 12 generations to produce a congenic strain (Flaherty, 1981).

Given the existence of a congenic strain, it was a trivial, but informative, experiment to set up hemizygous intercrosses and do a cursory analysis of the mutant phenotype on this different genetic background.

Intercrosses were performed between **Harry** hemizygotes congenic on 129J/Sv at the 12, 13 and 14th generation of backcrossing. Very few viable pups resulted, with many being consumed before analysis. The only full intercross litter to yield clear results consisted of 6 pups with 1 found dead on the day of birth. Two of the remaining 5 went on to show clear evidence of the mutant phenotype, with growth retardation and abnormal skin pigmentation. One mutant presumably died and was consumed before day 6, and the other was found dead on day 6. After culling all the pups, the remainder of the litter was analyzed.

The mutant which survived until day 6 had the customary bulging abdomen, and dissection revealed the expected megacolon. This was relatively severe, since it died only 6 days after birth with significant growth retardation compared to wild-type siblings, but this animal showed significantly greater skin pigmentation than any mutant bred on the C57/CBA background described previously. Essentially, the animal had only a small unpigmented patch covering some 50% of the right lateral head and shoulder, and lacked pigmentation on the skin of the limbs and tail. The bulk of the dorsal surface was fully pigmented. Fur growth had not yet commenced in these pups at the time of death, so it was impossible to determine whether the mutant animals would have developed fur of the parental strain colour (agouti), or whether it would have been black as with all mutants on the original C57/CBA background.

Discussion

The coat colouration and retinal histology show that neural crest-derived melanocytes were severely reduced or absent in **Harry** mutants. The gut histology shows that neural crest-derived myenteric neurons were also severely reduced in these animals, leading to toxic megacolon and death within 4 weeks of birth. This experiment may seem to have been redundant, but it should be noted that *hyper*ganglionosis can also lead to megacolon, as seen in mice which overexpress *HoxA-4* (Tennyson *et al.*, 1998) or in mice which lack *Ncx/Hox11L.1* (Hatano *et al.*, 1997) (although these can probably be ruled out as candidate loci in **Harry** mutants on the grounds that they appear to have no effect upon melanocyte development). It was therefore deemed important to assess whether the megacolon observed in **Harry** mutants was truly caused by a lack of enteric neurons.

The variation in the degree of hypoganglionosis (as measured by the point of constriction seen in the gut and variation in time of death), as with the variation in coat spotting, could be accounted for by postulating the presence of modifier genes segregating independently in these crosses. In this context, it should be noted that during comparative studies of the *Ednrb* -/- knockout mouse (made by

targeted deletion) and the classical s^l/s^l piebald lethal mouse (which has a spontaneously derived deletion of the entire ednrb gene), it was found that coat colouration in the s^l/s^l mice was almost entirely absent, compared with the significant dark patches seen in almost all *Ednrb* knockout mice. Since both mice have essentially the same genetic defect, this anomaly was ascribed to strain background differences (Hosoda *et al.*, 1994).

This explanation could account for the phenotype observed when the transgene was transferred onto the 129 background. In effect - although it should be noted that the following conclusions are drawn from very limited data and must be viewed as highly tentative - the mutant phenotype was similar to that seen on a C57/CBA background, except that the severity of the gut phenotype (as evidenced by early lethality) increased whilst the hypopigmentation decreased dramatically.

Overall, the phenotype seen in **Harry** mutants closely resembled that seen in *Ednrb* and *Edn3* null mice, with the only possible difference being the occasional observation of presumptive hypoganglionosis extending beyond the colon into the small intestine. Although hypoganglionosis was seen never to extend beyond the ileo-cecal junction in studies of *Ednrb* and *Edn3* mutants (Baynash *et al.*, 1994; Hosoda *et al.*, 1994), this could perhaps be ascribed to strain background effects, with both knockouts generated and maintained on a 129/Sv x C57BL/6J hybrid background, as distinct from the mixed C57BL/6J x CBACa background of the **Harry** transgenic line.

As a further cautionary argument against ruling out either *Ednrb* or *Edn3* as candidate loci purely on the grounds that these mutations restrict their effect to the colon, it should be noted that in the rat, mutations at the *Edn3* locus can cause an essentially identical piebald lethal phenotype (the spotting lethal rat), but that the hypoganglionosis often does extend beyond the ileo-cecal junction into the distal small intestine (Nagahama *et al.*, 1985). Furthermore, in the equine equivalent of piebald-lethal, a mis-sense mutation in the endothelin-B receptor gene leads to Lethal White Foal Syndrome, in which homozygosity for the mutant allele results in aganglionosis from the jejunum to the rectum - a more severe effect than that seen in other species (Metallinos *et al.*, 1998). Taking the above

into account, it could therefore be argued that a novel allele of either *Ednrb* or *Edn3* in the mouse might generate the same phenotype.

The final strong candidate locus, *Sox10*, presented a more complex case. The locus was originally identified as *Dom* (dominant megacolon), a spontaneously-occurring mutant in stocks maintained at the Jackson Labs (Lane & Liu, 1984). With the identification of the gene, the locus has now been renamed *Sox10* and the mutation formally reclassified as $Sox10^{Dom}$ (http://www.informatics.jax.org, 1999). As the original name suggests, this mutation is an autosomal semidominant, with a milder phenotype seen in heterozygotes than in homozygotes. $Sox10^{Dom}$/ $Sox10^{Dom}$ homozygotes are usually embryonic lethal by E13. Heterozygous $Sox10^{Dom}$/+ mice show white belly-spotting and white feet, coupled with megacolon. This was shown to vary on different genetic backgrounds, but coat spotting was never found to be as extreme as that seen in **Harry** mutants. The time of death due to toxic megacolon was found to vary more widely with genetic background, with a more severe enteric phenotype on a C57BL/6J background. The enteric hypoganglionosis in $Sox10^{Dom}$/+ heterozygotes was found to extend beyond the ileo-cecal junction in some cases (Kapur *et al.*, 1996). Although the cause of death in $Sox10^{Dom}$/ $Sox10^{Dom}$ homozygotes prior to E13 is not known, they have been reported to completely lack enteric neurons below the rostral foregut (Herbarth *et al.*, 1998).

Many transgene insertional mutations exert an effect via loss-of-function, and since the **Harry** mutation was essentially fully recessive, it seems reasonable to speculate that the transgene insertion in **Harry** might have caused a loss-of-function mutation at the affected locus, particularly given the similarity of the phenotype to the two known recessive null mutations at *Ednrb* and *Edn3*.

Sox10 encodes an HMG-box transcription factor which has been shown to play an essential role in neural crest development, discussed more fully in chapter 7 (Herbarth *et al.*, 1998; Southard-Smith *et al.*, 1998). The $Sox10^{Dom}$ mutation is a frameshift truncation which leaves the DNA-binding HMG-box domain intact but removes almost all the amino acids carboxy-terminal to it. This carboxy-terminal region has been shown to contain transactivation domains which interact with other transcription factors of the POU domain class. The intact amino-terminal

region upstream of the HMG-box may also contain transactivation domains. It has been suggested that the *Sox10^{Dom}* mutation might exert its effect due to haploinsufficiency of wild-type Sox10 protein, but it is just as reasonable to speculate that the *Sox10^{Dom}* mutant might act as a dominant negative to suppress the wild-type molecule. Were this the case, then a true null mutant of *Sox10* might reasonably be supposed to have a similar phenotype to *Dom* heterozygotes, except it would be recessive. Although highly speculative, the above chain of argument allows for the possibility of **Harry** being a loss-of-function recessive mutation at the *Sox10* locus. However, this model does not account for the fact that *Sox10^{Dom}/Sox10^{Dom}* homozygotes are embryonic lethal by E13. It is possible that the truncated *Sox10^{Dom}* gene product might act as a dominant negative on other closely related Sox genes. Although the native targets of Sox10 are unknown, most Sox proteins recognise the core binding motif 5'-AACAAAG-3'. Some degree of Sox10 protein specificity is probably generated through interactions with POU domain transcription factors binding to nearby sites on the DNA (Kuhlbrodt *et al.*, 1998a; Kuhlbrodt *et al.*, 1998b). Since *Sox10^{Dom}* lacks some of the domains necessary to interact with these factors, but not the DNA-binding domain, it might non-specifically block binding sites required by other Sox proteins.

Even if the *Sox10^{Dom}* mutation does exert its effect through haploinsufficiency, this still does not rule out the mutation seen in **Harry** as being at this locus, since the transgene insertion may not necessarily have caused simple loss of function but something more complex. This is discussed in more detail in chapter 7.

Summary

Detailed characterisation of the phenotype seen in **Harry** mutants revealed all of the features consonant with it being a mutation in any of the *Ednrb*, *Edn3* or *Sox10* genes with little to discriminate between them at the phenotypic level.

CHAPTER SIX:
HARRY - LOCATION OF THE TRANSGENE INTEGRATION SITE

Introduction

As discussed in Chapters 4 and 5, with three strong candidate genes for the mutant phenotype observed in **Harry** homozygotes and no obvious way of distinguishing between them at a phenotypic level, it was deemed essential to map the transgene insertion site. This was initially pursued via fluorescent *in situ* hybridisation (FISH) on metaphase chromosome spreads, followed by linkage mapping using PCR-based microsatellite polymorphisms to corroborate and refine the map position.

FISH - background and considerations

Following the establishment of protocols for the gentle denaturation and hybridisation of chromosomal DNA, early *in situ* experiments using isotopic labelling and autoradiographic detection permitted the detection and localisation (in skilled hands) of single copy mammalian genes (Harper *et al.*, 1981). Improvements in banding protocols following ISH made the identification of successfully hybridised chromosomes easier, but the limitations of radioactive detection meant that localisation of the probe signal was still technically difficult, requiring the examination and statistical analysis of silver grains from 50-100 metaphase spreads. With the introduction of fluorescently-labelled probes, and the addition to the hybridisation cocktail of an excess of moderately-repetitive (C_0t-1) unlabelled genomic DNA to suppress non-specific background, FISH has become a routine method used widely to detect and localise single-copy sequences with high precision (Heng *et al.*, 1997).

The recent advent of affordable microscope cameras incorporating cooled charge-coupled devices (CCDs) has greatly enhanced the detection of faint FISH signals. CCD cameras are a spin-off from astronomical research, and have the advantage that digitised images can be generated using very long exposures, by virtue of integrating the light intensities captured at individual pixels on the CCD chip over long time periods (seconds to minutes) (Tanke *et al.*, 1995). Following

image-processing using sophisticated algorithms (again, a spin-off from astronomy), good results can be obtained from relatively poor FISH slides with very low signal-to-noise ratios.

One final recent innovation in FISH technology, or rather ISH technology (since the detected label need not be fluorescent), has been the introduction of peroxidase/tyramide detection protocols (Raap *et al.*, 1995; van Gijlswijk *et al.*, 1996). Essentially, these revolve around the use of horseradish peroxidase to catalyse the deposition of a tyramide-conjugated label (fluorescent or otherwise) covalently linked to the substrate around the site of enzyme activity. In the context of chromosomal *in situ,* the enzyme can be localised to the hybridised probe either by direct conjugation to the probe itself prior to hybridisation, or, post-hybridisation, by conjugation of the enzyme to a hapten-binding moiety such as streptavidin. Regardless of the method used, this technique offers at least 5-fold greater sensitivity (signal-to-noise ratio) than conventional FISH, due to the enzyme's ability to catalytically deposit far more label at the target site than can be achieved via the passive binding methodologies used to date. The use of non-fluorescent label bypasses the need for fluorescent microscopes and expensive digital imaging technology - simple brightfield photography suffices. Although relatively new, the rapid adoption and patenting of this technology by commercial concerns (in other words, the speed of its transfer from the laboratory to the marketplace) attests to its power and attractiveness (TSA™, NEN Life Sciences, 1999).

Use of FISH to detect transgene integration

Compared to many single-copy genes, for which cDNA is often the only sequence available for use as a probe, transgenic mice offer themselves particularly well to FISH protocols due to the multi-copy nature of most integrated transgene arrays. There can be said to be three key elements to successful FISH mapping of transgene integration sites: Firstly, generation of high-quality metaphase chromosome spreads; secondly, a good probe and a hybridisation protocol which generates strong signals from the transgene; and thirdly, unambiguous chromosomal identification.

With regard to the first point, various methods exist for making metaphase spreads, and these were discussed in more detail in the introduction to chapter 4. In the FISH experiments discussed therein, spreads were prepared from individual animals strictly for the purposes of genotyping and did not need to be of high quality. In contrast, during the mapping studies discussed in this chapter and chapter 11, spleens from multiple animals were pooled. Using this modification, the splenocyte culture method was found in our hands to routinely generate good spreads with the long, extended chromosomes that are essential for G-banding and mapping.

The second point, quality of probe, protocol and strength of signal, proved more taxing, but after several attempts, a working protocol was obtained and with slight modifications this was found to routinely generate a strong transgene signal which could easily be distinguished from background and from fainter signals caused by cross-hybrisation of the transgene probe to the endogenous *Igf2/H19* locus on distal Chr7 (since the transgene constructs carry elements of this region). Early experiments used conventional photography with high-speed colour film, but, unsurprisingly, a cooled CCD camera, coupled with image-processing algorithms, was found to greatly augment the detection and documentation of fainter FISH signals.

Given high-quality chromosome spreads and routine detection of the transgene signal, this left identification of chromosomes. In humans, karyotyping is routinely done by Giemsa-trypsin banding which generates a characteristic pattern of horizontal dark (G) and light (R) bands along the length of each chromosome, and the variation in size and centromere position throughout the human karyotype assists in chromosomal identification (Franke & Oliver, 1978). Unfortunately, for unknown reasons, mouse chromosomes are all acrocentric (with the centromere at one end) and they do not band as clearly as human chromosomes with the Giemsa-trypsin protocols.

This difference in the quality of G-banding may reflect the different nature of the short highly repetitive sequences (SINE elements) present in the human and mouse genomes. In humans and mice, the dark-staining G-bands correspond to AT-rich gene-poor regions containing long interspersed L1 (LINE) elements which

are retroposon-derived and homologous between species (Silver, 1995). However, the lighter R-bands correspond to GC-rich gene-rich regions containing short interspersed sequences (SINE elements). SINE elements appear to have evolved out of small cellular RNA species. Unlike LINE elements, they appear to have originated independently in different species. In humans, the SINE elements belong primarily to one family - the Alu sequence elements which derive from 7SL RNA, a small cytoplasmic species involved in protein synthesis. In the mouse, the majority of SINE elements belong to the B1 and B2 families which are quite divergent from the Alu sequences, although the B1 element also appears to have been derived from 7SL RNA independently of the Alu family. Early FISH experiments revealed the close correlation between G-banding patterns and these repetitive sequence families in the two genomes, and this is thought to reflect differences in chromosomal structure between G and R-bands, which may prejudice the differential integration of LINEs and SINEs into genomic regions. There is a report from a laboratory using atomic force microscopy to examine the physical structure of chromatin, which states that constricted regions exist on (untreated) metaphase chromosomes which correspond exactly to the G-banding pattern that would be obtained after giemsa-trypsin treatment (Musio *et al.*, 1994). Thus, the differently banded regions almost certainly relate to underlying structural differences at the chromatin level.

Regardless of the underlying mechanisms involved, G-banding mouse chromosomes and subsequent identification proved to be a significant challenge. G-banded chromosome spreads with transgene integration sites marked with arrows were sent to an independent cytogenetics laboratory (M. Lee, MRC HGU, Edinburgh) for an expert opinion as to the chromosomal identity. The preliminary assignments from this were used to design linkage mapping experiments by informing the choice of sets of primers for microsatellite PCR (discussed below).

In addition to this, as an alternative method for unambiguous chromosomal assignment, double FISH was attempted: Using the mouse genome database (http://www.informatics.jax.org, 1999) to identify suitable probes, various phage lambda clones containing some 12-20kb of genomic sequence were

obtained. The genomic clones were chosen on the basis of their origin within the "best guess" chromosomes from the G-banded FISH experiments, and were selected to lie in a region of the target chromosomes distinct from the transgene integration site. In the double FISH experiments, the genomic clones and the transgene probe were differentially labelled to yield a red and a green signal after FISH. Co-localisation of the signals on the same chromosome would provide an unambiguous map position for the transgene integration.

It must be pointed out that a similar experiment could have been performed using "chromosome paints". These are derived either from chromosome-specific repetitive sequences which span the full length of the chromosome, or from chromosome-specific alpha-satellite sequences localised to the centromere. They are therefore used to "paint" a specific chromosome a distinctive fluorescent colour following FISH. They can be purchased pre-labelled for all 21 mouse chromosomes (Ventana Medical Systems). However, each individual paint costs in excess of £200, and with several provisonally assigned target chromosomes to choose from, this was deemed to be a prohibitively expensive approach.

Linkage mapping - background and strategic considerations

Linkage mapping of loci - in this case a mutant allele associated with the transgene - is based upon the ability to detect other loci of known position on the genetic map, and showing some degree of association during breeding crosses between the allele of interest and mapped loci. This hinges upon two key factors:

Firstly, successful detection of a polymorphism at the locus of interest. In the case of the **Harry** line, this was trivial - the transgene itself acts as a dominant allele, and its presence can be easily detected by luciferase assay. Furthermore, from the genotyping experiments, it was known that any mutant animal, by definition, was homozygous for the transgene. Therefore, the exact transgenic genotype could readily be determined for all animals.

Secondly, detection of a variety of polymorphisms throughout the mouse genome at known map positions. There are a variety of approaches to this, and the main ones can broadly be classified as using: phenotypic loci (classical); restriction fragment length polymorphisms (RFLP); interspecific backcrosses;

recombinant inbred (RI) strains; PCR of microsatellite and other short sequence-tagged sites.

Classically (i.e. prior to the development of recombinant DNA techniques in the late 1970s), new mutant loci were mapped with respect to visible, phenotype loci. This required enormous breeding programmes, and had the distinct drawback that, even in an inbred laboratory animal like the mouse, where a novel allele can be bred onto a specialised genetic background carrying multiple visible genetic markers, there simply aren't enough visible traits which can be used as markers to provide detailed coverage of the genome. This is illustrated by the observation that when the first genetic map of the mouse was published in 1941, it listed a mere 24 loci, of which 9 had not been assigned to any linkage group (Silver, 1995). This should be viewed in light of the fact that mouse genetics was a 26-year old science at this point.

The application of recombinant DNA methodologies to the problem of detecting genetic polymorphisms resulted in the development of restriction fragment length polymorphism (RFLP) mapping. This hinges around neutral nucleotide substitutions creating or removing restriction enzyme recognition sites at various positions throughout the genome. Digesting genomic DNA with suitable restriction enzymes and probing with an appropriate DNA fragment gives a diagnostic pattern of bands on a Southern blot. In humans, given the highly out-bred nature of the population, a large number of RFLPs can invariably be found between two individuals, even closely related ones (excepting identical twins). Given a DNA probe for a test locus, a polymorphism can almost always be found.

In the mouse, RFLPs initially offered the possibility of an abundance of neutral (i.e. non-phenotypic) polymorphisms scattered throughout the genome which could be mapped and used as a reference framework for mapping novel alleles. Unfortunately, early studies of the mouse genome using RFLPs quickly revealed that all the classical inbred strains of laboratory mouse were more closely related than had been previously thought. For example, all the mitochondrial genomes were found to be identical, implying maternal lineage leading back to a single common female ancestor, who may have lived as recently as 1920 (Ferris *et*

al., 1982). It is highly probable that during the derivation of the classical inbred strains during the early 20th century, interstrain contamination and interbreeding was much more prevalent than the records of the time suggest. The end result is that it is relatively difficult to find sufficient RFLPs between two classical inbred strains to be useful for the purposes of genome-wide linkage scanning.

This frustrating situation was resolved with the discovery that a separate species of mouse - *M. spretus* - could be bred with laboratory mice (which are all strains of the species *M. musculus*) (Silver, 1995). Spretus males crossed with laboratory females generate viable offspring, of which the males are sterile but the females viable. These interspecific F_1 hybrid females can be backcrossed to inbred laboratory males in mapping crosses. The signal advantage of this interspecific breeding protocol is that some 3 million years of evolution separate the two species. As a consequence, the genomes are highly divergent and RFLPs can be found for practically every DNA probe tested.

The *spretus* backcross revolutionised mouse genetics in the 1980s and many hundreds of loci were quickly placed on the genetic map. Large "panels" of DNA samples from interspecific backcrosses were prepared and made available to the community. The power of these panels derives from the hundreds of loci that have already been typed on them. If a new locus is found to show a polymorphism, it can be tested against an existing panel. This effectively acts as a backcross without actually having to perform the breeding experiment, and the locus can be rapidly mapped. This approach has been most effective in the mapping of new genes following the cloning of their cDNA, and large-scale collaborative backcross panels exist for this purpose.

The fourth approach, the use of recombinant inbred strains (RI) bears some similarities to an interspecific backcross panel in that it gains its power from the accumulation of data from typing hundreds of loci on a pre-existing panel. Unlike interspecific backcross panels, however, where the DNA in a given panel is a finite resource, the DNA used is derived from sets of inbred RI strains and therefore represents an inexhaustible resource.

Briefly, since this approach is inappropriate for mapping a transgene (until a flanking polymorphism has been obtained), a set of RI strains is derived by

crossing two inbred lines to generate a population of genetically homogenous F_1 animals and then further in-crossing these F_1 progeny to generate a population of F_2 animals. The chromosomes of these F_2 animals will each contain a random assortment of segments derived from each parental genotype. At this stage, F_2 males and females are selected randomly and inbred for at least 20 generations to create a true, inbred strain, with >99.8% homozygosity fixed into the genome. Multiple strains can be created from the same initial inter-strain cross, and these are collectively known as a set of RI strains.

Each RI strain can effectively be viewed as a "frozen" set of meiotic cross-overs between the parental strains, with each chromosome containing alternating segments from each genome. With the accumulation of large datasets for sets of RI strains, new loci which are found to be polymorphic between the two parental strains of a given set can be very quickly mapped by testing the new probe against the relevant RI panel. Various panels now exist, and some have been typed for very large numbers of known markers to give strain distribution patterns (SDPs) for each locus. By way of illustration of the power of this approach to mapping, provided that a polymorphism can be demonstrated for a locus of interest between the two parental strains of the BXD RI set (C57L6 and DBA), all that is required is that each strain in the set is typed once for this polymorphism. In the case of the BXD set, this amounts to typing 26 strains by Southern blotting or PCR. With over 1500 loci already typed for the set, by comparing the SDP of the new locus to existing datasets this can immediately give a map position to within <10cM, and possibly much less (http://www.informatics.jax.org, 1999).

In the context of mapping a transgene integration site, the existing interspecific backcross and RI panels are unfortunately useless, since the polymorphism at the test locus (i.e. the transgene) simply will not exist in the test DNA (unless some genomic sequence flanking the transgene integration has been obtained and a polymorphism established). The easiest solution in this case would therefore be to generate a new panel by performing an interspecific backcross between *spretus* and the transgenic line of interest. Clearly, the resulting panel would have to be typed *de novo* for a large number of markers - a

formidable undertaking. Generating a set of RI strains from the transgenic line and some other strain would be an even larger task.

Fortunately, in the 90s, an alternative solution has become available utilising polymorphic PCR-based DNA markers, often microsatellites. The most common class of microsatellite-based markers consist of a variable-length region of di-nucleotide repeats flanked by unique sequences to which PCR primers can be designed. Their usefulness derives from the fact that the long dinucleotide repeat structures (microsatellites containing runs of $(CA)_n$ and $(GA)_n$ are most commonly utilised) will very frequently mispair during recombination or replication. This "slippage" leads to contraction or expansion of the length of the repeat. The actual size of the microsatellite is therefore highly polymorphic, even between inbred mouse strains. Estimates of the mutation frequency are complicated by position and sequence-dependent effects, but one detailed study concluded that the rate of mutation per microsatellite locus per generation was 5-50 fold higher than that observed at classical loci (Dietrich *et al.*, 1992). In practical terms, this means that the microsatellites mutate fast enough to generate polymorphism between inbred strains, but not so fast that they cannot be followed through several generations within a given strain background.

A given pair of PCR primers will generate a short product (generally primers generating products of 50-400bp are used), and the exact size of this product may well be polymorphic between mouse strains. Detecting polymorphism is simply a matter of running the PCR reactions out on a high-resolution gel. The power of this approach was quickly recognised, and a great deal of effort was therefore put into establishing a very large number of typed markers and placing them on the genetic map, with PCR product information (i.e. band size) available for a number of inbred strains. The report published by the team at the Whitehead Institute in 1996 contained 7,377 genetic markers, consisting of 6,580 highly informative simple sequence length polymorphisms (mainly microsatellite PCRs), integrated with 797 restriction fragment length polymorphisms (the difference between these two numbers speaks to the much lower rate of polymorphism found between mouse strains using restriction enzymes) and placed on the mouse genetic map (Dietrich *et al.*, 1996). This gave

an average of one marker per 0.2cM - roughly one every 400kb in the mouse. Many more have continued to be added since that time. The Whitehead Institute maintains a database which details map positions, microsatellite sequence, PCR primers, reaction conditions and predicted product sizes for a large number of typed strains (Whitehead Institute, MIT, 1999). Their last set of collated data lists some 12,000 markers for the mouse genome. Research Genetics have made most of the primer pairs detailed on the Whitehead Institute database available to the genetics community at low cost (Research Genetics Inc., http://www.resgen.com, 1999).

Transgene integration site mapping by genome-wide linkage scan

With reference to the Methods chapter, it will be seen that all transgenic lines in this study were originally derived by micro-injection of construct DNA into a C57/CBA F^1 zygote. With only one integration site in the case of **Harry**, it logically follows that the transgene integrated into either a paternally-derived C57 chromosome or a maternally-derived CBA chromosome. During subsequent breeding, a mixture of incrossing between hemizygous animals and outcrossing to non-transgenic C57/CBA F_1 animals was used. There was no particularly strict rationale to this - incrossing was used preferentially to maintain strains and generate mutants, with outcrossing as required when stocks were low to reinject "hybrid vigour" back into the line and quickly build up numbers. The end result of this has been the generation of transgenic lines containing an heterogenous mix of C57 and CBA genomes in variable proportions.

Although microsatellite PCRs are not well documented for the CBA strain, it is quite closely related to the C3H strain and data for this strain, and for C57, do exist. The degree of similarity between CBA and C3H lies in the fact that both lines derive from the same original cross, with CBA selected for a low mammary tumour incidence and C3H for a high incidence (Strains Listing http://www.informaticsjax.org, 1999). Hence, primers polymorphic between C57 and C3H are likely to also be polymorphic between C57 and CBA.

The chromosomal segment containing the transgene will have retained its original genetic character (i.e. C57 or CBA) out as far as the closest recombinational breakpoints. Thus, if the transgene integrated into the C57

chromosome, closely-linked markers for the transgene are highly likely also to be C57 alleles. Given the heterogeneity of the genetic background in **Harry** mice, it would have been difficult to perform a backcross to either C57 or CBA purebred mice, since many of the loci in **Harry** are likely to be homozygous for a given background.

One strategy would have been to backcross **Harry** hemizygotes to a third background containing a third allele at all test loci which could be distinguished from both C57 and CBA alleles.

An alternative would have been to transfer the transgene (and its associated chromosomal segment) onto a pure inbred background (introgression) and to perform a more standard 2-background backcross from there. Formally, this would have necessitated breeding each test line onto the chosen background for at least 10 generations followed by an intercross to create a congenic line (Flaherty, 1981). This can take upwards of 2.5 years. With the aid of test PCRs to determine which of the offspring at each generation carried the maximum amount of the target background this can be reduced to 5 generations (marker assisted selection protocols or "speed congenics") (Markel *et al.*, 1997; Wakeland *et al.*, 1997). However, even combined with super-ovulation of pre-sexual females and *in vitro* fertilization of the oocytes to reduce generation time ("super-sonic congenics"), this would still have required the best part of a year to achieve.

Regardless of the method used, given a suitable backcross protocol for the **Harry** line, a genome-wide linkage scan would require a bare minimum of a backcross panel of 72 animals typed for 46 well-spaced markers (Silver, 1995). This approach requires the investigator to perform and analyze >3000 PCR reactions and to purchase some £1000 worth of PCR primers, simply to gain an initial map position to within ≤20cM of the transgene integration site. Further primers would need to be purchased for finer mapping of the integration site and a larger backcross panel would be required. In the particular case of **Harry**, some of the primer pairs might prove not to be polymorphic between C57 and CBA (this was indeed found to be the case for ~10% of primers purchased and used in our laboratory), in which case more primers might need to be purchased to complete the scan.

Overall, genome-wide linkage scanning can be considered to be an effective and powerful method for rapidly mapping a transgene integration site provided the laboratory is already set up for performing and analyzing large numbers of PCR reactions, and provided that the expensive resources (hundreds of PCR primers) have already been purchased. For a small laboratory not already performing such analyses, such as ours, the cost and time involved was deemed prohibitive unless a large number of lines were to be analysed. The heterogenous genetic background of our transgenic lines added extra difficulties to such an approach.

Use of microsatellite PCR to rapidly screen candidate loci

Although, for the reasons discussed above, a genome-wide linkage scanning approach was ruled out, with some candidate loci emergent from the phenotype studies and with data from the G-banded FISH experiments, an attractive alternative presented itself: Microsatellite PCRs could be performed using only a few primers specific for markers known to be close to the putative integration site, or close to attractive candidate loci such as *Ednrb*.

The nature of the transgene integration assisted greatly in this, since, as discussed above, the transgene in **Harry** logically had to reside in a chromosomal segment containing either C57 or CBA alleles. Homozygous **Harry** mutants therefore would almost certainly be homozygous for closely-linked genetic markers unless a meiotic recombination breakpoint happened to lie close to the transgene. Rather than performing a backcross and analyzing all offspring, simple analysis of only the mutants from hemizygous intercrosses could be performed. Provided that at least one of the parents was shown to be heterozygous at a given test locus, homozygosity in a sufficient number of mutant animals would provide proof of linkage. In effect, this can be viewed as a rather complicated backcross:

It will be seen that if one parent is heterozygous and one homozygous at a test locus, this is identical to a conventional backcross protocol and each mutant animal resulting from the cross is the equivalent of one backcross offspring i.e. one informative meiosis (**Figure 14a**).

Fig. 14 Informative meioses from two different backcross schemes

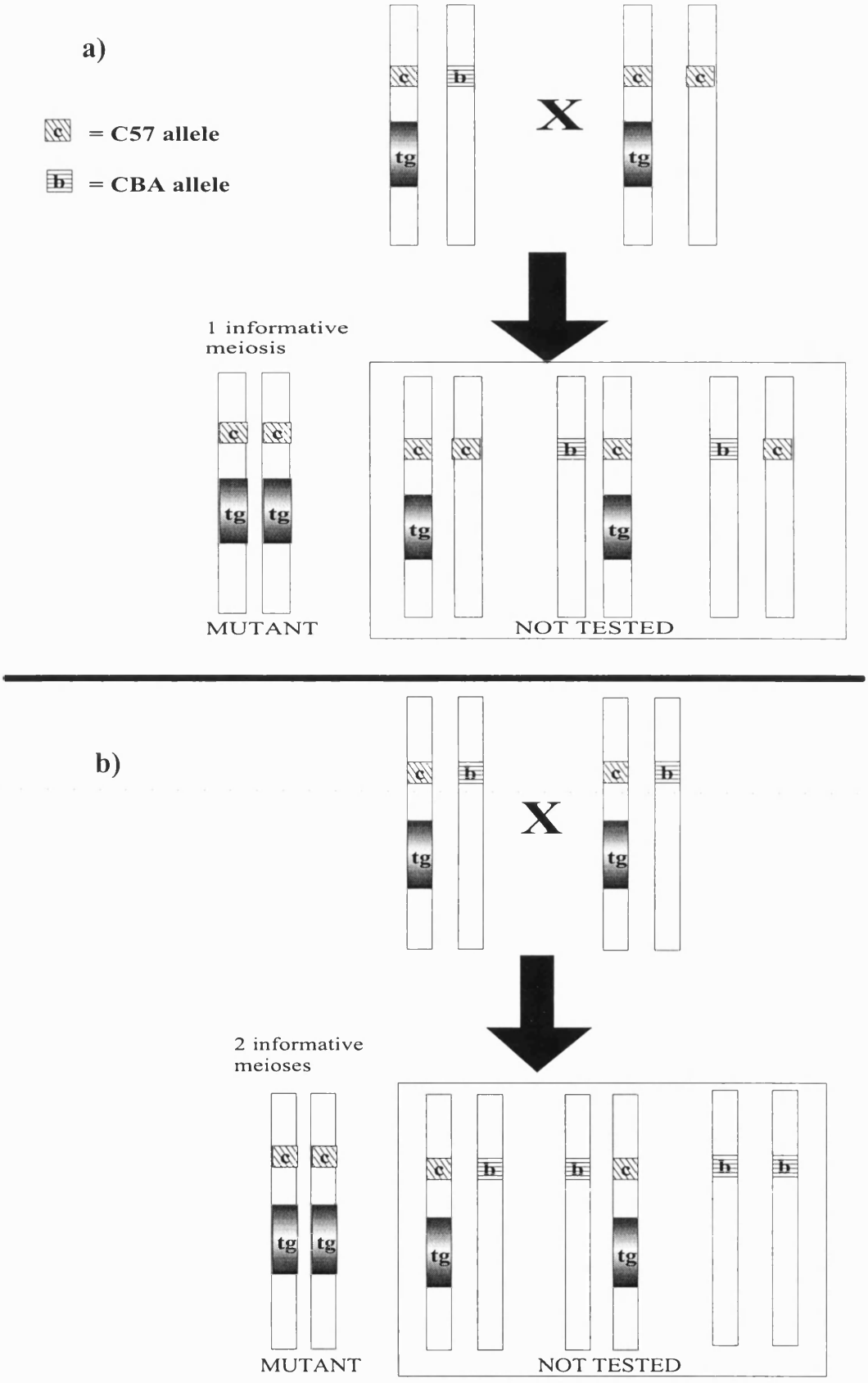

a) If only one parent is polymorphic (heterozygous) at a given test locus, the cross is equivalent standard backcross, yielding one informative meiosis per mutant offspring.
b) If both parents are heterozygous, each mutant (homozygous for the transgene by definition) yields **two** informative meioses at the locus under test.

Similarly, if both parents are heterozygous, each mutant animal is equivalent to two backcross samples i.e. two informative meioses (**Figure 14b**). In both cases, homozygosity at a given locus for any mutant animal indicates no recombination with respect to the transgene. No linkage between the transgene and the locus under test gives a Mendelian distribution of genotypes in the mutants, depending upon the exact genotypes of the parents.

Results

Mapping by FISH

A number of chromosome spreads derived from **Harry** hemizygotes were G-banded, destained and subsequently hybridised with the transgene probe. It was clear from these experiments that the transgene had integrated into a medium-length chromosome around two-thirds of the way down from the centromere. The G-banding pattern suggested Chr 15, but was not considered sufficiently unambiguous for confidence in this result (**Figure 15**).

Double FISH was attempted with the *Lifr* probe (which maps to proximal Chr 15) and the transgene construct, but this was unsuccessful - multiple signals were obtained with the *Lifr* probe and it was impossible to distinguish the Chr 15-specific signal (data not shown).

Linkage mapping

Following FISH analysis, the candidate locus microsatellite PCR linkage approach was adopted and primers were chosen, using the Whitehead Institute database, such that at least 2 primer pairs close to the *Dom, Ednrb* and *Edn3* loci on chromosomes 15, 14, and 2 respectively were tested (Whitehead Institute, http://www.genome.wi.mit.edu/, 1999; Copeland *et al.*, 1993;Dietrich *et al.*, 1994;Dietrich *et al.*, 1996) The primers chosen were selected on the bases that they were close to the candidate gene (within 1cM in all cases), and polymorphic between C57 and C3H strains, in the hope that this would extend to CBA mice, as explained earlier.

Figure 15. Transgene mapping by combined FISH and G-banding

Metaphase chromosome spreads from a hemizygous **Harry** animal, G-banded and then hybridised with a transgene probe using FISH.

a) FISH signal from the previously G-banded metaphase chromosome spread shown in b). One transgene signal is visible (arrow).

b) G-banding from the corresponding metaphase chromosome spread.

c) - f) Other G-banded spreads from the same slide, with transgene signals arrowed.

Figure 15

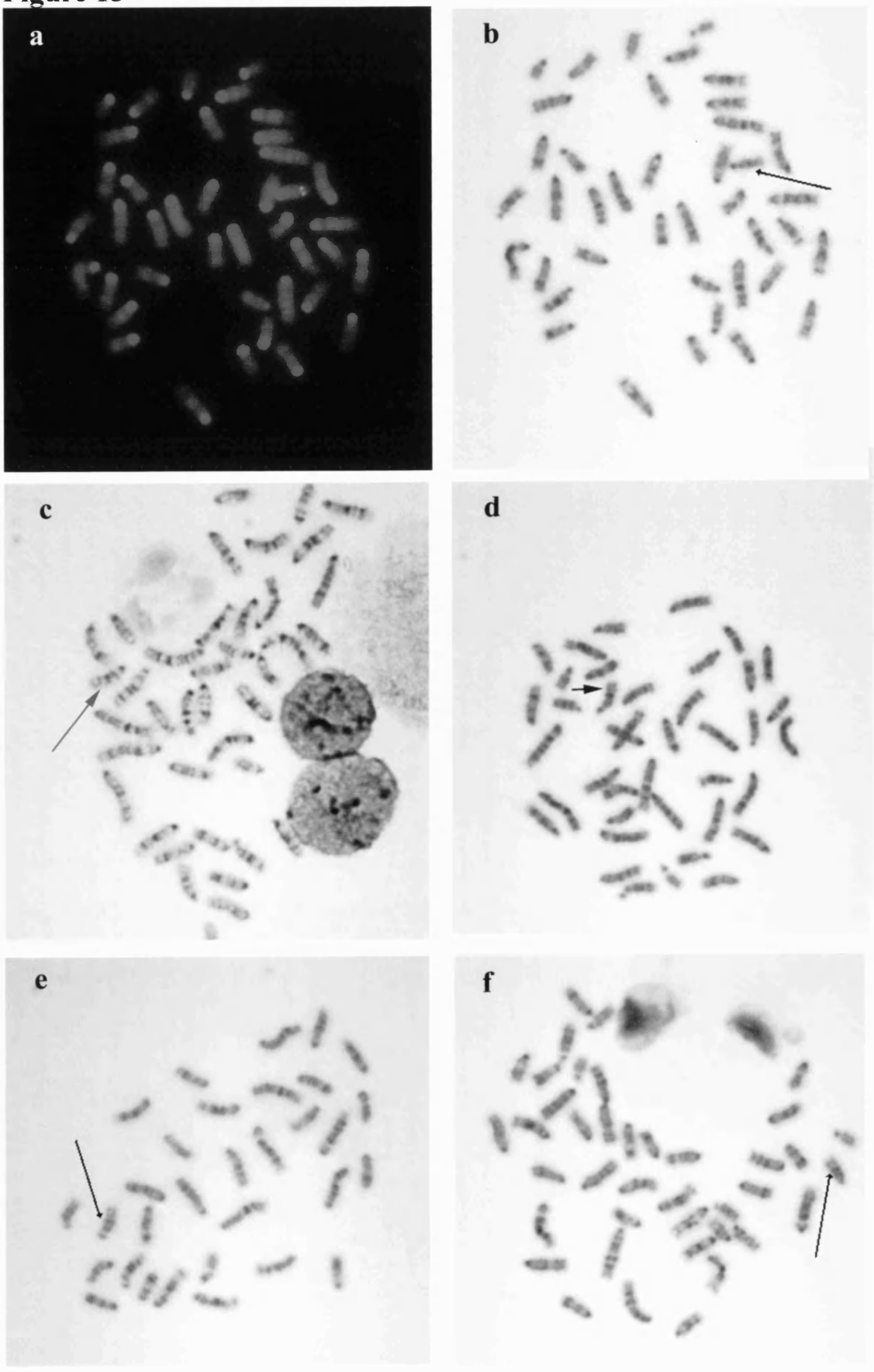

Table 8. Microsatellite PCR genotyping results for Harry

Animal	Parental Cross	D15Mit71 genotype	D15Mit1 genotype	D15Mit2 genotype	D14Mit197 genotype	D2Mit148 genotype
+/- parents						
4.2♂	n/a	C57	C57	C57	CBA	CBA
4.9f♀	n/a	F1	F1	F1	C57	C57
4.1♂	n/a	C57	C57	C57	CBA	F1
4.11♀	n/a	F1	F1	F1	C57	CBA
4.3♂	n/a	C57	C57	C57	F1	F1
4.5♀	n/a	C57	C57	C57	C57	F1
4.4♂	n/a	F1	F1	F1	F1	F1
4.6♀	n/a	F1	F1	F1	C57	CBA
+/+ mutants						
A1	4.4♂ x 4.6♀	C57	C57	C57	C57	F1
B1	4.3♂ x 4.5♀	n/t	n/t	n/t	C57	F1
B2	4.3♂ x 4.5♀	n/t	n/t	n/t	C57	F1
B3	4.3♂ x 4.5♀	n/t	n/t	n/t	F1	F1
C1	4.4♂ x 4.6♀	C57	C57	C57	F1	F1
C2	4.4♂ x 4.6♀	C57	C57	C57	F1	F1
D1	4.3♂ x 4.5♀	n/t	n/t	n/t	F1	F1
D2	4.3♂ x 4.5♀	n/t	n/t	n/t	F1	C57
E1	4.4♂ x 4.6♀	C57	C57	C57	C57	CBA
E2	4.4♂ x 4.6♀	C57	C57	C57	F1	F1
E3	4.4♂ x 4.6♀	C57	C57	C57	F1	F1
F1	4.3♂ x 4.5♀	n/t	n/t	n/t	F1	F1
F2	4.3♂ x 4.5♀	n/t	n/t	n/t	C57	n/t
J1	4.4♂ x 4.6♀	C57	C57	C57	C57	n/t
J2	4.4♂ x 4.6♀	C57	C57	C57	C57	n/t
K1	4.3♂ x 4.5♀	n/t	n/t	n/t	F1	n/t
K2	4.3♂ x 4.5♀	n/t	n/t	n/t	F1	n/t
L1	4.1♂ x 4.11♀	C57	C57	C57	F1	n/t
M1	4.2♂ x 4.9♀	C57	C57	C57	F1	n/t
M2	4.2♂ x 4.9♀	C57	C57	C57	C57	n/t
N1	4.4♂ x 4.6♀	C57	C57	C57	n/t	n/t
P1	4.2♂ x 4.9♀	C57	C57	C57	n/t	n/t
P2	4.2♂ x 4.9♀	C57	C57	C57	n/t	n/t
Q1	4.1♂ x 4.11♀	C57	C57	C57	n/t	n/t
R1	4.2♂ x 4.9♀	C57	C57	C57	n/t	n/t
S1	4.2♂ x 4.9♀	C57	C57	C57	n/t	n/t
S2	4.2♂ x 4.9♀	C57	C57	C57	n/t	n/t
S3	4.2♂ x 4.9♀	C57	C57	C57	n/t	n/t
S4	4.2♂ x 4.9♀	C57	C57	C57	n/t	n/t
S5	4.2♂ x 4.9♀	C57	C57	C57	n/t	n/t
T1	4.1♂ x 4.11♀	C57	C57	C57	n/t	n/t
T2	4.1♂ x 4.11♀	C57	C57	C57	n/t	n/t
U1	4.4♂ x 4.6♀	C57	C57	C57	n/t	n/t
V1	4.2♂ x 4.9♀	C57	C57	C57	n/t	n/t
V2	4.2♂ x 4.9♀	C57	C57	C57	n/t	n/t
V3	4.2♂ x 4.9♀	C57	C57	C57	n/t	n/t
W1	4.1♂ x 4.11♀	C57	C57	C57	n/t	n/t
W2	4.1♂ x 4.11♀	C57	C57	C57	n/t	n/t
W3	4.1♂ x 4.11♀	C57	C57	C57	n/t	n/t
W4	4.1♂ x 4.11♀	C57	C57	C57	n/t	n/t
X1	4.4♂ x 4.6♀	C57	C57	C57	n/t	n/t
Informative meioses		**43**	**43**	**43**	**17**	**18**

n/a = not applicable n/t = not tested

During test PCRs, some primers were found not to be polymorphic between these strains and these were discarded.

Four **Harry** hemizygous intercrosses were set up, and DNA samples prepared from the parents and from a number of resultant mutants. Initially, the parents were typed for all the markers used in this study, and only the mutants from informative crosses were tested for particular markers.

Following test PCRs to establish polymorphism (data not shown) genomic DNA from homozygous mutants was initially tested with 2 markers close to *Sox10* on Chr 15, one marker close to *Ednrb* on Chr 14 and one marker close to *Edn3* on Chr 2. From cursory inspection, it was clear that both the Chr 2 and 14 markers showed what appears to a Mendelian distribution of genotypes, particularly since hemizygous parents showed homozygosity for both CBA and C57 genotypes (**Figure 16**). While the numbers tested were not statististically significant, they strongly suggested non-linkage to either *Ednrb* or *Ednr*.

On the other hand, all the mutants tested were homozygous for the C57 allele of both the Chr 15 markers, suggesting linkage. Further mutants were tested with 3 separate Chr 15 markers to confirm linkage. The data from all microsatellite PCRs performed are summarised in **Table 8**

In all, 43 informative meioses were found to show no recombination between the transgene and D15Mit1, D15Mit2 and D15Mit71, with the C57 allele present in all cases (indicating that the transgene had integrated into the paternally derived C57 chromosome). Using Genelink software and the mapping data table from Silver (see Appendix B), given zero recombination between each of these three markers and the transgene, they are linked within 8cM of each other with a 95% confidence limit.

Discussion

The FISH mapping proved slightly ambiguous due to the technical difficulty of obtaining high-quality G-banding and making subsequent chromosomal assignments. However, the transgene had clearly integrated in the central region of a medium-length chromosome. This almost certainly ruled out *Edn3* as a candidate locus, since this lies at the distal end of Chr2 - a long

Figure 16. Microsatellite PCR gels

Scanned silver-stained sequencing gels, showing representative results obtained with 4 of the microsatellite PCR primer pairs used in the linkage mapping studies. Note that fainter satellite bands frequently appear above and below the specific major product, particularly when the PCR reaction is analyzed under denaturing conditions, as here.

Figure 16

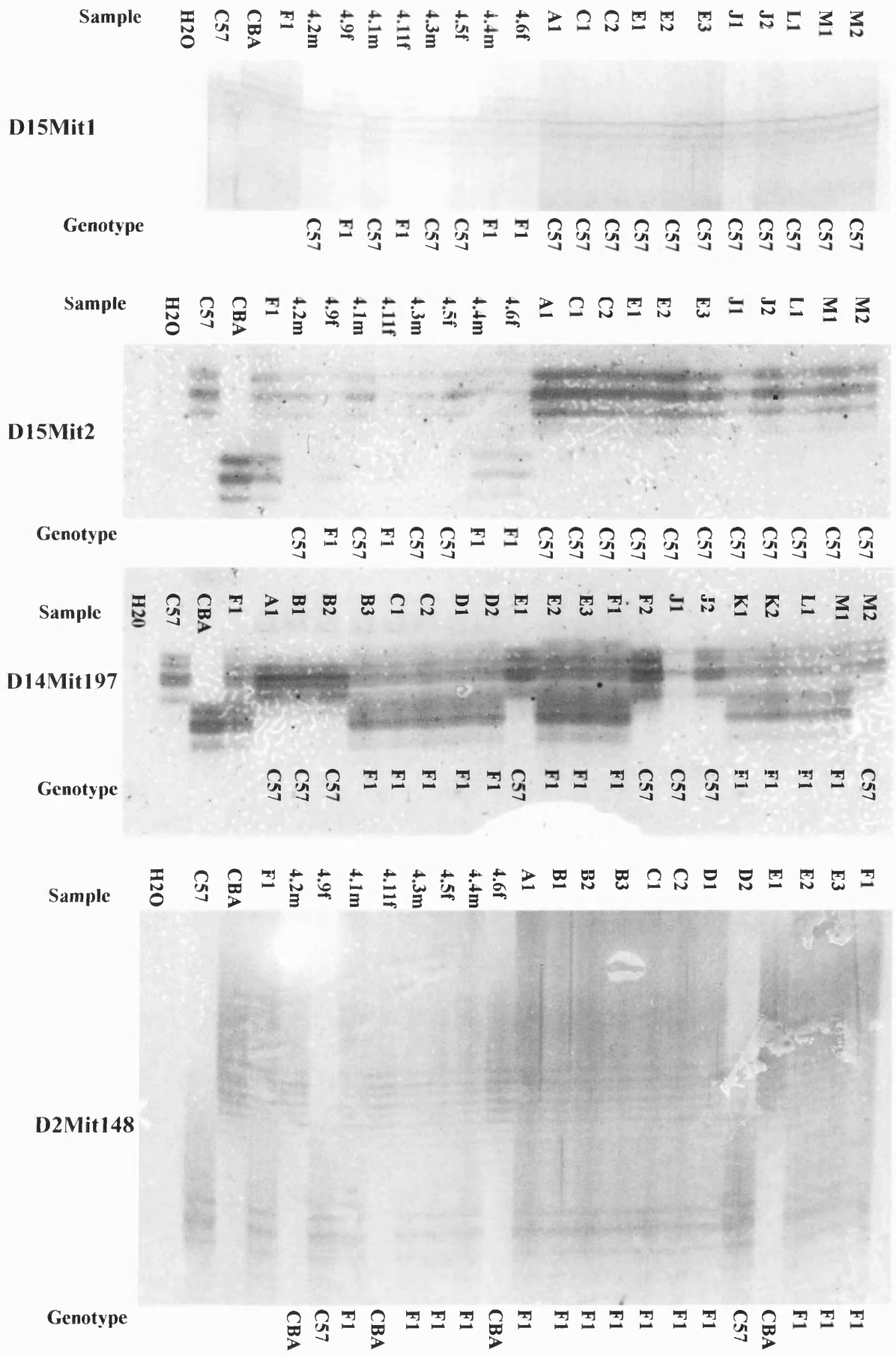
Sample
H2O C57 CBA F1 4.2m 4.9f 4.1m 4.11f 4.3m 4.5f 4.4m 4.6f A1 C1 C2 E1 E2 E3 J1 L1 J2 M1 M2
D15Mit1
Genotype
C57 F1 C57 F1 C57 F1 C57 C57 C57 C57 C57 C57 C57 C57 C57 C57 C57 C57 C57 C57 C57
Sample
H2O C57 CBA F1 4.2m 4.9f 4.1m 4.11f 4.3m 4.5f 4.4m 4.6f A1 C1 C2 E1 E2 E3 J1 L1 J2 M1 M2
D15Mit2
Genotype
C57 F1 C57 F1 C57 F1 C57 C57 C57 C57 C57 C57 C57 C57 C57 C57 C57 C57 C57 C57 C57
Sample
H20 C57 CBA F1 A1 B1 B2 B3 C1 C2 D1 D2 E1 E2 E3 F1 F2 J1 J2 K1 K2 L1 M1 M2
D14Mit197
Genotype
C57 C57 C57 F1 F1 F1 F1 C57 F1 F1 F1 F1 C57 C57 F1 F1 F1 F1 F1 F1 C57
Sample
H2O C57 CBA F1 4.2m 4.9f 4.1m 4.11f 4.3m 4.5f 4.4m 4.6f A1 B1 B2 B3 C1 C2 D1 D2 E1 E2 E3 F1
D2Mit148
Genotype
CBA C57 F1 CBA F1 F1 F1 F1 F1 F1 F1 F1 F1 F1 F1 F1 F1 F1 F1 F1 F1 F1

chromosome. However, both *Ednrb* and *Sox10* lie in the central region of Chrs 14 and 15, respectively. The preliminary assignment from the G-banded FISH experiments pointed towards Chr15, suggesting that the transgene might have integrated close to the *Sox10* gene.

Linkage mapping using microsatellite PCR primers confirmed this, first with non-linkage being strongly suggested between the transgene and markers close to *Ednrb* and *Edn3*, and then with no recombination observed between the transgene and three Chr 15 markers in 43 informative meioses. All three markers lie very close to *Sox10* on Chr 15. (D15Mit1, D15Mit2 and D15Mit71 have previously shown 0,2 and 1 recombinants with *Sox10* in a 252-animal interspecific backcross (Puliti *et al.*, 1995).

Given a distance of 8cM between the transgene and these markers with a 95% confidence limit, **Figure 17** shows a graphical representation of all loci within 15cM of *Sox10* which are known to cause a coat colouration phenotype.

Figure 17. Coat colouration loci within 15cM of *Sox10*

(Mouse Genome Database, 1999)

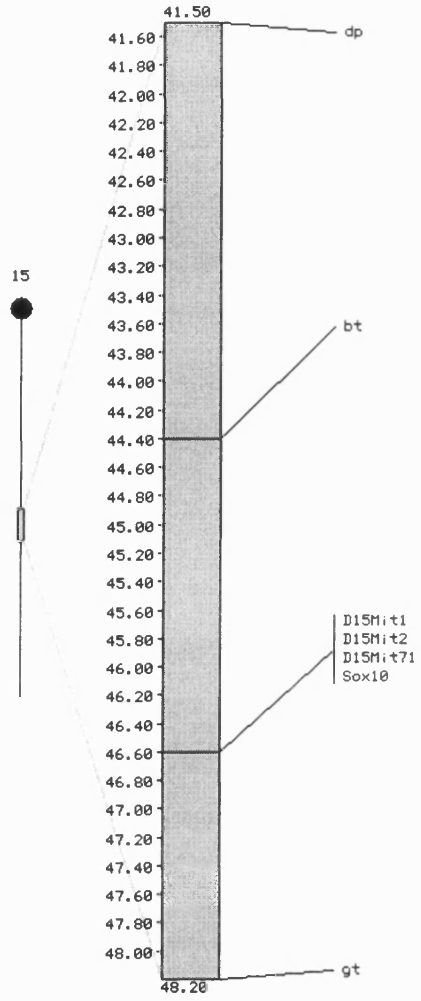

(Distances from the centromere are shown in cM down the left-hand side.)

Sox10 remains the obvious candidate, however there exist three other loci known to affect coat colour in the mouse which lie nearby which could also be considered as candidates, since all lie within the 95% confidence limit.

dp (Dilution-Peru)

The *dp* locus (Dilution-Peru) lies well within the 95% confidence limit, some 5cM away from the markers tested. *dp* arose from a cross between CBA and a Peru-Harland female. *dp* homozygotes show a relatively mild phenotype featuring only diluted coat colour, slightly darker than that of misty, which is itself merely a slight lightening of normal coat colour (*m/m*) (Lyon *et al.*, 1996).

The *dp* gene product is unknown and mutants are viable and fertile (Wallace, 1971). This can probably be eliminated as a candidate locus for transgene integration, largely on the grounds that whilst very little is known about the affected locus, the phenotype does not resemble that seen in **Harry** homozygotes whilst there are much stronger candidates nearby. Mutations which give rise to the coat spotting seen in **Harry** mutants tend to affect melanoblast migration and/or survival during development, giving rise to large patches of unpigmented skin which entirely lack melanocytes. On the other hand, mutations which dilute coat colour tend to exert an effect during melanocyte terminal differentiation, such as *Myo5a* (dilute) which affects melanocyte morphology, or mutations which affect melanogenesis, such as Tyr^{c} (albino) (Yokoyama *et al.*, 1990; Mercer *et al.*, 1991).

bt (belted)

A similar argument pertains to *bt*, the belted locus, which lies within the mean distance estimated between the transgene and the markers tested. *bt* arose as a spontaneous mutation in the DBA strain, and as the name suggests, shows a mild coat colour phenotype, with homozygotes having a white belt across the back in the midtrunk region and a white belly patch. These sometimes coalesce to form a continuous white belt. *bt* was first described in 1945 and has a long history of use as a visible marker in mapping crosses. As a consequence, there is a great deal more mapping data for this locus than for *dp*. (*bt* has however, been shown to show recombination with respect to the *dp* locus (Wallace & Green, 1974).) The gene product of *bt* is also currently unknown, and even although it shows no enteric phenotype it is not inconceivable that it is a hypomorphic allele of *Sox10*. However, in the original paper describing the *Dom* mutation at the *Sox10* locus, *Dom* was shown to recombine with *bt* in 26/252 animals in a *Dom*/+ x *bt*/+ cross, giving a recombination fraction of 10.3%, according to the author's calculations (Lane & Liu, 1984). This suggests close linkage between *bt* and *Sox10*, but not allelism. In support of this, recent fine mapping studies, as yet unpublished, have shown that *bt* lies at least 5cM away from *Sox10* (D. Foernzler, pers. comm.).

Even given that *bt* is a separate locus from *Sox10*, this does not preclude its being disrupted by the transgene. However, the gene function of *bt* would have

to closely parallel that of *Sox10*, since the phenotype observed in **Harry** homozygotes matches that seen in $Sox10^{Dom}$ heterozygotes almost exactly.

gt (grey tremor)

The third locus shown in figure 17, *gt* (grey tremor), lies within 2cM of *Sox10*. This locus is another recessive mutation in an unidentified gene which arose spontaneously in mouse stocks at the Jackson Labs, and homozygotes have reduced yellow coat pigment (hence grey), white feet, tail and belly and a white blaze on the head (Sweet, 1981). Besides this coat colour phenotype, they also display a neurological defect, with tremor and convulsions from around day 8 post-partum. Most homozygotes die by 3 months of age, but when *gt* was introgressed onto a heterogenous genetic background many mutants were found to survive and were viable. Histopathology revealed that *gt/gt* homozygotes suffer from extensive de-myelination in the peripheral and central nervous system, coupled with severe progressive spongiform encephalopathy in the CNS and early death. Heterozygotes appeared normal but suffer from mild spongiform encepalopathy in the CNS from around 2 months of age onward (Sidman *et al.*, 1985).

Detailed histopathological examination of *gt/gt* mutants revealed that in homozygotes, the encephalopathy manifested as extensive vacuolation of grey and white matter. Vacuoles in white matter were found to be caused by interlamellar splitting of myelin sheaths. Astrocytes lacked vacuoles and seemed substantially unaffected. Dendrites were focally swollen and contain irregular vacuoles. By the end of the first month post-partum, virtually the entire neuraxis was involved with vacuolation more severe in grey than in white matter. Astrocytic proliferation was mild and neuronal loss inconspicuous.

No virus particles or "scrapie-associated fibrils" were found. However, the progressive spongiform encephalopathy was highly reminiscent of the disease patterns seen in BSE, Creutzfeld-Jakob syndrome, kuru, scrapie and other such syndromes attributed to unconventional transmissible agents. In two separate studies, wild-type mice from strains susceptible or resistant to scrapie or certain murine viruses were inoculated intracerebrally with homogenised extract from the brains of severely affected *gt/gt* homozygotes (Sidman *et al.*, 1985; Hoffman *et*

al., 1987). In both cases, the mice were found to develop mild CNS phenotypes (slight tremor or hunching, some evidence of vacuolation) and *gt* mice were concluded to harbour a transmissible agent with an unusually long incubation time. It was unknown whether the *gt* locus itself represented a susceptibility locus to this agent, or whether it represented the site of integration of the agent into the host genome, permitting vertical transmission through the germline.

At the time the original studies were carried out, BSE had not become the *cause celébrè* it is today and no further reference to *gt* mice appears in the literature for ten years. However, a recent study flatly contradicted the transmissible agent hypothesis, finding no evidence of any phenotype transmitted by intracerebral inoculation of *gt/gt* brain homogenate (Carlson *et al.*, 1997). They suggest that the animals used in previous studies may have been harbouring an infectious agent which was completely independent of the *gt* locus.

The most suggestive piece of data from the 1985 histopathological study carried out by Sidman, Kinney and Sweet is the passing observation that mutant weanlings often develop a gastrointestinal illness with abdominal distension and watery fecal material with gas bubbles. This is highly suggestive of enteric hypoganglionosis, but no detailed examination of the status of enteric neurons was undertaken. The only known mutant at the *Sox10* locus, $Sox10^{Dom}$, features the coat spotting and enteric hypoganglionosis seen in **Harry** mutants. No other peripheral nervous system phenotype has been reported, nor has any effect upon the CNS. $Sox10^{Dom}$/ $Sox10^{Dom}$ homozygotes die before E13 of unknown causes, however. It is known that *Sox10* is highly expressed in the myelinating Schwann cells of the PNS, which are neural crest derived, and in non crest-derived glia and oligodendrocytes of the CNS (Kuhlbrodt *et al.*, 1998b). Given all this, it is reasonable to speculate that *gt* may well be a novel allele of *Sox10*, with a very mild melanoblast and enteric neuroblast phenotype, but a much more severe glial phenotype.

Strong support for this hypothesis comes from the recent description of a unique patient with a novel heterozygous mutation in SOX10 (Inoue *et al.*, 1999). The mutation consists of a 12bp deletion at the stop codon, leading to a frameshift and an extra 82 amino acid residues added onto the end of the full-length wild-

type SOX10 protein. The patient not only presented with Waardenburg-Shah syndrome, including long-segment Hirschprung disease, she also had profound peripheral neuropathy and leukodystrophy (degeneration of the white matter in the CNS), consistent with severe myelination defects in both peripheral and central nervous systems. The white matter defects are reminiscent of those seen in *gt* mice. Further evidence that SOX10 mutations can affect glial function comes from a pair of siblings heterozygous for a point mutation which truncates the SOX10 protein in the middle of the carboxy-terminal transactivation domain (Southard-Smith *et al.*, 1999). Both patients were classified as having WS4, but also suffered from ataxic cerebral palsy and nystagmus (rapid, jerky eye movements), both suggestive of peripheral neuropathy.

wn (white-nose)

A final locus *not* shown on the map in **Fig. 17** is *wn* (white nose), a recently described coat colour mutant which has been mapped to this region of Chr 15 (Marks *et al.*, 1999). *wn* is an autosomal recessive trait giving rise to an unpigmented region near the head, most often a white streak down the face, but with considerable variation in the size and position of this white patch. The only paper describing this mutation stated that it was not allelic with *Sox10*, but the mapping data gave a 6.3cM 95% confidence interval which comfortably overlaps the *Sox10* locus. It is therefore quite possible that *wn* represents a hypomorphic allele of *Sox10*, or if another coat colour locus really does exists close to *Sox10*, that *wn* and the **Harry** mutation are allelic.

Summary

In terms of the genetic mapping data from these experiments, *bt*, *Sox10* and *gt* can all be considered to be roughly equidistant from the transgene and all deserve consideration as candidate loci for the observed phenotype. *Dp* can probably be discounted, both on the grounds of distance and weakness of phenotype. Given the close similarity between the **Harry** mutant and the phenotype of the only known mutation at the *Sox10* locus, apart from the dominant nature of the latter, it seemed logical to assume that the transgene had disrupted Sox10 function in some way. Given also that neither *bt* or *gt* have been

cloned, the only straightforward experiment that presents itself with respect to these loci is to breed these mutant stocks against **Harry** to look for complementation. *bt* is still widely available, and mice carrying *gt* are still maintained in the McLaughlin Research Institute in Montana (G. Carlson, personal communication).

With detailed knowledge of the *Sox10* gene available, it was decided to investigate the status of this gene in **Harry** transgenic mice at the molecular level.

CHAPTER SEVEN:
HARRY - NATURE OF THE TRANSGENE INTEGRATION EVENT

Introduction

With the transgene integration site closely linked to the *Sox10* locus, it was decided to investigate the status of this gene in **Harry** mutants. At this point, it is worth reviewing the current state of knowledge about this gene and its function, paying particular attention to its properties in oligodendroglial cells *in vitro* and in the enteric nervous system *in vivo*, the two areas where most research to date has been focussed.

Origins of the enteric nervous system

The enteric nervous system (ENS) is the largest and most complex sub-division of the peripheral nervous system (PNS) (Gershon *et al.*, 1993). The adult ENS contains about the same number of intrinsic neurons as the spinal cord, and also contains a wide variety of types of neuron. Enteric neurons are grouped into complex microcircuits which resemble those seen in the brain and these collectively form complex neuronal networks which are capable of semi-autonomous function, even in the absence of any input from the CNS (Gershon *et al.*, 1981). Again, paralleling the situation in the brain, enteric neurons are not supported by the Schwann cells found in the remainder of the PNS, but by enteric glia, which resemble astrocytes, the support cells found in the CNS (Gershon & Rothman, 1991). (Outwith the ENS, glial cells of the PNS can be generally grouped into either myelinating or non-myelinating Schwann cells. Similarly, glial cells of the CNS can be broadly defined as myelinating oligodendrocytes and non-myelinating astrocytes, although there are several sub-types of astrocyte and other non-neuronal support cells exist in the CNS which may not strictly fall into either class) (Barres, 1997)).

Referring to **Figure 12b** in chapter 5, it will be seen that, at a gross level, the enteric nervous system is composed of two plexuses of interconnecting ganglion cells (neurons and glia), forming a pair of concentric meshes embedded in the gut wall. The outermost plexus of Auerbach lies in between the circular and

longitudinal muscularis and is commonly referred to as the myenteric plexus. The inner plexus of Meissner lies in the submucosae and these cells are far fewer in number than the Auerbach neurons. The myenteric plexus has been more closely studied and defined, and enteric ganglia in this region consist of dense clusters of neurons intermixed with glial cells, which partially ensheath axon bundles. These enteric glial cells express the same molecular markers as Schwann cells, but are ultrastructurally distinct (Gershon & Rothman, 1991).

Using *in situ* hybridisation and vital dye labelling, it has been shown that a common pool of neural crest cells gives rise to most of the ENS and the superior cervical ganglion in the mouse (Durbec *et al.*, 1996). In the chick, (where many of the original detailed anatomical studies of crest migration were performed using chick-quail chimerae), these cells originate from both cranial (somite 1-5 level) and anterior trunk (somite 6-7 level) regions of the neural tube and are referred to as vagal neural crest cells (Le Douarin & Teillet, 1973). Trunk neural crest cells arising posterior to somite 7 give rise to the more posterior sympathetic ganglia and contribute substantially to the foregut ENS. Posterior again to this, the sacral neural crest arises from the region caudal to somite 28 and contributes to the post-umbilical ENS (see discussion below). A similar arrangement pertains in the mouse and other organisms studied, although somite numbers differ.

Vagal neural crest cells migrate away from the neural tube around E9 in the mouse and colonise the wall of the developing gut. At some point, these neural crest cells become specified as "neuroblasts", and are fated to become enteric neurons or glia. The question of exactly when and how this fate is established and whether these cells are irreparably committed to a neuronal fate is an interesting and controversial one which exceeds the scope of this work. However, it is worth touching briefly upon some aspects of this debate.

The predominant model of neural crest patterning has postulated that multipotent neural crest cells are developmentally naïve and migrate haphazardly away from the neural tube. They then encounter environmental cues which both guide their migration and inform their differentiation. Some crest cell populations have been shown to be multipotent *in vitro* and crest derivatives such as the precursors of enteric or sensory ganglia backgrafted to new locations often

differentiate according to their new environment, although this plasticity can be limited to specific fates (Le Douarin, 1981). Subpopulations of neural crest cells may be partially specified at an earlier, pre-migratory stage, and neural crest cells have been shown to transiently accumulate in a cell-free region adjoining the neural tube which has been termed the migration staging area (MSA), where such specification may occur (Wehrle-Haller & Weston, 1997). Such a specified cell may be shown to be differentiated in the sense that it expresses unique lineage markers, but may not yet be irreparably committed to a particular fate. If this specification merely dictates which migratory route a neural crest cell will follow, then the environmental cues encountered en-route could determine the final distribution of crest derivatives. This "phenotype-directed model" of neural crest cell patterning has recently been shown to apply to melanocytes, where, in the chick, ventral migration of neural crest precedes dorsolateral migration by nearly 24 hours and ceases as dorsolateral migration begins. Melanoblast specification *precedes* migration and only melanoblasts migrate dorsolaterally (Reedy *et al.*, 1998).

Such a phenotype-directed model can be hypothesised to exist with respect to the vagal, trunk and sacral neuroblast precursors, which originate from distinct regions of the neural tube, migrate along distinct pathways and differentiate to form different final structures, but which all show at least partial plasticity of final cell fate when transplanted to an inappropriate migratory region (Le Douarin, 1981).

It is important to draw a distinction between instructive and selective signals. The former act to direct cells towards a particular fate, while the latter act to promote or block the survival of particular fated lineages. In crest development, it has proved easier to demonstrate the existence of selective signals, with instructive signals so far only being identified during *in vitro* studies. For example, the tyrosine kinase receptor *kit* and its ligand have been shown to be a crucial selective factor for the survival of melanoblasts (Wehrle-Haller & Weston, 1997), while bone morphogenetic protein (BMP2) acts as an instructive factor to fate crest cells towards the autonomic neuronal lineage in an *in vitro* system (Shah *et al.*, 1996). The difficulty in distinguishing instructive signals

which may be important *in vivo* lies in the fact that such signals are often important regulators of a number of different developmental processes, and mutations in such genes have pleiotropic effects which make it difficult to distinguish their role in the neural crest. This may not necessarily apply to selective signals to the same degree, however. With reference to the two example molecules given above, a null mutation in *kit* results in the dominant white spotting (*W*) phenotype. Mice homozygous for kit^{W} entirely lack melanocytes and erythropoetic stem cells and are sterile due to a lack of primordial germ cells, the three lineages where this molecule acts as a survival factor (Geissler *et al.*, 1988). On the other hand, a targeted null mutation in *Bmp2* has dramatic effects upon cardiac and amnion/chorion function, resulting in embryonic lethality long before any effect upon the neural crest can be discerned (Zhang & Bradley, 1996).

It has become increasingly clear from studies where neural crest cell explants have been cultured *in vitro* that one important mechanism of neural crest cell specification could act via the generation of a multipotent precursor population, with subsequent apoptosis and removal of unwanted cells during migration along specific paths. Neuronal precursors on the dorso-lateral pathway have been shown to exist, but to be subsequently removed during an episode of apoptosis (Wakamatsu *et al.*, 1998). A "proof-reading" mechanism, perhaps involving the differential expression of receptor tyrosine kinases has been postulated to act to cause removal of inappropriately specified neural crest cells by apoptosis (Wehrle-Haller & Weston, 1997).

Overall, neural crest cell specification is probably achieved via a mixture of the above mechanisms. Instructive signalling could initially direct cells towards multipotent lineages. Selective signals before or during migration could then act to promote survival of particular lineages and cause removal of inappropriately fated cells. Upon arrival at target tissues, further signalling would then occur in conjunction with the micro-environment in which the neural crest cells find themselves to regulate proliferation and differentiation.

Regardless of the exact nature and timing of neuroblast specification, vagal crest-derived neuroblasts are seen in the murine foregut at around E9.5 by virtue of their earliest known marker, dopamine β-hydroxylase (DBH). These cells are

referred to as transiently catecholaminergic (TC), as between E9.5 and E14 they express all the characteristics associated with sympathetic neurons (expression of tyrosine hydroxylase, aromatic L-amino acid decarboxylase and DBH, storage of a catecholamine and transmembrane transport of norepinephrine) (Gershon *et al.*, 1993). TC cells proliferate and migrate along the entire length of the developing gut, colonising the gut wall with cells which differentiate and proliferate *in situ* into enteric ganglia. Unlike sympathetic neurons, these TC cells are proliferative and do not express neuronal markers such as neurofilament proteins until after they have started to differentiate at their target sites. They are therefore considered to be genuine neuronal precursors.

During this time, the gut wall changes from a tube of uniform mesenchyme to a differentiated annular organisation, as observed by changes in extracellular matrix molecules such as tenascin, laminins and chondroitin sulfate proteoglycan (Newgreen & Hartley, 1995). Changes in these ECM molecules proceed in a rostro-caudal wave, and markers for differentiating enteric neurons also appear in such a wave, which lags slightly behind intestinal maturation. These changes in the micro-environment through which the neuroblasts migrate may inform their colonisation and differentiation at target sites.

It is thought highly likely that TC cells do not represent the totality of the vagal crest cells migrating through the gut, and that these cells only give rise to a subset of the enteric nervous system. It is also believed that TC cells cease to be catecholaminergic when they terminally differentiate into enteric neurons and glia, although a subset of enteric neurons are catecholaminergic in the mature ENS.

Simultaneous with the migration of enteric neuroblasts, trunk-derived neuroblasts migrate to and colonise their target tissues to give rise to the sympathetic ganglia (except for the most anterior ones), the dorsal root ganglia adjacent to the spinal cord and most of the foregut ENS (Durbec *et al.*, 1996) as well as the chromaffin cells of the adrenal medulla. Cells of this sympathoadrenal lineage can be distinguished from other trunk neural crest cells by their expression of catecholaminergic enzymes. They can be further distinguished from the enteric neuroblast lineage by the latter's absolute dependence upon the *ret*

tyrosine kinase receptor for correct development. *ret-/-* null mice entirely lack structures derived from the vagal neural crest (their intestines are completely aganglionic below the stomach), while the sympathoadrenal lineage remains unaffected.

The contribution of the sacral neural crest, originating caudal to somite 28, to the ENS has been controversial. The original studies of Le Douarin and Teillet using chick-quail chimerae suggested that sacral crest made a substantial contribution to the post-umbilical ENS (Le Douarin & Teillet, 1973). However, in studies where the vagal crest contribution was removed, either by severing the bowel during development, or by culturing aneural hindgut segments *in vitro* with sacral neural tube explants, no sacral crest contribution was seen (Gershon *et al.*, 1993). Despite these findings, vital dye and retroviral labelling clearly indicated an ascending contribution to the distal gut from the sacral neural crest. It recently became possible to definitively resolve this controversy, at least in chick, with the development of a completely quail-specific monoclonal antibody. In a set of experiments using chick-quail chimerae, the authors made the interesting discovery that the sacral neural crest does indeed make a significant contribution to the ENS, but that the vast bulk of the sacrally-derived cells are found in the colon, and display a proximo-distal gradient of distribution with the greatest number at the terminal end of the gut (Burns & LeDouarin, 1998). Furthermore, these sacrally derived enteric neurons are not seen in the gut until after the vagally-derived enteric neuroblasts have begun to colonise the terminal colon. This raises the possibility that sacral crest cells require interaction with vagally-derived cells in order to colonise and/or proliferate in the colon. This would explain why severing the bowel above the ileo-cecal junction during development leads to a complete absence of enteric neurons in the colon (Allan & Newgreen, 1980).

The Sox10^{Dom} mutation

As mentioned previously, *Sox10* had been described only as the mutant locus *Dom* for a number of years, but the gene product was identified recently by two independent groups (Herbarth *et al.*, 1998; Southard-Smith *et al.*, 1998). The original description of the locus in 1984 was as a spontaneous mutation arising in

stocks kept at the Jackson Laboratories (Lane & Liu, 1984). The white spotting phenotype of *Dom/+* mice is relatively mild compared to **Harry** mutants, even on similar genetic backgrounds (C57BL/6J and C3HeB/FeJLe-*a/a*, which is similar to CBA, as discussed in the previous chapter), with usually only white feet and a white belly spot of variable size being observed. However, the megacolon observed in *Dom/+* mutants presented in a very similar manner to that seen in **Harry** mutants, with affected animals having a thin, malnourished appearance and the characteristic bulging abdomen due to fecal impaction in the gut. Time of death varied from 2 days to 12 months, and was found to be somewhat dependent on genetic background. No *Dom/Dom* homozygotes were observed in the original breeding studies and homozygosity has been found to be lethal before E13 for unknown reasons. The only exception to this is seen on a C57BL/6J x C3H/HheOuJ hybrid background, where a very few homozygous embryos develop to term and *Dom/Dom* pups die within a few hours of birth (Herbarth *et al.*, 1998). Histopathological studies of the enteric nervous system in *Dom/+* animals revealed a consistent lack or reduction of enteric ganglion cells in the terminal gut. This showed wide variation in the level at which innervation ceased, but in all cases, the terminal 2mm of the gut was either fully aganglionic or severely hypoganglionic (Puliti *et al.*, 1996). Occasionally, the aganglionic segment was seen to extend throughout the colon up to the cecum.

Migration of enteric neuroblasts

A useful system for the study of enteric neuroblast migration through the gut has been the development of a line of transgenic mice carrying the *lacZ* reporter gene driven by the upstream reporter region of the human DBH gene (Kapur *et al.*, 1992). Enteric neuroblasts (and other TC cells) in these *DβH-nlacZ* mice can be easily detected using stains for the reporter enzyme, and under normal circumstances, these cells were found to migrate rostrally-to-caudally along the gut from E9.5 until E13.5, at which point the entire length of the gut was colonised. (It is important to stress that although expression of DBH is considered to be the definitive marker for enteric neuroblasts, it has not been proven that *all* enteric neuroblasts express this gene i.e. it is possible that the developing gut also contains vagal crest derivatives which are not transiently catecholaminergic. The

cells which stain blue for *lacZ* in the gut of transgenic embryos may therefore not represent the totality of enteric neuroblasts.)

When this transgene was introgressed into the *ls* (lethal spotting) mutant strain, which carries a null allele of the endothelin-3 gene, enteric neuroblasts in *ls/ls* mice were found to progress normally through the gut and then to halt abruptly at the ileo-cecal junction around E12.5. Colonisation of the proximal and mid-colon proceeded thereafter, but at a retarded rate and in an irregular pattern. The terminal colon was never colonized in these mutant mice. Similar results were obtained in s^l mutants, which are null for the endothelin-B receptor (Kapur *et al.*, 1995).

In contrast, when the transgene was introgressed into the *Dom* mutant strain and used to track enteric neuroblasts, it was found that in *Dom/+* embryos, colonisation of the entire gut was impaired from the earliest stages examined (E11) (Kapur *et al.*, 1996). Again, migration was found to be delayed at the ileo-cecal junction around E12.5. However, vagal neural crest cells normally reach the distal colon on E13.5 in wild-type embryos, and a number of presumptive enteric neuroblasts (which stained blue for the transgene) were observed in the distal colons of a subset of *Dom/+* embryos on a C3HeB/FeJ background. This observation suggested a degree of "catch-up" in *Dom/+* enteric neuroblast migration, via some mechanism which does not exist in *ls* or s^l mutants, or in *Dom/+* mutants on a C57BL/6J background, where this phenomenon was never observed.

Sox10 expression during development

Following fine-scale mapping studies, the product of the *Dom* locus was identified by two independent groups of researchers as the transcription factor *Sox10* (Puliti *et al.*, 1995; Pingault *et al.*, 1997; Herbarth *et al.*, 1998; Southard-Smith *et al.*, 1998). This gene had previously been partially sequenced and classified based on its highly conserved HMG-domain. This DNA-binding motif is the hallmark of the Sox (*Sry*-type HMG box) genes, and a degenerate PCR strategy had previously amplified seven different HMG box sequences from a mouse embryo cDNA library and classified them as various Sox genes (Wright *et al.*, 1993).

The structure of the *Sox10* gene and the known salient features of the 466 amino acid protein itself are summarised in **Figure 18**. In the *Dom* mutation, renamed *Sox10^{Dom}*, a single nucleotide insertion causes a frameshift just downstream of the HMG-box, resulting in a wild-type amino-terminus and HMG-domain attached to 99 novel amino acids and premature termination. *In situ* and Northern hybridisation studies showed that *Sox10* is expressed in newly forming neural crest cells at E9.5 and that expression is maintained in a subset of crest cells as they migrate to their target tissues. Subsequent to this, *Sox10* expression is also seen in the developing CNS and correlates with oligodendrocyte precursors. *Sox10* expression in the CNS of adult rodents, consistent with its expression in cultured oligodendrocytes, corresponds to glial cells, with expression greatest in regions with high myelinated fibre content (Kuhlbrodt *et al.*, 1998b). Outwith the CNS, expression in adults is confined to glial cells of the peripheral nervous system, including Schwann cells (Kuhlbrodt *et al.*, 1998b; Southard-Smith *et al.*, 1998).

In *Sox10^{Dom}* /+ and *Sox10^{Dom}/Sox10^{Dom}* embryos, neural crest cells expressing *Sox10* are seen to be developmentally delayed in their migratory pathways at E10.5, and by E11.5 no *Sox10* expression is detectable in homozygous mutant embryos. This appears to be due to apoptosis and loss of neural crest cells near this time (Kuhlbrodt *et al.*, 1998b; Southard-Smith *et al.*, 1998). This ablation of a subset of neural crest cells almost certainly accounts for the fact that *Sox10^{Dom}/Sox10^{Dom}* embryos entirely lack enteric neurons below the rostral foregut, and show substantial reductions in peripheral ganglia which normally have a substantial contribution from the vagal neural crest (Herbarth *et al.*, 1998). In addition, no early melanoblasts were detectable in E10.5 and E11.5 *Sox10^{Dom}/Sox10^{Dom}* embryos, as assayed by dopachrome tautomerase (*Dct*), a marker for this lineage (Southard-Smith *et al.*, 1998).

It should be stressed at this point that although Sox10 expression is seen in neural crest cells emerging along the full length of the neural tube, the *Sox10^{Dom}* mutation only affects melanoblasts and derivatives of the vagal neural crest. Clearly, however, the *Sox10* signal in emergent melanoblasts fated to migrate down the dorso-lateral pathway could overlay and mask any signal from cells

migrating along the earlier ventral route. However, a more detailed study of the expression pattern of *Sox10* in emergent neural crest cells suggests that ventrally migrating trunk neural crest cells do express *Sox10*, and that such expression precedes the formation of dorsal root ganglia (Pusch *et al.*, 1998).

It should also be stressed that although Sox10 is expressed widely in glial cells of both central and peripheral nervous systems, including those which originate from trunk neural crest, the $Sox10^{Dom}$ mutation only appears to cause a phenotype in vagal neural crest cell derivatives and melanoblasts, at least in heterozygotes. The cause of death in homozygotes remains unknown.

It is tempting to speculate, in light of the apoptosis observed in $Sox10^{Dom}/Sox10^{Dom}$ embryos, that one initial important role of *Sox10* in the developing embryo is as a survival factor specific to vagal neural crest and melanoblasts and that subsequent to this, it fulfils a less critical role throughout the lifespan of all or most glial cells. Similar apoptosis has recently been shown to occur in undifferentiated enteric neuroblasts lacking the *ret* gene product, and it has been suggested that one function of *ret* is to promote the survival of these cells (Taraviras *et al.*, 1999). Since *ret* appears to serve no function in melanoblasts, this might imply that *ret* lies downstream of *Sox10* in vagal neural crest but not the melanocyte lineage (where *c-kit* may subsume the role of *ret*).

The molecular nature of the $Sox10^{Dom}$ mutation

Work in oligodendroglial cell cultures has shown that the mouse and rat Sox10 protein, as with many other Sox genes, possesses no intrinsic transcriptional activation (transactivation) properties, but rather that it functions synergistically with other transcription factors to modulate transcription (Kuhlbrodt *et al.*, 1998b). The HMG box is known to act as a DNA-binding domain and many Sox proteins recognise the motif 5'-AAACAAAG-3'. This motif was used in an *in vitro* reporter assay in glioblastoma cells to show that Sox10 itself would not activate transcription, but that it would interact with the POU domain transcription factor Tst-1/Oct6/SCIP to significantly increase the latter's ability to activate transcription. Sox10 was also shown to interact with Pax3 and the zinc finger transcription factor Krox20 in the same system, upregulating and downregulating the respective transcriptional activation ability of these two factors. (All three

transcription factors are known to be involved in the development of Schwann cells.) Thus Sox10 was hypothesized to be a transcriptional modulator, rather than a transcription factor, at least in glial cells.

From deletion construct experiments using the system described above, it was hypothesized that Sox10 contained a synergy domain amino-terminal to the HMG-box which could interact with nearby transcription factors to modulate their activity. Human SOX10 was cloned and 4 separate mutations in the gene were implicated in familial cases of Waardenburg-Shah syndrome (Pingault *et al.*, 1998; Pusch *et al.*, 1998). These 4 mutations were replicated in the cloned human and rat Sox10 cDNAs and all were tested in a follow-up study using the same oligodendroglial cell culture system for their ability to intrinsically transactivate a reporter gene with a Sox binding site upstream and for their ability to synergise with Tst-1/Oct6/SCIP (Kuhlbrodt *et al.*, 1998c). Interestingly, human SOX10 was found to have a weak intrinsic transcriptional activation ability, unlike the situation in rodents. This was found to reside in the carboxy-terminal 113 amino acids of the human protein. The ability to bind DNA was also required, as two mutations which removed or affected the HMG-box also abolished DNA binding and synergy. The synergy domain which interacts with the N-terminal region of Tst-1/Oct6/SCIP was found to reside in the amino-terminal 60 amino acids of SOX10, although this synergistic enhancement was found to be reduced in the absence of the carboxy-terminal transactivation domain. The authors postulate that the human carboxy-terminal transactivation domain interacts with the synergy domain in some way.

Since the synergy domain resides in the amino-terminus of the protein, and since the *Sox10^{Dom}* mutation does not affect either this region or the HMG box, it is therefore puzzling that the synergistic effect is completely abolished in the Sox10^{Dom} protein. Based on the presumptive interaction between the carboxy-terminal domain and the synergy domain, Kuhlbrodt *et. al.* speculate that the novel 99 amino acid carboxy terminus of the Sox10^{Dom} protein might act as a repressor of synergy, rather than simply being a passive deletion of the carboxy-terminus (Kuhlbrodt *et al.*, 1998c). Hence the *Sox10^{Dom}* mutation might act as a true dominant, rather than via haploinsufficiency of wild-type Sox10 protein.

The differences between human and rodent Sox10 are also evident in the observation that during human development, SOX10 is expressed in the cranial neural crest-derived cephalic mesectoderm, which gives rise to facial cartilages (Bondurand *et al.*, 1998). This is not seen in mouse or rat and the authors suggest that human SOX10 may have additional roles in development. Dystopia canthorum (widening of the medial canthus of each eye) is due to defects in the cephalic crest contribution to the facial cartilages, and is a classic indicator of WS type 1 and 3. It is not normally associated with WS4, however, the unique patient with the novel mutation in SOX10 giving rise to extremely severe PNS and CNS defects also presented with WS4, including profound deafness, long-segment Hirschprung and heterochromia iridis (Inoue *et al.*, 1999). Unusually, she also had dystopia canthorum, indicating that SOX10 does seem to play some role in cephalic neural crest, consistent with its expression pattern in human embryos.

Sox genes and POU domain transcription factors in Schwann cells

The role of POU domain transcription factors in the differentiation of Schwann cells is now beginning to be unravelled. *Tst-1/Oct6/SCIP* is essential for terminal differentiation of myelinating Schwann cells and is also expressed in CNS oligodendrocytes. A targeted deletion of this gene resulted in a severe defect in peripheral nerve myelination but failed to give any CNS phenotype (Bermingham *et al.*, 1996; Jaegle *et al.*, 1996). The closely related transcription factors *Brn-1* and *Brn-2* also show a similar expression pattern to *Tst-1/Oct6/SCIP* in oligodendrocytes and some degree of functional redundancy may well apply. Thus, it is possible that a double or triple knockout of these genes might be required to give a phenotype in the CNS.

Following on from the detailed investigation of Sox10's ability to synergise with *Tst-1/Oct6/SCIP*, oligodendroglial cells were found to express *Sox11*, and this protein was found not to interact with *Tst-1/Oct6/SCIP*, but to synergise with *Brn-1* and *Brn-2*, which do not interact with Sox10 (Kuhlbrodt *et al.*, 1998a). The comparison between the two Sox genes is informative, as rat *Sox11* possesses a strong carboxy-terminal transactivation domain. The synergy domain is unidentified as yet, but does not lie within the amino-terminal 43 amino acids.

It is hypothesized by the authors that Sox proteins interact with class III POU domain transcription factors in a combinatorial manner to help specify or maintain cell identity in the PNS (Kuhlbrodt *et al.*, 1998a). It is furthermore suggested that there is considerable overlap in the functions of these class III POU domain transcription factors in glial cells. By implication, this may extend to their transcriptional partners, the Sox genes. In support of this argument, it has been observed that Sox10 is actively transcribed in both the precursor and the mature oligodendrocyte, however Sox11 expression is down-regulated during the early stages of differentiation of both oligodendrocytes and Schwann cells. The Sox11 expression pattern closely resembles that of Brn-1. Sox4 is also expressed in a similar pattern to Sox11 in the oligodendrocyte lineage, and functional compensation by other, closely-related Sox genes may explain why there is no glial phenotype in the *Sox4-/-* knockout mouse (Schilham *et al.*, 1996).

This suggested mechanism of specific gene activation by combinatorial interactions accords well with a proposed similar model involving POU domain and LIM homeodomain proteins. It has been estimated that there may be hundreds of different POU-domain proteins, each expressed in different subclasses of neurons (He & Rosenfeld, 1991). Similar numbers of LIM-domain genes exist, and it has been suggested that combinatorial interactions between POU and LIM domain proteins could confer neuronal identity (Tsuchida *et al.*, 1994; Anderson & Jan, 1997).

Sox gene function in chicken and *Drosophila*

In parallel with the studies of Sox10 and Sox11 discussed above, detailed domain-swap experiments have been performed using a similar *in vitro* reporter assay system to dissect and compare the functions of *Sox1*, *Sox2*, *Sox3* and *Sox9* (cloned from chicken) (Kamachi *et al.*, 1999). The closely related Sox1/2/3 proteins are all expressed in the lens and will all activate a δ-crystallin minimal enhancer element. The distantly related Sox9 protein plays a crucial role in chondrogenesis, and will activate a minimal enhancer element derived from the collagen gene *Col2a1*. Using these enhancer elements in a reporter assay system, constructs containing various domains of these Sox genes were tested. It was found that the HMG-box domain conferred only limited specificity on each Sox

gene, and that specificity was conferred mainly through interaction with partner factors which bound to nearby enhancer elements, and that interactions between Sox genes and partner factors were mediated by the region of the protein immediately carboxy-terminal to the HMG-box. The actual transactivation domains were found to be distal to this, lying closer to the carboxy-terminus of each molecule. Interestingly, the amino-terminal domain of Sox9 was found to act as a repressor of transactivation activity.

A similar arrangement has been found to pertain within the TCF/LEF family of HMG-box transcription factors, which were initially identified as being important in lymphocyte differentiation, but have now been grouped with the Sox gene family (Schilham & Clevers, 1998). Four human *Tcf* (T-cell factor) genes have been identified, with one ancestral homologue in *Drosophila*, named dTCF or Pangolin (Castrop *et al.*, 1992; Brunner *et al.*, 1997). It has now been shown that dTCF binds to the enhancer region of *engrailed* via its HMG-domain, and that it synergistically interacts with *Groucho* to repress *engrailed* expression (Cavallo *et al.*, 1998). However, following activation of the β-catenin signalling pathway, a separate domain of the dTCF protein can interact with Armadillo (the β-catenin homologue) and synergistically upregulate expression of *engrailed* (van de Wetering *et al.*, 1997).

Sox9 is co-expressed with *Sox5* and *Sox6* in regions of chondrogenesis and further work on the *Col2a1* enhancer element has shown that all three proteins bind to nearby sites in this region and upregulate expression of the gene (Lefebvre *et al.*, 1998). In addition, it was found that the long isoforms of Sox5 and Sox6 (L-Sox5 and L-Sox6) heterodimerise via a coiled-coil (leucine zipper) domain lying amino-terminal to the HMG box, and that this interaction greatly enhanced their binding to adjacent HMG target sites. Studies of this coiled-coil domain in L-Sox6 (also known as Sox-LZ) have shown that it can mediate homodimerisation, resulting in repression of transactivation ability (Takamatsu *et al.*, 1995; Lefebvre *et al.*, 1998). Thus, it is entirely possible that some of the important partner factors for Sox proteins are actually other Sox proteins, with homo- and heterodimerisation occurring.

Given the importance of dimerisation for the mode of action of Sox5 and Sox6, it would be useful to know whether Sox10 contains a coiled-coil domain which might mediate homo- or heterodimerisation. Coiled-coil domains consist of a bundle of α-helices - generally two, but occasionally three or four - wound together into a superhelix (Lupas, 1996). The packing in the centre of the superhelix involves a distinctive "knobs-into-holes" packing, in which a residue from one α-helix packs into a space surrounded by four sidechains of the facing α-helix. Negative supercoiling reduces the number of residues per turn of each α-helix to 3.5, allowing sidechains to repeat every seven residues, the hallmark "heptad repeat" of a coiled-coil domain. Prediction of coiled-coil domains therefore hinges around scanning the amino acid sequence with a "window" of multiples of seven residues, looking for heptad repeat motifs. The prediction algorithm COILS is available on the Web, and is the heart of a program that compares a sequence to a database of known parallel two-stranded coiled-coils and derives a similarity score (http://www.isrec.isb-sib.ch/software/COILS_form.html) (Lupas *et al.*, 1991). By comparing this score to the distribution of scores in globular and coiled-coil proteins, COILS then calculates the probability that the sequence will adopt a coiled-coil conformation. Given a query sequence, COILS scans the amino acid sequence with a "window" of 14, 21, or 28 residues (based on the diagnostic heptad repeat) and assigns a probability value from 0 to 1.0 for each residue forming part of a coiled-coil domain. A coiled-coil domain can be confidently assigned if more than one window results in a high probability score and the 21-residue window appears to be the most accurate predictor of coiled-coils.

Both L-Sox5 and Sox-LZ (i.e. L-Sox6) gave very strong predictions for coiled-coil domains amino-terminal to the HMG box when their sequences were run through the COILS program, and this accords perfectly with published data on the functional leucine-zipper coiled-coil domain in these proteins (Lefebvre *et al.*, 1998). However, not only do Sox10, Sox10^{Dom} and Sox9 lack (so far as is known) the alternatively-spliced amino-terminal domain of L-Sox5 and L-Sox6 where this coiled-coil domain lies, but none of these three proteins showed any significant predictions for a coiled-coil domain (data not shown). While it is

dangerous to draw firm conclusions from a cursory analysis of Sox10 using only one algorithm, it is probably safe to assume that Sox10 does not have a leucine-zipper dimerisation domain analogous to that found in Sox5 and Sox6. The $Sox10^{Dom}$ mutation may therefore be viewed as being less likely to exert its effect by acting as a dominant negative inhibitor of Sox10 homodimerisation via a coiled-coil domain.

A proposed general mechanism of Sox gene function

Although many Sox genes are still poorly characterised, the published data allows the postulation of a general mechanism for Sox gene function. The HMG-box domain is responsible for binding DNA, and introduces a bend in the DNA when it does so (Werner *et al.*, 1995). However, the specificity of Sox gene function is probably not solely conferred by the region, since Sox genes appear to be fairly promiscuous in binding to their target sequences. It is likely that Sox genes achieve target specificity through interactions with partner factors such as POU domain proteins or other Sox proteins, which bind to nearby sequences in the promoter region. An individual Sox protein may interact with more than one partner factor, and these combinatorial interactions could mediate repression or activation of genes in specific tissues.

***Sox10*^{Dom} and enteric pathogenesis**

Many of the studies on the expression pattern and the molecular nature of the *Sox10* gene have been carried out with regard to glial cells of the PNS and CNS. However, the critical defect observed in $Sox10^{Dom}$ mutant mice and human WS4 patients is the intestinal aganglionosis (indeed there is no observed phenotype in either the PNS or CNS in *Sox10*^{Dom}/+ heterozygotes). There are several possibilities as to the pathogenic mechanism of this condition.

Firstly, since enteric neuroblasts are entirely absent in homozygotes due to apoptosis of the neural crest cells which give rise to them, it is possible that in hemizygotes the pool of neural crest cells available to generate enteric neuroblasts is somewhat reduced. Since the terminal colon is the last region to be colonised, such a reduction in starting numbers of precursor cells might reasonably be expected to affect this region. The numbers of enteric neuroblasts observed

migrating down through the gut in the *DβH-nlacZ* transgenic experiments argues against this, however (Kapur *et al.*, 1996). It is also known that enteric neuroblasts have enormous proliferative capacity during their migratory phase (Young *et al.*, 1998).

A simple explanation for the aganglionic phenotype observed in *Sox10^{Dom}*, *ls* and *s^{l}* mutant embryos has been proposed by Newgreen *et al.* who made a detailed study of the growth kinetics of the gut itself relative to the migration of enteric neuroblasts during chick and quail embryogenesis (Newgreen *et al.*, 1996). They found that the rate of growth of regions of the gut was relatively slow until the time at which neural crest derived cells (as determined by those cells which expressed the HNK-1 epitope) arrived, at which point the growth rate dramatically increased. Although it is not possible to use the same antibody in mouse in order to repeat this study in mutant embryos (the HNK-1 epitope is a conserved carbohydrate moiety associated with glycoproteins found mainly on the cell surface of migrating neural crest, but current monoclonal antibodies to HNK-1 do not cross-react with mouse), they hypothesize that any delay in the arrival of vagal neural crest derivatives might jeopardise their ability to fully colonise the rest of the gut due to a growth wave outstripping their migration. While this is an attractive hypothesis, it does not account for Kapur's observation of a few cells labelled with *DβH-nlacZ* arriving in the terminal gut at the correct time during *Dom/+* embryogenesis, despite an earlier delay in migration (Kapur *et al.*, 1996). These might, of course, correspond to some few sacrally-derived enteric neuroblasts, if such were shown to be transiently catecholaminergic at this time. Although sacral neural crest derivatives are almost certainly not TC during migration to the gut, and probably do not express the HNK-1 epitope during migration, if a few cells successfully colonised the terminal gut, they might become TC at this time or shortly after differentiation to enteric neurons.

The exact nature of sacral neural crest during murine development is somewhat under-characterised, due to a lack of specific markers. However, a recent study using antibodies to the transcription factor *Phox2b*, which appears to be a good marker for both migratory enteric neuroblasts and differentiated enteric neurons in rodents, has shown that no Phox2b-labelled cells appear in the hindgut

until after the vagal wave of enteric neuroblasts arrives (Young *et al.*, 1998). Vital dye labelling studies have shown that sacral crest has migrated into this region prior to the arrival of the vagal wave, hence these early sacral crest cells either do not contribute to the ENS or absolutely require some interaction with the vagally-derived cells before they can acquire enteric neuroblast characteristics(see below) (Serbedzija *et al.*, 1991).

Cell autonomous and non-autonomous effects during enteric neurogenesis

It was found, using aggregation chimerae between wild-type and mutant embryos, that the defect in colonisation of the colon seen in both *ls* and s^{l} mutants was not strictly cell-autonomous (i.e. did not solely reflect a defect in the mutant neuroblasts). There are sharp differences in morphology, ECM expression patterns and enteroendocrine secretory products between the colon and the small intestine immediately below and above the ileo-cecal valve. It is possible that the defect observed in *ls* and s^{l} mutants partly reflects changes in the micro-environment of the gut wall which impairs the migration and/or colonisation of neuroblasts in this region and this has been suggested to be the case with respect to an observed abnormal accumulation of basal lamina components in the colonic wall of *ls* adult mutant mice (Payette *et al.*, 1988).

Further studies using an *in vitro* culture system have shown that the hindgut of *ls/ls* mice is a non-permissive environment for both mutant and wild-type neural crest cells, and it seems clear that in this mutation, at least, failure to express endothelin-3 in the hindgut mesenchyme creates a non-permissive microenvironment and causes aganglionosis independently of any defects in neural crest cells (Jacobs-Cohen *et al.*, 1987). Excess axonal innervation is seen in the aganglionic region of *ls/ls* mice and it has been suggested that the gut micro-environment may be permissive for axonal growth in the absence of intrinsic innervation (Payette *et al.*, 1987).

Using aggregation chimerae between wild-type and $Sox10^{Dom}$/+ embryos, it was found that the $Sox10^{Dom}$ mutation was also not strictly cell-autonomous (Kapur *et al.*, 1996). In other words, the ability of a neuroblast to colonise the distal gut is not solely an intrinsic property dictated by the presence or absence of the $Sox10^{Dom}$ mutation, but can be affected by the cellular environment in which

the neuroblast finds itself. Chimeric mice with aganglionic distal colons were found to lack both wild-type and *Sox10^{Dom}* /+ neurons in the affected regions, implying that the presence of mutant cells in some way affected the migration and/or proliferation of wild-type enteric neuroblasts.

This finding is curious, since, given that *Sox10* is a transcription factor, the gene might reasonably be expected act in a cell-autonomous manner, and indeed, aggregation chimera experiments with its closest relative, *Sox9*, have shown that this gene does act in a cell-autonomous manner to direct cell fate along a cartilage formation pathway at an early stage (Bi *et al.*, 1999; Healy *et al.*, 1999).

If the *Sox10^{Dom}* defect truly is non cell-autonomous, it is possible that *Sox10^{Dom}* fails to fulfil some role in conditioning the micro-environment of the colonic wall so as to be suitable for colonisation by enteric neuroblasts. Given the lack of observed expression of *Sox10* in this region, this seems unlikely, although it is conceivable that *Sox10*-expressing enteric neuroblasts might activate *Sox10* expression in the gut wall via interaction with mesenchymal cells upon arrival, constituting part of a paracrine/autocrine feedback loop necessary for the proliferation of neural crest cells in their target micro-environment. This has been directly refuted by recent work from the same lab that performed the original aggregation chimera studies with *Sox10^{Dom}* mutants: wild-type neural crest can colonise *Sox10^{Dom} /Sox10^{Dom}* intestinal grafts placed under the renal capsule of wild-type host mice (Kapur, 1999). This suggests that the enteric microenvironment is probably normal in *Sox10* mutants.

An attractive alternative hypothesis for the mechanism of hypoganglionosis suggests itself from the recent findings of Burns and Le Douarin, with regard to the putative interaction required between vagal and sacral neural crest derivatives in order for the latter to successfully colonise the terminal gut (Burns & LeDouarin, 1998). This interaction was also mooted by Young *et al.* who point out that sacral neural crest cells are highly unusual in that they express none of the markers associated with enteric neuroblasts until after the arrival of the vagally-derived cells (Young *et al.*, 1998). Young and co-workers could not categorically state whether the sacral neural crest did in fact make a

contribution to the ENS, but Burns and Le Douarin have definitively proved that this is the case, at least in the avian embryo.

Given that sacrally-derived wild-type crest cells would not have been detected in Kapur and co-workers earlier study (since they would likely not have expressed the *DBH-nlacZ* transgene), it is possible that in those chimeric animals most affected, there was a very substantial mutant contribution to the sacral neural crest. This could have led to a severely hypoganglionic distal colon, even in the presence of substantial numbers of vagally-derived wild-type enteric neuroblasts migrating down the gut rostral-to-caudally. However, if this model were to prove correct, the aganglionosis would reflect a cell-autonomous defect in $Sox10^{Dom}$/+ neural crest cells.

If this hypothetical interaction between the two groups of neural crest cells were further postulated to have a narrow window of opportunity, it might also explain why the delay in the migration (rather than a complete absence) of vagally-derived enteric neuroblasts in $Sox10^{Dom}$/+ (non-chimeric) embryos could lead to a severe reduction in the number of neurons in the terminal gut, since the sacral crest cells might "miss their chance" to interact with them and hence fail to become potentiated for a neuronal or glial fate.

Glial cells and the pathogenesis of megacolon

It is known that the ganglia of the myenteric plexus are composed of multiple neurons and glia clustered together in small groups with inter-linking fibres which stain positive for neurofilament, and that individual enteric neuroblasts are capable of giving rise to both cell types (Gershon & Rothman, 1991; Natarajan *et al.*, 1999). This is in accord with the multi-potent nature of neural crest cells of the sympathoadrenal lineage, which are known to form neurons, glia and the chromaffin cells of the adrenal medulla (Durbec *et al.*, 1996; Burns & LeDouarin, 1998). It has further been established during the course of the *DBH-nlacZ* <-> wild-type aggregation chimera studies that the enteric ganglia are not necessarily of clonal origin i.e. that more than one enteric neuroblast may contribute to each ganglion (Kapur *et al.*, 1993). Since *Sox10* expression is maintained in the developed PNS and CNS only in glial cells, it is possible that its expression in the ENS becomes restricted to the glial cells after the neuroblasts*

*** Strictly speaking, the term *neuroblast* refers to a purely neuronal precursor, but is used, in this context, to refer to neuronal-glial precursors.**

have fully differentiated. If this were the case, *Sox10^{Dom}* mutation might reasonably be expected to exert an effect upon enteric glia directly, rather than upon the migratory precursors.

In support of this "glial effect" hypothesis, a recent experiment specifically ablated glia in adult mice. and found that reducing the number of enteric glia in the mature ENS had a particularly dramatic phenotypic effect (Bush *et al.*, 1998). The mutant mice in these experiments carried a GFAP-HSVTk transgene consisting of a viral thymidine kinase gene driven by the mouse glial fibrillary acid protein (GFAP) promoter. When gancyclovir was administered to these mice, a dramatic loss of the glial cells of the jejunum and ileum (but not the stomach or colon) was found, due to the production of cytotoxic nucleotide metabolites by the action of thymidine kinase upon gancyclovir. These mice developed a fulminating jejuno-ileitis and died less than 20 days after commencement of gancyclovir treatment. The pathology of this rapid onset intestinal disease was quite reminiscent of that seen in megacolon, with inflammation of the bowel and degradation of the mucosal lining. It had been previously thought that such inflammation might be a consequence of the sepsis seen in mice with megacolon (Caniano *et al.*, 1989), but the condition seen in the GFAP-HSVTk mice was claimed to be independent of bacterial overgrowth. This has led to a resurgence of interest in entero-glial cells, with some researchers claiming that they may act as a bi-directional interface between the nervous and immune systems, by virtue of being both responsive to and producers of both cytokines and neurotransmitters (Ruhl & Collins, 1995).

There certainly exists strong evidence from other studies of inflammatory bowel diseases such as Crohn's disease and ulcerative colitis that reduced or abnormal enteric innervation can lead directly to an inflammatory response (Dvorak *et al.*, 1993). The plexus of Meissner almost certainly interacts intimately with the immune system. It has been shown by careful morphometry that in the human lower bowel, enteric nerve fibres of the plexus of Meissner are very closely apposed to most lymphoid cells in the gut wall, and that significant loss of these fibres is implicated in inflammatory bowel disease (Kubota *et al.*, 1992). The plexus of Meissner is much more severely affected in the *ls* mutant than the

myenteric plexus, and abnormal distributions of enteric lymphoid cells have been demonstrated in the affected intestines of s^l mutants (Payette *et al.*, 1987; Fujimoto, 1988; Caniano *et al.*, 1989).

Further to this, Fihn and co-workers claim to show that the myenteric plexus regulates fluid secretion and epithelial permeability in the rat small intestine, although since this work is in the form of a meeting abstract, it cannot be fully assessed as yet (Fihn *et al.*, 1997).

Overall, the pathogenesis of the inflammatory reaction seen in the gut wall lying above the constricted region in megacolon probably does not simply reflect defects in the myenteric plexus and is unlikely to be merely a secondary effect of sepsis .

Enterochromaffin and APUD cells

One final consideration is the possible role of the enterochromaffin cells in the ENS and in the pathogenesis of megacolon in *Sox10* mutant mice.

The endocrine system can be divided into two main components, with the first being the classical endocrine organs such as pituitary and thyroid glands, and the second being the so-called "diffuse endocrine system" (MacSween & Whaley, 1992). This consists of cells dispersed singly or in small groups throughout various non-endocrine organs including the gastrointestinal tract. Indeed, it has been estimated that the total mass of the diffuse enteric endocrine system may well exceed that of many of the classical endocrine organs (Pearse, 1973).

All of the cells of the diffuse endocrine system stain with silver salts when an exogenous reducing agent is added during incubation. In addition, a subset of these cells will reduce silver salts directly, and this is known to be associated with expression of 5-hydroxytryptamine (5-HT) These are known as argentaffin or enterochromaffin cells and can be delineated using Fontana-Masson staining (Culling, 1974).

Enterochromaffin cells fall within the gamut of APUD cells (amine precursor uptake and decarboxylation), which also include the neural crest-derived endocrine chromaffin cells of the adrenal medulla. APUD cells are known to comprise a large part of the enteric endocrine system, and consist of at least 20 different cell types, responsive to different stimuli and secreting different

products (Pearse, 1973). Their exact origin has been controversial, but it seems clear that at least some enterochromaffin cells are neural crest-derived, whilst others are not, and instead derive from differentiation of local multi-potent stem cells (Le Douarin & Teillet, 1973; Pearse, 1973; Andrew, 1974; MacSween & Whaley, 1992). The use of their biochemical properties as a marker for a purely neural crest origin is therefore inappropriate.

The original studies on the aganglionic gut of *Sox10^{Dom}*/+ heterozygotes included Fontana-Masson staining, and the authors showed that enterochromaffin cells were also severely reduced in parallel with the reduction in enteric ganglia in these mutant mice (Lane & Liu, 1984). Since the origin of these cells was controversial, the authors refused to speculate on the significance of this. Regardless of the mechanism of their ablation in these mutants, since the enterochromaffin cells are clearly part of the enteric endocrine system, it might be predicted that their absence would have a dramatic effect on the ability of the animals to absorb nutrients, or even upon gut motility, since endocrine secretions are thought to feed back into the intestinal neuromuscular complex and promote an increased motile response (Tortora & Anagnostakos, 1990).

Overall, the actual mechanism by which the *Sox10^{Dom}* mutation produces the dramatic megacolon phenotype is somewhat unclear. It is emphatically clear that a reduction or loss of enteric glia cells can have drastic physiological consequences, even if enteric neurons remain intact. Thus, it is possible that the *Sox10^{Dom}* mutation might exert an effect at two levels: Firstly, in the neuronal precursor cells, by a delay in their migration with consequential reduction in the number of enteric ganglia in the terminal gut (by whatever mechanism). Secondly, the mutation might act to reduce survival within a subset of enteric glial cells after neuroblast colonisation and differentiation.

Sox10^{Dom} in melanogenesis

Surprisingly little work has been done on the role of *Sox10* in melanoblasts, although a great deal is known about the differentiation of melanoblasts into melanocytes.

Melanoblasts migrate away from the MSA along the dorso-lateral pathway and colonise the developing epidermis around E12.5. Subsequent to this, they

colonise and proliferate in the developing hair follicles around E14.5 (Aubin-Houzelstein *et al.*, 1998). At around the same time, other melanoblasts migrate to and colonise the inner ear, the eye and, curiously, the leptomeninges covering the ventrolateral surfaces of the medulla oblongata and the upper cervical cord (Morse & Cova, 1984; Boissy & Nordlund, 1997). The melanocytic cells of this latter region are believed to give rise to extremely rare primary malignant melanomas of the CNS (Fish *et al.*, 1990).

In the adult skin of the mouse, therefore, there reside two distinct populations of melanocyte. The first consists of a group of melanocytes in the basal epithelial layer of the epidermis, and the second consists of those melanocytes populating the germinative bulb of the hair follicle. The former differentiate and start to produce melanin around E16. Their numbers dramatically increase shortly after birth, with skin pigmentation readily visible by day 3 post-partum in the mouse. Epidermal pigmentation in the trunk of wild-type C57BL6 mice remains for several weeks after birth (Mayer, 1967b). Hair follicle germination also begins around E16, although fur growth lags somewhat behind skin pigmentation in the post-natal mouse. Throughout the growing phase of the hair cycle (anagen), melanogenesis occurs, with the melanocytes in the hair follicle actively transferring melanin granules to the surrounding keratinocytes which form the hair shaft (Aubin-Houzelstein *et al.*, 1998). These two processes are considered to occur separately and to be regulated independently, although they share important regulatory molecules such as the *c-kit/SCF* receptor-ligand system.

While it is relatively straightforward to envision a mode of action for a mutation which completely abolishes skin pigmentation, the mechanism by which only certain large areas lacking pigmentation are generated in coat spotting mutants such as piebald (*s*) has long been a bone of contention. Three major hypotheses have been put forward (reviewed in (Mayer, 1967b)). Schaible proposed that only 14 stem melanoblasts survive and migrate to specific pigment centres in the epidermis, and that subsequent proliferation of melanocytes from these centres results in a fully pigmented coat. In this model, mutations which generate coat spotting do so by eliminating certain stem melanoblasts or

restricting their proliferation, resulting in large unpigmented regions (Schaible, 1969).

Alternatively, following early experiments in various patterning mutations, Mintz suggested that two types of melanoblast were created: one viable, and one "pre-programmed" to die. According to this model, after the initial stages of migration are complete, the death of certain melanoblast clones leaves gaps in the coat that may never be filled in by the viable melanoblasts (Mintz, 1967).

A third hypothesis, favoured by Mayer and others, suggested that melanoblasts migrate in large numbers to all regions of the integument, but that in spotting mutants they fail to differentiate in certain areas of the skin (Mayer, 1965; Mayer, 1967a). This model permits a mutation to affect either the melanoblast (cell autonomous) or the surrounding environment (cell non-autonomous), but the end result is a failure of differentiation of melanoblasts rather than a defect in proliferation or migration.

Although far more is now known about the molecules involved in these processes, little progress has really been made beyond Mayer's studies towards determining the exact mechanism of coat spotting in the mouse and in human pigmentary disorders reviewed in (Boissy & Nordlund, 1997)). It has become apparent though that, as with enteric neuroblasts, mutations in the endothelin-3/endothelin-B receptor act both cell autonomously in the melanoblast and cell non-autonomously in the tissue environment in which the melanoblast differentiates and that this may be a consequence of different actions of these molecules during different times in melanoblast development (Mayer, 1967b; Mayer, 1977). Endothelin-3 in particular has been found to regulate survival and proliferation of early melanoblasts and to directly stimulate their differentiation into melanocytes at a later point in development. (Reid *et al.*, 1996). The *Ednrb/Edn3* receptor-ligand system therefore acts in a similar fashion to *c-kit/SCF* in the melanoblast lineage.

One suggestive finding has been the discovery of a "community effect" postulated to act during the proliferation of melanocytes in hair follicles during development (Aubin-Houzelstein *et al.*, 1998). The recessive patchwork (*pwk*)

mouse mutation appears to be in a gene which encodes a non cell-autonomous signal for melanoblast survival in hair follicles. Patchwork mice show a variegated coat colour pattern with individual hairs either fully coloured or entirely white. In homozygous *pwk/pwk* embryos, most melanocytes were seen to apoptose around E18.5 and the majority of hairs were white. However, a number of different melanoblasts colonise each single hair follicle (Mintz, 1967), and aggregation chimerae between *pwk/pwk* and wild-type embryos showed that the patchwork effect disappeared or was severely ameliorated if sufficient wild-type cells were present. It was also clear from these experiments that *pwk/pwk* melanoblasts could survive and proliferate if an above-threshold number of melanoblasts (wild-type or mutant) were present, hence the "community effect".

If borne out, this result might have relevance to the findings of Kapur and co-workers when they examined aggregation chimerae between wild-type and s^l, *ls* and *Dom* mutant embryos and observed that a relatively small wild-type contribution could completely rescue the aganglionic phenotype. This could be explained by the existence of a similar community effect with respect to enteric neuroblast proliferation upon reaching their target sites. Intriguingly, it has been found that when trunk neural crest cells are cultured *in vitro*, they progressively lose the ability to form neurons, and become restricted to a glial-melanocyte fate. It was established that cell-cell contact leads to loss of the neurogenic subpopulation by apoptosis (Maynard & Weston, 1998). This phenomenon is almost a mirror image of the "community effect".

It is known that melanoblast migration is somewhat delayed compared to other neural crest lineages. One attractive hypothesis is that early neural crest cells are biased towards a neuronal-glial fate, while later ones become biased towards a glial-melanocyte fate. In addition, there may be a restricted window of opportunity for melanoblasts to migrate and successfully proliferate in the epidermis, since melanoblasts express the *c-kit* tyrosine kinase receptor and have an absolute requirement for its cognate ligand, SCF (stem cell factor or Steel factor), to be presented to these cells before they can migrate and proliferate. SCF is transiently produced by the dermamyotome and is localised on the lateral migration pathway shortly before melanoblasts begin to migrate away from the

MSA (Wehrle-Haller & Weston, 1995). If *Sox10* mutations caused a delay in melanoblast migration, this might lead to the melanoblasts missing their chance to encounter SCF and begin migration. Alternatively, the *Sox10* mutations might down-regulate *c-kit* or SCF expression in migrating melanoblasts and cause apoptosis and loss of significant numbers of melanoblasts. Similar arguments can clearly be applied with respect to *Sox10* and other receptor/ligand complexes such as *Ednrb/Edn3*, and this might be considered more likely than *c-kit*/SCF, given that this latter does not appear to play any significant role in enteric neurogenesis.

This is somewhat in accord with the model put forward by Wehrle-Haller and Weston, who suggested that different combinations of tyrosine kinase receptors expressed by neural crest cells in combination with their cognate ligands (which can be found on migratory pathways in soluble or cell-bound form) act to direct the migration and differentiation of neural crest cell populations (Wehrle-Haller & Weston, 1997). *kit* and *ret* clearly fit this model, and although *Ednrb* is not itself a tyrosine kinase receptor, ligand binding does cause the receptor to activate the nonreceptor tyrosine kinase $p125^{FAK}$ (focal adhesion kinase), as well as interacting with intracellular signalling pathways likely to be shared by the "true" receptor tyrosine kinases, such as G-proteins (Zachary & Rozengurt, 1992).

While it is unknown whether *Sox10* acts cell autonomously or not in the melanoblast, it might be predicted from the close similarity between the phenotype of $Sox10^{Dom}$ and the *Ednrb* and *Edn3* null mutants that it acts both at the level of the early melanoblast and during their final differentiation in the skin. The most parsimonious explanation, of course, would be to postulate that *Sox10* lies immediately upstream of one or either of these genes.

No downstream targets of *Sox10* have yet been identified, however, hence the above is purely speculative.

Function of *Sox10* in neural crest cells

Returning to the specification of neural crest fates, although *Sox10* clearly plays some role in setting up both autonomic nervous system and melanocyte lineages, the central question is whether *Sox10* plays an instructive or permissive role. At the time of writing, this remains unanswered, but experiments (as yet unpublished except in abstract form), using retrovirus to shuttle tagged wild-type

SOX10 protein into mouse embryo explant cultures should go some way towards addressing this issue (Dunn *et al.*, 1999).

Investigation of the nature of the transgene integration event

The nature of the Harry mutation

With the transgene closely linked to *Sox10* in **Harry** mice and given a phenotype which was very similar to a known Sox10 mutant, it was decided to investigate the status of this gene at a molecular level, to try and assess the nature, if any, of a transgene-induced mutation at this locus.

Strategy

To investigate the status of *Sox10* in **Harry** mutants, initial experiments were designed simply to assess whether the *Sox10* gene was being expressed at all, and this was achieved using RT-PCR. Following
this, Northern blotting was used to determine the status of the mRNA in mutant animals.

The nature of the transgene integration was investigated by determining the number of copies of the construct present in the **Harry** genome using a method of titrating out a transgene-specific signal until it matched the intensity of a 2-copy endogenous signal. Following this, the transgene integration site was mapped in some detail.

This done, the status of the *Sox10* gene itself was assessed by restriction mapping the region containing the gene in transgenic and wild-type samples and looking for polymorphisms which might be associated with the transgene.

Results

Sox10 *RT-PCR*

With no Sox10 probe available initially, primers were designed to amplify a specific product from Sox10 mRNA. These are detailed in the methods chapter, but were chosen to lie outside and to flank the highly conserved HMG box and to prime from regions which were also not homologous to the closely related Sox8

and Sox9 genes (**Figure 18**). It should also be noted that the HMG box contains a large intron, hence no PCR product should have amplified from contaminating genomic DNA, and this was shown to be the case in control amplifications (data not shown). RT-PCR was performed using the Promega Access kit, which has the advantage that the inital reverse transcription reaction occurs at 48°C, rather than the more usual 45°C. This helps to alleviate the problem of secondary structure in the mRNA, which can often cause RT reactions to terminate prematurely. A conventional RT-PCR method, with reverse transcription at 45°C was found to give no product with these primers (data not shown).

Sox10 RT-PCR reactions were performed on total brain RNA from all 6 pups in a **Harry** intercross litter containing one mutant animal. Although very faint, the predicted 700bp product was amplified from and detected in 4 of the 6 animals in the litter, including the homozygous mutant (**Figure 19**). This showed that the **Harry** mutation was not a simple deletion of the *Sox10* locus, since at least the central portion of the message is expressed in the CNS.

Rather than try and repeat this RT-PCR for the remaining two animals in the litter, since the mutant was clearly expressing Sox10 at some level, it was decided to use Northern blotting to investigate the transcript.

Sox10 Northern blotting

The RT-PCR product was unsuitable as a probe for Southerns and Northerns, since the HMG box comprised a large proportion of the sequence. This region is so highly conserved that it could confidently be predicted to cross-hybridise to other Sox sequences, except under highly stringent conditions (Sox8 and Sox9 are respectively 86% and 83% identical at the nucleotide level over a 160bp region of the HMG box).

Total brain RNA from the same intercross litter tested by RT-PCR was transferred to a filter by Northern blotting and hybridised with a Sox10 probe derived from the 3' end of the cDNA (probe Sox10B on **Figure 18**) which does not contain the HMG box. A separate filter prepared in parallel with the same samples was hybridised with a probe to a housekeeping gene, glyceraldehyde-3-phosphate dehydrogenase (GAPDH) for use as an RNA loading control. Wild-type levels of full-length Sox10 message were seen in all lanes (**Figure 20**). This

Figure 18. Structure of the Sox10 gene and protein

Composite diagram showing Sox10 intron/exon structure, the frameshift in the *Dom* mutation and restriction sites based on a combination of published work (Kuhlbrodt *et al.*, 1998b;Pusch *et al.*, 1998; Southard-Smith *et al.*, 1998), unpublished data (G. Scherer, personal communication) and restriction mapping in this laboratory using the two probes shown at the bottom of the figure.

The putative domains in the protein are based upon published work (Kuhlbrodt *et al.*, 1998a; Kuhlbrodt *et al.*, 1998b; Kuhlbrodt *et al.*, 1998c; Pusch *et al.*, 1998).

The RT-PCR primers used to amplify Sox10 are shown as arrows marked 96, 97, 98 and 99 (see Materials and Methods, chapter 2).

Sox10A and Sox10B are cDNA fragments used as probes in Southern and Northern blotting experiments.

Figure 19. *Sox10* RT-PCR from brain total RNA.

A Sox10-specific 700bp product amplified via nested RT-PCR using primers 98/99 followed by primers 96/97 (see Materials and Methods, chapter 2). Product can be seen in 4 out of the 6 animals in the litter, including the homozygous mutant.

Fig. 18

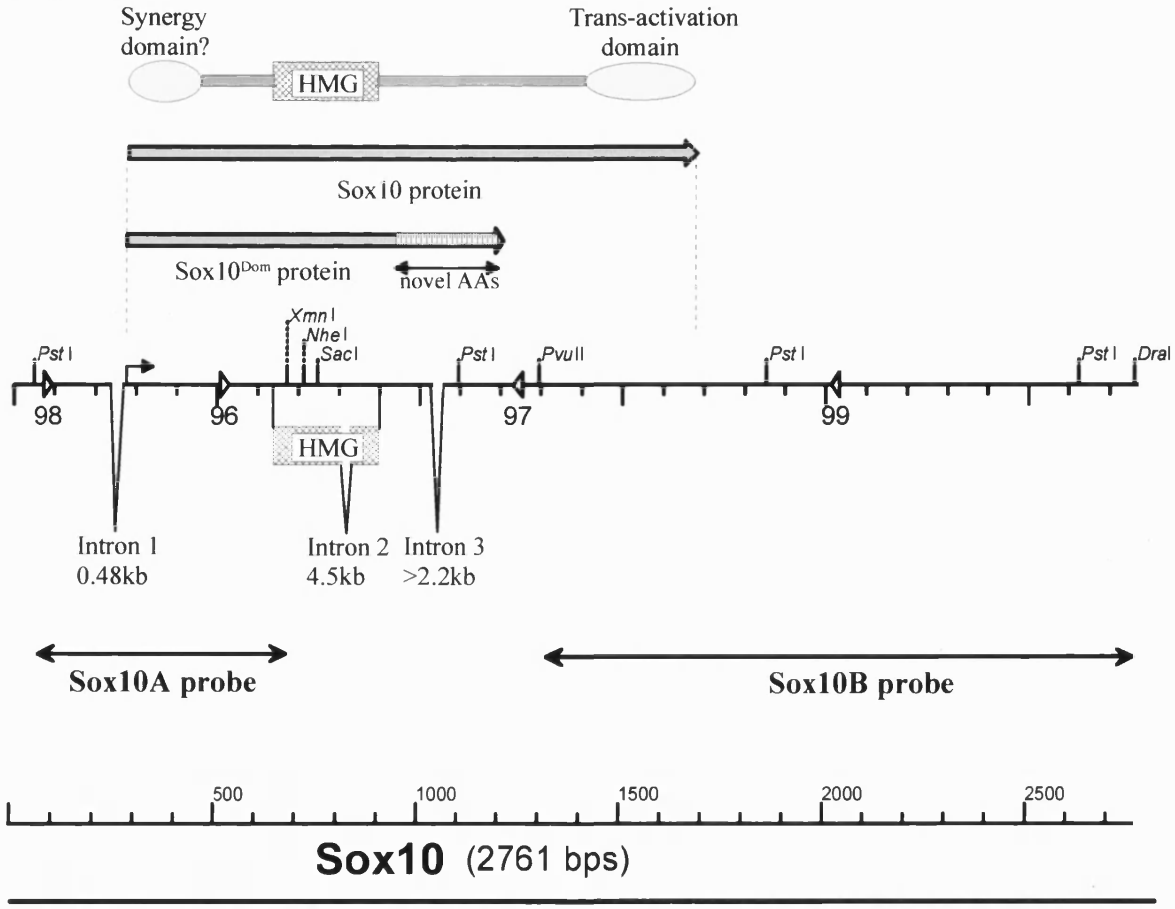
Synergy domain?
HMG
Trans-activation domain
Sox10 protein
Sox10Dom protein
novel AAs
Xmn I
Nhe I
Sac I
Pst I
Pvu II
Pst I
Pst I
Dra I
98
96
97
99
HMG
Intron 1
0.48kb
Intron 2
4.5kb
Intron 3
>2.2kb
Sox10A probe
Sox10B probe
500
1000
1500
2000
2500
Sox10 (2761 bps)

Fig. 19

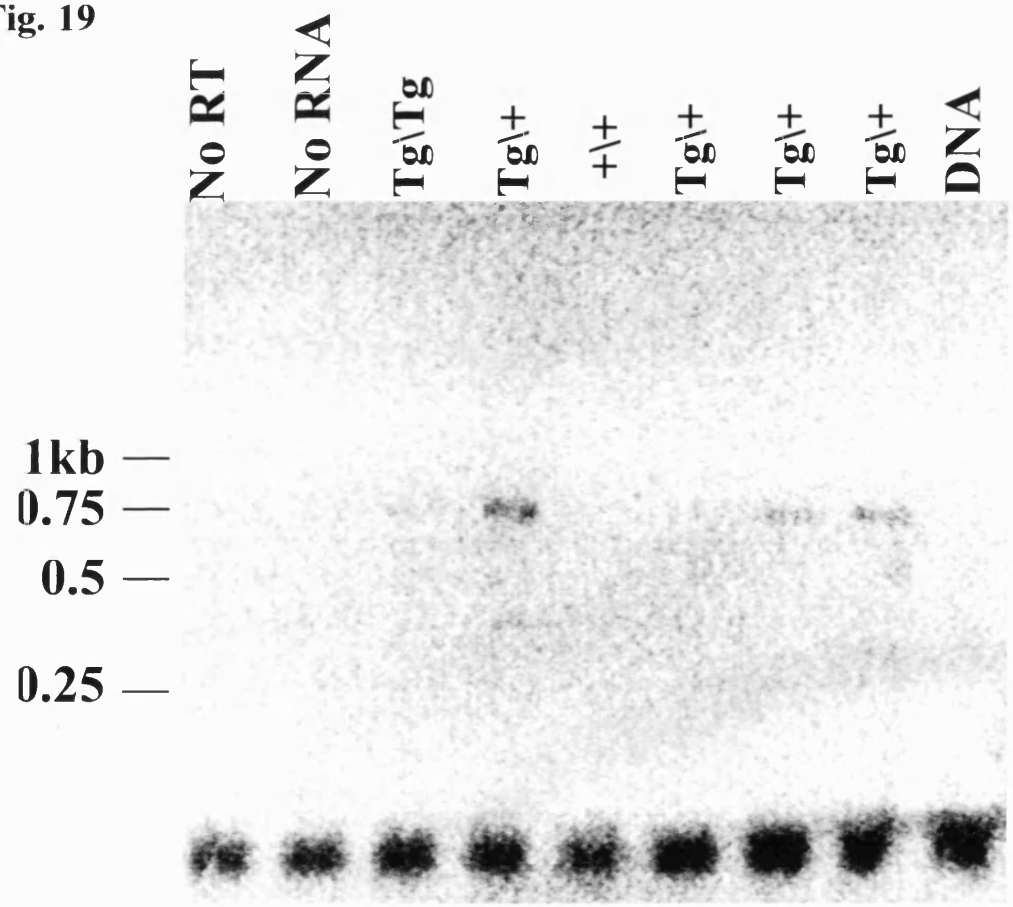
No RT
No RNA
Tg\Tg
Tg\+
+\+
Tg\+
Tg\+
Tg\+
DNA
1kb
0.75
0.5
0.25

experiment was repeated using RNA samples from a different intercross litter and similar results were obtained (data not shown).

Transgene copy number determination

Since densitometric measurement of bands was previously found to be unreliable as a quantititative method in our hands (see chapter 4), this experiment was based on logarithmic dilution of a transgene-specific band and comparison to an undiluted endogenous band, with both bands being obtained simultaneously in the sample using the same probe and the same restriction digest. A KpnI digest using a probe to the 3' portion of the CCD was chosen as being ideally suited for this purpose. In non-transgenic DNA this gives a single band around 12kb, whereas in digested **Harry** DNA, it gives a single, strong, transgene-specific band of around 5kb, along with some fainter, subsidiary bands that probably correspond to junction fragments or truncated transgene constructs. In undiluted transgene DNA, the upper endogenous band provides a "gold standard" of 2 copies (since there are 2 endogenous copies of the genomic region containing the CCD). During progressive dilution of the transgenic DNA, the stronger transgene band would be predicted to fade out. Dilutions based on a logarithmic progression were chosen to correspond to integral values of the transgene relative to the original sample. The dilution which gave a transgene band of the same intensity as the endogenous band in the undiluted lane could therefore be used as a yardstick to estimate transgene copy number. (For example, if the transgene band were to display equal intensity to the original 2-copy endogenous reference band after the sample had been diluted 4-fold, then there would be roughly 8 copies of the transgene represented in this band.)

Table 9 below shows the dilutions performed with each sample made up to 20µl final volume and digested overnight with KpnI in a final volume of 25µl. Each lane on the blot corresponds to an entire digested sample.

Table 9. Dilutions of Harry genomic DNA used for copy number titration

Sample	NTG	TG	TG	TG	T G	TG	T G	TG	TG	T G	TG	TG	TG	TG
Volume of DNA (µl)	20	20	13.33	10.0	8.0	6.67	5.7	5.0	4.44	4	3.63	3.33	3.07	2.86
Transgene copy #	0	2	3	4	5	6	7	8	9	10	11	12	13	14

The results of this are shown in **Figure 21**. The X-ray film was pre-flashed to give a linear response (Sambrook *et al.*, 1989), however it is obvious that the transgene band does not begin to diminish towards the intensity of the 2-copy reference band until the very lowest dilution tested in this experiment, which corresponded to 14 copies of the transgene. Judging from the relative intensity at the 14-copy dilution, there are unlikely to be significantly more than 14 copies. Taking into account the extra bands on the blot, which probably correspond to junction fragments or partial copies of the transgene, the copy number was therefore deemed likely to lie somewhere between 15 and 30 copies, pending further investigation.

Restriction map of the transgene array

Samples of non-transgenic, hemizygous and homozygous genomic DNA were digested with various restriction enzymes, Southern blotted and the filters hybridised with 3 different probes corresponding to various regions of the transgene construct, specifically the 5′ end (probe P3), the 3′ end (probe CCD) and the middle (probe LUX). These are shown diagramatically in **Figure 22a**. There are four potentially methylation-sensitive restriction sites in the construct, three EcoRI and one SacI (restriction sites which overlap a CpG dinucleotide). No information was available concerning the methylation-sensitivity of BstEII.

A preliminary map of the transgene array with the relevant restriction sites marked is shown in **Figure 22b**. This map cannot be viewed as definitive, as some of the bands in various lanes remain unexplained or open to multiple

Figure 20

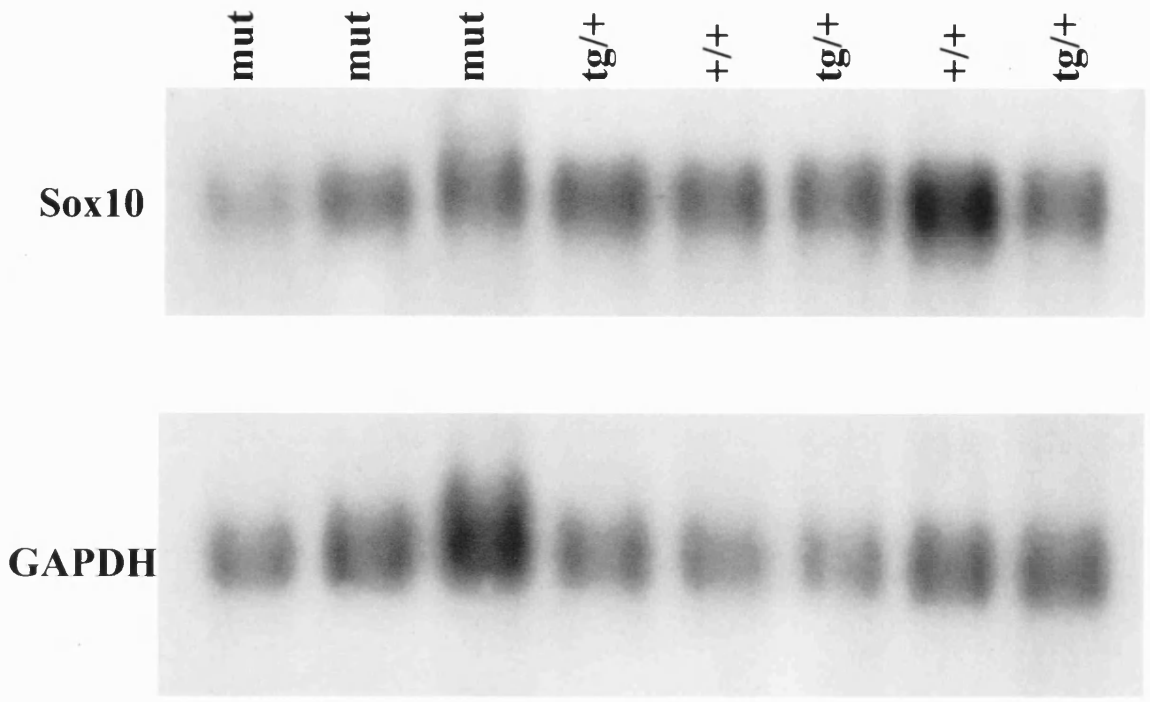

Figure 21

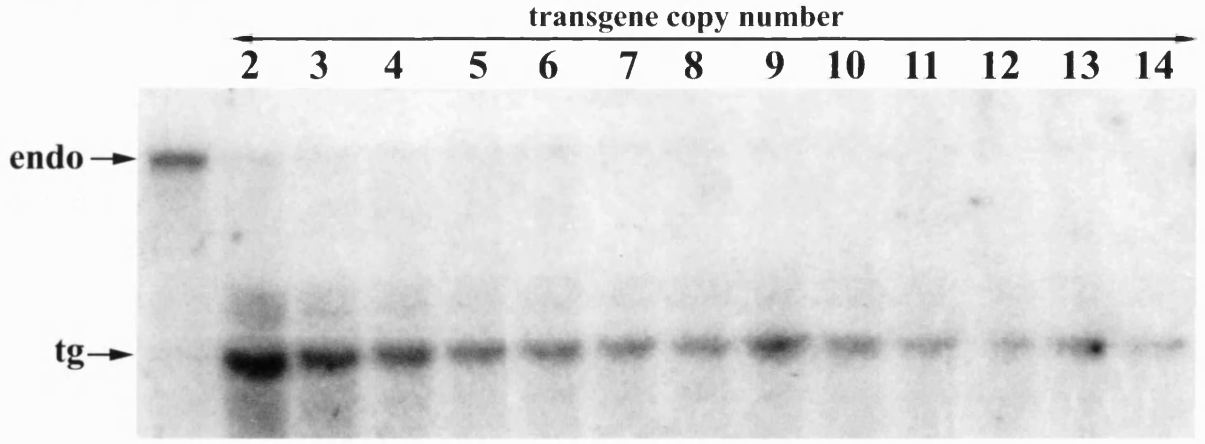

interpretations. It is almost certain that at least some of the unexplained bands were due to methylation-sensitive enzymes failing to cut at methylated sites in a fraction of the DNA sample. It is also likely that strain-specific RFLPs existed between the parental strains, since such was shown to be the case during restriction mapping of the *Sox10* locus (discussed below).

A representative autoradiogram from DNA hybridised with the CCD probe is shown in **Figure 22c**. As an example, both KpnI and ApaI are predicted to cut the transgene construct only once, near the centre. In a head-to-tail array, digestion with either of these enzymes should give a full-length construct band of 5.2kb. In the corresponding lanes on the blot, multiple fainter bands can clearly be seen flanking the more intense predicted 5.2kb band.

Sox10 polymorphism mapping

In an effort to detect transgene-associated polymorphisms in or near the *Sox10* gene, wild-type, hemizygous and homozygous genomic DNA was digested with various restriction enzymes, Southern blotted and the filters hybridised with probes Sox10A and Sox10B which corresponded to the 5′ and 3′ end of the gene (see **Figure 18**).

No polymorphisms were detected on blots probed with Sox10A and Sox10B (**Figure 23**) apart from naturally occurring ones found to be present between C57 and CBA following test Southerns using parental strain DNA (data not shown). Although the *Sox10* gene had a dearth of restriction sites appropriate for use with these probes to scan the flanking regions, it was possible to determine that there was no polymorphism either within the gene itself or within ~3kb of the 5′ end of the gene and ~1.5kb of the 3′ end of the gene.

Figure 22a. Map of the "H" transgene construct

Detailed map of the "H" construct used to generate the **Harry** transgenic line, including restriction sites used in mapping. Potentially methylation-sensitive sites are marked with an asterisk. Regions of the construct are indicated (P3 = *Igf2* promoter P3; Luc = luciferase coding region; SV40 = SV40 large t intron and polyadenylation signal; CCD = centrally conserved domain from *Igf2/H19* intergenic region). Probes used in restriction mapping are shown arrowed below.

Figure 22b. Map of the Harry integration site

Preliminary map of the structure of the integration event in the **Harry** transgenic line. Suspected deletions are circled at **a** and **b**. Flanking and interspersed genomic DNA is indicated by dotted lines.

Figure 22c. Representative autoradiograph from restriction mapping experiments

Southern blot of wild-type and hemizygous transgenic DNA digested with various enzymes and hybridized with probe CCD shown in Figure 22a.

Fig. 22a

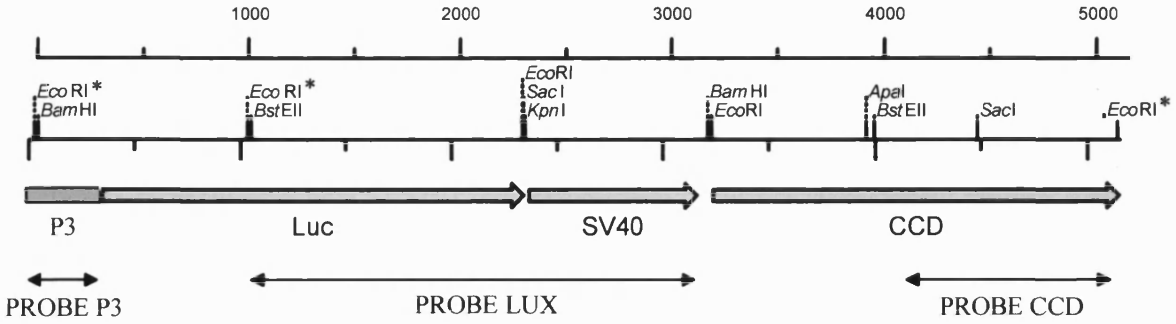

H construct (5145 bps)

Fig. 22b

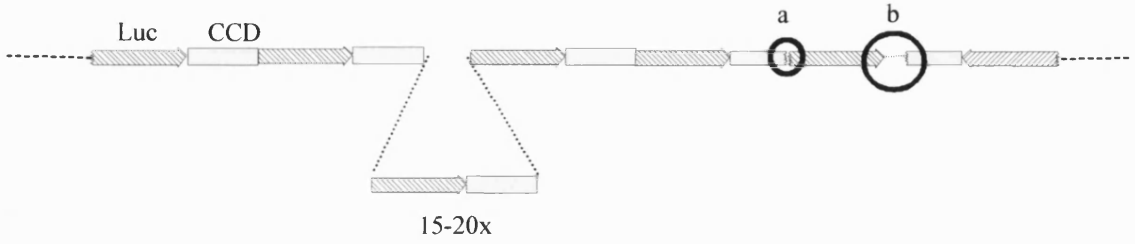

Fig. 22c

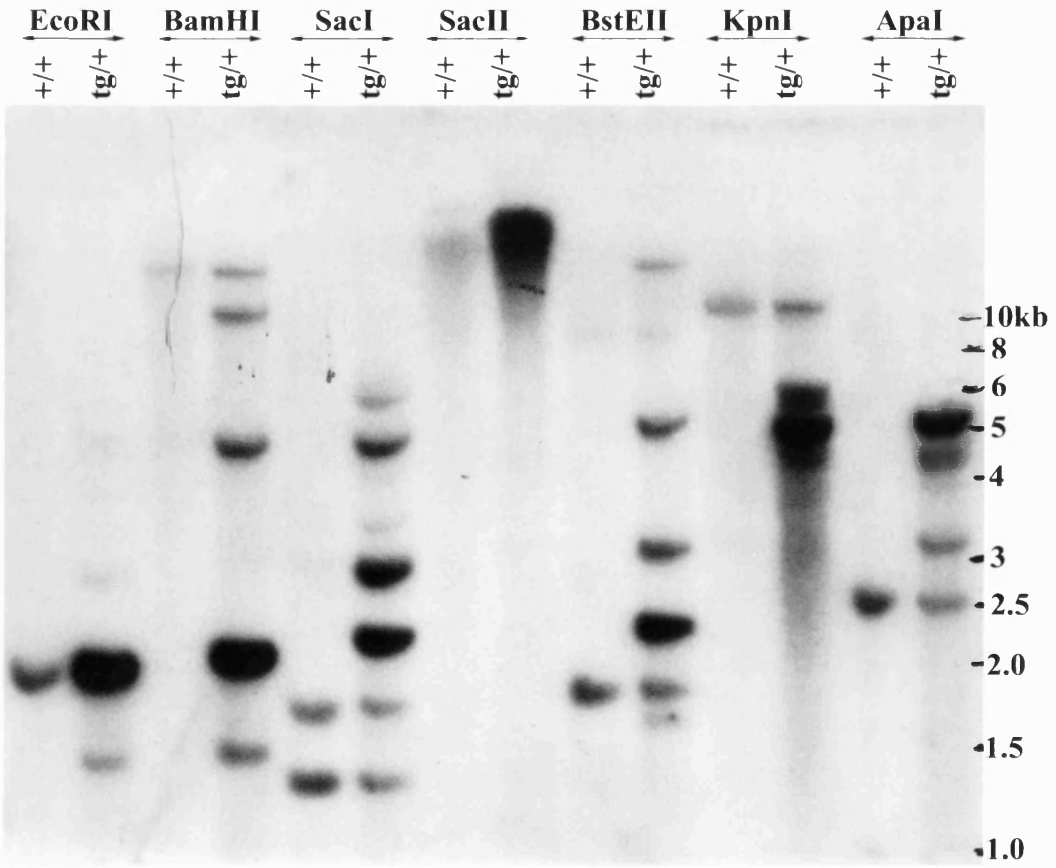

Figure 23a. Polymorphism mapping with 5' *Sox10* probe

Homozygous, hemizygous and non-transgenic genomic DNA digested with various restriction enzymes, run out on 0.3% agarose, Southern blotted and hybridised with a probe derived from the 5' end of the *Sox10* cDNA (probe Sox10A on Figure 18).

Figure 23b. Polymorphism mapping with 3' *Sox10* probe

Homozygous and non-transgenic genomic DNA digested with various restriction enzymes, run out on 1% agarose, Southern blotted and hybridised with a probe derived from the 3' end of the *Sox10* cDNA (probe Sox10B on Figure 18).

Figure 23

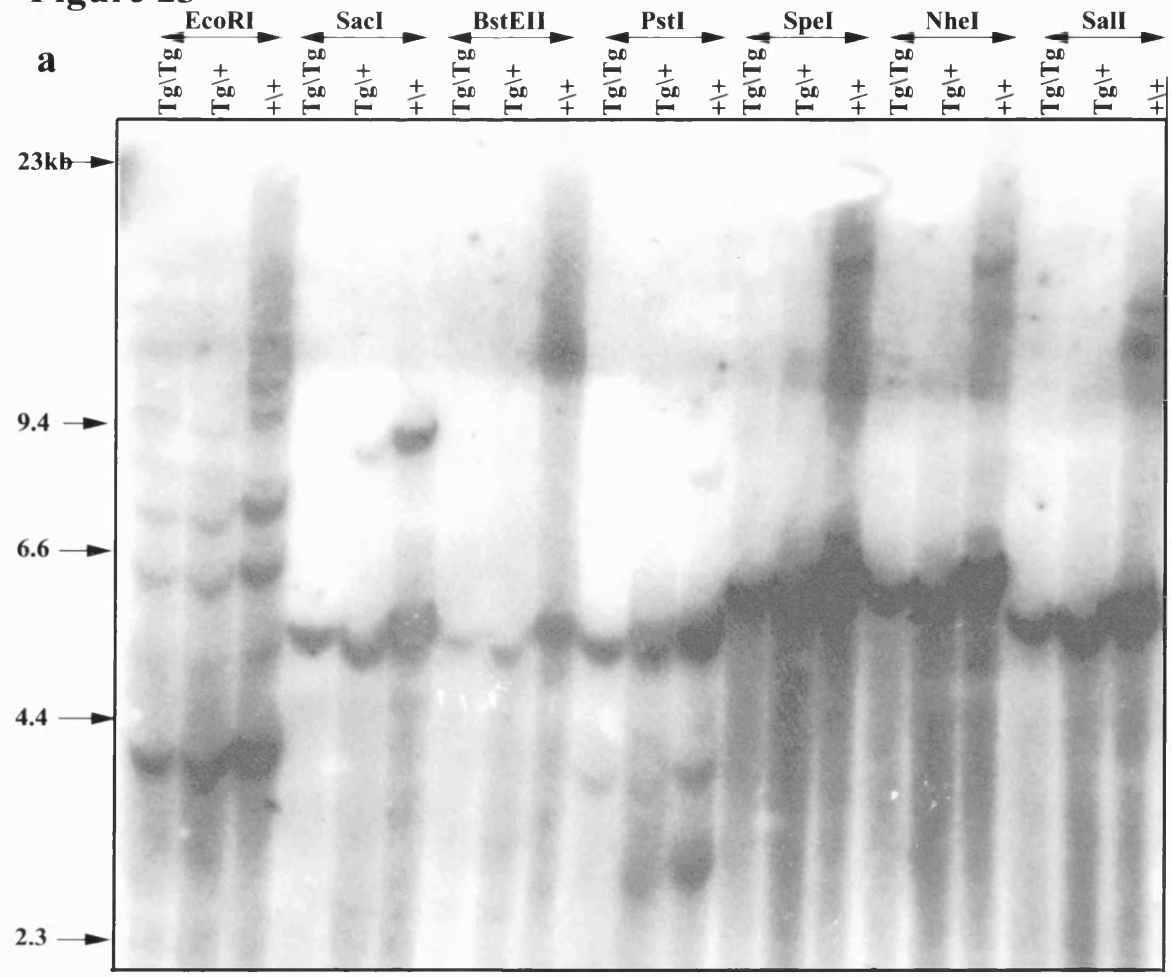
a
EcoRI
SacI
BstEII
PstI
SpeI
NheI
SalI
Tg\Tg
Tg\+
+\+
23kb
9.4
6.6
4.4
2.3

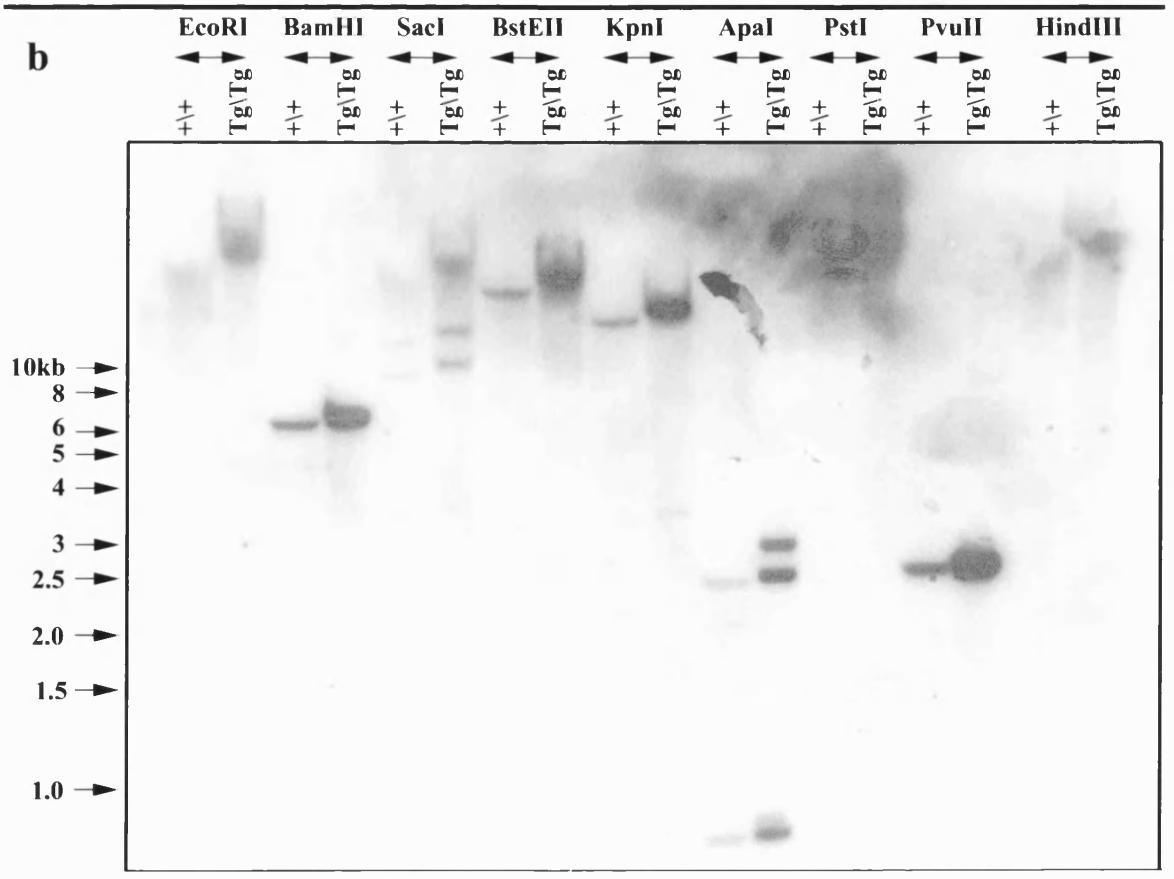
b
EcoRI
BamHI
SacI
BstEII
KpnI
ApaI
PstI
PvuII
HindIII
+\+
Tg\Tg
10kb
8
6
5
4
3
2.5
2.0
1.5
1.0

Discussion

From the RT-PCR results and Northern blotting, it is clear that **Harry** mutants express essentially wild-type levels of full-length Sox10 mRNA in the CNS, at least post-natally. Furthermore, it is also clear, that despite a large and complex integration site containing at least 15 copies of the transgene, there is nodisruption within or in the immediate vicinity of the *Sox10* gene itself. There are a number of possibilities arising from these data.

Firstly, it is possible that the gene affected is simply not *Sox10*. Although it seems highly improbable that a second gene performing a very similar function would exist within 1.6cM of *Sox10*, tandem gene duplications are not unheard of and a gene derived by such an event would be predicted to be closely linked to *Sox10*. Furthermore, given the existence of two nearby loci which also affect coat colour in some respect (*gt* and *bt*), it is not inconceivable that one or both of these loci represent genes distinct from *Sox10* which also play a role in neural crest cell development. The transgene could therefore be disrupting gene function at a locus distinct from *Sox10*. Applying Occam's Razor, however, given the close similarity between the phenotype observed in **Harry** mutants and $Sox10^{Dom}$ heterozygotes , this explanation must be classed as being of low probability.

Assuming that *Sox10* is the affected locus, it is possible that the transgene insertion induced some rather subtle mutation in the Sox10 gene which would not affect the length of the transcript, such as the nucleotide insertion leading to the frameshift seen in the $Sox10^{Dom}$ mutation. Given the often chaotic events usually associated with transgene insertion, this can also be considered as low probability, but it is not inconceivable that a small region of the gene could have been affected during the upheaval accompanying transgene insertion, perhaps by a small insertion, translocation or deletion event.

It is possible that alternative splicing of Sox10 mRNA occurs and that the transgene insertion has reduced the level of or entirely ablated a minor transcript which plays a crucial role in neural crest. There have been reports in the literature of a 2.7kb Sox10 major transcript in human testis, quite distinct from the normal 3.1kb transcript in other tissues (Bondurand *et al.*, 1998). No alternate transcripts have been reported for the mouse, however, despite published results

from several Northern blotting experiments (Herbarth *et al.*, 1998; Kuhlbrodt *et al.*, 1998b; Pusch *et al.*, 1998).

The gene structure of Sox10 is uncharacterised upstream of the canonical start site indicated by the very 5′ end of the cDNA shown in **Figure 18**, and there could certainly be other exons and alternative start sites in this region. If such an alternative transcript was roughly the same size as the known 3kb message, or if it was simply expressed at low levels relative to the major transcript in the CNS, then its reduction or absence in mutant brain total RNA might not be detected on Northern blots. It should be noted that a neural crest-specific transcript would be predicted to be present at very low levels compared to the CNS transcript detected on the blot shown in **Figure 20**, by virtue of the fact that there are almost no neural-crest derived tissues present in the brain. All glial cells in the CNS are of neurectodermal origin.

There is good evidence for the existence of alternatively-spliced transcripts in other Sox genes, with *Sox5* and *Sox6* in particular possessing well-characterised long isoforms, L-Sox5 and L-Sox6 (SoxLZ) (Takamatsu *et al.*, 1995; Hiraoka *et al.*, 1998; Lefebvre *et al.*, 1998). L-Sox5 and L-Sox6 both possess a large amino-terminal region not present in the short isoforms which contains the leucine-zipper coiled-coil domain critical for dimerisation between Sox proteins. It has also been shown that the long form of *Sox5* is expressed in the early mouse embryo (E8.5), as well as in the adult testis at a low level compared to the short isoform (Hiraoka *et al.*, 1998).

Sox10 is known to be expressed from around E9.5 onwards by *in situ* hybridisation studies, but the earliest published Northern blot data is from E12.5 embryos (Southard-Smith *et al.*, 1998). Other studies, including this one, have only looked at RNA derived from neonatal or adult tissues (Herbarth *et al.*, 1998; Kuhlbrodt *et al.*, 1998b).

It is therefore at least a formal possibility that *Sox10* has an alternate long isoform which is chiefly expressed in the early embryo.

Another possible explanation is that, rather than disrupting an alternative transcript, the transgene could have disrupted an enhancer region which controls expression of Sox10 in developing neural crest cells, but plays no role in

governing expression in the CNS. This "distant enhancer" hypothesis is attractive, because such an element could lie quite distant from the gene (which would explain the lack of polymorphisms detected by restriction mapping), and because disruption of such an enhancer could specifically influence expression during neural crest development whilst leaving CNS expression unaffected (which would explain the Northern blotting results).

There is some support for this hypothesis from studies of the closely-related *Sox9* gene, in which it was shown that there existed important regulatory elements scattered across a large upstream region (Wunderle *et al.*, 1998). In these experiments, a number of transgenic mouse lines were derived bearing YACs containing a *lacZ* reporter construct driven by varying amounts of the genomic region surrounding *Sox9*. A YAC containing some 350kb of upstream DNA gave patterns of expression of the reporter which corresponded to the normal patterns observed for *Sox9*, although no expression was seen in the gonads. The absence of elements lying at least 50kb upstream of the coding region caused significant down-regulation of *Sox9* expression in chondrogenic tissues during murine embryonic development. It was found that the regulatory elements required for correct tissue-specific expression of *Sox9* lay in various regions between 50 and 350kb upstream of the gene. Deletion of these elements in human patients by virtue of translocation breakpoints located at least 200kb upstream of *Sox9* was found to recapitulate the campomelic dysplasia (a genetic syndrome involving severe dysfunction of chondrogenesis and autosomal sex reversal) found in patients containing mutations within the coding region of the gene.

Staying within the confines of this "distant enhancer" hypothesis, it is possible that the transgene integration has caused a slight global decrease in the level of transcript, rather than a tissue-specific effect. This might well not be detectable by Northern blotting, but such a slight decrease might be enough to "tip the balance" and cause a dramatic phenotype. This model would imply that the wild-type levels of Sox10 expression lie very close to a threshold level, below which a phenotype manifests. Threshold dosage effects have been observed for other transcription factors such as *Pax6* and *Gli3*, particularly in the context of

human clinical genetic defects with variable expressivity or partially penetrant phenotypes, and haploinsufficiency has been mooted as a possible mechanism by which *Sox10^{Dom}*/+ mutants display their phenotype. In support of this mechanism, the molecular defect present in a single patient classified as suffering from a rare congenital disease - the Yemenite deaf-blind hypopigmentation syndrome - has recently been elucidated as a single base-pair transversion within the HMG box of SOX10 (Bondurand *et al.*, 1999). Functional analysis of the mutation showed that binding of the protein to a DNA target was completely abolished, at least *in vitro*. The phenotype seen in the patient consisted of skin hypopigmentation and hearing impairment, although no Hirschprungs was described (Hennekam & Gorlin, 1996). Since the proband was heterozygous for what was apparently a null mutation of SOX10, this would suggest that haploinsufficiency could account for at least the melanoblast component of the *Sox10^{Dom}*/+ phenotype.

However, such a model seems inconsistent with the robust, fully penetrant recessive phenotype observed in **Harry** mutants.

CHAPTER EIGHT:
HARRY - FINAL DISCUSSION

Nomenclature of the Harry mutant

In the absence of any firm molecular evidence of transgene-associated disruption at the *Sox10* locus, the evidence that the **Harry** mutation is truly a novel allele of *Sox10* remains circumstantial, pending further investigation. However, given the very close similarity between the $Sox10^{Dom}$/+ mutant phenotype and that seen in **Harry** homozygotes, the tight linkage to the *Sox10* locus and the absence of any other strong candidate loci in the immediate vicinity, it is suggested that **Harry** does in fact represent a transgenic insertional mutation at the *Sox10* locus. According to the rules laid down by the Committee on Standardized Genetic Nomenclature for Mice (Lyon *et al.*, 1996), it is therefore proposed that this allele be given the designation $Sox10^{TgNRpLucH1Ward}$ [with the superscripted suffix composed of Tg (transgene);N (non-homologous insertion);Rp (reporter); LucH (luciferase H construct); 1(allele number);Ward (designated laboratory code)].

Future work

Complementation between $Sox10^{TgNRpLucH1Ward}$ and $Sox10^{Dom}$

A number of possible experiments suggest themselves in order to resolve the question of the exact nature of the $Sox10^{TgNRpLucH1Ward}$ mutation. The most apparently straight-forward of these would be to cross transgenic hemizygotes with $Sox10^{Dom}$ /+ animals of breeding age and see if the mutations complement. This is rather a complex experiment, however, since $Sox10^{Dom}$ heterozygotes display the full phenotype observed in $Sox10^{TgNRpLucH1Ward}$ homozygotes. If the two mutations are allelic at the *Sox10* locus, this might be predicted to result in a more severe phenotype. On the other hand, even if they are allelic, given the recessive nature of $Sox10^{TgNRpLucH1Ward}$ and the dominant nature of $Sox10^{Dom}$, it is possible that a compound $Sox10^{Dom}$/ $Sox10^{TgNRpLucH1Ward}$ animal might display exactly the same phenotype as a $Sox10^{Dom}$/+ heterozygote. Furthermore, due to the severity of the phenotype in heterozygotes, it is difficult to maintain a

breeding colony of *Sox10^{Dom}* animals. They are currently maintained on a B6C3Fe-*a/a* background by the Jackson laboratory, however, where the phenotype is relatively mild and are therefore commercially available (http://www.jax.org, 1998).

Complementation between *Sox10^{TgNRpLucH1Ward}* and *bt*

Similarly, it might also prove worthwhile to test both *Sox10^{TgNRpLucH1Ward}* against *bt* (belted) for complementation. Although *Sox10^{Dom}* and *bt* were shown to recombine with respect to each other, current mapping data available shows that they are closely linked (Mouse Genome Database, 1999). Recent mapping studies have shown that these two loci actually lie some 5cM apart, but this remains unconfirmed, pending publication (D. Foernzler, pers. comm.). Even if *Sox10* and *bt* do prove to correspond to different genes, given that both loci are involved in melanocyte differentiation and/or proliferation, the two genes might interact in a doubly heterozygous animal to give a compound phenotype.

Irrespective of the allelic or non-allelic nature of these two loci, in the absence of firm molecular evidence of transgene-associated disruption at the *Sox10* locus in **Harry** mice, the presence of a second nearby locus with an effect on melanoblast proliferation makes it imperative to test whether the mutation seen in these mice might be at the *bt* locus rather than *Sox10*. *bt* mice are widely available, with the mutant allele having been bred onto multiple genetic backgrounds due to its utility as a visible, viable phenotypic marker (http://www.informatics.jax.org, 1998).

Complementation between *Sox10^{TgNRpLucH1Ward}* and *wn*

Exactly the same arguments pertain to a complementation test between the **Harry** line and the mutant *wn* (white nose), perhaps with even more force, given that the mapping data for *wn* places it much closer to *Sox10* than *bt* (Marks *et al.*, 1999).

Transgenic rescue of the *Sox10^{TgNLucH1Ward}* phenotype

If a transgenic line could be constructed that over-expressed *Sox10* under the influence of a neural crest-specific promoter such as the human *DβH* promoter

region used to successfully tag enteric neuroblasts and catecholaminergic neurons, this could be crossed with the *Sox10*^{TgNLucH1Ward} line to see if it could rescue the mutant phenotype. This could provide definitive proof that the locus affected by transgene insertion was indeed *Sox10*, but must be considered as a rather chancy experiment with a number of possible pitfalls.

In order to rescue the phenotype seen in *Sox10*^{TgNLucH1Ward} mutants, the exogenous wild-type *Sox10* would have to be expressed in the same subset of neural crest cells which are most affected by the mutant allele. If the *DβH* promoter fulfilled this requirement and the transgene did indeed rescue the phenotype, then the matter would settled. However, if the transgene failed to rescue the phenotype, it would be unclear whether this was because the mutation affects a critical role of *Sox10* in some other subset of neural crest cells, or whether the mutation seen in **Harry** homozygotes was caused by disruption of a different gene. Different promoters, such as a constitutive one from a housekeeping gene, would have to be harnessed to drive expression of *Sox10* in this event. However *Sox10* is clearly a potent transcriptional modulator, if not a transcriptional activator in its own right, and over-expression in a transgenic line might well lead to some undesirable phenotypic side-effects. Constitutive over-expression of *Sox10* might be predicted to have dramatic effects upon Schwann cells in the PNS, for example, which might well compromise viability of the transgenic line. The use of a large genomic region containing the Sox10 gene (such as a cosmid or a BAC) as the injected transgene construct might obviate this problem.

While the transgenic rescue approach is attractive, therefore, it has to be approached with a degree of caution.

Further genetic and physical mapping

It is clearly possible to continue to refine the map position by genotyping more animals, and since the D15Mit260 marker has been placed on the physical map less than 40kb away from the *Sox10* gene, this might prove to be the most useful marker in order to unambiguously link the transgene mutation to the *Sox10* locus. However, this marker was found not to be polymorphic between C57 and CBA, so the transgene would first have to be introgressed onto another background.

A more direct approach would be to extend the physical mapping by obtaining probes for regions flanking the *Sox10* gene and scanning for transgene-associated polymorphisms at progressively greater distances from the gene. This has the danger that should the transgene prove to have disrupted a very distant regulatory element, or should it prove to have disrupted an entirely separate locus, a great deal of time and effort could be expended establishing such polymorphisms. One useful approach to physical mapping could take advantage of the fact that a BAC containing the gene has been identified and mapped and is commercially available (Research Genetics Inc., http://www.resgen.com, 1998). The *Sox10* gene lies within 25kb of one end of this BAC (Southard-Smith *et al.*, 1998). With the use of Cre-loxP mediated end-labelling to efficiently and quickly restriction map the BAC (Mullins *et al.*, 1997), probes flanking the gene could be rapidly isolated and used to scan flanking genomic DNA in wild-type and $Sox10^{TgNRpLucH1Ward}$ mice for transgene-associated polymorphisms.

A useful starting point for such an exercise would be to take advantage of the sequence already in the database for a 40kb human cosmid covering the entire SOX10 gene, and a database detailing the 431 sub-clones obtained after shotgun cloning BAC 43P19, containing the mouse *Sox10* gene (Pusch *et al*, 1998; Southard-Smith *et al.*, 1999c). The human cosmid ends some 3kb upstream of exon 1 of SOX10, however comparative BLAST analysis of the subclones obtained from the murine BAC reveals a short region of 160bp with >95% conservation at the nucleotide level between mouse and human. This conserved region lies some 2.7kb upstream of exon 1 of SOX10, and shows no BLAST hits to any protein or EST databases. It is possible that this region represents an alternative exon of *Sox10*, something which has been suggested to exist by several authors, but not yet defined (Pingault *et al.*, 1998; Southard-Smith *et al.*, 1999). It is also possible that it is an upstream enhancer element. Regardless of its nature, it could be used as a probe to scan for transgene-associated polymorphisms upstream of *Sox10*. Unfortunately both the mouse BAC and the human cosmid terminate shortly upstream of this element, so no further comparative sequence analysis is possible at the present time. However, when the human and mouse genome sequences are

published, it will be possible to compare large segments of the genomes in this way to identify regulatory elements upstream of genes.

One important consideration with respect to this long-range mapping approach is that there exists good evidence that important regulatory elements exist >350kb upstream of the closely-related *Sox9* gene, and that such a mapping exercise might have to cover a very large region (Wunderle *et al.*, 1998).

Is there an alternate *Sox10* transcript in the early embryo?

One key experiment which might help to shed light on the nature of the $Sox10^{TgNRpLucH1Ward}$ mutation would be to perform Northern hybridisation using RNA derived from E9.5-E12.5 embryos, to determine whether there might exist any alternatively-spliced transcripts. $Sox10^{TgNRpLucH1Ward}/Sox10^{TgNRpLucH1Ward}$ homozygotes can be detected at any stage of development by use of the closely-linked polymorphic microsatellite markers D15Mit2, D15Mit1 and D15Mit71. RNA could therefore be isolated from genotyped embryos at various stages and hybridised with *Sox10* probes.

No published data exists prior to E12.5, and since *Sox10* is known to be expressed from E9.5 onwards in the developing peripheral nervous system and presumptive pre-migratory neural crest, the existence of such an alternate transcript would provide an attractive mechanism for the mode of action of the $Sox10^{TgNRpLucH1Ward}$ allele.

Neural crest cell apoptosis

Even without detailed knowledge of the precise molecular nature of the mutation, the $Sox10^{TgNRpLucH1Ward}$ mutant embryos represent a unique resource for the dissection of neural crest cell migration and ontogeny during development.

It might prove informative to ascertain the degree of apoptosis in $Sox10^{TgNRpLucH1Ward}/ Sox10^{TgNRpLucH1Ward}$ embryos during neural crest cell migration. Using the TUNEL (Tdt-mediated dUTP-X nick end labelling) assay for apoptotic cells, extensive apoptosis of presumptive neural crest derivatives has been observed in $Sox10^{Dom}$ homozygotes , with essentially no melanoblast or enteric neuroblast precursors present by E11.5 (Southard-Smith *et al.*, 1998). Interestingly, in $Sox10^{Dom}$ homozygotes, which are embryonic lethal by E13,

apoptosis was also seen in structures not known to be affected in heterozygotes, such as dorsal root ganglia. The obvious experiment would therefore be to obtain staged *Sox10*^{TgNRpLucH1Ward}/ *Sox10*^{TgNRpLucH1Ward} embryos and perform TUNEL assays to see whether and where any apoptosis of neural crest cells occurs. The microsatellite markers known to be closely linked to the transgene can be used to genotype DNA prepared from yolk sacs to identify homozygous embryos.

Aggregation chimera studies

Even if significant apoptotic loss of enteric neuroblast precursors was observed in *Sox10*^{TgNRpLucH1Ward} mutants, this would not directly answer the question of how the aganglionosis arises in the terminal gut. One crucial (and long-standing) question has been the exact nature of the contribution of the sacral neural crest to the hindgut and its relevance to enteric neurogenesis. Since it is now known that a large component of the enteric nervous system in the colon is derived from sacral neural crest, at least in avian embryos, but that sacral crest cells express none of the markers traditionally associated with enteric neuroblasts, it is important to determine the exact timing and nature of murine sacral crest migration and proliferation in the gut (Burns & LeDouarin, 1998). A number of experiments with *Sox10*^{TgNRpLucH1Ward} mutant embryos might prove fruitful in this regard.

Since the mouse lacks specific markers for enteric neuroblasts, it would be difficult to track the progress and proliferation of these cells in the gut without introgressing the mutant allele onto the *DβH-nlacZ* strain of mice (Kapur *et al.*, 1992). One attractive alternative would be to make aggregation chimerae between *Sox10*^{TgNRpLucH1Ward} homozygotes and ROSA-26 embryos, which are available and maintained in Bath (Prof. J. Slack). This line of transgenic mice contains a *lacZ*-based enhancer trap event which has been bred onto an albino background to make homozygotes fully viable and fertile (Zambrowicz *et al.*, 1997). This results in essentially wild-type embryos which constitutively express β-galactosidase in all cells. In aggregation chimerae stained with X-gal, therefore, all wild-type cells would stain blue and mutant cells would be unstained. This would allow a direct visual assay for the level of wild-type contribution to the chimera. It would be predicted, from the results obtained in aggregation chimera experiments in

Sox10^{Dom}, *Ednrb* and *Edn3* mutants, that a relatively small wild-type contribution could rescue the aganglionic phenotype in *Sox10^{TgNRpLucH1Ward}* mutants. *lacZ* staining can be combined with immunohistochemical staining (Bernex *et al.*, 1996), and immuno-staining for glial or neuronal markers in fully developed colons would allow assessment of wild-type versus mutant contribution to the ENS. In combination, these data might help elucidate how a relatively small number of wild-type cells can rescue the aganglionic phenotype, if such were found to be the case.

Sox10^{TgNRpLucH1Ward} mutant embryo cells clearly contain an exogenous transgene which might be used to track mutant cells in aggregation chimerae with fully wild-type or other (different) mutant embryos such as *Sox10^{Dom}* . However, it has proven technically difficult to reliably detect the transgene in tissue sections or wholemount preparations, either by luciferase immunohistochemistry or by *in situ* hybridisation (M. Charalambous, unpublished results). Tissue-specific luciferase activity has been imaged directly by simply placing enzyme substrate onto explanted organs and thick tissue slices, however this required the use of a highly-sensitive photomultiplier linked to a cooled CCD camera, and the cellular resolution was rather poor (A. Ward & M. White, unpublished results). Thus, at the present time, the transgene unfortunately cannot be considered useful as a high-resolution marker for mutant cells when planning experiments. However, Northerns, RNAse protection assays or Westerns for luciferase could provide a useful measure of the relative contribution of transgenic to wild-type tissue in chimeric mice, albeit not with the high spatial resolution achievable through microscopy-based methods.

Determination of the cell autonomous or non-autonomous nature of the *Sox10^{TgNLucH1Ward}* mutation by organ culture

An organ culture system has recently been developed in which mouse fetal gut can be cultured *in vitro* in such a way that its three-dimensional organisation is maintained, and that supports morphogenesis and development of the ENS (Natarajan *et al.*, 1999). It was used to show that a null mutation in *c-ret* functions

cell autonomously with respect to enteric neuroblasts by demonstrating that isolated wild-type neuroblasts could successfully colonise and proliferate in *c-ret-/-* segments of gut lacking intrinsic neuroblasts. On the other hand, older experiments in a similar, but less sophisticated organ culture system, proved that the *ls* mutation was non cell-autonomous in nature (Jacobs-Cohen *et al.*, 1987).

The new organ culture system offers a decisive means of determining the cell autonomous or non-autonomous nature of mutations which affect enteric neurogenesis. Although isolation of enteric neuroblasts is technically demanding and requires a fluorescence-activated cell sorter (FACS) and whilst it is currently unclear whether the organ culture method is robust and replicable, it offers an attractive system for studying the nature of the *Sox10*^{TgNLucH1Ward} mutation.

***Sox10* expression patterns**

Another aspect of the mutant phenotype which has not been studied in any detail is the expression pattern of *Sox10* in the ENS of post-natal mutant animals. It is clear that the gene is expressed in early neural crest and in enteric neuroblasts, but it is unclear in which subsets of neural crest derivatives *Sox10* expression is maintained during adult life. From the data available in the PNS, it would be predicted that *Sox10* might be restricted to the enteric glia, and antibodies to glial fibrillary acidic protein (GFAP) combined with *in situ* hybridisation with the *Sox10* message could be used to investigate this hypothesis.

Studies of enteric neural crest derivatives outwith the myenteric plexus

While the experiments described in the preceding paragraph do not require *Sox10*^{TgNRpLucH1Ward} mutants, it might also be informative to use similar methods to investigate the status of the plexus of Meissner and the enterochromaffin cells in wild-type and mutant animals. While there are no specific markers for the plexus of Meissner, and these cells are small and difficult to observe, GFAP antibody staining can be used to reveal glia in this plexus and Fontana-Masson staining can be used as a straightforward method of assessing the status of enterochromaffin cells in *Sox10*^{TgNRpLucH1Ward} mutants (Culling, 1974).

Studies of melanoblasts in *Sox10^{TgNRpLucH1Ward}* mutants

This area has received very little attention, both in the current and in other studies. It remains an open question as to whether *Sox10* is important for early melanoblast specification or migration or whether the known mutations act later on during migration along the dorso-lateral pathway to reduce the number of melanoblasts reaching the epidermis. It might well prove interesting to use early melanoblast markers such as dopachrome tautomerase or *c-kit* to study melanoblast migration in *Sox10^{TgNRpLucH1Ward}* mutant embryos.

The wide variation in coat spotting patterns seen between different genetic backgrounds in both *Sox10^{Dom}* and *Sox10^{TgNRpLucH1Ward}* points to a number of modifier genes interacting epistatically with *Sox10* to regulate melanoblast survival and/or proliferation. One possible approach to this problem would be to follow on from the work of Pavan and Tilghman, who mapped six QTLs which modify the severity of coat spotting in the *s* (piebald) mouse, which expresses low levels of the *Ednrb* gene product (Pavan *et al.*, 1995). In order to replicate this type of experiment with the *Sox10^{TgNRpLucH1Ward}* mutation, the transgene would need to be introgressed onto to two separate genetic backgrounds and bred to congenicity. One background would need to show a relatively mild coat spotting phenotype and the other a severe one (either C57 or CBA would fulfil this latter requirement). Mutant F_1 offspring from a cross between these two inbred strains could then be scored for severity of phenotype, and a genome-wide scan instigated, preferably using an established RI panel for rapid mapping of modifier loci. Given that the QTLs mapped in the Pavan and Tilghman study pertain to *Ednrb*, it would be interesting to see which loci might exert an effect upon *Sox10*.

In fact, this experiment has now been performed and published with respect to the *Sox10^{Dom}* allele (Southard-Smith *et al.*, 1999). The mutant allele was introgressed onto both C57BL/6 and C3H backgrounds, and a C3H allele on Chr 10 was found to act as a recessive modifier of white forelock in hypopigmented mutants (Southard-Smith *et al.*, 1999). The *kit* ligand on Chr 10 presents itself as an obvious candidate for the modifier locus.

Coat colour

Following on from the observation that all mutant animals which lived long enough to develop fur had black coats, and hence lacked phaeomelanin in their hair follicles, it would be interesting to see whether this still held true following transfer of the transgene onto a fully agouti background such as CBA/Ca. Agouti strains carry the wild-type *A* allele at the agouti locus, which gives rise to a sub-apical yellow band in an otherwise black hair. In genotypes having both black and yellow pigment in the hair, the melanocytes can switch back and forth between black and yellow, but the mechanism controlling the switch is not known. If the *Sox10*^{TgNLucH1Ward} mutation were found to specifically abrogate the production of yellow pigment in some manner, this mutation could provide an interesting avenue of approach to the long-standing problem of how variegated colour is established in hairs (Galbraith & Arceci, 1974).

One simple experiment which could be profitably done is simply to microscopically examine pigmented and non-pigmented regions of *Sox10*^{TgNLucH1Ward}/*Sox10*^{TgNLucH1Ward} mutant skin. It has been reported that in the lateral flanks (outwith the pigmented regions at head and rump, which are considered to be special cases) the classical *s* allele results in entirely unpigmented epidermis, even in those regions where the fur is coloured (Mayer, 1967b). Given the early appearance of occasional pigmented patches on the flanks of *Sox10*^{TgNLucH1Ward} mutants, it would prove interesting to know what effect the mutation has on the different populations of epidermal and follicular melanocytes in those regions where pigmentation does occur.

Amelioration of *Sox10*^{Dom} /*Sox10*^{Dom} lethality on a particular genetic background

One outstanding puzzle about the exact nature of the *Sox10*^{Dom} mutation is the question of why a few homozygotes survive to term on a C57BL/6J x C3H/HheOuJ hybrid background. On the surface, this would seem to be very similar to the original background on which the mutant allele is consistently lethal during embryogenesis, however, it presumably contains one or more modifier genes which act to ameliorate the lethal nature of the allele. Since the cause of lethality is currently unknown, and seems unlikely to be related to enteric

neurogenesis, it might prove interesting to introgress the *Sox10*^{TgNRpLucH1Ward} allele onto this background and examine the level of severity of the post-natal mutant phenotype.

Neural crest contribution to inner ear development

A further possible aspect of the *Sox10*^{Dom} and *Sox10*^{TgNRpLucH1Ward} mutant phenotypes which has not been investigated is the status of the neural crest contribution to the inner ear. It is known that the integrity of the stria vascularis in the inner ear is crucially dependent upon the presence of intermediate cells of neural crest origin (which are actually of melanoblast derivation), and that these are frequently reduced or absent in mice mutated at the *Ednrb* locus (Deol, 1967). It is further known that deafness to varying degrees is a common pathological feature of WS4, and that some human patients with mutations in the SOX10 gene had this symptom (Pingault *et al.*, 1998). It is therefore a strong possibility that at least a subset of *Sox10*^{TgNRpLucH1Ward} homozygotes might have had inner ear defects. This was not studied during the course of these investigations, since the preparation of histological specimens from the inner ear requires specialised skills, and the interpretation of histopathology in this structure might well have proven difficult in inexperienced hands. However, the scope of future investigations could encompass the inner ear (if sufficient justification could be found). Again, the use of aggregation chimerae between ROSA-26 and *Sox10*^{TgNRpLucH1Ward} homozygous mutants might prove fruitful in illuminating poorly-understood aspects of the role of neural crest in inner ear development.

At a less technically demanding level, it is also possible to use non-invasive hearing tests on mice, such as the "click box" developed at the Institute of Hearing Research in Nottingham. This generates a brief 20KHz tone at 90dB SPL when held 30cm above the mouse, and is used as part of the more comprehensive SHIRPA protocol, which tests for behavioural and functional abnormalities (http://www.mgc.har.mrc.ac.uk/mutabase/shirpa_summary.html, 1998). However, given that *Sox10*^{TgNLucH1Ward} mutants generally present in a rather debilitated manner, due to the toxic megacolon component of the phenotype, the use of such a behavioural hearing test might well be inappropriate.

The role of *Sox10* in the CNS and the *gt* (grey tremor) mutation

Perhaps the most baffling aspect of both the *Sox10*^{Dom} and the *Sox10*^{TgNRpLucH1Ward} mutations is the lack of any apparent phenotype in either the CNS or PNS. Given that *Sox10* is known to be abundantly expressed in glial cells of multiple lineages throughout adult life, it seems odd that neither of the two *Sox10* mutants display any apparent peripheral or central nervous system pathologies. In the case of *Sox10*^{TgNRpLucH1Ward} , this can perhaps be explained by recourse to an enhancer-specific reduction in the *Sox10* message which does not affect *Sox10* expression in adult life, and the Northern result from brain RNA from 6-day old animals supports this hypothesis. In the case of *Sox10*^{Dom}, however, this explanation will not suffice. The simplest explanation would be to postulate a threshold effect, whereby haploinsufficiency of *Sox10* has a dramatic effect during neural crest development, but has little impact upon mature glial cells. Another explanation might be that *Sox10*^{Dom} acts as a true dominant allele to repress or activate inappropriate genes during neural crest development to detrimental effect, but again, that such transcriptional modulatory activity has little effect in mature glial cells, since these clearly utilise quite a different set of genes during their lifetime. A third explanation, which applies equally well to both *Sox10* mutants, is that in some lineages, there is functional compensation for reduced levels of *Sox10* by other, closely-related Sox genes such as *Sox4* and *Sox11.* Recent work has shown that not all oligodendrocytes of the CNS can be considered equal, since. although all oligodendrocytes express platelet-derived growth factor alpha-receptor (PDGFRα), ablation of the ligand, platelet-derived growth factor A (PDGF-A), by targeted mutagenesis has revealed that only a subset of myelinating cells are affected in this knockout (Fruttiger *et al.*, 1999).

Another explanation which pertains to both mutants is that there actually is an effect in the CNS and PNS, but that mutant animals simply do not live long enough for this to become readily apparent. The only mutants to survive to breeding age are *Sox10*^{Dom}/+ heterozygotes on a B6C3Fe-*a/a* background, and these rarely survive much beyond 18 months. It is possible that a neurological phenotype developing in these animals might be masked by and attributed to the more obvious and dramatic enteric phenotype. It is certainly true that *Sox10*^{Dom}

homozygotes were generally very wobbly and uncertain in their movements, however this was attributed to their severely debilitated condition, with systemic sepsis and presumptive malnourishment, rather than a myelination defect caused by any mutant phenotype in Schwann cells.

One intriguing possibility is that *gt* (grey tremor) mice might represent a third mutant allele at the *Sox10* locus (see discussion in chapter 6). The phenotype seen in *gt* mutants is almost the complement of that seen in $Sox10^{TgNRpLucH1Ward}$ homozygotes with only a very mild effect upon some neural crest derivatives (a mild coat colour defect and possible slight enteric defects) but very severe progressive defects in glia of both PNS and CNS, the two regions known to express *Sox10* throughout adult life, but seemingly unaffected in $Sox10^{TgNRpLucH1Ward}$ and $Sox10^{Dom}$ mutants. Although *gt*/+ heterozygotes show an abnormal phenotype, this is comparatively mild and of late onset. If, by breeding *gt* and $Sox10^{TgNRpLucH1Ward}$ heterozygotes together, these two mutations were shown to be non-complementary (i.e. to be allelic), this might help resolve two separate questions: the nature of the $Sox10^{TgNRpLucH1Ward}$ locus and that of the *gt* locus. This latter may prove to be of particular interest to the virology community, since *gt* was originally found to act as as a transmissible agent causing a spongiform encephalopathy (Sidman *et al.*, 1985). This was confirmed by other workers (Hoffman *et al.*, 1987), but subsequently refuted by a third group (Carlson *et al.*, 1997). Linkage of the *gt* phenotype to a mutation at a molecularly-defined locus might resolve this controversy.

In this context, it is worth mentioning that the phenotype of the unique patient described by Inoue *et al* appears to be, in effect, a combination of *gt* and $Sox10^{Dom}$ (Inoue *et al.*, 1999).

The *gt* strain was actually discontinued by the Jackson labs, due to its potential nature as a biohazard. However, it is currently maintained at the Institute of Virology in Montana, where studies by Carlson and co-workers refuted the transmissible nature of the *gt* phenotype (Carlson *et al.*, 1997). The line was subsequently downgraded from biohazardous status and is now maintained under standard conditions. It might therefore be possible to cross *gt* with $Sox10^{TgNRpLucH1Ward}$ and test for complementation.

Conclusion

In summary, the mutant phenotype seen in the **Harry** transgenic line appears to be caused by transgene-associated disruption of unknown nature at the *Sox10* locus. This gives rise to a fully recessive mutant phenotype which closely resembles that seen in animals heterozygous for the other known mutation of this gene, the $Sox10^{Dom}$ allele. The mutant phenotype is characterised by white coat spotting and enteric aganglionosis, caused by a reduction in the numbers of melanoblasts and vagal neural crest derivatives.

Although the precise nature of the transgene insertion event is currently unknown, this does not preclude the use of this mutation as a potentially useful tool for the investigation of migration and ontogeny of the neural crest during murine embryogenesis.

CHAPTER NINE:
HOLLY - INITIAL CHARACTERISATION OF THE PHENOTYPE

Introduction

As discussed in chapter 3, during primary screening an initial hemizygous intercross using **Holly** mice generated 3 abnormal animals with corneal opacity in a single litter of 7 animals - a frequency consistent with a recessive mutant phenotype. Following Caesarean re-derivation and establishment of the **Holly** line in Bath, further hemizygous intercrosses were therefore set up with three initial aims as given for **Harry** mutants in Chapter 4. Firstly, to see if the phenotype was reproducible, recessive and fully penetrant. Secondly, to characterise the phenotype itself at a gross level with a view towards assigning candidate loci, should such exist. Thirdly, and vitally, to ensure that the phenotype truly was associated with the transgene i.e. that the transgene insertion site was genetically linked to the phenotype.

Results

Gross phenotype

Following establishment of the **Holly** line in Bath, hemizygous intercrosses throughout four subsequent generations of animals have generated mutant animals at frequencies consistent with a recessive trait.

All animals appeared normal at birth, but from around day 15 onwards progressive opacity of the corneas was visible. This was difficult to detect in the early stages, usually requiring that animals be inspected closely for a slight but distinctive greying and dullness of the corneal surface. However, by about 4-6 weeks of age, regions of the cornea were very obviously opaque and grey-white in colour. The affected region varied in size from 30-100% of the cornea, but was most commonly an elliptical patch covering some 50% of the visible corneal surface. Older mutant animals (>2 months) frequently had a "half-shut" appearance to their eyes, with the eyeball sunken in its socket behind half-closed eyelids.

Several **Holly** mutants showed reduced size (20-40%) compared to their littermates at an advanced age, although no such difference was observed prior to weaning, and this effect was not seen consistently.

The **Holly** line has been found to be a rather poor breeder, particularly in hemizygous intercrosses, and the root cause of this appears to be the consumption of litters shortly after birth by the parents, rather than any defect in the pups themselves.

Association between the transgene and phenotype

Unlike **Harry**, the mutant phenotype seen in **Holly** mice did not seem to compromise life-span and all mutants which were allowed to live reached breeding age. It was therefore decided to use crosses between mutants and non-transgenic animals to assess whether the mutant animals were homozygous for the transgene.

In all, 5 adult **Holly** animals showing the corneal phenotype were mated with non-transgenic animals, but only one male successfully sired offspring and these were limited to one litter with each of two non-transgenic females. These two litters totalled 15 pups, all of which were transgenic. Given a null hypothesis that the father is hemizygous for the transgene, it would be predicted that 50% of the offspring would be non-transgenic. Using a simple χ^2 test, this gives

$\chi^2 = 15$

and for 1 degree of freedom this gives $P < 0.0001$

This gives statistically significant rejection of the null hypothesis, which is to say that the mutant **Holly** father was probably homozygous for the transgene.

Although mutants appeared to be at least partially viable, attempts to determine homozygosity for the transgene by this method were unsuccessful, since no further offspring were derived from any of the **Holly** mutants, although only 5 such animals were tested.

Using the more laborious breeding protocol detailed in chapter 4, data for 111 pups from **Holly** hemizygous intercrosses were collated and are summarised below into a 2x2 contingency table. As before, with the null hypothesis that there

is no association between the "dominant" transgene and a recessive mutant trait, expected ratios would be 9/16 transgenic wild-type, 3/16 wild-type non-transgenic, 3/16 mutant transgenic, 1/16 mutant non-transgenic.

Table 10. Collated breeding data from multiple Holly intercrosses

	wild-type	**mutant**	Σ
transgenic	60 (62.4)	19 (20.8)	79
non-transgenic	32 (20.8)	0 (6.9)	32
Σ	92	19	
Overall Σ = 111			

Expected values are given in brackets below each observed value. Using the formula given in Appendix A, this gives

$\chi^2 = 7.67$

and for 1 degree of freedom this gives $P < 0.01$

This means that the null hypothesis can be rejected with a 99% confidence limit, or, to put it another way, that the data obtained would be expected to occur at a frequency of less than 1% if the transgene and mutant locus were not linked.

FISH genotyping was performed by hybridising the transgene probe to metaphase chromosome spreads prepared from a single transgenic mutant and a single transgenic wild-type littermate (**Figure 24**). The mutant was homozygous for the transgene while the wild-type animal was hemizygous.

Figure 24. FISH genotyping of mutant and wild-type Holly mice

a) Metaphase chromosome spread from wild-type transgenic **Holly** male. One transgene signal can be seen (arrow).

b) Metaphase chromosome spread from mutant **Holly** male. Two transgene signals are present (arrows).

Figure 24

a

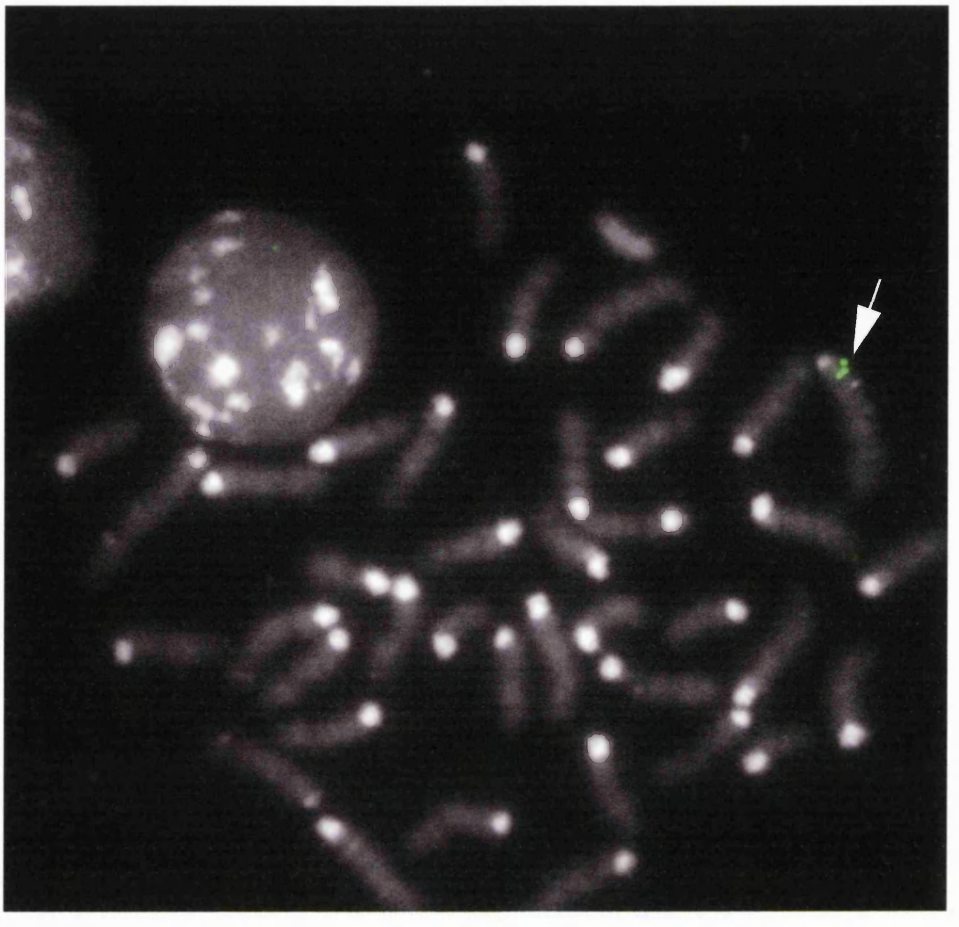

b

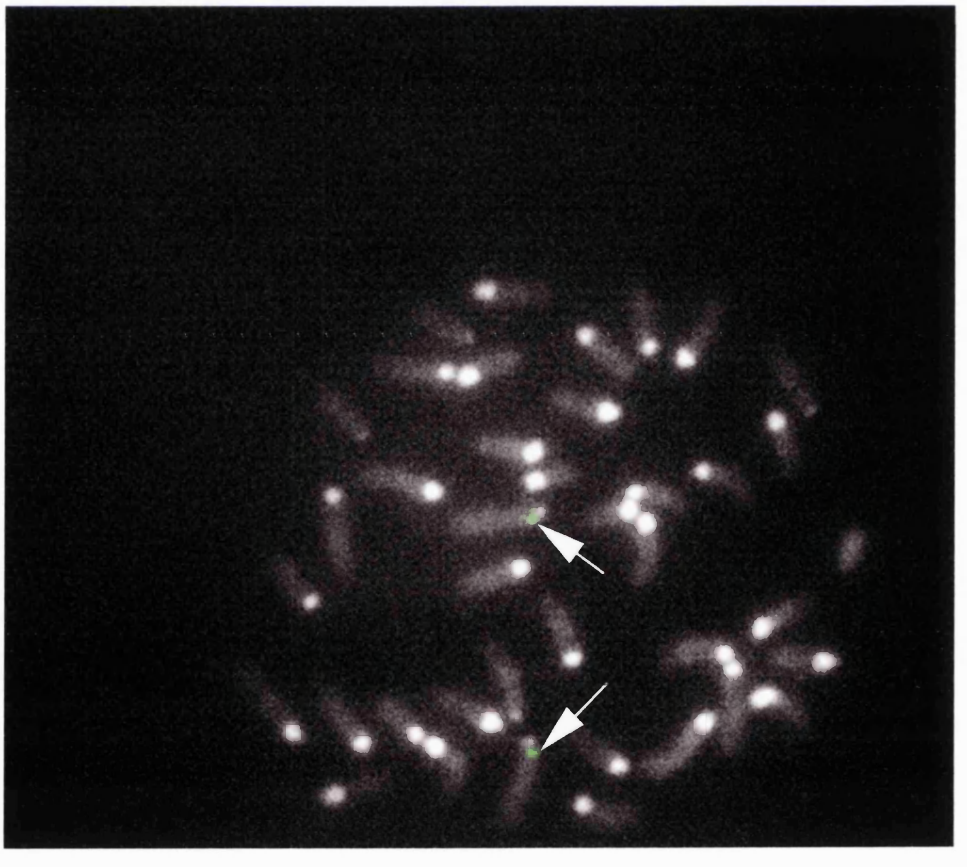

Discussion

While FISH analysis was not performed as rigorously as was done for the **Harry** line, in combination with the statistical analysis, the data obtained was taken as reasonable proof that the **Holly** transgenic line carried a recessive mutant trait which was associated with the transgene and primarily affected eyes from around day 15 post-partum. It was therefore decided to characterise this phenotype more fully.

CHAPTER TEN:
HOLLY - DETAILED CHARACTERISATION OF THE PHENOTYPE

Introduction

With a distinct opthalmopathy developing in homozygous **Holly** transgenics from around post-natal day 15 onwards, examination of the eye at a gross and histological level was undertaken (see Results). This rapidly led to the conclusion that the observed phenotype was strongly suggestive of pathology relating to glaucoma, a condition caused by prolonged elevation of intra-ocular pressure.

At this point, with a potentially glaucomic phenotype, a discussion of the details of eye physiology seems pertinent. Although there are some differences in the fine details, particularly in the iris and the irido-corneal angle, the murine and human eye are very similar in construction and the details described below for the human eye apply equally to the mouse in their essential aspects (Chew, 1996; Tomarev *et al.*, 1998).

Anatomy and physiology of the anterior mammalian eye

For a variety of reasons, not least the maintenance of its spherical shape, the eye maintains a considerable intra-ocular pressure (IOP). In humans, an IOP of around 12-20mm Hg is considered normal, but this value can drop as low as 6mm or range as high as 25mm Hg without being considered pathological (Gorin, 1977). Data for IOP in the mouse has been somewhat scarce in the past, but John and coworkers have recently rectified this situation by developing an invasive assay using a glass microneedle attached to a pressure transducer, which is inserted into the anterior chamber directly through the cornea (John *et al.*, 1997). Measurements in four common inbred strains maintained under identical conditions revealed considerable inter-strain variation in average IOP, ranging from 7.7±0.5mm Hg in BALB/cJ mice up to 13.7±0.8mm Hg in the C3H/HeJ strain, with C57BL/6J and A/J strains falling somewhere in the mid-range. Further to this, recent work in the DBA/2J strain, a model for primary open-angle glaucoma, suggests that the normal range for these mice (prior to the onset of

glaucoma) is around 4-15mm Hg, although there is a marked difference between the sexes in this strain (John *et al.*, 1998).

As mentioned above, IOP is critical in maintaining the shape of the eye, with correct curvature of the cornea being particularly important for clarity of vision. The curvature of the cornea is maintained by the pressure of the aqueous humour in the anterior chamber. The cornea is the chief refractive element of the eye, being even more important than the lens in the establishment of the path that light rays will take on their way to the retina (Ross *et al.*, 1989). The advantage of the lens, of course, is that its shape can be adjusted to focus on objects at different distances.

Aqueous humour is produced in the posterior chamber of the eye, which lies between the lens and the iris. It has an ionic composition similar to that of plasma, although it contains a much lower protein content (<0.1%, compared to around 7% in plasma), and is considered to be largely produced by active secretion from the ciliary body, rather than passive diffusion of fluid under pressure from the capillaries, (although this may contribute some small fraction) (Gorin, 1977). Following production in the posterior chamber, the aqueous humour (often referred to as simply aqueous) then flows through the iris into the anterior chamber, and exits via outflow channels at the corneal periphery. In addition to the constant production of aqueous by the ciliary body, which has been estimated to be around 1% of the volume of the anterior chamber per minute, there is a constant and substantial exchange of fluid and ions by simple diffusion between the anterior chamber and the iris capillaries. Overall, this results in a rapid turnover of aqueous in the anterior chamber, coupled with a sustained level of pressure in the chamber, which maintains corneal curvature.

The outflow system for the drainage of aqueous lies in the anterior chamber angle, where the iris meets the cornea at the limbus. This has been best characterised in humans, where the fluid first passes through a loose trabecular meshwork of tissue which, under normal conditions, probably presents no significant obstacle to the passage of fluid or macromolecules. At some point thereafter, the aqueous enters the outflow tract proper, the canal of Schlemm, which encircles the limbus and communicates with scleral veins and hence out to

the systemic circulation (Ross *et al.*, 1989). Despite several ultra-structural studies, the exact nature of the junction between the trabecular meshwork and the canal of Schlemm remains contentious, however the outflow of fluid is considered likely to be via active transport rather than passive diffusion or dialysis, and to be mediated by the single, continuous layer of endothelial cells lining the canal (Tripathi, 1972; Gorin, 1977; Lütjen-Drecoll & Rohen, 1996).

Within the angle itself, only higher primates and humans actually possess a true *trabecular* meshwork, consisting of laminated sheets and beams of extracellular matrix material surrounding an organised outflow vessel wall (canal of Schlemm). Most other mammals possess a *reticular* meshwork, spread over a wider area of the sclera. Many smaller vessels bend into this meshwork, rather than a single, large outflow channel (Lütjen-Drecoll & Rohen, 1996). The chamber angle itself is filled with radial, interlacing strands of pectinate ligament. However, the essential nature of the outflow mechanism appears to be conserved in animals, with cells secreting and laying down copious extracellular matrix to create a filtering mesh surrounding the outflow vessel walls, across which an endothelial layer of cells mediate active transport to remove fluid.

The outflow pathway in mice has traditionally been thought to conform with that seen in the other lower mammals, but interestingly, a recent detailed ultrastructural study of the murine angle has contradicted this model (Tamm *et al.*, 1999). The authors found that mice actually possess a single, large circumferential outflow vessel directly equivalent to the canal of Schlemm, and that the fine structure of the trabecular meshwork is closer to that of primates than other mammals. They therefore suggest that the mouse may be the superior model animal for conditions affecting aqueous outflow in humans.

Under normal circumstances, aqueous is produced in the posterior chamber by the ciliary body, circulates through the pupil into the anterior chamber and exits via the outflow system in the chamber angle (**Fig. 25a**). The rate of inflow and outflow are finely controlled and delicately balanced to maintain IOP. As previously mentioned, the composition of aqueous is substantially similar to that of de-proteinated plasma, and, apart from the

Figure 25a Production and outflow pathway of aqueous

Section through a wild-type adult mouse eye, with the anterior to the right (cornea) and the posterior to the left (retina and sclera). x40

The aqueous is produced by the ciliary body (**cb**) in the posterior chamber (**pc**), which lies between the iris and the lens. It should be noted that the region immediately posterior to the ciliary body is entirely filled by the vitreous humour (**vh** - invisible in this histological preparation) and the lens and offers little room for aqueous to circulate. The boundaries of this region are indicated by dotted lines. The secreted aqueous therefore largely flows (thick arrows) through the posterior chamber, out into the anterior chamber (**ac**) through the valve-like pupil of the iris and exits via the outflow system in the anterior chamber angle where the cornea meets the iris.

The disruption of the lens fibres is an artifact of sectioning, and is very common in histological preparations from mature crystalline lens tissue.

Figure 25b. Pupillary block

This diagramatically illustrates the pathological mechanism of angle closure by pupillary block, the most common cause of angle-closure glaucoma. As the lens comes into contact with the iris, fluid is retained in the posterior chamber. This causes the iris root to balloon out and make contact with the cornea and close the angle.

Fig. 25 a

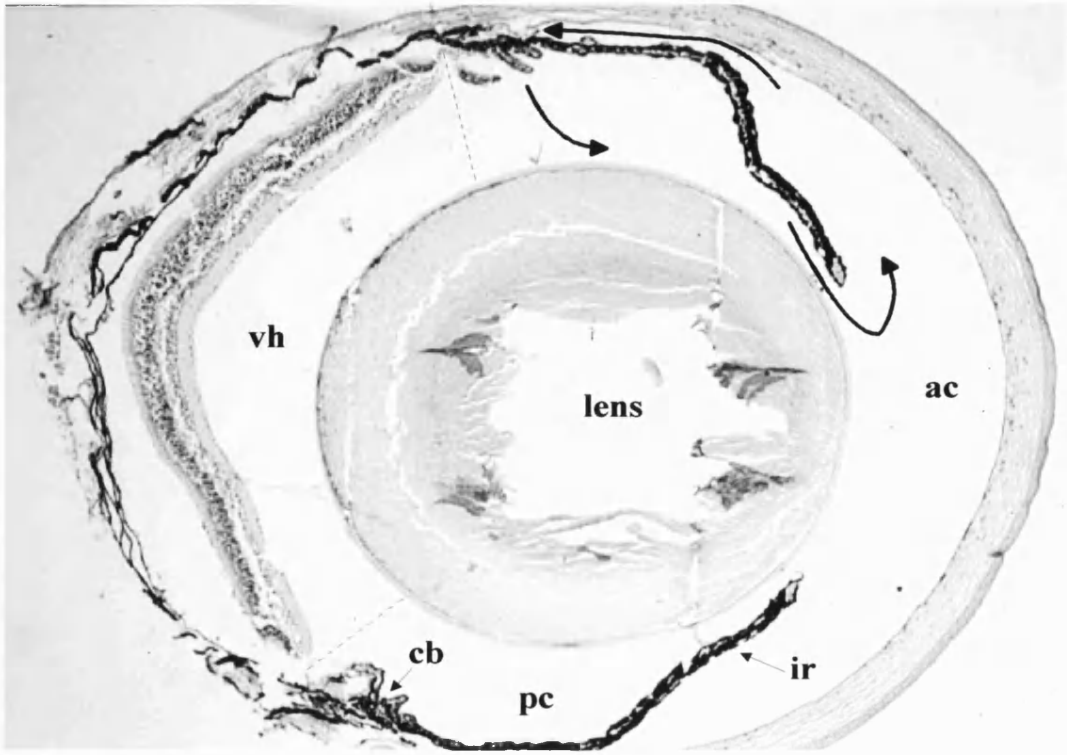

Fig. 25 b

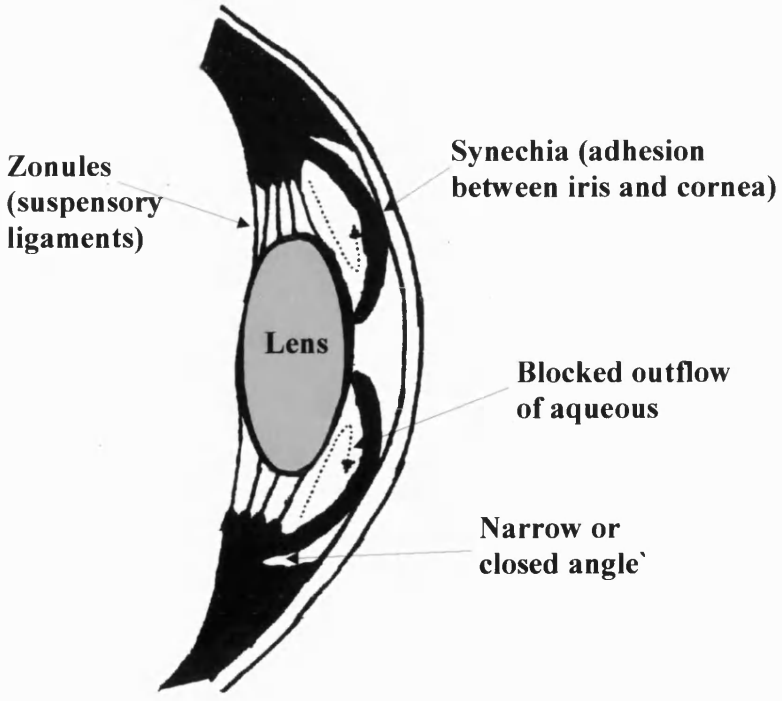

maintenance of IOP, the primary role of the aqueous is to exchange nutrients and metabolites with the avascular cornea and lens tissues.

The cornea itself is composed of three major structural layers (seen clearly in **Fig. 27e**). The outer corneal epithelium consists of five or six layers of stratified non-keratinised squamous epithelium and shows a high regenerative capacity, concomitant with its rapid turnover under normal conditions (Ross *et al.*, 1989). Slow-cycling stem cells in the limbus provide the corneal epithelium with a steady supply of transiently amplifying (transit) cells, which proliferate briefly before terminal differentiation (Matic *et al.*, 1997). The epithelial cells show a typical proliferative cycle, with a basal layer of columnar cells underlying several layers of cells which become progressively flatter as they approach the surface. As cells migrate towards the surface, their metabolic activity decreases and the cytoplasmic organelles disappear. The entire corneal epithelium turns over roughly every seven days (Ross *et al.*, 1989; Chung *et al.*, 1992). The corneal epithelium is continuous with the conjunctival epithelium and under normal circumstances, the undersurface of the former presents a flat appearance and the undersurface of the latter is more rugose.

The corneal epithelium sits upon Bowman's membrane - a thin, homogenous basement membrane layer. Underlying this is the thick corneal stroma, which consists of many thin lamellae of parallel bundles of collagen fibrils, with successive layers laid down at various angles across each other. The collagen fibrils form a transparent crystalline lattice, surrounded by a poorly-defined "ground substance" containing corneal proteoglycans. The highly specialised nature of the corneal ECM, which contains several unusual collagens, contributes to the transparency of this structure (Wessel *et al.*, 1997). There are a few flattened fibroblasts and a number of lymphocytes scattered between the lamellae, although during an inflammatory response (e.g. due to corneal infection), enormous numbers of lymphocytes and leukocytes migrate into and infiltrate the stroma.

Underlying the stroma is a further basement membrane layer, Descemet's membrane, which, as with Bowman's layer, is believed to act as a barrier to the spread of infection (Ross *et al.*, 1989). The corneal endothelium forms the

innermost layer, and consists of a single layer of flattened polygonal cells. This is continuous with the endothelium covering the anterior surface of the iris. The corneal endothelium is involved in the diffusion of nutrients from the aqueous into the corneal stroma, and is also known to actively transport water out of the stroma. This is important for the maintenance of corneal transparency, and injury to the endothelium or interruption of this transport process can rapidly result in corneal clouding (clearly evident in mouse eyes examined within less than a minute of death). The most significant differences between the stromal layers of the sclera and the cornea are the avascularity and the active dehydration of the latter, and the opacity of the sclera is primarily due to its high water content.

The lens is a transparent, avascular structure, which in adult life is composed of >80% dry weight of crystallins (Wistow, 1993; Robinson & Overbeek, 1996). These are contained in the lens fibres, which are hugely elongated flattened cells which have lost their nuclei and organelles during terminal differentiation. The lens fibres are derived from the subcapsular epithelium, which is present only on the anterior half of the lens as a single layer of cuboidal cells. New lens fibres derive from the equatorial subcapsular epithelial cells, which increase greatly in height and then undergo terminal differentiation into lens fibres (Ross *et al.*, 1989). The entire lens is surrounded by the capsule, which is a greatly thickened basal lamina (some 10 to 20μm under normal circumstances) produced by the subcapsular epithelium. The lens capsule is elastic and composed primarily of type IV collagen. This is laid down in lamellar fashion, similar to that seen in the corneal stroma (Ross *et al.*, 1989). The lens capsule is thickest at the equator, where the zonules or suspensory ligaments are attached. These run between the lens and the ciliary body, and hold it tautly in position. Contractions of the ciliary muscles result in changes in the shape and hence the focal length of the lens.

The cornea does not appear to contain any of the crystallins found in abundance in the lens. Crystallins are generally thought to have been recruited in a taxon-specific manner from metabolic enzymes and stress-protective proteins, with the same molecules being expressed and playing quite different roles in non-ocular tissues - a process known as "gene-sharing" (Piatigorsky & Wistow, 1989).

It is believed that the lens exploits the heat shock protein function of some crystallins to protect against protein aggregation during aging

In contrast to the lens, the cornea contains mostly water-insoluble structural proteins such as collagen, but the water-soluble component warrants further examination. The corneal epithelium appears to have independently recruited metabolic enzymes such as aldehyde dehydrogenase class 3 (ALDH3), a tumour-inducible detoxification enzyme (Piatigorsky, 1998). ALDH3 is present at very high levels in the bovine cornea (10-40% of all water-soluble protein) (Cuthbertson *et al.*, 1992). Similarly, the enzyme transketolase (TKT) makes up some 10% of the total water-soluble corneal protein in the mouse (Sax *et al.*, 1996). Both enzymes probably play a role in protecting the corneal epithelium against oxidative stress, vital given its frequent exposure to UV light, but the very high levels of expression suggest a possible structural role as well, analogous to that of the lens crystallins.

Pathology of glaucoma

The clinical condition known as glaucoma encompasses a group of complex diseases involving the death of retinal ganglion cells and the degeneration of the optic nerve head, with consequent visual impairment. Glaucoma is the second leading cause of blindness in the United States, and causes around 10-15% of blindness in most countries (John *et al.*, 1997; John *et al.*, 1998). It is generally caused by a disturbance in the delicate balance between the inflow and outflow of aqueous, most often by obstruction of the outflow system, although there are a variety of other conditions which can lead to glaucoma besides simple obstruction of this kind. Many forms of glaucoma are therefore associated with an increased IOP.

While a detailed discussion of clinical glaucoma is beyond the scope of this thesis, it is broadly accepted that "normal" IOP in humans is around 16mm Hg ± 3mm, although this may vary much more widely and still be considered to be non-pathological (Gorin, 1977). Observed IOP above ~20mm Hg usually warrants further examination, and sustained levels of pressure above ~26mm Hg generally lead to opthalmological problems. The clinical symptoms resulting from a rise in IOP vary depending on the degree and duration of such elevation,

but the most common and serious defect is visual loss due to ischaemic atrophy of the axons in the nerve fibres of the optic disc and secondary atrophy in the inner nerve fibre layer of the retina (MacSween & Whaley, 1992).

Types of glaucoma

Glaucoma is classified as either primary or secondary, the latter being a complication of some other condition, such as diabetes. The primary form of the disease is further divided into open and closed angle glaucoma, and population-specific genetic modifiers pertain to each, with open angle more common amongst Caucasians, whilst closed angle glaucoma is more common amongst Chinese and shows highest incidence amongst Inuits (Gorin, 1977; Lim & Constable, 1987; Johnson *et al.*, 1996). A third primary form of the disease is congenital glaucoma.

Open angle glaucoma

The most common form of glaucoma, and the leading cause of preventable blindness in the United States, is chronic primary open angle glaucoma (POAG). This is an insiduous disease which can lead to severe visual impairment with few or no symptoms during progression. It is viewed as a condition in which the anterior chamber angle stays open, but the trabecular meshwork becomes defective. The resultant increased resistance to the outflow of aqueous leads to a gradual rise in IOP, which may be chronic or periodic in nature. The retina becomes damaged quite slowly in open angle glaucoma, although the exact mechanism by which elevated IOP causes this damage remains somewhat contentious. One important aspect of the retinopathy associated with glaucoma is that the ganglion cells of the inner nerve fibre layer degenerate long before the deeper photoreceptor layers of the retina.

Several theories have been proposed for the extreme sensitivity of the glial and ganglion cells of the optic disc and retina to elevated pressure, ranging from purely mechanical (where the vitreous humour physically damages the retina by pressing against it), through ischaemia (in which the pressure causes a loss of efficient blood supply to the cells) to blockage of axoplasmic transport of nutrients and enzymes from the neuronal perikaryon along the axons (Anderson, 1972; Gorin, 1977). The primary site of damage is actually the optic nerve-head and

advanced glaucoma often results in extensive excavation or "cupping" of this area. Recent work has lent weight to the hypothesis that the damage is actually caused by the blockage of mitochondria in this region (Levy, 1996). It is clear that elevated IOP leads to physical compression of the axons in the optic nerve-head by the extracellular basement membrane surrounding them - the *lamina cribrosa.* This much is uncontentious, however proponents of the mitochondrial exclusion hypothesis contend that this compression blocks axoplasmic transport of the mitochondria to more distal regions of the nerve fibres, with the consequent lack of ATP leading to cellular degeneration. Regardless of the exact mechanisms involved, elevated IOP in chronic open angle glaucoma frequently results in visual field loss, particularly in arc-shaped well-defined regions (arcuate scotomas), but this is gradual in progression.

Angle-closure glaucoma

Due to the subtle nature of open angle glaucoma, it is not often diagnosed at an early stage. In stark contrast, angle-closure glaucoma has a very rapid onset and most frequently presents in middle-age as a unilateral red eye associated with blurred vision, pain or headache (Lim & Constable, 1987). It is caused, as the name suggests, when the periphery of the iris suddenly apposes itself to the corneal periphery and blocks the anterior chamber angle. During an acute attack of angle-closure glaucoma, the vessels of the iris frequently become congested, and there is oedema of the corneal stroma, leading to loss of transparency. The pupil dilates and becomes irregular in shape and insensitive to light. In severe or prolonged attacks, adhesions (synechiae) can form between the peripheral iris and the anterior wall of the angle, or between the pupillary region and the lens.

The IOP increases very rapidly in angle-closure glaucoma, and as a result of this, specific opacities (*Glaukomflecken* of Vogt) can develop on the anterior surface of the lens. These regions appear to be areas of anterior epithelial necrosis and as they become covered up by newly formed lens fibres, cataract develops (Anderson, 1972).

Attacks of angle-closure glaucoma can resolve as rapidly as they occurred, but recurrent acute attacks lead to atrophy of the iris, with consequent irregularity

of the pupillary opening and localised depigmentation (Gorin, 1977; Lim & Constable, 1987).

Chronic congestive angle-closure glaucoma is not as dramatic as the acute form, and is rarer, but the mechanism of angle closure remains the same. In the chronic form of the disease, patients generally have minimal symptoms: recurrent mild ache over the eyes, halos around lights and slightly blurred vision. Closure of the angle appears to be more gradual, and the eye has a chance to adjust to the slowly rising IOP. This gradual rise in IOP probably blocks further formation of aqueous, and the eye stabilises at a lower IOP than that seen in acute cases - generally around 40mm Hg, as opposed to 60mm Hg or higher in the acute condition (Gorin, 1977). Of particular relevance to the pathology seen in **Holly** mutants is the observation that in chronic congestive angle-closure glaucoma, the full thickness of the iris usually comes into contact with the anterior wall throughout a large portion of its circumference. This usually results in broad peripheral anterior synechiae and permanent partial blockage of the outflow system.

The possible association between the lens and angle-closure glaucoma is self-evident. Conditions in which the anterior surface of the lens comes into contact with the iris will frequently result in pupillary block and this is the most common clinical cause of angle-closure glaucoma (**Fig. 25b**). Predisposing conditions include formation of tumours within the eye, frequently melanomas, which physically push the lens forward; the formation of cataracts, which can sometimes induce absorption of water and consequent swelling of the lens; and loosening or ruptures of the zonules which hold the lens in position, leaving it free to move forward. This last condition - anterior dislocation of the lens - causes a rapid rise in IOP as the pupil becomes blocked. The lens may protrude into the anterior chamber and come into contact with the cornea. If this happens, both cornea and lens become opacified, since the corneal endothelium and the lens epithelium can no longer carry out metabolic exchange with the aqueous (Anderson, 1972; Gorin, 1977; Lim & Constable, 1987). The lenticular opacity associated with such anterior synechiae has been shown in some cases to be associated with sub-capsular fibrous metaplasia (Kissane, 1990).

Congenital glaucoma

This has traditionally been considered separately by clinicians with respect to the adult onset forms of glaucoma, but numerous developmental conditions which feature abnormalities of the anterior chamber give rise to glaucoma which can be either open or closed-angle in nature (Shields *et al.*, 1996). True congenital glaucoma is already manifest at birth, but infantile and juvenile glaucoma become apparent during the first two or sixteen years of life, respectively (Kanski, 1994). The subsequent development of such congenital glaucomas essentially mirrors that seen in adults, although diagnosis and treatment presents obvious difficulties (Dickens & Hoskins, 1996).

Results

General appearance

Older Holly mutants (>6 months) frequently had a "sunken", half-shut appearance to one or both eyes. It was found that eyes with this appearance frequently tore during enucleation. This was not observed with eyes from younger animals (3-6 weeks) and may reflect some structural defect in the sclera which developed in parallel with the cataract and corneal opacity. Eyeballs were occasionally (2 out of 20) found to be smaller on one side than the other i.e. there was occasional unilateral micropthalmia.

Corneal opacity and iris dysplasia

When enucleated eyes were examined under the dissecting microscope, eyeballs from an 8-week old mutant animal displayed very obvious abnomalities of the cornea, manifesting as opacity and greyness, and a distorted appearance at the limbus (**Fig. 26**). Superficially, this resembled hyperplasia of the corneal epithelium, with thickening and overgrowth at the edges (**Fig. 26a**).

Obvious dysplasia of the iris was visible in around 30% of cases, particularly in older animals, with occasional patches of reduced pigmentation visible around the iris (**Fig. 26b**).

In addition to this, bulges in the sclera were frequently seen around the circumference of the limbus (**Fig. 26c** and **d**). These had a translucent appearance

Figure 26. Morphological abnormalities in Holly mutant eyes

a) Whole eyeballs removed from wild-type (left) and mutant (right) **Holly** littermates, culled at 16 weeks of age. The limbus (corneo-scleral junction) is indicated by arrows

b) Iris dysplasia in a mutant **Holly** eye, culled at 6 weeks of age. Breakdown of iris pigmentation is also apparent (arrows)

c) and d) Dark bulges (arrows), apparently herniated protrusions visible at intervals around the limbus in mutant **Holly** eyes.

e) and f) Wild-type and mutant lenses from littermates culled at 8 months of age. The cataract has fully progressed to fill almost the entire lens.

g) and h) Lenses from two sibling mutants culled at 18 days post-natally, looking down upon the anterior pole. Remnants of the ciliary body can be seen attached around the lens equator (cb). Only very slight corneal opacity was visible in these mutants at this time, and cataracts can be seen starting to form at the anterior pole of each lens.

Figure 26

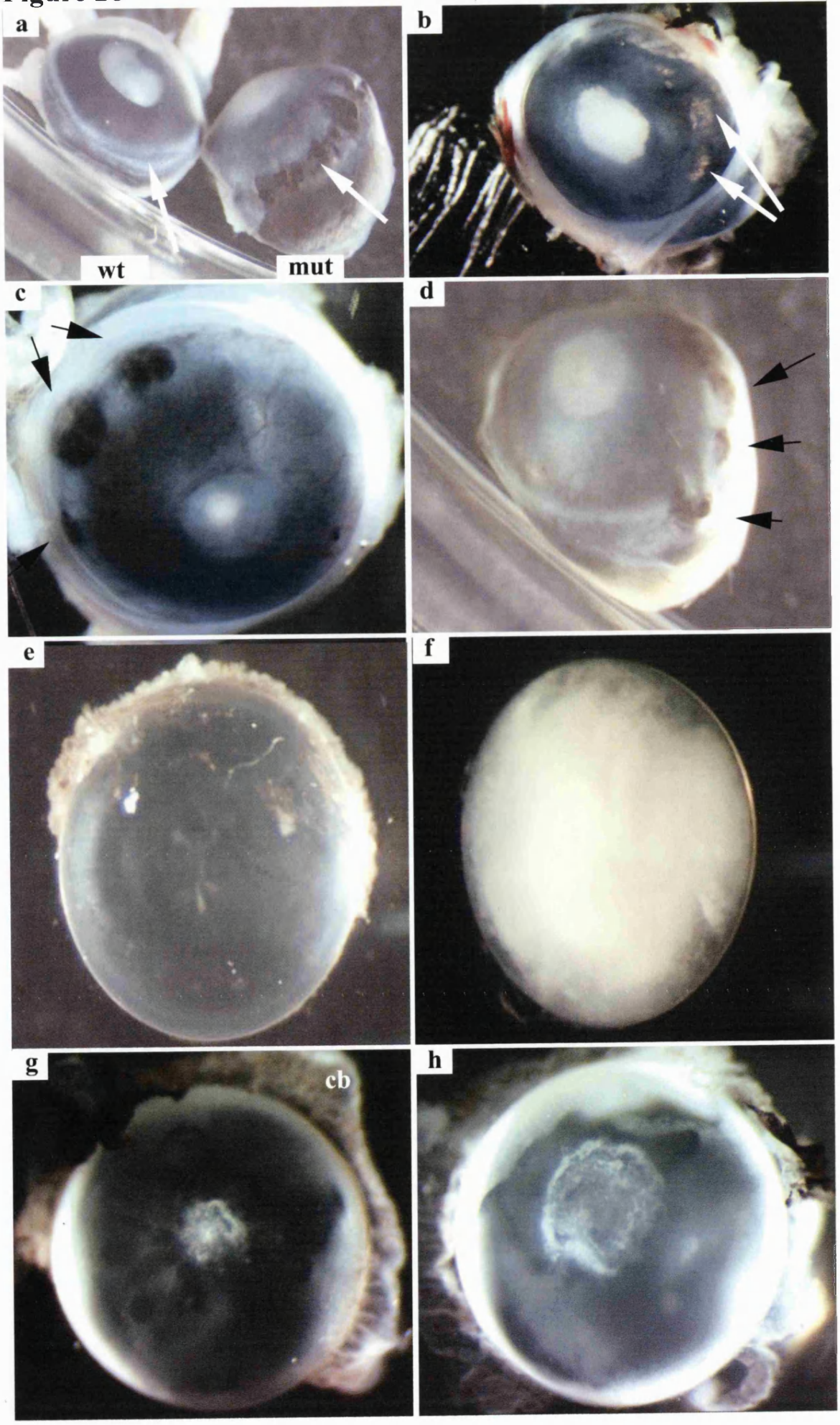

with reduced scleral pigment, and superficially resembled "blebbing" caused by a weakening or thinning of the wall of the eye in these regions, with the vitreous humour bulging out, perhaps under intra-ocular pressure. Eyes removed from older mutants (>6 months) were frequently found to be misshapen, having an ovoid or "squashed" appearance, and this may have reflected presumptive structural defects in the sclera or around the limbus.

Lens cataracts

When lenses from older (>6 months) mutants were examined, these were found to be severely cataractous, with the bulk of the lens having a milky white appearance when compared to wild-type (**Fig. 26e** and **f**). Examination of lenses from 18-day old mutants, which were just beginning to show slight corneal opacity revealed slight opacities at the anterior pole of the lens (**Fig. 26g** and **h**). Examination of ~20 mutant lenses subsequently confirmed that in all cases, mutant animals developed bilateral cataracts, which originated at the anterior pole around or shortly after the corneal opacity at day 15, and that in most cases, these cataracts progressed to fill most of the lens by around 6 months of age.

Histology

Whole eyes from 13-month old wild-type and mutant **Holly** females were sectioned and stained with H&E as detailed in Methods. While the wild-type eyes had a round, firm appearance following enucleation, the mutant eyes displayed the typical ovoid, squashed appearance seen in older mutant animal (**Fig. 27a** and **b**). It was also clear that the anterior chamber in the mutant eye had virtually disappeared, with the angle fully closed (**Fig. 27c** and **d**). The corneal epithelium itself was substantially unaffected in the mutant eye, but the corneal stroma and endothelium were both severely affected (**Fig. 27e** and **f**). The mutant lens had a grossly thickened capsule, and showed severe disorganisation of the nuclei of the lens fibres and epithelium (**Fig. 27g** and **h**). Finally, the retina was almost completely degenerated (**Fig. 27i** and **j**).

Sectioning of two more eyes from 13-month old mutant animals revealed histopathology consistent with the initial tentative diagnosis of glaucoma induced by angle closure. The anterior chamber angle was fully closed in all cases, with

Figure 27. Ocular histopathology of Holly mutants.

5μm sections from 13-month old wild-type and mutant **Holly** females. All sections stained with H&E.

KEY: angle = anterior chamber angle; cb = ciliary body; cen = corneal endothelium; cep = corneal epithelium; cor = cornea; ir = iris; lc = lens capsule; le = lens epithelium; ret = retina; str = corneal stroma.

a) Wild-type eye, with a rounded appearance, and an open anterior angle. x40
b) Mutant eye, showing a distorted, flattened appearance and a closed angle. x40
c) Wild-type anterior chamber, showing corneal layers, iris and lens. x100
d) Mutant anterior chamber, showing complete angle closure, grossly thickened and distorted lens capsule and a dysplastic cornea. x100
e) Wild-type cornea, showing corneal layers. x400
f) Mutant cornea. The corneal epithelium appears relatively normal, but the stroma is disorganised and thickened and the corneal endothelium cannot be clearly distinguished. The cornea is apposed to the lens, but the two structures are distinct. x400
g) Equatorial region of wild-type lens, showing well-organised lens fibres containing nuclei close to the sub-capsular lens epithelium. x200
h) Equatorial region of mutant lens, showing thickened lens capsule and disorganised lens epithelium. x200
i) Wild-type retina. x200
j) Mutant retina, showing almost total retinal degeneration. x200

Fig. 27

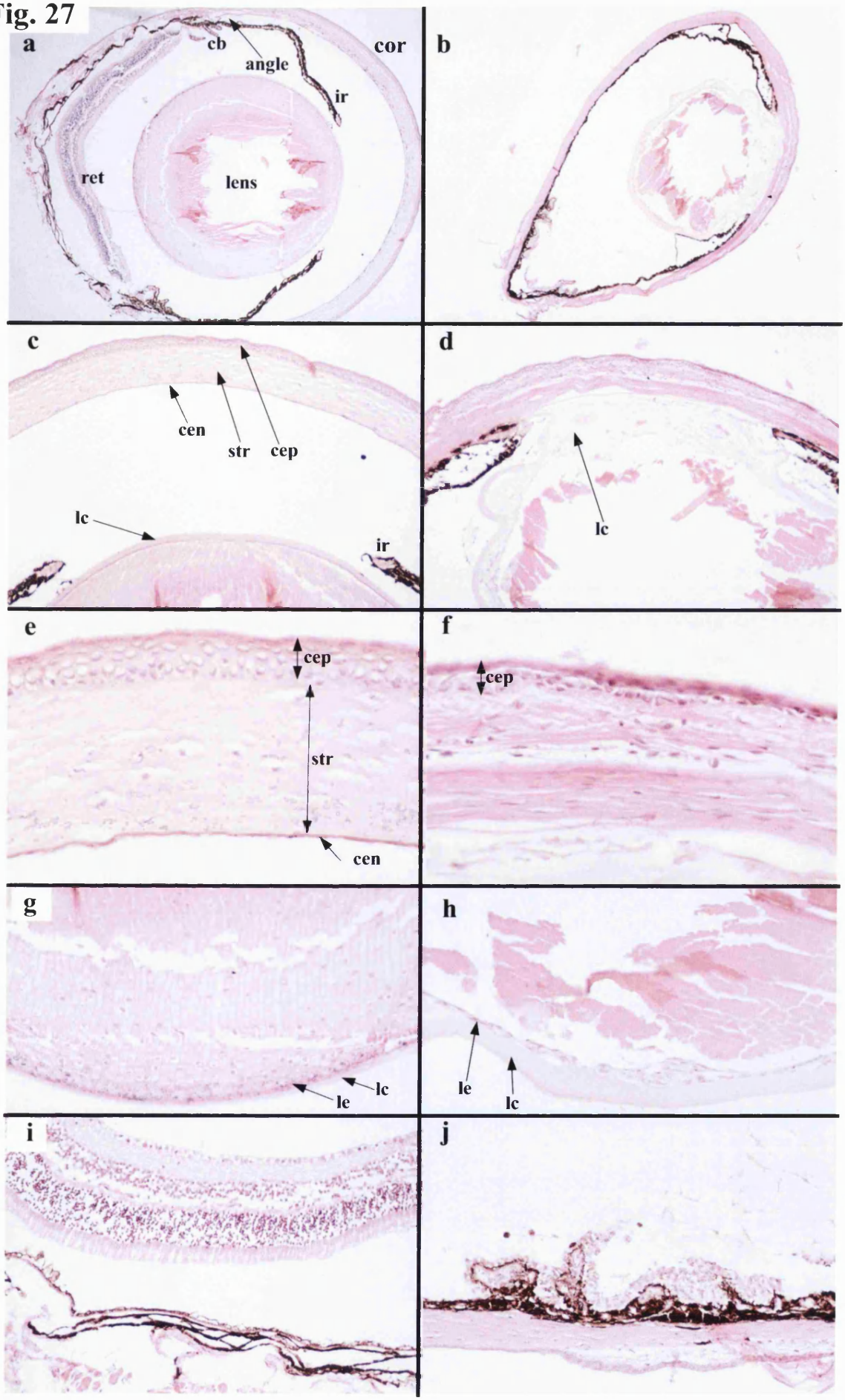
a
cb
angle
cor
ir
ret
lens
b
c
cen
str
cep
lc
ir
d
lc
e
cep
str
cen
f
cep
g
lc
le
h
le
lc
i
j

the iris closely apposed to the cornea. The corneal stroma was thickened and disorganised, with the undersurface of the corneal epithelium displaying a rugose appearance in some cases, reminiscent of its appearance in the conjunctiva (**Fig. 28a** and **b**). The lenses showed severe degeneration of lens fibres, disorganisation and proliferation of the sub-capsular epithelium and thickening of the lens capsule. In one case, the lens was attached and fused (anterior synechia) to the cornea. Serial sectioning revealed that the point of attachment was highly localised, but both the corneal stroma and the lens capsule showed over-proliferation in and around this region. In addition, massive sub-capsular fibrous metaplasia could be seen underlying this region of attachment (**Fig. 28a** and **b**). PAS staining revealed that the subcapsular fibrosis observed had a strong glycoprotein component, consistent with the notion that it was caused by abnormally proliferating lens epithelium cells laying down capsular material (**Fig. 28c** and **d**).

As previously mentioned, the retinal degeneration associated with glaucoma in human patients tends to occur in localised regions and typically, the innermost ganglion cells and nerve fibre layer degenerate much earlier than the remaining layers of the retina (Anderson, 1972; Kissane, 1990). This was observed in the retinas of **Holly** mutants, with serial sections revealing that some regions of the retina had a substantially normal appearance, while other areas were almost entirely degenerated. Intermediately affected regions showed the characteristic thinning of the nerve fibre layer and reduced numbers of ganglion cells, with the remaining retinal layers unaffected (**Fig. 28e** and **f**). It was not clear whether there was any cupping of the optic disc.

Figure 28. Anterior synechia and retinal degeneration

a) and b) Synechia between lens and cornea in 13-month old **Holly** mutant eye. Apart from the usual thickening of the lens capsule itself, there appears to be large-scale sub-capsular fibrous metaplasia immediately below the point of attachment. The sub-capsular epithelial cells also show abnormal foci of proliferation, accompanied by significant cortical degeneration of lens fibres. H& E x200.

c) Prominent synechial attachment (**syn**) between lens and anterior choroid. The lens capsule (**lc**) and the fibres underlying it stain strongly with PAS. Abnormally proliferating lens epithelium (**le**) can be seen underlying the point of synechic attachment. It should be noted that the structure outside the choroid is sclera, not cornea, due to the plane of section. PAS-Haematoxylin, x200.

d) Wild-type cornea and lens, PAS-haematoxylin stain, making Descemet's membrane (**DM**) and the lens capsule (**lc**) prominent. The twin purple lines running vertically through the cornea are artifacts due to folding during sectioning. The lens epithelium (**le**) can be seen underlying the lens capsule. x200

e) Wild-type retina, with an almost continuous layer of ganglion cell nuclei (**GCN**) surmounting a thick nerve fibre layer (**NF**). H&E x200

f) Mutant retina from a 13-month old animal, showing relatively intact inner and outer plexiform layers and cell nuclei, but significantly thinned nerve fibre layer and reduced numbers of ganglion cells. H&E x200.

Fig. 28

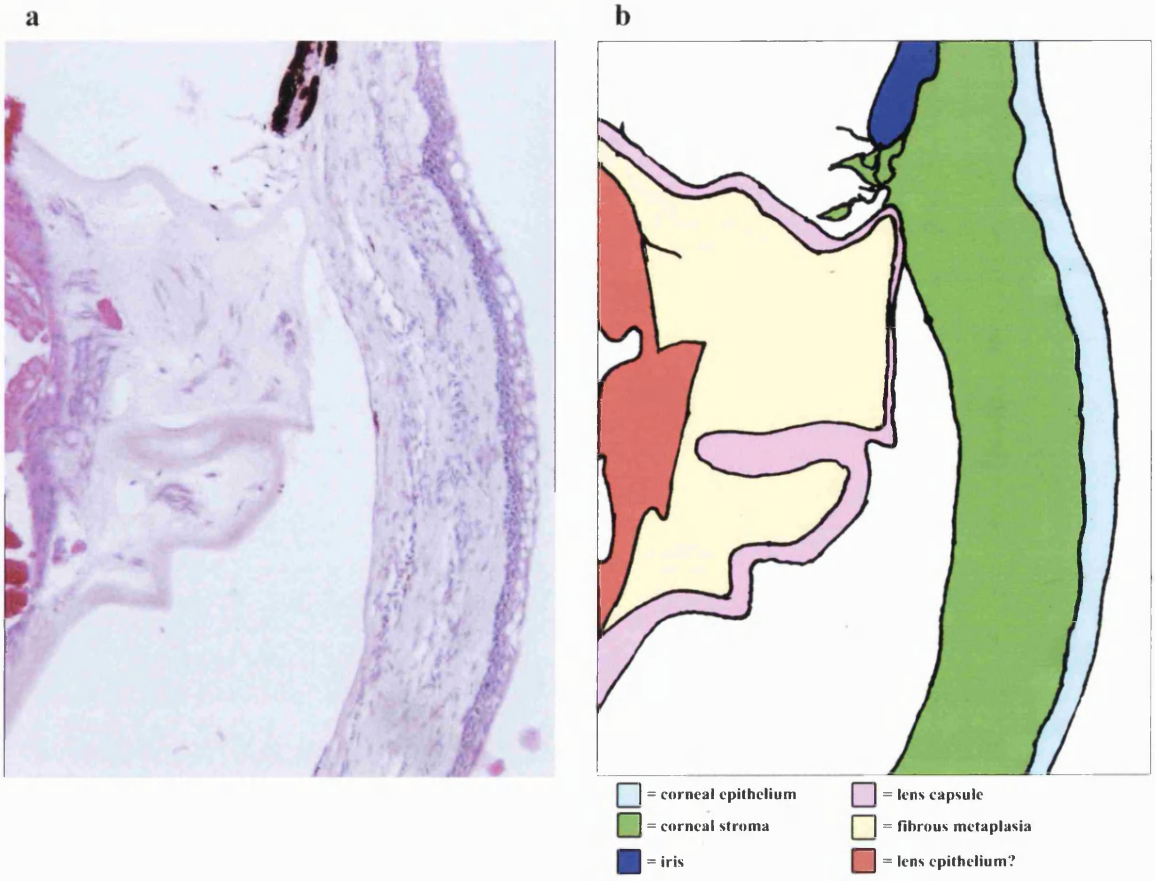
a
b
= corneal epithelium
= corneal stroma
= iris
= lens capsule
= fibrous metaplasia
= lens epithelium?

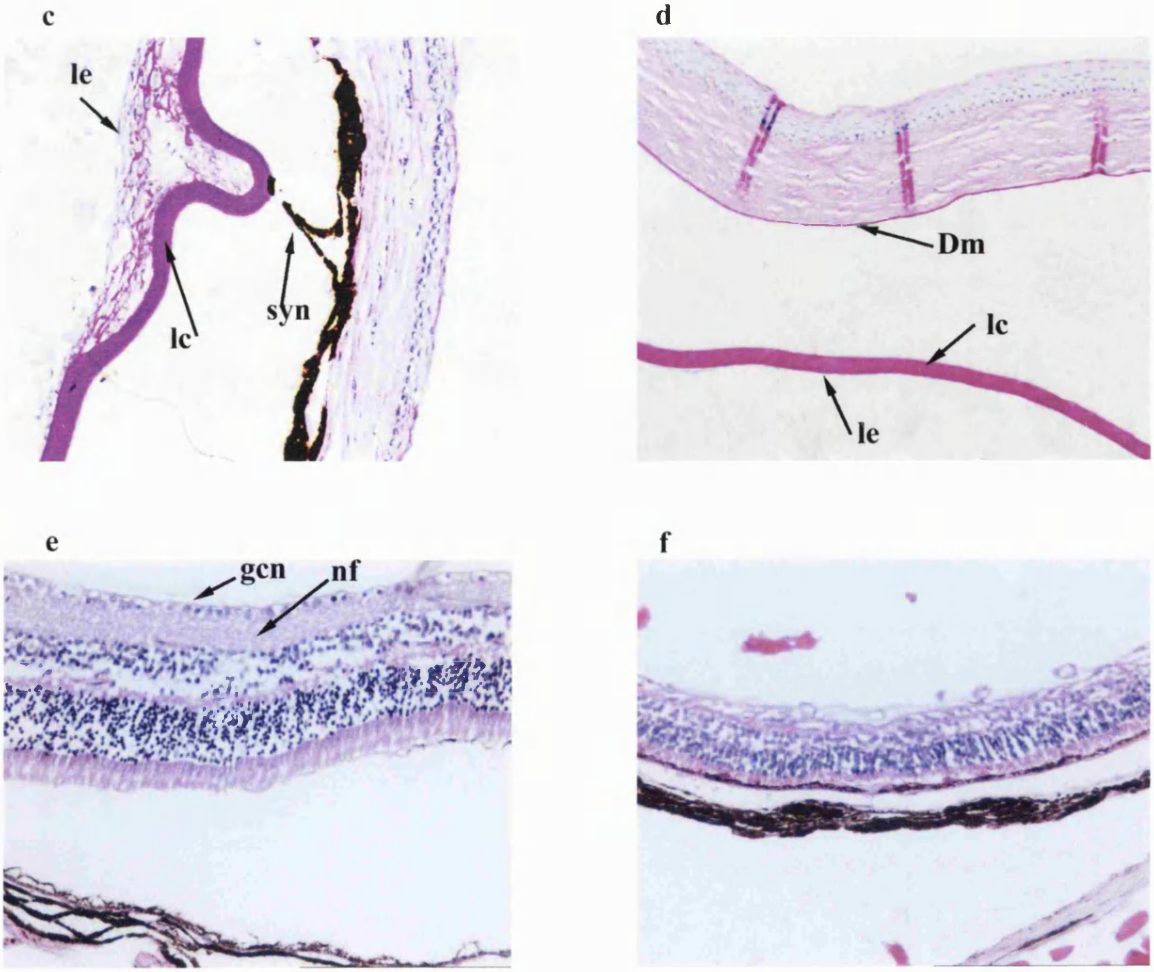
c
le
lc
syn
d
Dm
lc
le

e
gcn
nf
f

Examination of a single eye sectioned at an earlier stage from an 18-day old mutant revealed that even at this time, the anterior angle was fully closed, with the iris adhered to the cornea (**Fig. 29a**). In addition, the cornea was apposed to the lens, leading to the characteristic sub-capsular metaplasia of the lens epithelium cells. Immunostaining for proliferating cell nuclear antigen (PCNA) is a marker for DNA synthesis, and hence a useful marker for actively proliferating cells (McCormick & Hall, 1992). Immunostaining of the 18-day old mutant eye sections and age-matched controls revealed that cell proliferation in the mutant cornea was unaffected, but that proliferation in the lens was severely downregulated, despite the appearance of numerous extra cells in the anterior polar region of the lens, where it had been apposed to the cornea (**Fig. 29c-f**).

Figure 29. Anterior developing cataract in an 18-day mutant eye

a) Whole eye from an 18-day **Holly** mutant. The eye cup itself can be seen to be substantially normal, with correct curvature and the retina normal in appearance. The cornea is however collapsed and draped over the lens, with the anterior angle fully closed. The anterior pole of the lens has a disorganised appearance where it lies apposed to the cornea. H&E x 40

b) The anterior pole of the lens, showing that the cornea and lens lie apposed to each other, but have not fused. The cornea appears superficially normal, although there may be some breakdown of the endothelium in the region apposed to the lens. There is a large region of abnormal fibrous metaplasia (**fm**) in the subcapsular epithelum underlying the region of contact. H&E x100

c) α-PCNA staining of a wild-type age-matched control eye, showing a continuous single layer of stained nuclei in the corneal basal epithelium (**ce**) and in the lens epithelium (**le**). The corneal endothelium shows little signs of proliferation, consistent with its non-renewing nature x100

d) Detail of figure c) showing the subcapsular lens epithelium. Practically every cell at the anterior pole of the lens is proliferating. x400

e) α-PCNA staining of the mutant eye shown in a) and b). The corneal epithelium (**ce**) still shows a continuous layer of proliferating cells, but the lens epithelium shows very few proliferating cells until one moves well away from the region apposed to the cornea. In particular, the region of fibrous metaplasia (**fm**) whilst containing numerous cells, as evinced by H&E staining in b), contains almost no proliferating cells.

f) Detail of figure e) showing proliferation in the lens epithelium starting some distance away from the abnormal polar region.

Figure 29

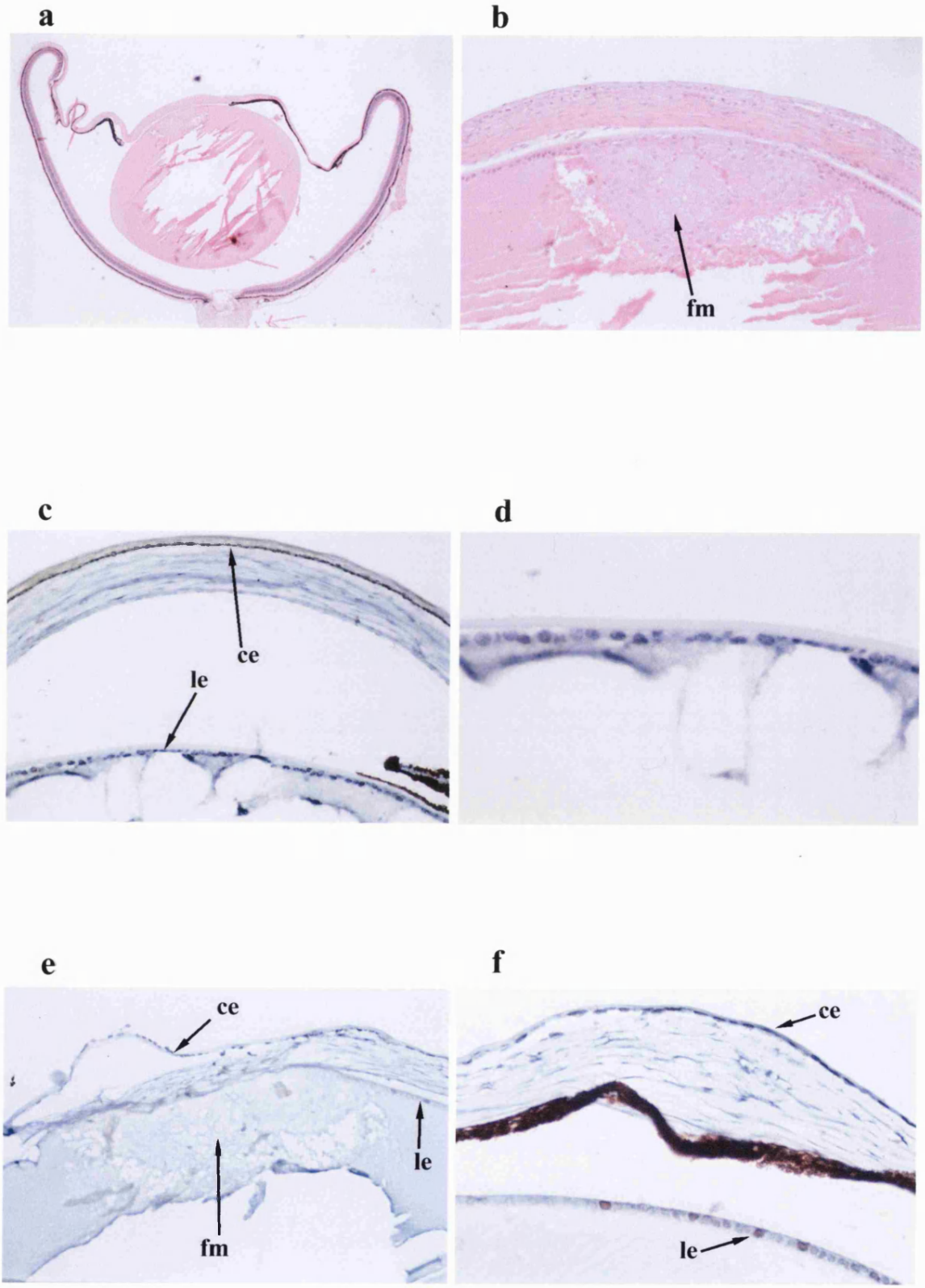

Discussion

General appearance

Histology revealed that the structures affected in **Holly** mutants eyes were not restricted to the cornea and lens. The anterior chamber of the eyes of **Holly** mutants had practically disappeared, with concomitant closure of the anterior chamber angle. In human patients, this invariably leads to the clinical condition known as acute angle-closure glaucoma, which has a variety of side-effects.

The ocular phenotype seen in **Holly** mutants becomes obvious only at some point after the eyes open, since no opacity of the cornea was observed until at least day 16 or 17.

During mouse development, as with other mammalian species, the eyelids close and then reopen at a later stage. In the mouse, the eyelids close at some point between E15.5 and E17, but the exact timing of closure varies widely, even within a single litter (Kaufman, 1992). Although the reason why the eyelids fuse closed in the first place is somewhat unclear, it is considered likely that the conjunctival sac formed by eyelid closure provides protection for the developing cornea and shields it from potentially toxic metabolites in the amniotic fluid during differentiation.

At some point during development, the eyes re-open, but the exact timing of this re-opening varies widely across the animal kingdom, with calves and guinea pigs born with open eyes, and dogs, cats and mice with closed eyelids. This is thought to reflect the developmental stage at which the animal is born, since eyelid closure is one of the last morphogenetic events of embryogenesis. The eyes re-open in the mouse around days 12-14 post-partum.

Around the time that the eyes open in mouse, the cornea undergoes a massive program of differentiation and change, with the corneal epithelium becoming multilayered and stratified (Piatigorsky, 1998). It might be predicted that mutations which affect the differentiation or stratification of the corneal epithelium would become manifest around this time. However, histological examination clearly showed that the corneal epithelium was substantially

unaffected, even in advanced stages of the phenotype, in which the eye was distorted and shrunken (phthisical), the lens was fully or mostly cataractous and the retina was almost entirely degenerate.

It is also the case that the aqueous outflow pathway only becomes active at around day twelve post-natal, just as the eyes open. A detailed study of the formation of the trabecular meshwork and other outflow structures in the murine angle has been performed using fluorescently-tagged lectins to label both cells and extracellular matrix (Vanden Hoek *et al.*, 1987). It was found that at the time of birth, the aqueous outflow structures exist only as anlägen, comprising loosely arranged cells and extracellular matrix. There is little change during the first six days post-partum, but they differentiate into functional structures during days 6-14. The outflow pathway becomes active around day 12, after which point some further maturation occurs. It might therefore be predicted that a mutation which compromises aqueous outflow would only exert a phenotype from day 12 onwards, as seen in **Holly**.

The Holly ocular phenotype – primary causal candidate loci

As stated previously, there are a very large number of loci which can cause lens cataracts (at least 48 independent loci are listed in the Mouse Genome Database as of early 1999), but very few which cause associated corneal defects. There are a large number of crystallin genes, for example, and mutations in many of these are known to cause cataracts. However, as mentioned previously, the cornea does not contain any of the crystallins found in abundance in the lens. This in no way precludes transgene-associated disruption at a locus which encodes a gene common to both lens and cornea. Three pertinent examples of genes of this type are worth mentioning at this point: the gap junction genes *Gja3* and *Gja8* and transforming growth factor β1 (TGFβ1).

The gap junction genes (formerly known as connexins, but reclassified partly due to conflicting nomenclature of the *Cx* genes in different species) are expressed in a highly tissue-specific manner and are known to play important roles in mediating cell-cell communication, often critical for the maintenance of tissue integrity (Bruzzone *et al.*, 1996). The connexin gene *Gja3* (formerly *Cx46* in mouse) is expressed in the lens and a targeted null mutation in this gene has been

shown to cause cataracts in mice (Gong *et al.*, 1997). *Gja3* is not expressed in the cornea, however, where the epithelial cells express mainly *Gja8* (formerly *Cx50*) and *Gja1* (formerly *Cx43*) (Matic *et al.*, 1997). This latter is also expressed in the lens and although *Gja1-/-* null mutants die at birth due to cardiac defects (hence no information is available on possible corneal defects), the knockout phenotype includes developing cataracts in the lens (Reaume *et al.*, 1995; Gao & Spray, 1998). Similarly, *Gja8* is expressed in both lens and cornea, and although the gene has not yet been knocked out in mouse, it is considered to be an excellent candidate for the *No2* bilateral congenital cataract mutation (Steele *et al.*, 1998). Furthermore, mutations in *GJA8* are now known to cause *autosomal dominant pulverulent* (Coppock) cataract, which also happened to be the first autosomal disease condition mapped in humans (Renwick & Lawler, 1963; White *et al.*, 1992; Geyer *et al.*, 1997; Shiels *et al.*, 1998).

Mutations in connexin genes have therefore been convincingly shown to cause congenital cataracts, and given their overlapping expression (in some cases) in the cornea, might be predicted to cause corneal defects as well, although this does not appear to be the case for the mutations studied so far.

Lens epithelial cells can be induced to differentiate into fibroblast-like cells by wounding or under prolonged metabolic stress such as that induced by synechial attachment of the lens to the cornea, and these can lead to anterior subcapsular cataracts (Srinivasan *et al.*, 1998). TGFβ1 is thought to be involved in this process, since intact rat lenses or epithelial explants cultured in the presence of this growth factor develop similar changes (Liu *et al.*, 1994; Hales *et al.*, 1995). The exact nature of these alterations bears some resemblance to the cataracts seen in **Holly** mutants, with subcapsular fibrous metaplasia, an accumulation of ECM and thickening of the lens capsule. Transgenic mice which overexpress TGFβ1 under the control of a lens-specific αA-crystallin promoter also develop anterior subcapsular cataracts, as well as corneal opacification and structural changes in the iris and ciliary body (Srinivasan *et al.*, 1998). This phenotype bears some resemblance to that seen in **Holly** mutants at a superficial level, however at the histological level the corneal epithelium presents with a disorganised and

exfoliating appearance, quite distinct from the well-organised epithelial structure seen in **Holly.**

The point has been made, however, that lens and cornea do share common genes of critical importance to the maintenance of structural integrity and transparency, and that mutations in such genes can lead to phenotypes resembling that seen in **Holly** homozygotes.

The ocular phenotype as a secondary effect of glaucoma

On the other hand, angle-closure glaucoma in human patients is known to be capable of inducing all or most of the histopathological abnormalities seen in the eyes of **Holly** mutants, at least in the advanced stages of the phenotype, and could reasonably be invoked as an explanation for the dramatic changes seen in the eyes of older mutant animals. To deal with these in sequence: the corneal opacity is the first obvious manifestation of the phenotype, and corneal oedema and opacity is one of the first consequences of elevated IOP. The localised regions of opacity observed on the cornea may be explained either by regions of contact (i.e. incipient synechiae) between the iris and the cornea, or between lens and iris, or even, in extreme cases, between lens and cornea. Alternatively, the cornea may not be truly opaque, but the developing cataracts in the lens give this impression. This is speculative, however, and really requires slit-lamp microscopy to confirm or refute this hypothesis. Detailed dissection might prove sufficient, but it is technically difficult to avoid any displacement of internal structures such as the lens during micro-dissection of unfixed eyes. The 18-day mutant sections shown in **Fig. 29** came from a mouse where corneal opacity could only just be detected by careful examination of the eye. The cornea appears relatively normal in the section, but corneal opacity would be difficult to discern in H&E sections. Certainly the anterior pole of the lens shows a large region of fibrous metaplasia, adjacent to the region where the lens and cornea are in contact in the sections. The fact that the lens epithelial cells have largely ceased to proliferate in this region suggests the following scenario: the lens and cornea come into contact with each other, creating a region in which the aqueous cannot circulate freely. Under these hypoxic conditions, the lens epithelium appears to proliferate abnormally, then ceases, giving rise to an anterior polar cataract. The corneal endothelium in the

hypoxic region may also be affected, leading to partial breakdown of the endothelium and Descemet's membrane. This could lead to localised corneal oedema, giving rise to opacity. In this scenario, the pronounced cataracts seen in older mice are a consequence of sustained hypoxia in the anterior pole of the lens.

The development of this kind of cataract is poorly understood, since in human patients, anterior synechiae of this type almost invariably cause early pain and discomfort, with consequent rapid medical intervention to alleviate the contact between the affected tissues. However, in one rare case, a patient presented with an anterior lens dislocation which had been present for well over four months, and the result was an entirely cataractous lens affixed to the iris by fibrous tissue (Hein & Maltzman, 1975). In addition, the sub-capsular fibrous metaplasia observed in mutant **Holly** lenses bears some resemblance to photographs reproduced in articles on the pathology of glaucoma, showing similar regions underlying synechiae (Anderson, 1972; Kissane, 1990).

As mentioned previously, in addition to the metabolic stress caused by synechiae of this kind, wounding or the presence of exogenous TGFβ1 can both induce lens epithelial cells to differentiate to a proliferative fibroblast-like morphology, leading to anterior subcapsular cataract (Font & Brownstein, 1974; Hales *et al.*, 1995; Srinivasan *et al.*, 1998). The morphology observed in isolated lenses cultured in the presence of TGFβ is not dissimilar to that seen in **Holly** mutants, with characteristic spindle-shaped cells being seen below the lens capsule in both cases (Hales *et al.*, 1995).

Overall, it seems plausible to suggest that the cataracts observed in **Holly** mutants were secondary to such anterior synechiae, although an expert second opinion from an experienced pathologist would be required to establish this beyond question.

It is possible that the "angle closure" seen in sectioned eyes is secondary or even artifactual - since the mutant eyes appeared ovoid and squashed upon removal, an alternative explanation might be a rather low IOP, leading to the collapse of the cornea onto the iris and lens during handling and processing for histology. Two factors argue against this, however: firstly, the synechiae seen between lens and cornea strongly suggest prolonged apposition of these two

structures during the lifetime of the affected animal; secondly, the pattern of degeneration of the retina in intermediately affected regions is pathognomonic for prolonged elevation of IOP.

IOP was not measured directly in this study, hence the above is conjectural, albeit based on strong circumstantial evidence. Measurement of IOP in mice is highly technically demanding, with only one group in the world currently capable of performing it (John *et al.*, 1997).

In fact, the distorted shape of the eyes in older mutants is consistent with *phthisis bulbi* - the final stage of ocular degeneration following a prolonged glaucomic period. In a phthisical eye, the production of aqueous is reduced, leading to lowered IOP (hypotony), deformation and atrophy of the globe, and widespread atrophy of internal structures (Kissane, 1990) . This may well explain the "half-shut" appearance of one or both eyes in older mutants, and the fragility of these tissues during extirpation. It can also be invoked as an explanation for the total degeneration of the retina seen in some areas.

The blebbing seen around the limbus remains unexplained, however, and no such bulges were successfully identified and analyzed at the histological level. There are reports of bulges or weaknesses in the sclera following prolonged glaucoma, termed *staphylomas*, but these are not restricted to the limbus (MacSween & Whaley, 1992).

What is unclear from these results is how the angle actually closes. The two most likely scenarios, based on studies of human glaucoma, are that either the lens becomes dislocated, perhaps due to defects in the ciliary ligaments, and moves forwards to cause so-called pupillary block angle-closure glaucoma (c.f. **Fig. 25b**). Alternatively, the anterior angle itself may close first, with the iris adhering to the cornea, perhaps through some abnormality of the corneal or irideal endothelium (which share the same embryological origin). This would cause a rapid rise in IOP, but production of the aqueous would be downregulated, perhaps leading to pressure drop in the anterior chamber and collapse of the corneal onto the lens.

Summary

In summary, the ocular component of the phenotype seen in **Holly** homozygotes is consistent with acute angle-closure glaucoma, with the prolonged condition leading to bilateral cataracts, retinal degeneration and severe corneal dystrophy, terminating in phthisis bulbi. There are currently no genes known to lead directly to angle-closure glaucoma.

CHAPTER ELEVEN:
HOLLY - LOCATION OF THE TRANSGENE INTEGRATION SITE

Introduction

There are a very large number of genes which can cause cataracts and other defects in ocular development. Indeed, it has been estimated that some 2500 genes participate in the development of the Drosophila compound eye, and that some important molecular mechanisms are highly conserved in mammals (Halder *et al.*, 1995). Although there are relatively few loci which cause glaucoma, given the large number of cataractogenic mutations in the database, the observed phenotype did not allow specific candidate genes to be confidently assigned without a map position (http://www.informatics.jax.org, 1999).

Although seven genes have now been identified which are susceptibility loci for open-angle glaucoma, some of which have been cloned in mice, no loci are currently associated with angle-closure glaucoma in mice or humans (Sarfarazi, 1997; Wirtz *et al.*, 1998). The DBA/2J strain of mouse has been found to develop progressive open-angle glaucoma of a highly specialised type (pigment dispersion with iris atrophy) from around 4 months onwards, due to the interaction of two loci on Chr 4 and Chr 6 (John *et al.*, 1998; Chang *et al.*, 1999). This inbred strain of mice has therefore been mooted as a useful model for this disease and for the study of retinal degeneration in other forms of glaucoma.

The genetics of angle-closure glaucoma in humans are much less well described than the pathology and diagnosis of the disease. In human patients, the most common aetiological factor predisposing towards an acute attack of angle-closure glaucoma is the combination of a shallow anterior chamber and a narrow angle (Gorin, 1977). The genetics of this have been investigated for a number of years, and point to at least one major autosomal dominant gene which significantly affects the depth of the anterior chamber and acts as a susceptibility locus for angle-closure glaucoma (Miller, 1970).

Peters' anomaly is a clinical condition which features corneal clouding and adhesions between lens, iris and cornea, often leading to glaucoma and cataracts.

Since it has been found in association with several different genetic and nongenetic clinical syndromes, it is considered to be a morphological entity rather than a distinct clinical entity. In particular, it has been shown that mutations in *Pax6* can cause a variety of different types of aniridia, some of which feature Peters' anomaly, but that, conversely, this gene is normal in most cases of Peters' anomaly (Churchill *et al.*, 1998). This leaves a large number of cases of this condition with a definite genetic component where the loci affected are unknown.

Since the genetics of angle-closure glaucoma are so poorly defined, the identification of a major locus in mice could provide useful data as a starting point for a genetic screen. Mapping this locus would permit investigators to target the syntenic region when screening human DNA obtained from familial pedigrees involving this disease.

Consequently, as with the **Harry** mutant, mapping by FISH and linkage mapping using microsatellite PCRs was performed to determine the transgene integration site. Partly due to the poor breeding performance of the **Holly** line, no productive hemizygous intercrosses were available at the time the linkage mapping studies were carried out. A modified backcross protocol was therefore adopted, crossing hemizygous **Holly** males against non-transgenic C57/CBA F_1 females. With no prior knowledge of which genetic background the transgene had integrated into, each transgenic pup tested from these crosses was effectively worth "half" a backcross offspring. It follows from this that twice as many offspring needed to be tested to reach statistical significance, compared to a standard backcross. In addition, only offspring of transgenic parents shown to be heterozygous at the locus under test provided informative meioses in this protocol.

Results

Mapping by FISH

Initial FISH results clearly indicated that the transgene had integrated very close to the centromeric end of a long chromosome, although the G-banding was rather poor (data not shown). This led to preliminary assignment to either Chr 1 or Chr 4. Subsequent G-banding experiments gave higher quality results and

following successful FISH of these spreads, the transgene was deemed to have integrated into proximal Chr 1 (**Figure 30**).

The transgene was also shown not to have integrated into Chr 4 by double FISH. A genomic probe to distal Chr 4, consisting of some 15kb of genomic sequence from the *Dvl* (dishevelled) locus was differentially labelled and hybridised to metaphase chromosome spreads derived from a homozygote at the same time as the transgene probe. Although the background levels were very high in these experiments, examination of multiple spreads confirmed that the green transgene-specific signal lay on a discrete chromosome from the red *Dvl* signal on Chr 4 (**Figure 31**).

A Chr 1 specific probe was obtained, containing some 17kb of genomic DNA from distal Chr1 cloned into phage lambda vector. Unfortunately, however, the phage stock failed to infect host bacteria, and no DNA could be obtained for use in FISH experiments.

Figure 30. Transgene mapping by combined FISH and G-banding

a) G-banded metaphase chromosome spread from a homozygous **Holly** male with hybridisation sites arrowed following FISH with a transgene probe.

b) Corresponding FISH signals from the same spread shown in a). Two transgene signals are visible (arrowed).

c) to h) Different G-banded spreads from the same slide, with hybridisation signals arrowed.

Figure 30

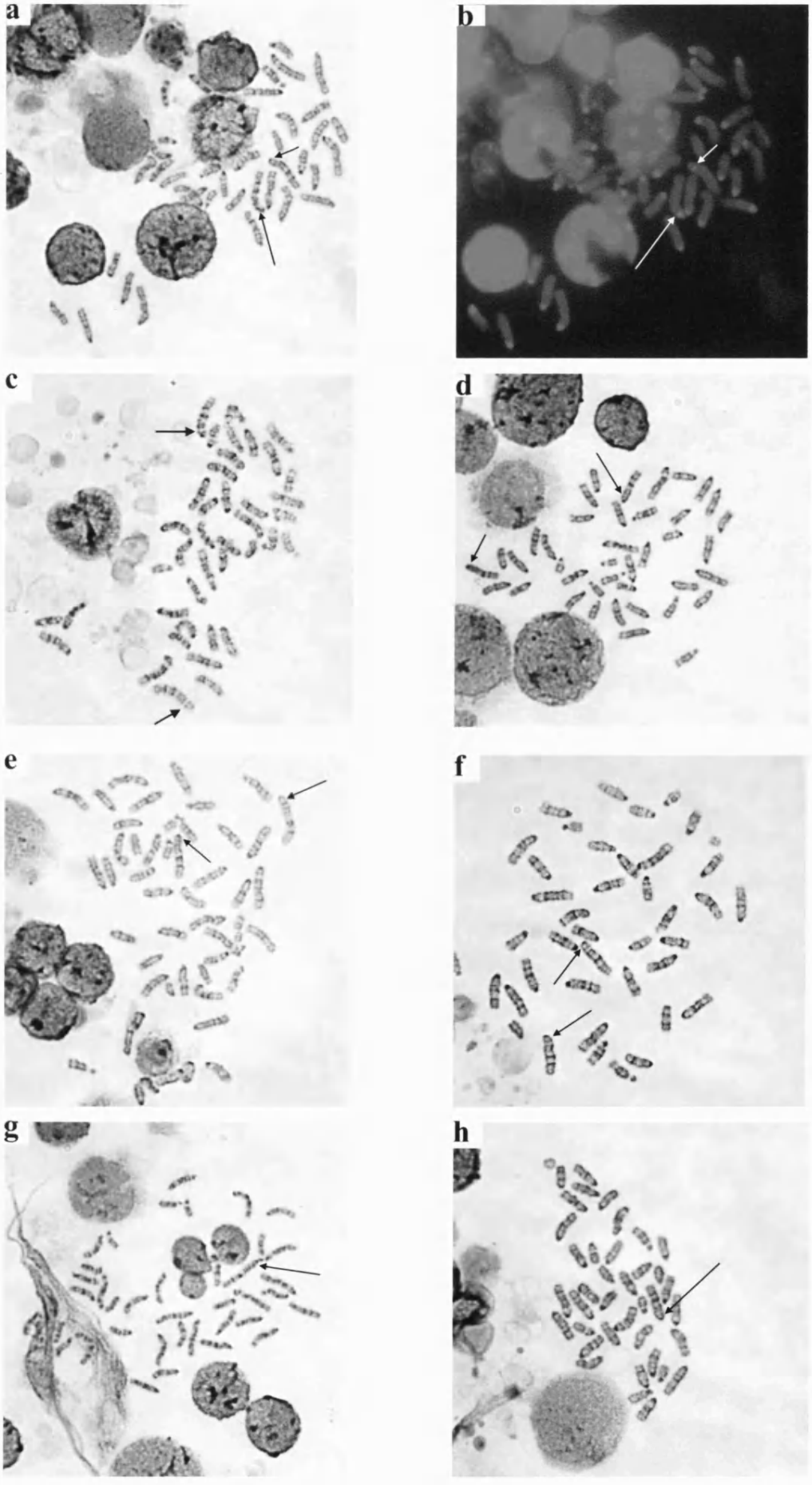

Figure 31. Double FISH with a Chr 4-specific probe and the transgene

Two representative metaphase chromosome spreads from a homozygous **Holly** male with hybridisation signals (arrowed) corresponding to the transgene (green) and a *Dvl* probe specific to distal Chr 4 (red).

Figure 31

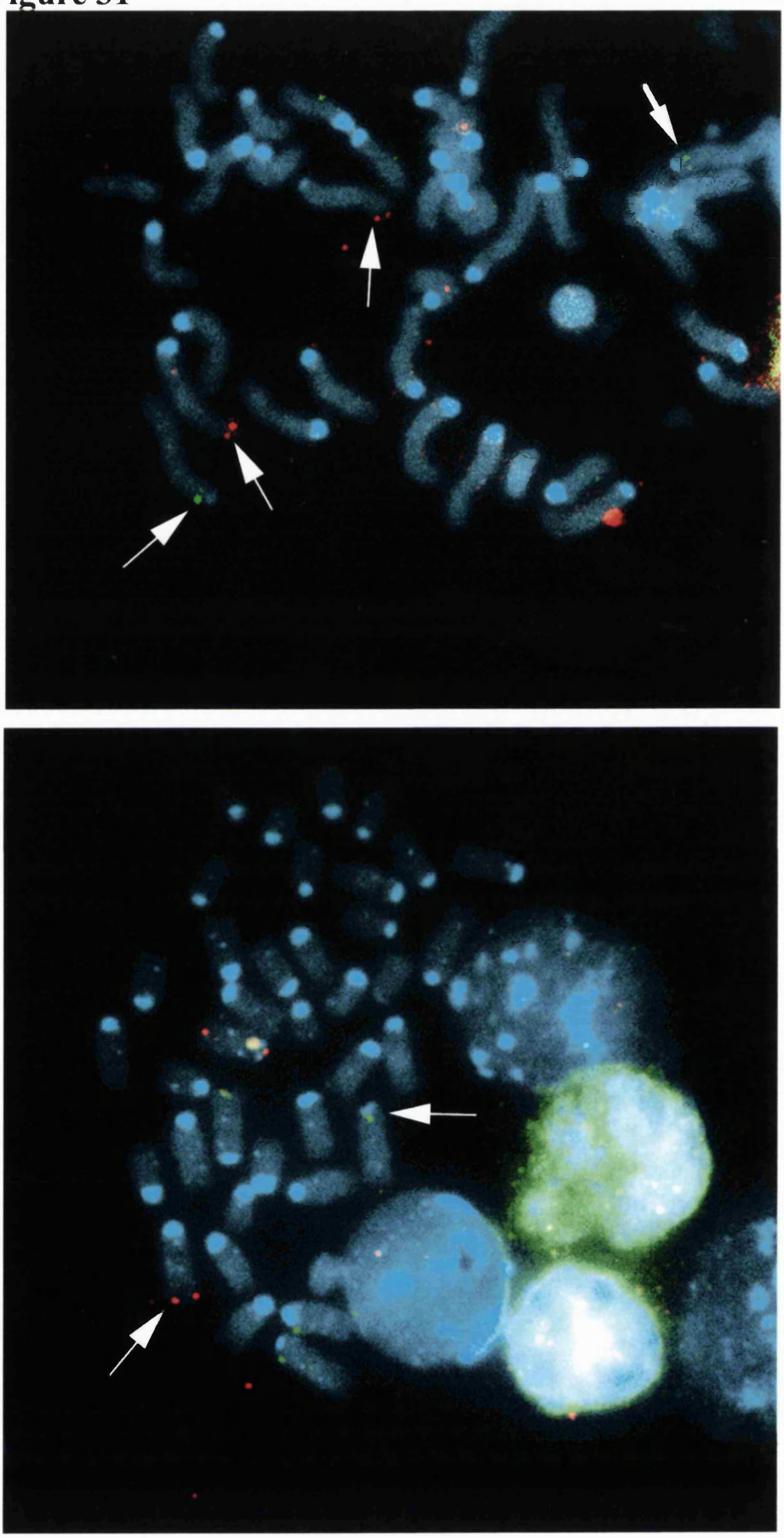

Table 11. Microsatellite PCR genotyping results for Holly

Data gathered from hemizygous (+/-) transgenic male parents crossed with non-transgenic F_1 females and from transgenic offspring of these crosses.

Animal	Father	D1Mit66 genotype	D4Mit101 genotype
+/- parents			
3.1A♂	n/a	F1	F1
3.2A♂	n/a	F1	F1
3.2B♂	n/a	CBA	F1
3.2C♂	n/a	F1	n/t
2.2♂	n/a	F1	n/t
+/- offspring			
A1	3.1A♂	F1	F1
A3	3.1A♂	CBA	F1
A4	3.1A♂	F1	CBA
A5	3.1A♂	F1	C57
A6	3.1A♂	F1	F1
A7	3.1A♂	CBA	C57
A8	3.1A♂	F1	F1
B1	3.2A♂	F1	C57
B2	3.2A♂	CBA	F1
B3	3.2A♂	F1	C57
B4	3.2A♂	F1	F1
C1	3.2B♂	n/t	C57
C2	3.2B♂	n/t	F1
C3	3.2B♂	n/t	F1
C4	3.2B♂	n/t	C57
C5	3.2B♂	n/t	CBA
E1	3.2C♂	F1	n/t
E2	3.2C♂	CBA	n/t
E3	3.2C♂	F1	n/t
E4	3.2C♂	CBA	n/t
F1	2.2♂	CBA	n/t
F2	2.2♂	F1	n/t
F3	2.2♂	F1	n/t
F4	2.2♂	F1	n/t
F5	2.2♂	CBA	n/t
G1	3.2C♂	F1	n/t
G2	3.2C♂	F1	n/t
G3	3.2C♂	CBA	n/t
H1	2.2♂	CBA	n/t
H2	2.2♂	F1	n/t
H3	2.2♂	F1	n/t
H4	2.2♂	F1	n/t
H5	2.2♂	CBA	n/t
H6	2.2♂	CBA	n/t
Informative meioses		**29**	**16**

n/a = not applicable n/t = not tested

Linkage mapping

Based on the preliminary assignments of Chr 1 and Chr 4, two pairs of primers were chosen for the proximal region of each of these chromosomes. D1Mit64 failed to amplify a specific product, even under a range of annealing temperatures, buffers and magnesium concentrations and this primer pair was abandoned. On Chr 4, all **Holly** parents tested with D4Mit263 were found to be CBA homozygous at this locus, and therefore this primer pair could not be used without first crossing **Holly** animals onto a C57 background to generate heterozygous parents. D1Mit66 and D4Mit101 were found to be both polymorphic between C57 and CBA, and to be heterozygous in some of the parents used in the backcross.

Since all useful parents are heterozygous at the locus tested, if there is no linkage between transgene and marker, then transgenic offspring should show a Mendelian distribution of 25% C57, 50% F1 and 25% CBA. For statistical significance in a χ^2 test, expected numbers in each class must be 5 or more, therefore at least 20 offspring must be tested.

Although the numbers for D4Mit263 were not sufficient for significance, it was clear from early results that both C57 and CBA homozygotes were present at this locus in numbers approximating to a Mendelian distribution, suggesting non-linkage, whilst no C57 homozygotes were observed for D1Mit66 amongst transgenic offspring. Further offspring were tested for D1Mit66 alone. In total, 29 transgenic offspring of doubly heterozygous parents were tested for this marker, resulting in 29 informative meioses. The data obtained for both loci are summarised in **Table 11.**

Taking the null hypothesis to be that there is no linkage between the transgene and D1Mit66, the data from 29 transgenic offspring can be summarised into a 1x3 contingency table thus:

Table 12. Contingency table for linkage between the transgene and D1Mit66

	C57 homozygotes	F1	CBA homozygotes	
Observed	0	18	11	$\Sigma = 29$
Expected	7.25	14.5	7.25	

Applying a simple χ^2 formula, this gives:

$\chi^2 = 10.03$

And for 2 degrees of freedom, this gives $P < 0.01$

The null hypothesis can therefore be rejected, and the transgene is probably linked to this marker and hence to proximal Chr 1.

Discussion

Candidate genes based on map position and phenotype

The results from the initial G-banding experiments were somewhat ambiguous, but the preliminary chromosomal assignment of the transgene integration site to the proximal end of either Chr 1 or Chr 4 allowed judicious choice of microsatellite primers. Chr 4 was eliminated by double FISH, and further G-banding experiments yielded high-quality results which strongly favoured proximal Chr 1. Linkage mapping using microsatellite PCR confirmed this map position, with statistically significant linkage shown between the transgene and D1Mit66, which lies around 9cM from the centromeric end of Chr 1. Since the number of offspring tested in the backcross was quite low (due to poor breeding performance), linkage to this marker is not particularly tight, however the FISH data places the transgene integration site very close to this

region, somewhere in cytogenetic band A3. A linkage map of known genes in this region is shown below (**Fig. 32**).

Figure 32. Linkage map of proximal Chromosome 1.

(Mouse Genome Database, http://www.informatics.jax.org, 1999)

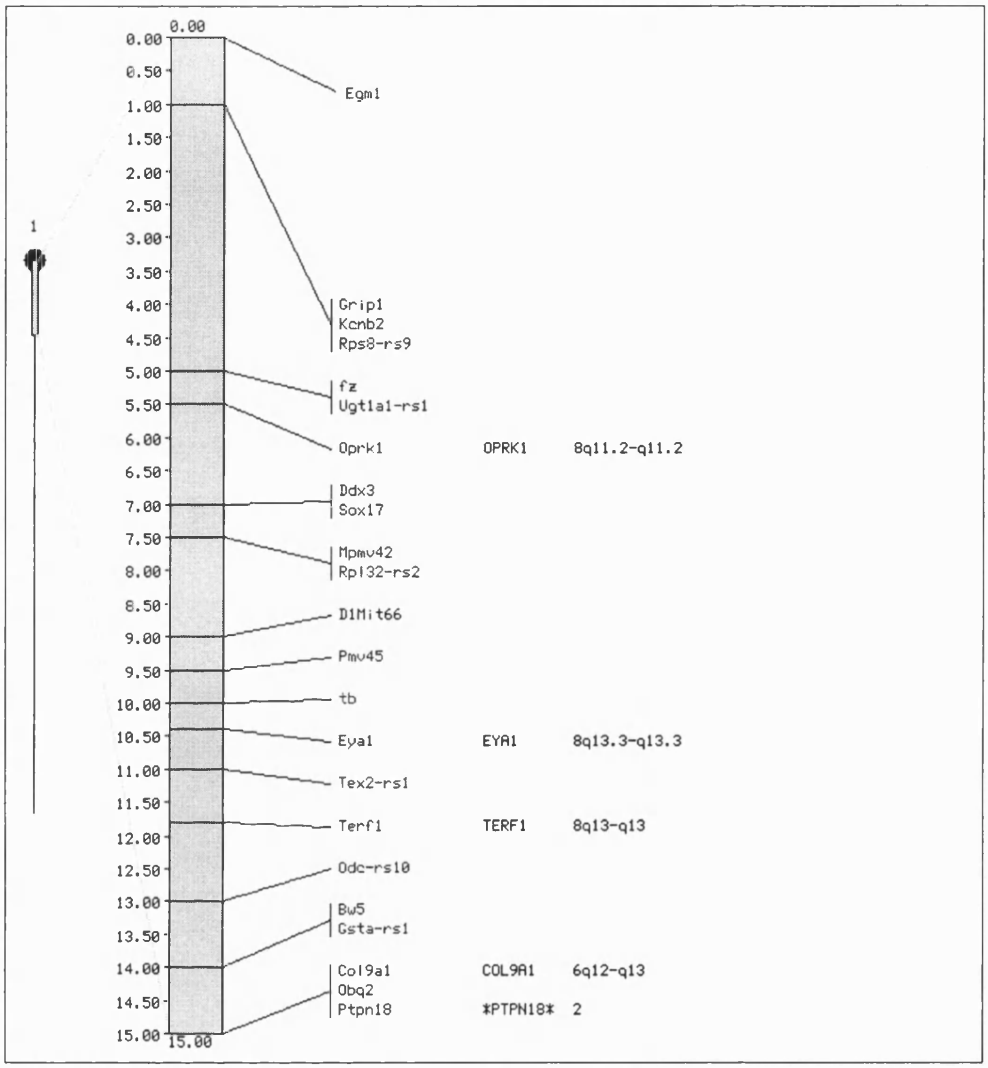

(Known human homologues are shown to the right, with their chromosomal positions.)

There are no genes known to cause any ocular phenotype in mouse in this region. Mouse chromosome 1 is syntenic to human chromosome 8q and chromosome 6q, with the syntenic breakpoint lying somewhere between *Terf1* and *Col9a1* (Human-Mouse Homology Maps; http://www.ncbi.nlm.nih.gov/Homology/, 1999). There are no loci known to cause either cataracts or glaucoma which map to either of these syntenic regions in humans, although the gene causing autosomal dominant Stargardt disease is

known to lie in the syntenic region Chr 6q13-15. This condition is restricted to retinal degeneration, however, and the causative gene has recently been identified as the interphotoreceptor matrix proteoglycan-1 (IMPG1) gene (Felbor *et al.*, 1998; Gehrig *et al.*, 1998).

Of the genes shown in **Figure 32,** both *Eya1* and *Col9a1* can be considered as reasonable candidates on the grounds that they might cause an ocular phenotype if disrupted, and these possibilities are discussed below. A third gene, *Grip1,* might be viewed as a candidate on the ground that it may be associated with non-insulin dependent diabetes. Since diabetes can cause glaucoma, *Grip1* must be considered as a candidate gene, and this is also discussed below in more detail. The other known genes in this region which have been discounted as being much less likely candidates are as follows: *Egm1* represents the egg modifier locus 1, mapped using RI strain distribution patterns, which is involved in imprinting effects. *Kcnb2* is a potassium voltage gated channel with neurological and smooth muscle functions. *fz* (fuzzy) is a recessive mutation in an unknown gene giving rise to wrinked skin and frizzy hair. *Oprk1* encodes the opioid receptor kappa 1, which is thought, from its expression patterns in the brain, to be involved in the control of autonomic and neuroendocrine functions (Yasuda *et al.*, 1993). *Ddx3* encodes a member of the DEAD-box (aspartate-glutamate-alanina-aspartate box) group of proteins, which are believed to act as RNA helicases. *Ddx3* is believed to be the murine homologue of Xenopus *An3,* which is differentially expressed in the oocyte and is believed to play an important role in translational activation in the early embryo (Sowden *et al.*, 1995). The exact function of *Ddx3* is unclear at present, but it is known to be expressed abundantly during embryonic development and to show only low levels of expression during adult life, with expression being largely restricted to specific regions of the brain. The lack of known expression in the post-natal eye argues somewhat against disruption at this locus being responsible for the **Holly** mutant phentotype. *tb* (tumbler) is a mutation in an unknown gene giving rise to a neurological phenotype with locomotor dysfunction (Mouse Genome Database, 1999). *Terf1* encodes a telomeric repeat binding factor. *bw5* and *Obq2* are QTLs for body weight and obesity, respectively, which have been mapped but whose genes

remain uncloned. *Ptpn18* encodes protein tyrosine phosphatase non-receptor type 18, which is believed to play a critical role in the maintenance of the undifferentiated state of haematopoetic stem cells, but shows very limited expression outside the bone marrow in the adult mouse (Cheng *et al.*, 1996). Apart from *Eya1* and *Col9a1*, all remaining loci shown in **Figure 32** are either pseudogenes (suffixed with -rsN where N is some integer) or represent known retrovirus integration sites in various strains of mice(*Mpmv42* and *Pmv45*).

***Grip1* as a candidate gene**

Grip1 encodes a glucocorticoid receptor interacting protein which interacts with the hormone-binding domain of the glucocorticoid receptor and may mediate its interaction with the nuclear transcription machinery (Hong *et al.*, 1996). It appears to be the murine orthologue of human TIF2 (transcriptional intermediary factor 2) (Voegel *et al.*, 1996). Although no mutations at this locus have been identified, a closely related molecule, steroid receptor coactivator 1 (SRC-1) has been knocked out by targeted deletion (Xu *et al.*, 1998). This resulted in a mild phenotype in which target organs such as uterus, prostate, testis and mammary gland exhibited a mild decrease in organ growth in response to steroid hormones, hence the mice are considered to be partly steroid hormone resistant. It was also found that expression of *Grip1/TIF2* was upregulated in the SRC-1 null mice, suggesting a degree of functional compensation by the former molecule in the absence of the latter. This might imply that disruption of the *Grip1* locus by transgene insertion would only result in a mild phenotype, due to functional compensation by SRC-1, but this cannot be asserted with confidence, as *Grip1* may perform roles which SRC-1 cannot compensate for.

It has been found that both *Grip1* and SRC-1 functionally interact with hepatocyte nuclear factor 4 (HNF-4), and mutations in this latter gene are known to cause type I mature onset diabetes of young (MODY), a form of non-insulin-dependent diabetes mellitus (Wang *et al.*, 1998). Since the hypertension associated with some forms of diabetes can cause glaucoma, *Grip1* cannot be ruled out as a candidate gene. However, the secondary glaucoma associated with diabetes tends to be of the open-angle variety, and acute angle-closure is rarely, if ever seen in diabetics (Gorin, 1977).

Although little is known about the expression pattern of *Grip1*, it is known that one of its cognate partners, *Hnf4*, is not expressed in the eye (Freeman *et al.*, 1998). Furthermore, given the functional redundancy between this gene and SRC-1, it seems likely that even if transgene insertion had entirely abolished *Grip1* function in **Holly** homozygotes, this would result in only a mild phenotype, rather than the dramatic acute onset glaucoma seen in these mice

***Eya1* as a candidate gene**

A much stronger candidate gene is *Eya1*, one of four known mouse homologues of the *Drosophila eyes absent* (*Eya*) gene (Xu *et al.*, 1997b; Zimmerman *et al.*, 1997; Borsani *et al.*, 1998).

The ancestral *Drosophila* gene, as the name suggests, is known to be an important regulator of eye development and encodes a transcription factor which acts immediately downstream of the "master regulator" eye gene, *Eyeless* or *Pax6*, and in tandem with another gene vital for eye development, *sine oculis* (Cheyette *et al.*, 1994; Xu *et al.*, 1997b; Bonini *et al.*, 1998). Murine *Pax6* has been shown to functionally compensate for a lack of *Eyeless* in Drosophila, and the same has been shown to be true for *Eya* in experiments where the murine *Eya2* cDNA was expressed in *Drosophila eyes absent* mutants (Bonini *et al.*, 1997). As with Pax genes, Eya genes are highly conserved throughout evolution, and both ancestral gene families are thought to have been initally involved in functions not related to vision, with subsequent recruitment to the developing visual system (Duncan *et al.*, 1997).

Continuing this theme of extreme conservation of developmental pathways in vastly disparate organisms, two murine homologues of *sine oculis* have been cloned, *Six1* and *Six2* and these homeobox genes have been shown to lie immediately downstream of *Pax6*, and to interact synergistically with *Eya* genes (Oliver *et al.*, 1995; Bonini *et al.*, 1998). The *Pax-Six-Eya* hierarchy is considered to be highly conserved throughout evolution, and is thought to play an important role in the development of the eye, from the early placode stage onwards (Xu *et al.*, 1997a; Xu *et al.*, 1997b).

Although at the time these experiments were performed there were no known mouse mutants of *Eya1* (but see Chapter 12 Discussion), it is highly

conserved between mouse and fly and is known to be expressed in developing anterior chamber structures during murine eye development (Xu *et al.*, 1997b). These include expression in the developing lens, ciliary body and prospective corneal ectoderm, precisely the structures most affected in **Holly** mutants. In contrast, *Eya2* is expressed in more posterior structures during eye development, including the retina and the sclera. *Eya3* is also expressed in the eye, although less is known about this gene, and still less about *Eya4* (Zimmerman *et al.*, 1997; Borsani *et al.*, 1998).

All four genes lie on different chromosomes, and the first three genes also show expression in regions of the embryo other than the developing eye, with *Eya1* and *Eya2* thought to play important roles in the patterning of the tendons in the distal limb of the mouse and similarly, in the patterning of connective tissues in the developing avian limb (Xu *et al.*, 1997a; Mishima & Tomarev, 1998). *Eya1* also shows significant expression in the developing kidney and inner ear.

Although no mouse mutants of *Eya2* exist, as mentioned previously the gene can functionally compensate for a lack of the ancestral gene in the *eyes absent* mutant fly (Bonini *et al.*, 1997). In addition, murine *Eya2* maps very close to a known cataract locus, *lop4* on Chr 2 (Duncan *et al.*, 1997). *Eya2* is therefore likely to have an important role in eye development.

Given the expression pattern and the high degree of homology between *Eya1* and *Eya2*, it seems reasonable to suppose that *Eya1* might play an important role in murine eye development, and that disruption of expression of this gene by transgene insertion might give rise to the phenotype seen in **Holly** homozygotes.

Arguing somewhat against this supposition is the accumulation of a weight of evidence concerning mutations in the human *EYA1* gene. It has recently become clear that multiple independent mutations in this gene are responsible for familial and some sporadic cases of branchio-oto-renal dysplasia (BOR syndrome) (Abdelhak *et al.*, 1997a; Abdelhak *et al.*, 1997b; Vincent *et al.*, 1997; Kumar *et al.*, 1998). An association between branchial arch defects and hearing loss has been recognised since the nineteenth century, but Melnick and colleagues identified associated renal defects in 1976, and BOR syndrome was formally classified as a clinical entity, featuring a pathognomonic triad of branchial arch, otic and renal

abnormalities (Melnick *et al.*, 1976). The syndrome features incomplete penetrance and variable expressivity, concomitant with the large number of independent mutations (at least fourteen at last count) in the *EYA1* gene (Abdelhak *et al.*, 1997a; Abdelhak *et al.*, 1997b; Vincent *et al.*, 1997; Kumar *et al.*, 1998). Hearing loss is common, as is renal agenesis or severe abnormalities of the collecting system, and these are consistent with the observed expression of *EYA1* in the developing ear and kidney (Kalatzis *et al.*, 1998).

However, despite the observed expression in anterior structures of the developing eye, this syndrome has no ocular component, which might suggest that *EYA1* does not play a critical role in eye development. Balanced against this, however, is the fact that the investigators were specifically looking for mutations which cause BOR syndrome. It is possible that there are other mutations in the EYA1 gene which give rise to a quite different clinical set of symptoms, and that hitherto these have not been grouped along with BOR syndrome, hence the DNA from these patients has simply not been screened for mutations in the EYA1 gene.

In light of this, it is suggestive that a second clinical entitity, branchio-oculo-facial (BOF) syndrome, has been proposed to be genetically related to BOR syndrome, largely on the grounds of observed similarities in defects in the branchial arches in these patients, and sporadic renal abnormalities in patients classified as having BOF syndrome (Legius *et al.*, 1990; Fielding & Fryer, 1992; McCool & Weaver, 1994; Lin *et al.*, 1995b; Su *et al.*, 1998). The putative genetic overlap between BOR and BOF syndrome is hotly contested, however, and there are currently no genetics available for BOF syndrome which might support this hypothesis (Legius & Fryns, 1992; Lin *et al.*, 1992). The vast bulk of data on BOF syndrome resides in the realm of detailed clinical observation (Lin *et al.*, 1995a).

BOF syndrome, as the name suggests, does feature a variety of ocular abnormalities, including micropthalmia, coloboma, anopthalmia, myopia and cataract, and the broad range of these is consistent with multiple mutations in a transcription factor likely to regulate a number of processes during eye development such as *EYA1* .

Both mouse and human *Eya1* are expressed in connective tissue precursor cells and in developing tendons along with *Pax6* and *Six* genes, and the conserved

Pax-Six-Eya hierarchy is thought to play an important role in connective tissue development, in addition to its critical role in eye and ear development (Oliver *et al.*, 1995; Xu *et al.*, 1997a; Mishima & Tomarev, 1998). Despite this, no peripheral connective tissue disorders have been observed in BOR syndrome. This could reflect functional compensation by other members of the *Eya* family, or might again point towards the restricted nature of the *EYA1* mutations so far discovered in these patients.

A Japanese research group has recently presented a poster detailing a mutation in the *EYA1* gene in three separate patients with congenital eye abnormalities, with one patient being classifed as having Peter's anomaly - a condition showing considerable overlap with the **Holly** mutant phenotype (Azuma *et al.*, 1999). Although this work is as yet unpublished, if verified, it clearly allows for the possibility that mutations in murine *Eya1* might generate the phenotype seen in **Holly** mice.

Overall, despite the lack of any proven association between EYA1 and congenital eye defects, the mouse *Eya1* gene must be considered a good candidate for disruption by transgene insertion in the **Holly** transgenic line.

***Col9a1* as a candidate gene**

Col9a1 encodes the α1 chain of type IX collagen. The fibrils of type IX collagen, as with most collagens, are composed of triple helical heterotrimers of three genetically distinct subunits, the α1(IX), α2(IX) and α3(IX) chains. Unusually, however, these triple helices are interrupted by non-collagenous domains, hence type IX collagen is classified as a member of the FACIT (fibril-associated collagen with interrupted triple helices) class of extracellular matrix proteins (Shaw & Olsen, 1991).

Individual type IX molecules contain three triple-helical sections, COL1, COL2 and COL3 interrupted by globular non-collagenous domains, designated NC1, NC2 and NC3 (van der Rest *et al.*, 1985; Irwin & Mayne, 1986). In hyaline cartilage, assembled collagen type IX molecules are found attached at periodic intervals to the surface of type II collagen fibrils (consisting of bundles of cross-linked staggered type II collagen chains) with the long arm, comprising COL1, COL2, NC1 and NC2 thought to lie along the surface of these fibrils, covalently

crosslinked to the underlying type II collagen. The NC3 domain acts as a flexible hinge, so that the short arm, COL3 projects out from the surface into the perifibrillar matrix (Muragaki *et al.*, 1990). The α1(IX) chain has two alternatively spliced transcripts, encoding a long and a short form of the message, and the short form lacks the large amino-terminal globular domain NC4 (Muragaki *et al.*, 1990). This is shown diagrammatically in **Fig. 33**

Figure 33. Structure of type IX collagen in association with a type II fibril
(drawn after (Linsenmayer *et al.*, 1998))

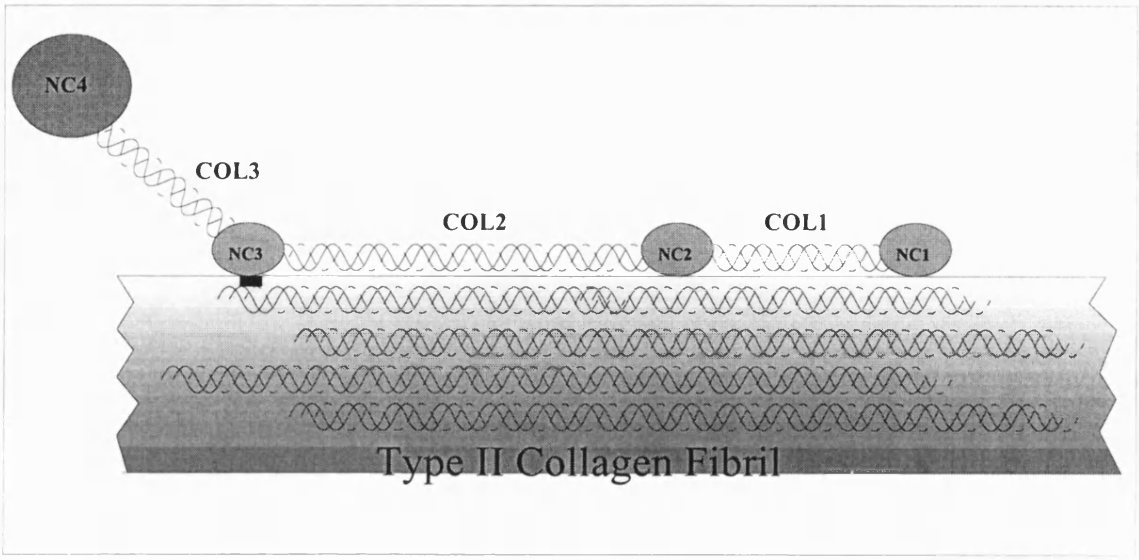

The alternatively spliced NC4 domain at the end of the projecting short arm is believed to interact with other, as yet unidentified, molecules, hence, type IX collagen, as with other members of the FACIT group, is believed to mediate interactions between collagen fibrils and other components of the extracellular matrix. This may provide the basis for anchoring and precisely positioning collagen fibrils within a three-dimensional matrix. *In vitro* studies with chondrocyte cell cultures have led to the suggestion that type IX collagen might act as a "spacer" to keep adjacent collagen fibrils from fusing together (Shaw & Olsen, 1991; Mallein-Gerin *et al.*, 1995). Apart from joints, type II and IX collagens are abundant in cartilage and in the vitreous of the eye (Swiderski & Solursh, 1992; Liu *et al.*, 1993b).

Detailed studies of the expression patterns of these two transcripts revealed that, in the mouse, the long form was preferentially expressed in cartilage and

lung, while the short form was preferentially expressed in the eye and heart (Muragaki *et al.*, 1990; Liu *et al.*, 1993a). Both transcripts are down-regulated around the time of birth, although low levels of message persist throughout adult life (Abe *et al.*, 1994). This probably reflects a low turnover of type IX collagen fibrils during adult life.

The expression pattern of *Col9a1* in the developing eye is particularly suggestive (Liu *et al.*, 1993a). *In situ* hybridisation studies revealed that this gene (predominantly the short form) is first expressed at E10.5 in the neural ectoderm but not the surface ectoderm. This becomes restricted to the anterior neural retina by E13.5, but around the time of birth expression is dramatically up-regulated for a brief period of time. In the neonatal mouse, expression is exclusive to the inner non-pigmented layer of the presumptive ciliary epithelium. During the first three weeks post-partum, the ciliary epithelium becomes fully differentiated and becomes, of course, largely responsible for the production of aqueous (Gorin, 1977). After this time, *Col9a1* expression was found to be greatly reduced and entirely restricted (in the adult eye) to the junction between the folds of the mature ciliary body and the neural retina. By 6 weeks of age, expression was undetectable by *in situ* hybridisation.

Collagen IX fibrils are known to be present in the vitreous, which contains large amounts of extracellular matrix proteins, and it is tempting to speculate that the expression pattern of *Col9a1* during embryonic development correlates with the production of vitreous to fill the globe (Yada *et al.*, 1990).

Given the specialised and highly restricted expression pattern of *Col9a1* in the ciliary body, it is reasonable to speculate that disruption of this gene by transgene insertion might have some effect upon either a structural element of the developing eye, such as the vitreous, or upon the maturation of the ciliary body itself. In particular, such a defect might not give rise to any phenotype until around the time the eyes open and the aqueous flow becomes established, precisely the time of onset of glaucoma in **Holly** mutants. This gene must therefore be considered as a very attractive candidate for transgene disruption.

Set against this hypothesis are detailed studies of the phenotype resulting from targeted deletion of the *Col9a1* gene in mice (Fassler *et al.*, 1994; Hagg *et al.*,

1997). Absence of the α1(IX) chain leads to a functional knockout of the entire type IX collagen molecule, since the triple-helix cannot assemble without all three subunits being present. Homozygous null mutants are viable and appear normal at birth, but as they age, they develop a severe noninflammatory degenerative joint disease, which is considered to be a model for osteoarthritis in humans (mutations in the human COL9A2 gene, encoding one of the other subunits of the collagen IX heterotrimer, are known to cause *multiple epiphyseal dysplasia 2*, which progresses to include osteoarthritis (Briggs *et al.*, 1995)). This accords well with the postulated role of collagen IX in maintaining the long-term structural integrity of cartilage, but since no opthalmopathy is present in *Col9a1-/-* mice, it argues against this gene being disrupted in **Holly** mutants.

Fortuitously, however, a second directed mutation of a slightly unusual nature was also generated in *Col9a1* at around the same time that the conventional knockout experiment was being performed, and this mutant provides strong circumstantial evidence to support *Col9a1* as a candidate gene for disruption in **Holly** mutants (Nakata *et al.*, 1993). These researchers took a different tactic, and decided to generate a *trans*-dominant form of the α1(IX) chain which would interfere with the correct assembly of type IX collagen. To this end, they generated a transgene construct containing the α1(IX) long form cDNA with a central deletion encompassing a large portion of the two major triple-helical domains and the flexible hinge region between them. This truncated form of the molecule, consisting of the regions amino- and carboxy-terminal to the central deletion, fused together in-frame, was driven by an upstream collagen type II promoter, and had a collagen type II enhancer region placed immediately downstream. This mutant form of the α1(IX) chain was predicted to act as a *trans*-dominant allele, interfering with the correct assembly of type IX collagen, and the authors showed that the severity of the phenotype observed correlated with the transgene dosage, suggesting that such was indeed the case.

Three transgenic founder mice were derived containing this construct, although it is perhaps not strictly accurate to call the single female a "founder", since she proved to be sterile, even after ovary transfer to wild-type female hosts. This female transgenic was also found to have opaque and irregular corneas when

her eyes opened. The remaining two founder males appeared normal, but a number of F_1 mice from both of these animals had somewhat small eyeballs.

Following incrosses between hemizygous F_1 animals, some 15% of the F_2 generation were found to develop opaque and irregular corneas, which were sometimes infiltrated with blood vessels. The published photographs, although poor quality, suggest the presence of localised grey patches on the corneal surface, highly reminiscent of those seen in **Holly** mutants. These animals were assumed to represent transgenic homozygotes, although this was not proven. These putative homozygotes also showed mild proportionate dwarfism and had a mild ossification defect leading to ovoid vertebral bodies. Transgenic hemizygotes showed no overt skeletal or ocular abnormalities, but, as with the knockout mutant mice, tended to develop progressive osteoarthritis, most noticeably in the knee joint, with changes in the articular surfaces visible by light microscopy at around 6 weeks of age.. The final conclusion was that the transgene did act in a dominant fashion to disrupt assembly of type IX collagen, leading, in the hemizygous state, to a mild chondrodysplasia predisposing for early onset osteoarthritis, a condition closely resembling the phenotype observed in the knockout animals.

The ocular phenotype was not investigated in any great detail, hence it is impossible to say whether the corneal opacity was caused by glaucoma, as in **Holly** mice, or by some structural defect in the cornea. In this regard, the authors suggest that, in light of the fact that type IX collagen is not thought to be expressed in the cornea normally, it is possible that the use of the type II collagen promoter may have driven expression of the transgene in the cornea, leading to ectopic phenotypic effects in this region. Clearly, if this were to be the case, it would weaken the argument for *Col9a1* being affected by transgene integration. However, no evidence was presented in support of this hypothesis.

Given the apparent similarity between the **Holly** phenotype and aspects of the phenotype seen in mice homozygous for the centrally deleted α1(IX) transgene, the *Col9a1* gene presents itself as an excellent candidate for transgene-associated disruption.

***Col19a1* and *Col12a1* as candidate genes**

Two loci not shown on the map in **Figure 32** are *Col12a1*and *Col19a1*, both close relatives of *Col9a1*, which encode the α1 chain of type XII and type XIX collagens respectively. *Col19a1* was initially isolated from a human rhabdomyosarcoma cDNA library, and has been mapped by FISH analysis in mouse and shown to lie very close to *Col9a1*, with both genes localised to cytogenetic band A3 on proximal Chr 1 (Inoguchi *et al.*, 1995; Khaleduzzaman *et al.*, 1997).

While very little is known about this gene, type XIX collagen is also a member of the FACIT group, and in humans, shows significant expression in many basement membranes (Myers *et al.*, 1997). In the mouse, initial ubiquitous expression during embryogenesis becomes restricted to strong expression in brain, eyes and testis of the adult (Sumiyoshi *et al.*, 1997). Given its expression in the eye, this gene also cannot be ruled out as a candidate gene.

Similarly, although even less information is available, COL12A1 encodes yet another closely related FACIT collagen subunit, and maps very close to COL9A1 and COL19A1 on Chr 6q12-13 in humans (Gerecke *et al.*, 1997). Collagen type XII also has long and short alternatively spliced isoforms and is found in abundance in stroma of the cornea, where it is considered to play a role in the spacing of the fibrils and hence the maintenance of corneal transparency (Gerecke *et al.*, 1997; Wessel *et al.*, 1997; El Shabrawi *et al.*, 1998). Intriguingly, COL12A1 is rapidly and reversibly upregulated at the mRNA level in response to mechanical stress (Trachslin *et al.*, 1999).

Given that COL12A1, COL9A1 and COL19A1 are closely related and lie together, it has been suggested that all three genes arose by gene duplication (Gerecke *et al.*, 1997). The murine homologue *Col12a1* is known to be expressed in the cornea, and would present an excellent candidate gene were it not for the fact that it lies just beyond a syntenic breakpoint with respect to human Chr 6 and actually maps to mouse Chr 9 (Oh *et al.*, 1992). It can therefore be discounted as a candidate for transgene disruption in **Holly** mutants.

As mentioned in chapter one, transgene integration can often lead to wide-spread disruption around the integration site, and it is possible that multiple

genes have been affected in **Holly** mutants. A compound phenotype involving both *Col9a1* and another gene such as *Col19a1* might explain the observed differences between **Holly** mutants and the phenotype resulting from targeted mutations in the *Col9a1* gene (Nakata *et al.*, 1993; Fassler *et al.*, 1994; Hagg *et al.*, 1997).

***MyoC/TIGR* as a candidate gene**

It should be noted that the myocilin (*Myoc*) gene, also known as Trabecular meshwork-Inducible Glucocorticoid Receptor (*TIGR*) is one of the few well-characterised glaucoma susceptibility loci, and that this gene maps to distal Chr 1 in the mouse (Tomarev *et al.*, 1998). Although it lies some 83cM from the centromere, and therefore lies at least 70cM away from the site of transgene integration in **Holly** mice, long-range effects cannot be entirely discounted in cases of transgene-associated insertional mutation, although they must be classed as being of low probability, given the map distances involved.

Prolonged exposure to gluocorticoids such as dexamethasone has long been known to cause a rise in IOP associated with increased resistance to outflow of the aqueous. The TIGR gene encodes an extracellular glycoprotein which is expressed at very high levels by the endothelial cells lining the trabecular meshwork in response to prolonged exposure to dexamethasone. It has been proposed that the TIGR protein may become deposited in the extracellular spaces of the trabecular meshwork and impede aqueous outflow, although this remains contentious (Nguyen *et al.*, 1998). Notwithstanding the fact that the exact function of the *Myoc/TIGR* gene is still somewhat obscure, mutations in the human gene are known to cause primary open-angle glaucoma, and may be responsible for at least 3% of cases of this condition (Adam *et al.*, 1997; Stoilova *et al.*, 1997; Stone *et al.*, 1997; Stoilova *et al.*, 1998). Although no known mutations in the mouse gene exist, the molecule is 82% conserved at the amino acid level between mouse and human, and in particular all fourteen residues where mutations in human TIGR can lead to glaucoma are conserved (Tomarev *et al.*, 1998). Furthermore, the mouse gene is expressed in the correct regions (retina, iris and ciliary body) to play a role in glaucoma. It therefore seems highly likely that mutations in this gene could lead to glaucoma in the mouse. Circumstantial

evidence to support this hypothesis comes from comparative sequencing of this gene in three inbred mouse strains with varying levels of "normal" IOP. The average IOP in C3H/HeJ, C57BL/6J and BALB/cJ strains is 13.7 , 12.3 and 7.7 mm Hg respectively (John *et al.*, 1997). The latter strain has a significantly lower IOP than the first two, and also possesses an alanine residue at position 164, whereas C3H and C57 both have threonine. This residue is not affected in any of the known mutations in the human TIGR gene, however, and it is not known whether the observed polymorphism has any physiological significance (Tomarev *et al.*, 1998).

All the known mutations in humans are single amino acid substitutions predisposing to the relatively mild, or at least slow-onset, primary open-angle form of glaucoma. It is tempting to speculate that a more disruptive mutation in mouse *MyoC* such as truncation or complete ablation might have a dramatic effect upon the ultrastructure of the trabecular meshwork, and could lead to acute angle-closure glaucoma, but this remains conjectural pending a knockout experiment. Given the distance between the transgene and this locus, *Myoc/TIGR* must be viewed as a valid but low probability candidate gene.

CHAPTER TWELVE:
HOLLY - NATURE OF THE TRANSGENE INTEGRATION EVENT

Introduction

With a firm map position for the transgene and two strong candidate genes in this region, it was decided to investigate the status of both *Eya1* and *Col9a1* in **Holly** mutants at the molecular level by performing Northern blotting on total RNA from wild-type and mutant animals using appropriate probes.

Preparation of the probes and RNA proved quite time-consuming, so in the interim some preliminary analysis of kidneys in **Holly** mutants was undertaken on the grounds that mutations in *Eya1* (in BOR syndrome) and in collagen genes (such as mutations in type IV collagen in Alport's Syndrome) can cause renal defects. In addition, there exists clinical evidence for genetic links between nephropathy and closed angle glaucoma (Fiore *et al*, 1985).

In BOR syndrome, the renal abnormalities cover a broad spectrum, even within individual pedigrees, ranging from fairly subtle glomerular lesions, through megaureter (gross enlargement of the collecting system) up to bilateral agenesis in extreme cases (Melnick *et al.*, 1976; Dumas *et al.*, 1982).

Clearly **Holly** mutants do not feature renal agenesis, but a significant number of these mice showed reduced bodyweight, and breeding performance, even in hemizygotes, had been markedly poor. In the homozygotes, this could of course be secondary to distress caused by the ocular phenotype (since acute angle-closure glaucoma often causes considerable discomfort or pain in humans), but in hemizygotes, which have apparently unaffected eyes it might be due to partial renal dysfunction and attendant distress.

The *Eya1* gene

The complete structure of the human EYA1 gene has been determined, and consists of some nineteen exons spread over around 156kb of genomic DNA. (Abdelhak *et al.*, 1997a). The overall size and exon-intron structure of the mouse *Eya1* gene appears to be similar, as revealed during an investigation of an interesting *Eya1* mouse mutant: A spontaneous mutation causing deafness and

circling behaviour (most often associated with defects in the vestibular system of the inner ear) has recently been characterised at the molecular level, and proved to be due to the insertion of an intracisternal A particle (IAP) element into intron 7 of the *Eya1* gene (Johnson *et al.*, 1999). This retrotransposed IAP element, of which around 2000 exist in the mouse genome, affects splicing and causes reduced expression levels and aberrant transcripts of *Eya1*. The resulting phenotype strongly resembles BOR syndrome in humans. The mutation is considered to provide a good model of BOR syndrome, and has been designated $Eya1^{bor}$. It should be noted that no ocular anomalies were observed in $Eya1^{bor}$ mutant mice.

Furthermore, although the results were not published at the time these experiments were undertaken, a targeted null mutation of *Eya1* has now been generated (Xu *et al.*, 1999). Heterozygous mutants showed hearing loss and renal abnormalities consistent with BOR syndrome, although the phenotype was somewhat milder than that seen in mice homozygous for the $Eya1^{bor}$ allele. No ocular anomalies were observed. Homozygous knockout mice entirely lacked ears and kidneys, and were born with open eyelids, although no detailed investigation of the eye was undertaken. Homozygotes died around the time of birth, however, long before any glaucomic phenotype could be discerned, even if such were present.

Alternative splicing generates different length mRNA transcripts in both humans and mice, and the probe generated to mouse *Eya1* by RT-PCR (see Methods) hybridised to two bands of approximately 4.3 and 2.9kb. The upper band is in accordance with published results from Northern blots of mouse RNA hybridised with probes derived from the 3'UTR of *Eya1* (Abdelhak *et al.*, 1997b) and almost certainly corresponds to an *Eya1* signal. The lower 2.9kb band has not been previously reported and cross-hybridisation of the probe to another *Eya* homologue cannot be excluded. However, over the region of the *Eya1* mRNA used to generate the probe, the closest known homologue, *Eya2*, is 53% homologous at the nucleotide level, which would not be expected to generate a strong band at the stringency used in these hybridisations. Over the same region, *Eya3* and *Eya4* are 37% and 28% homologous to *Eya1* at the nucleotide level, respectively.

The *Col9a1* gene

The gene itself contains 38 exons. The long form contains the large globular amino-terminal NC4 domain, which is encoded by exons 1-7 (Savontaus *et al.*, 1998). The short form utilises an alternative promoter located in intron 6 to drive expression and entirely lacks the NC4 domain. The two isoforms of *Col9a1* are very similar in size, hence although the probe pMCol9a1-1 (derived from exons 36-38 at the 3' end of the coding sequence) recognises both isoforms, only a single band at around 4kb is visible on hybridisation (Abe *et al.*, 1994). The probe pMCol9a1-2 (derived from exons 2-6) is specific for the long isoform.

The functions of the two different isoforms are unknown, although both forms are expressed in prechondrogenic mesenchyme and then differentially regulated thereafter (Abe *et al.*, 1994). A detailed study of the two isoforms during mouse development revealed that in the perichondrium and periosteum of E14.5-E18.5 embryos (i.e. during cartilage condensation and differentiation) the long isoform was preferentially expressed in the cartilaginous anlage, whilst the short form was confined to the surrounding mesenchyme (Savontaus *et al.*, 1998). In the eye, only the short form was detected, with expression in the vitreous, the ganglion layer of the retina, and weak expression in the lens. No signal was detected in the cornea or sclera at any stage of embryonic development, and no trace of the long isoform could be found. This is in marked contrast to the situation in the developing chick eye, where type IX collagen is believed to play a critical role. During avian corneal development, the acellular primary stroma swells and becomes populated by neural crest-derived mesenchymal cells which migrate in from the periphery. Type IX collagen is strongly expressed in the chick cornea, and stromal swelling correlates with proteolysis of the α1(IX) chain, with loss of the NC4 domain essentially converting the long isoform to the short one, albeit post-translationally (Fitch *et al.*, 1998). It has been suggested, although not proven, that this proteolysis changes the nature of the interaction of collagen fibrils with the ECM, allowing stromal swelling and the ingress of mesenchymal cells. Another study on chick has shown that the type IX collagen found in abundance in the vitreous contains only the short form of the α1(IX) chain, which agrees with the *in situ* data from mouse (Yada *et al.*, 1990).

The function of type IX collagen was probed directly in mouse by two separate groups of researchers making directed mutations in the gene. The first of these consisted of the *trans*-dominant transgene construct mentioned in the previous chapter, consisting of a truncated form of α1(IX) which interfered with the assembly of type IX collagen (Nakata *et al.*, 1993). Apart from the major component of the phenotype in these transgenic mutants, namely osteoarthritis, most intriguingly some 15% of the F^2 generation - putatively homozygous for the transgene - developed opaque or irregular corneas, which were sometimes infiltrated with blood vessels. The authors offered no explanation, but suggest that, perhaps the use of the rat type II collagen promoter/enhancer to drive expression of the transgene might have contributed to this aspect of the phenotype. They conceded that "the clarification of the eye phenotype....will need further study", but the only further reference in the literature to this mutant is a subsequent X-ray study on the joint and vertebral degeneration (Kimura *et al.*, 1996), with the eye component of the phenotype seemingly dropped after the publication of Fassler *et al*'s paper the following year, when they generated a *Col9a1* null allele (Fassler *et al.*, 1994). This group generated a targeted mutation in the gene and showed that no α1(IX) chain was generated in homozygotes. They subsequently went on to prove that lack of this chain completely abolishes the assembly of type IX collagen i.e. that the other two subunits cannot compensate for the lack of the first (Hagg *et al.*, 1997). They also showed that the absence of type IX collagen in no way compromised fibrillogenesis in all tissues examined, and suggested that type IX collagen was primarily important for the long-term maintenance of tissue stability in certain cartilages. The knockout study performed by Fassler *et al* essentially backed up Nakata and co-workers with respect to the osteoarthritic phenotype, but they found no ocular anomalies, even though they were looked for.

Leaving aside the possibility that the corneal abnormalities seen in the earlier study were merely a result of ectopic expression of the transgene under the control of the type II collagen promoter, one plausible explanation for the lack of an ocular phenotype in the knockout mice lies in the strain backgrounds, and perhaps most particularly in the special nature of the C57BL/6 strain. Fassler *et al*

made their knockout in ES cells, which are 129 derived, and following initial crosses of chimeric crosses to either BALB/C or C57BL/6, they proceeded to breed their knockout back onto a pure 129/Sv background. In contrast, Nakata and co-workers generated and maintained their transgenic line on a pure C57BL/6 background. Not only are these strains very distinct, but it has been known for many years that C57BL/6 mice spontaneously develop ocular abnormalities at low frequency.

Some 5-15% of C57BL/6 mice develop a range of ocular defects, including micropthalmia, anopthalmia, corneal opacity and cataracts (Pierro & Spiggle, 1967). This was originally attributed to a delay in separation between the lens vesicle and the surface ectoderm, but more recently, studies using chimeric mice made by aggregation of embryos from C57BL6 and other strains have shown that the lens cells of C57BL/6 appear to be developmentally retarded (Robinson *et al.*, 1993). The lens appears to be able to catch up in growth later on, but on occasion, the abnormally small lens vesicle can become completely enveloped by the optic cup, leading to arrested development and micro- or anopthalmia.

Given this established defect in the C57BL/6 strain, it is possible that this might contribute additively to the *Col9a1* mutation introduced by Nakata *et al* on this strain background, but not on the 129 background used by Fassler *et al.* In other words, that the defect in lens development in C57BL/6 acts as a modifier to enhance an ocular phenotype in *Col9a1* mutants.

Results

Northern blotting

No detectable signal could be resolved with either *Eya1* or *Col9a1* probes hybridising to RNA prepared from adult tissues, both mutant and wild-type (data not shown). However, RNA prepared from the head (both brain and surrounding mesenchyme, excluding eyes) and hindlimbs of E17 and E15 embryos gave a strong signal with all three probes used (**Figure 34**). RNA prepared from kidney and eye gave only very weak signals, even though there was sufficient RNA to give a strong signal with GAPDH.

Figure 34. Northern blotting of embryo RNA from Holly hemizygous intercrosses

Band sizes: *Eya1* 4.3kb and 2.9kb

Col9a1 3.5kb

GAPDH 1.3kb

a) **Holly** 5.3♂ x 4.3♀ E17 embryos (x 3)
1) Reference RNA from an E9 non-tg embryo
2) Head RNA from non-tg E17 embryo #1
3) Hindlimb RNA from non-tg E17 embryo #1
4) Head RNA from tg E17 embryo #2
5) Hindlimb RNA from tg E17 embryo #2
6) Head RNA from tg E17 embryo #3
7) Hindlimb RNA from tg E17 embryo #2

b) **Holly** 5.4♂x5.1♀ E15 embryos (x4)
1) Head RNA from tg E15 embryo #1
2) Head RNA from tg E15 embryo #2
3) Head RNA from tg E15 embryo #3
4) Head RNA from tg E15 embryo #4
5) Hindlimb RNA from tg E15 embryo #1
6) Hindlimb RNA from tg E15 embryo #2
7) Hindlimb RNA from tg E15 embryo #3
8) Hindlimb RNA from tg E15 embryo #4
9) Kidney RNA from tg E15 embryo #1
10) Kidney RNA from tg E15 embryo #2
11) Kidney RNA from tg E15 embryo #3
12) Kidney RNA from tg E15 embryo #4
13) Eye RNA from tg E15 embryo #1
14) Eye RNA from tg E15 embryo #2
15) Eye RNA from tg E15 embryo #3
16) Eye RNA from tg E15 embryo #4

c) **Holly** 6.1♂x6.4♀ E17 embryos (x8)
1) Head RNA from tg E17 embryo #1
2) Head RNA from tg E17 embryo #2
3) Head RNA from tg E17 embryo #3
4) Head RNA from tg E17 embryo #4
5) Head RNA from tg E17 embryo #5
6) Head RNA from tg E17 embryo #6
7) Head RNA from tg E17 embryo #7
8) Head RNA from tg E17 embryo #8
9) Hindlimb RNA from tg E17 embryo #1
10) Hindlimb RNA from tg E17 embryo #2
11) Hindlimb RNA from tg E17 embryo #3
12) Hindlimb RNA from tg E17 embryo #4
13) Hindlimb RNA from tg E17 embryo #5
14) Hindlimb RNA from tg E17 embryo #6
15) Hindlimb RNA from tg E17 embryo #7
16) Hindlimb RNA from tg E17 embryo #8

Fig. 34

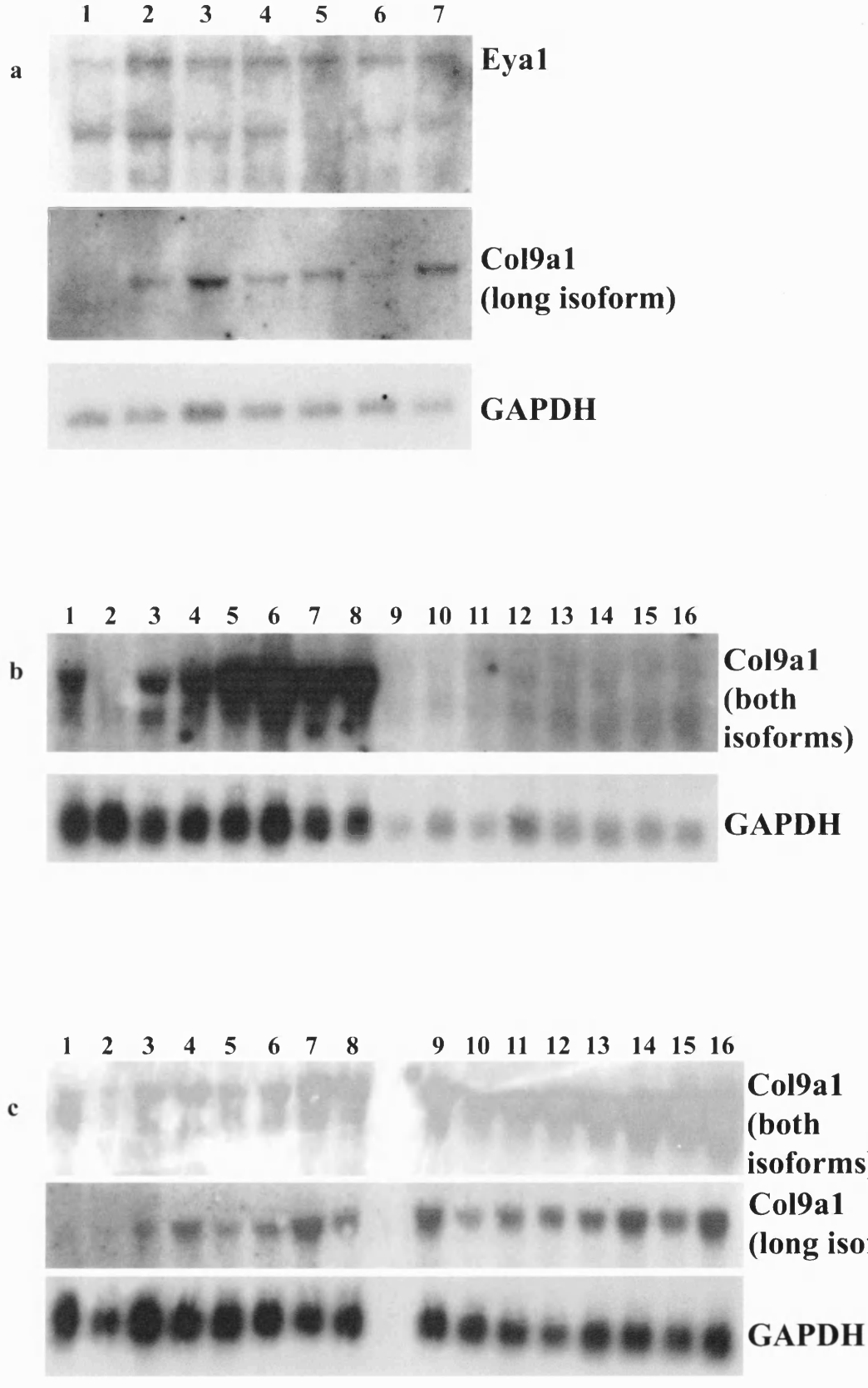
1 2 3 4 5 6 7
a
Eya1
Col9a1
(long isoform)
GAPDH
1 2 3 4 5 6 7 8 9 10 11 12 13 14 15 16
b
Col9a1
(both
isoforms)
GAPDH
1 2 3 4 5 6 7 8 9 10 11 12 13 14 15 16
c
Col9a1
(both
isoforms)
Col9a1
(long isoform)
GAPDH

Referring to **Fig 34a**, the *Col9a1* signal is entirely absent from the E9 embryo, as predicted, since there is practically no connective tissue present at this stage. In addition, the signal seems to be reduced in the head RNA of embryo #3 (track 6). The *Eya1* signal (upper band) is present in all samples.

In **Fig 34b**, the *Col9a1* signal (both isoforms) is greatly reduced in the head RNA of embryo #2 (track 2), while hindlimb expression remains unaffected (track 6). Kidney and eye show insignificant levels of expression of the gene at this stage, although it should be noted that less RNA was obtained from these tissues, as evinced by the GAPDH signal.

In **Fig. 34c**, although the signal obtained with the Col9a1-1 probe (both isoforms) is somewhat indistinct, embryo #2 shows a clear reduction in expression in head (track 2) but not hindlimb (track 10). This is confirmed with the cleaner result using Col9a1-2 (long isoform), where again, embryo #2 shows a sharp reduction in head expression.

Eya1 showed no difference in expression across all samples, but in some embryos *Col9a1* showed a dramatically reduced level of expression in RNA prepared from the head. In total, embryos from three separate intercrosses were tested, and one embryo from each cross was found to show definite reduction in *Col9a1* expression in head RNA (3/15 embryos). *Eya1* expression was examined in two of these three crosses and was not found to be affected (data not shown for one cross).

Renal histopathology

The kidneys of homozygous mutants were found to be visibly enlarged in some mice older than two months (3 out of 5 examined). Younger mutants (15-21 days old) showed no obvious enlargement (4 examined). Sectioning and PAS staining of three grossly enlarged kidneys from separate mice and comparison to age-matched controls revealed that in the cortex, the glomeruli and Bowman's capsule appeared normal, but that the nephrons were grossly dilated, probably in the proximal convoluted tubules (**Figure 35**). The loop of Henle and the collecting apparatus appeared less affected, as the innermost region of the medulla appeared normal, although some dilation may have been present.

Figure 35. Renal histopathology

a) Sagittal section showing wild-type nephrons from a two month old wild-type female. PAS-Haematoxylin x100.
b) Sagittal section showing nephrons from a **Holly** homozygous mutant (2 month old female) with a grossly enlarged kidney. PAS-Haematoxylin x100
c) Diagram of two types of nephron: juxtamedullary and cortical nephrons.

It should be noted that although the mutant kidney was significantly larger than the wild-type, the difference in size between the two regions shown in a) and b) is partly due to the oblique plane of section in b) which has rendered the mutant nephrons somewhat extended compared to the wild-type. The regions which can be seen in the photomicrographs from outside to inside are: the **cortex**, containing the glomeruli (**glom**) and some shorter cortical nephrons; the **outer medulla**, containing the descending and ascending limbs of the longer (and more numerous) juxtamedullary nephrons, along with collecting tubules; the **inner medulla**, containing the thinner loops of Henle and where the collecting ducts (**CD**) come together to drain into the **calyx** and hence into the ureter.

PAS staining accentuates the proximal convoluted tubules (**PCT**) by virtue of staining their lumenal brush borders. The distal convoluted tubules (**DCT**), the descending and ascending limbs of the nephron in the outer medulla and the loop of Henle do not stain strongly with PAS. PAS also stains the basement membrane of the glomerulus.

In the mutant, grossly dilated structures can be seen in the cortex, and all have brightly stained lumenal surfaces, indicating that they are proximal convoluted tubules. The undilated tubules which can also be seen in this region lack strong PAS staining, suggesting that they are either distal convoluted tubules, collecting tubules or blood vessels. Little or no dilation can be seen in the inner medulla. Some dilated structures can be seen in the outer medulla, and these may correspond to the descending limbs (**DL?**), although without the diagnostic brush border found in the proximal convoluted tubules, this is unclear.

The glomeruli appear relatively unaffected, at least by light microscopy.

Fig. 35

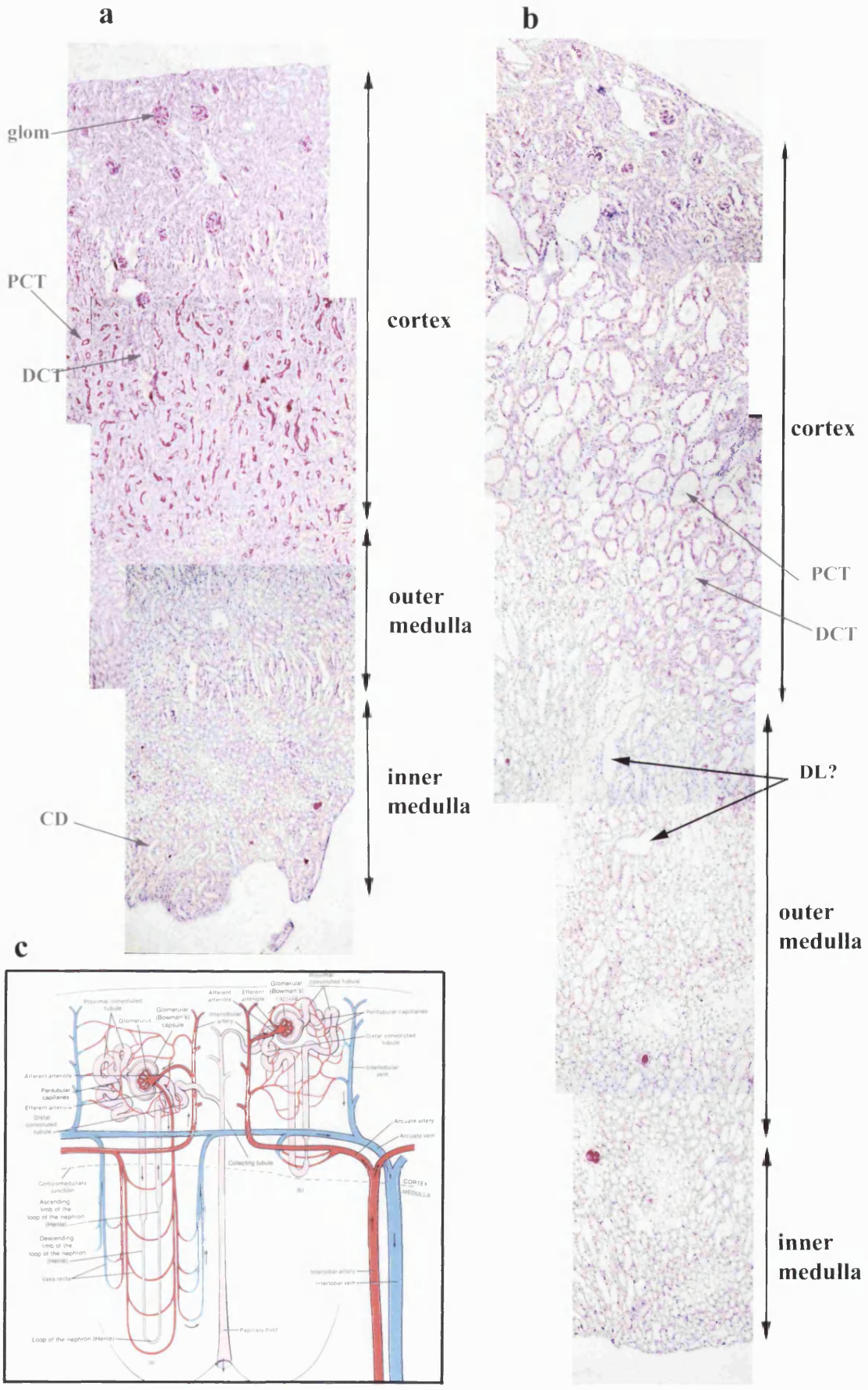
a
glom
PCT
DCT
CD
cortex
outer medulla
inner medulla
b
cortex
PCT
DCT
DL?
outer medulla
inner medulla
c

Some dilation was visible in the outer medulla, probably corresponding to the descending limbs, but this was not as marked as that seen in the proximal convoluted tubules in the cortex.

Transgene copy number determination

This was performed exactly as discussed previously in chapter 7, with the same KpnI digest giving separate transgene and endogenous reference bands. Although the structure of the array in the **Holly** genome was such that the transgene gave two major bands, both transgene signals were visibly fainter than the reference endogenous signal by the 8-9 copy dilution, indicating that probably between 5-10 copies of the transgene have integrated (**Figure 36**).

Figure 36. Holly transgene copy number titration

Southern blot of various dilutions of KpnI-digested transgenic DNA corresponding to discrete transgene copy numbers (shown above each lane) hybridised with a probe which gives a separate endogenous (endo) and transgene bands (tg).

Figure 36

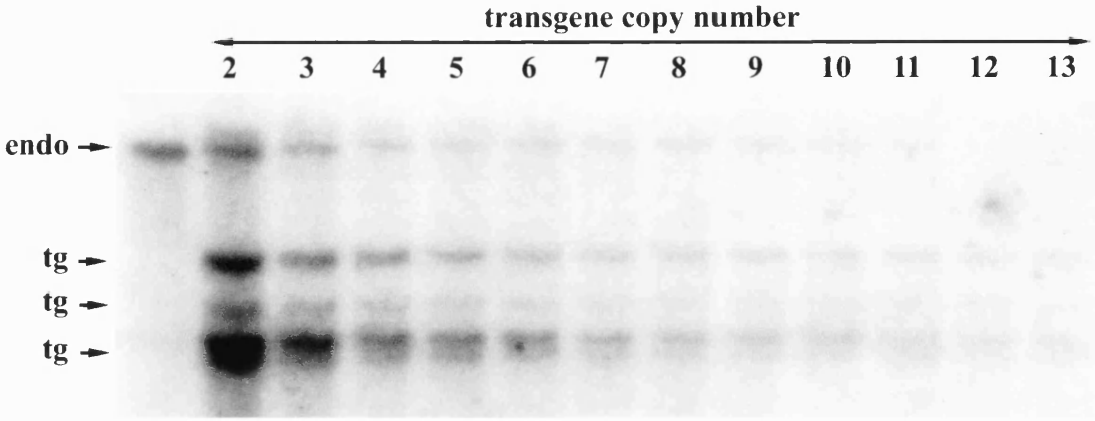

Discussion

It proved impossible to obtain a clear signal on Northerns using RNA from adult tissues, hence no defined mutants could be tested. 25% of the E15 embryos from hemizygous intercrosses should have been homozygous, and the number of embryos (3/15) showing a definite reduction in the *Col9a1* signal in head mesenchyme was consistent with this ratio.

In principle, the known polymorphism at D1Mit66 could have been used to assign genotypes to the E15 embryos. Crossing two mice which were each heterozygous at this locus would be informative, since embryos homozygous for the CBA allele would most likely also be homozygous for the transgene. Unfortunately, all parents of breeding age were genotyped and no heterozygous mothers could be found at the time these experiments were performed (data not shown).

Eya1

Given that *Eya1* expression was unaffected in two litters, each of which contained one sample showing a substantial reduction in *Col9a1* expression, and given that *Eya1* lies at some distance from *Col9a1* (some 5cM on the linkage map), it seems reasonable to conclude that the transgene integration has disrupted *Col9a1*, but has left *Eya1* unaffected.

It might seem, in light of the *Eya1* knockout mouse showing no ocular abnormalities, that *Eya1* can safely be discounted from playing a critical role in eye development (or at least a role which cannot be functionally compensated for by another gene), but if the findings of Azuma and co-workers with respect to mutations in EYA1 in human patients with developmental eye anomalies are verified, then other alleles of *Eya1* might yet be found to give rise to an ocular phenotype in mouse (Azuma *et al.*, 1999).

Transgene integration

The exact nature of the integration event remains unclear. The presence of multiple strong bands on the Southern blot shown in **Fig. 36** points towards a

complex integration, although the array was not restriction mapped during the course of this study. *Col9a1* has a large and complex gene structure, with some 38 exons spread over around 56kb of genomic DNA. (Savontaus *et al.*, 1998). The fact that wild-type levels of both isoforms of *Col9a1* are expressed in embryonic hindlimbs argues against disruption of the coding sequence. This suggests that the transgene might be acting to perturb regulation of the gene, perhaps by disruption of tissue-specific enhancers.

Col9a1 in the eye

The lack expression of *Col9a1* in RNA from the eyes of E15 embryos, or indeed of documented expression of *Col9a1* in the developing mouse cornea should not necessarily be taken as a sign that transgene-associated disruption to this gene could not be responsible for the phenotype. Firstly, although a significant amount of RNA (around 10μg) was obtained from the eyes of a single embryo, the vast bulk of this RNA could be from cells which simply do not express *Col9a1*, such as the neuroectoderm. The actual *Col9a1* expressing moiety could be a small fraction of the total, reducing the chances of detecting any signal on Northerns from single embryos. The published *in situ* data suggests that the short form only is expressed in the vitreous and in the posterior lens (Savontaus *et al.*, 1998). There is no data on expression of *Col9a1* in post-natal mouse eyes, and given that this is precisely the time when the aqueous outflow pathway is being set up, it might be predicted that type IX collagen is only expressed in the cornea post-natally. Although type IX collagen is clearly important for the development of the embryonic avian cornea the timing of mouse and chick eye development is quite different.

Osteoarthritis

The fact that **Holly** homozygotes do not develop osteoarthritis can be explained by the observation that wild-type levels of *Col9a1* are expressed in the hindlimbs. Of course, it is not certain that **Holly** mutants entirely lack joint defects, since these were not looked for, and could be relatively subtle. A few animals did show slight dwarfism, an observation made by Nakata *et al* with respect to their transgenic mutant (Nakata *et al.*, 1993).

Renal defects

Although renal pathology is complex and difficult to interpret, the overall picture pointed towards severe dilation of the ascending and descending limbs of the nephrons, perhaps caused by fluid retention, but featuring relatively normal glomeruli. This is important, because compromise of Bowman's capsule (glomerulonephritis) is one of the pathological hallmarks of Alport's syndrome, a multifactorial genetic disease featuring hematuria (blood in the urine), sensorineural hearing loss, progressive renal failure and frequently ocular defects such as lenticonus (anterior bulging and dysmorphology of the lens), cataract and retinal abnormalities (Colville & Savige, 1997). The autosomal recessive forms of the disease are frequently caused by mutations in either COL4A3 or COL4A4, components of type IV collagen and the sex-linked form of the disease is caused by mutations in COL4A5 (Kalluri *et al.*, 1994). Essentially, Alport's Syndrome features, to a varying degree, defects in basement membranes found in glomeruli, the inner ear, the retina and the lens capsule. The lens capsule abnormalities are quite distinct from that seen in **Holly**, and this appears also to be true for the renal defects, but the point stands that mutations in a single collagen subunit can lead to characteristic defects in a range of structures dependent upon basement membrane integrity (Streeten *et al.*, 1987).

It is unclear whether **Holly** heterozygotes have similar renal problems, although the poor breeding performance points either towards reduced fertility or towards some form of stress. The latter explanation is supported by the observation that, in two of the three crosses utilised for the Northern experiments, the mothers were found to contain several resorbed embryos upon dissection, resulting in only three or four live embryos.

Col19a1

Returning to the differences between **Holly** mutants and the documented lack of an ocular phenotype in *Col9a1* null mice, another possible explanation is that the transgene integration has also disrupted a neighbouring gene. There is in fact, an attractive candidate gene for such an event - *Col19a1* encodes the α1 subunit of type XIX collagen, and this gene is known to sit somewhere fairly close to *Col9a1*. Type XIX collagen, although poorly-characterised, is another FACIT

collagen with initial expression throughout the mouse embryo at E11, with expression subsquently restricted to certain tissues in the adult, specifically brain, eye and testis (Sumiyoshi *et al.*, 1997). In humans, expression of type XIX collagen has been shown to be largely confined to basement membranes in a wide variety of organs (Myers *et al.*, 1997).

It has been suggested that *Col9a1* and *Col19a1* arose by tandem duplication of the same gene, as the human homologues of these two genes also map to the same syntenic region, Chr 6q (Yoshioka *et al.*, 1992). Not only does *Col19a1* lie next to *Col9a1* in both mouse and human, but analysis of the human gene sequences has led Khaleduzzaman *et al* to support the hypothesis that the two genes arose by tandem duplication of an ancestral FACIT collagen (Khaleduzzaman *et al.*, 1997). The human gene is large and complex, spanning over 250kb of genomic DNA, and has an unusually large (>10kb) mRNA transcript, with numerous splice variants (Gerecke *et al.*, 1997; Sumiyoshi *et al.*, 1997). The significance of this is unknown, as the translated region is relatively small.

Although detailed expression studies have not been performed, it is possible that *Col19a1* plays a role in murine eye development. The possibility therefore cannot be excluded that the ocular phenotype seen in **Holly** mutants is caused by disruption to *Col19a1*, or to *both* collagen genes.

Summary

Holly transgenic homozygotes appear to show tissue-specific reduction of both isoforms of the *Col9a1* gene. The question of whether the ocular phenotype seen in **Holly** mutants is actually caused by a reduction in *Col9a1* remains somewhat of a moot point.

The data from the Northerns argues in favour, however the knockout study of Fassler *et al* argues that a complete lack of *Col9a1* does not compromise eye development, at least in the 129/Sv strain (Fassler *et al.*, 1994). **Holly** transgenic mice are maintained on a somewhat mixed background, comprising C57BL/6 and CBA to varying degrees, and it is entirely possible, given the known defects in C57BL/6 lens development and the fact that Nakata and coworkers *did* see an ocular phenotype in a *Col9a1* mutant on their C57BL/6 background, that the strain

background combined with a tissue-specific reduction in *Col9a1* generates the phenotype in **Holly** mice.

CHAPTER THIRTEEN:
HOLLY - FINAL DISCUSSION

Future work

Nature of the transgene integration

Restriction mapping of both the transgene array and the *Col9a1* genomic region is required to shed some light on the exact nature of the disruption at this locus. While more precise genetic mapping of the transgene is possible with the use of additional markers and a larger backcross, *Col9a1* has only been mapped with respect to three other genes in proximal Chr 1 with a 114-mouse Spretus backcross panel, hence no accurate data (<1cM) exists to link *Col9a1* to any genetic marker, such as a microsatellite (http://www.informatics.jax.org, 1999). If no polymorphism were found in or around the *Col9a1* gene with respect to **Holly** transgenic mice, then having an accurate position on the linkage map for the transgene would not be of any great benefit, as a chromosome walk would still have to be performed moving away from *Col9a1* in both directions.

Gene expression

While knowing where the transgene has integrated with respect to *Col9a1* is important, probably more pressing is determining the expression pattern of both isoforms in the developing mouse. The expression of *Col9a1* is maximal between E12 and E15 (depending on the isoform) (Perala *et al.*, 1997). It is technically difficult to perform wholemount *in situ* on mouse embryos after E12.5, but it would be most informative to serial section embryos first, then perform *in situ* hybridisation and examine the temporo-spatial expression of each isoform in **Holly** mutants. A detailed study of the expression pattern of this gene in wild-type mouse embryos has already been published and would provide a useful reference series for such a study (indeed, the pMCol9a1-1 and pMCol9a1-2 probes used in this work were a gift from the authors) (Savontaus *et al.*, 1998).

Status of type XIX collagen (*Col19a1*)

As discussed in the previous chapter, one reason for the observed discrepancy between **Holly** mutants and *Col9a1* knockouts might be that the adjacent *Col19a1* locus has also been affected by the transgene, and that altered expression of type XIX collagen might account for the ocular phenotype. It would therefore be important to obtain a probe and establish whether the expression of this gene is affected in mutants, by Northerns or *in situ*.

Type IX collagen deposition

Given that the aqueous outflow pathway forms and differentiates post-natally, it would probably be more informative to examine gene expression in eyes and possibly kidneys from post-partum days P0-P12 mice, rather than embryos. Unfortunately, expression of the gene declines after birth, reflecting the low rate turnover of collagen in connective tissues, but even if *in situ* failed to reveal gene expression patterns, it might still be possible to examine type IX collagen using immunohistochemistry. Commercial antibodies are available, but the only isoform-specific ones are two mouse monoclonals which presumably do not recognise mouse type IX collagen. Although it might not be possible to dissect out the expression of each individual isoform of *Col9a1*, therefore, it should be feasible to study the expression and deposition of the protein throughout embryonic and post-natal development.

Complementation with other *Col9a1* mutants

Another possible explanation as to why *Col9a1* knockouts show no ocular phenotype refers to the strain background on which the knockouts were maintained. To re-iterate: the *trans*-dominant truncated α1(IX) transgene on a C57BL/6 background gave rise to an ocular phenotype which superficially resembles that seen in **Holly** mutants (Nakata *et al.*, 1993). In contrast, the targeted null on a 129/Sv background showed no ocular phenotype, even though this was looked for (Fassler *et al.*, 1994). It might prove informative to cross **Holly** hemizygotes with *Col9a1*-/+ heterozgotes to see if the transgene insertion complements the targeted null allele.

Another, equally interesting experiment, would be to simply introgress the transgene onto purebred strain backgrounds - C57BL/6 and CBA would be logical choices to see if the phenotype is greatly exaggerated on the C57BL/6 background. This would, however, require at least 5 generations of backcrosses.

Osteoarthritis

The logical corollary to the question of why *Col9a1* knockout mice lack an ocular phenotype is to ask whether **Holly** mutants develop osteoarthritis through damage to the articular cartilage or show changes in the vertebral bodies. This could be addressed most easily by allowing some mutants to go to advanced age (9 months being sufficient time to show considerable alteration in the joints of *Col9a1* knockouts) and then sectioning knee joints and spines for histology. In light of the apparent wild-type levels of expression of *Col9a1* in RNA from the hindlimbs of presumptive mutant embryos, it may well be the case that **Holly** mutants show little or no change in articular cartilage

Histopathology

In tandem with gene expression studies, it will be important to track the pathological progression of this mutant phenotype from birth onwards by simply sectioning eyes and kidneys from a series of mutant mice ranging from P0 up to full adulthood. Of particular interest will be whether the lens becomes displaced and moves forwards to contact the iris (pupillary block angle-closure) or whether the iris or cornea is misplaced and adheres to the lens. In addition, if a temporal series of PAS stained sections through the cornea were to be assembled, it should prove straightforward to determine whether Descemet's membrane is compromised *before* the onset of the phenotype or whether the corneal endothelium degenerates as a secondary consequence of prolonged glaucoma and presumptive hypoxia in the regions of contact between cornea and lens. This question is of considerable interest, since attenuation or absence of Descemet's membrane is pathognomonic for Peters' Anomaly (Kanski, 1994; Schottenstein, 1996).

The renal histopathology is suggestive of some dysfunction in the nephron, but this needs to be tracked through different stages of development as for the

ocular pathology. In addition, assaying for urea nitrogen in serum is a useful marker for renal stress and blood samples could be taken for assay at the same time as samples are collected for histology.

Animal modelling of glaucoma

Current animal models of glaucoma can be divided into two classes: spontaneous and iatrogenic (i.e. arising from treatment of a wild-type animal). True inherited glaucomas are relatively rare in animals, but are particularly common in certain breeds of dog (cocker spaniels, Basset hounds, St Bernards and others). These have the disadvantage that the phenotypes generally take several months to manifest and such large animals are expensive to keep in any quantity (Chew, 1996). The New Zealand White rabbit also carries a semilethal autosomal recessive allele involving both ocular abnormalities (buphthalmos i.e. grossly enlarged eyes, outflow pathway defects) combined with systemic abnormalities, which give rise to high mortality in this strain (Hanna *et al.*, 1962; Chew, 1996). More recently, a genetically isolated colony of rhesus monkeys was found to have a high incidence of chronic open-angle glaucoma (Dawson *et al.*, 1993). Apart from the expense and difficulties in keeping and handling such large primates, these provide an excellent model for glaucoma in humans, since the outflow pathway is considered to be much more similar to humans than that seen in lower animals.

Albino (Al) mutant quails (*Coturnix coturnx japonica*) carry a sex-linked recessive trait leading to bupthalmos and acute angle-closure glaucoma by around 6 months of age (Takatsuji *et al.*, 1986). The phenotype bears some similarity to that seen in **Holly** mutants, with thickening of the lens, cataract formation, angle closure and anterior synechiae. After about one year, corneal oedema, optic disc cupping and retinal ganglion cell degeneration are all apparent (Takatsuji *et al.*, 1988). Thus, at least superficially, the progression of the phenotype in these birds seems to mirror that seen in **Holly** mice, apart from the timing. This strain of quail appears to have been somewhat under-utilised in glaucoma research, although there exists a body of work concerning the relationship between retinal dopamine metabolism, the day-night cycle and the progression of this mutant phenotype (Dkhissi *et al.*, 1996; Dkhissi *et al.*, 1998; Dkhissi *et al.*, 1999).

Glaucoma can be induced in most species of animal artificially by a variety of techniques, mostly relying on mechanical blockage of the outflow channels. This can be achieved by the injection of various substances into the anterior chamber, or, in a more sophisticated manner, by high energy argon laser photocoagulation of the trabecular meshwork in monkeys. Other methods include the administration of steroids to American cocker spaniels bred for susceptibility to glaucoma, and, bizarrely, exposing Japanese quail chicks (and certain other species of chickens and turkeys) to continuous daylight during rearing results in so-called light-induced avian glaucoma (LIAG) (Lauber & Cheng, 1989; Chew, 1996). LIAG is quite distinct from the angle-closure glaucoma seen in the aforementioned albino mutant quails.

Traditionally, argon laser trabeculoplasty of rhesus monkeys has been widely used to study the effects of chronic IOP elevation. However, the expense and also the dwindling supply of these animals preclude their use in large-scale studies. Also, the need for frequent IOP measurements, preferably in an unanaesthetised state (since general anaesthesia can significantly alter IOP) further weighs against the use of primates. One recently developed animal model of glaucoma involves the scarring of the outflow pathway in rats by the injection of hypertonic saline into the episcleral veins (Morrison *et al.*, 1998). This model has significant advantages of both cost and ease of handling, since rats are sufficiently docile that their IOP can be measured by the non-invasive use of a TonoPen ultrasound tonometer using topical anaesthesia. The saline regime administered was shown to regulate the duration and degree of elevation of IOP, and furthermore, the administration of glaucoma drops (β-blockers) was shown to control IOP and prevent optic nerve damage. This system represents an excellent model for chronic open-angle glaucoma, therefore, although it does require some skill and specialised equipment for the injection of saline.

Mice have been a somewhat under-exploited resource in glaucoma research until recently, since despite the vast wealth of genetics available, only one defined inherited condition leading (on occasion) to glaucoma had been described: the corneal opacity observed in some older C57BL/6 mice and discussed in more detail in the introduction to the previous chapter (Pierro &

Spiggle, 1967). However, with the superb recent characterisation of heritable open-angle glaucoma in the DBA/2J strain of mice at both the pathological and molecular level, this deficit has been amended (John *et al.*, 1998; Chang *et al.*, 1999). The advent of the DBA/2J model, coupled with the recent finding that the ultrastructure of the murine outflow pathway is more similar to that found in humans than had previously been thought, linked to the more obvious benefits of the mouse as a model animal, may lead to a rise in status of the mouse in glaucoma research (Tamm *et al.*, 1999).

In light of current progress in the use of mice as a model organism for the study of glaucoma, the **Holly** transgenic line might also prove useful in this regard.

Anti-glaucoma drug therapy

Another interesting possibility is whether the progression of the phenotype, particularly the retinal degeneration, could be delayed using anti-glaucomic drugs. This depends upon the phenotype showing a reproducible, consistent timecourse, which could be determined by referring to the temporal series of eye sections mentioned above. It will be particularly important to study the retinal degeneration during the first two to three months, since most retinas examined after this point showed very severe degeneration, whereas the earlier samples (18 day) showed little or no change.

Most anti-glaucoma drug therapy centres around lowering IOP, either by lowering the induction of aqueous (β-blockers and carbonic anhydrase inhibitors) or by increasing the outflow capacity (miotics) or both (sympathomimetics such as adrenaline) (Kanski, 1994). These drugs are generally effective in treating open-angle glaucoma.

Closed-angle glaucoma is a medical emergency requiring surgery, and given the severe nature of the angle-closure glaucoma in **Holly** mice, it seems unlikely that simply lowering IOP by administration of drug therapy would significantly retard the progression of the phenotype. However, recent work has shown that α-adrenergic agonists such as clonidine, which are routinely used to lower IOP might have a protective effect against the secondary neurodegeneration seen in glaucomic retinas (Yoles *et al.*, 1999). This secondary degeneration

continues, with consequent further loss of vision, in glaucomic patients whose IOP has been returned to safe levels. It is believed to be caused by the release of cytotoxic substances following the primary insult to ganglion cells under conditions of raised IOP, and this parallels the situation seen in traumatic injuries to the CNS, where neurons adjacent to the site of trauma are seen to degenerate for some time afterwards. The α2-adrenoreceptor agonists clonidine and dexmedetomidine are known to ameliorate such secondary neurodegeneration following cerebral ischaemia (i.e. strokes), and when tested in a rat model of optic nerve degeneration (by unilateral crush injury to the optic nerve) were found to exhibit the same neuroprotective effect.

In all likelihood, the crush injury inflicted in the study by Yoles *et al.* does not accurately reflect the neurodegenerative syndrome found in glaucoma, and it remains an open question as to whether such drugs might retard the progression of retinal degeneration in a glaucomic eye. If **Holly** mutant retinas degenerate in a reproducible fashion, this could provide a useful model system for testing such drugs.

In the *Al* mutant quail model of glaucoma, it is interesting to note that the presence of high glutamate levels in the vitreous correlates with the presence of TUNEL-positive apoptotic retinal ganglion cells (Dkhissi *et al.*, 1999). Glutamate is considered to be an excitotoxic amino acid with respect to nerve cells, and this may underly the observation that even ganglion cells dying by apoptosis in glaucomic eyes cause secondary death of nearby cells. It might therefore prove interesting to examine the apoptotic status of the retinal layers in **Holly** mutants, and to test the vitreous for the presence of glutamate.

Conclusion

In summary, **Holly** homozygous transgenics develop closed-angle glaucoma as a probable consequence of the transgene integrating close to the *Col9a1* locus and disrupting expression of this gene in a tissue-specific manner. Although a number of questions remain to be answered, particularly with respect to the early ontogeny and the reproducibility of progression of the mutant phenotype, the **Holly** line is potentially an important and useful model of angle-closure glaucoma.

Once the precise nature of the pathology arising in **Holly** mutants has been established, it may well prove worthwhile to try and correlate this with human congenital glaucomas, such as Peters' Anomaly, and hence to test appropriate patients for mutations in COL9A1. Thus **Holly** may also shed light on the molecular mechanisms underpinning certain rare human genetic diseases.

CHAPTER FOURTEEN:
FINAL CONCLUSIONS

Overall, the screen of some 55 transgenic lines represents one of the largest screens of this nature performed so far, and has to date revealed five bona fide transgenic insertional mutations representing a hit rate of ~10%, in accord with previously published figures (Meisler, 1992). The mapping strategy employed, comprising FISH, followed by confirmation and fine mapping using linkage to a few PCR-based microsatellite markers is proposed as a good strategy for small laboratories unequipped for a full-genome linkage scan. This is made possible by virtue of the transgene's nature as a unique, multicopy sequence-tagged site at a locus closely linked to the mutant phenotype.

However, of the two mutations selected for characterisation in this study, both turned out, in all likelihood, to be mutations in previously characterised genes with existing mutant alleles.

In the case of *Sox10*, the **Harry** mutant phenotype adds little that was not already known about the role of this transcription factor in a subset of neural crest cells during development. On the other hand, the transgene provides a useful tag for studying the effects of the mutant allele in wild-type tissue, and vice-versa. The recessive nature of this mutation makes it easier to maintain stocks as compared to $Sox10^{Dom}$, particularly on backgrounds where $Sox10^{Dom}$ causes lethality before breeding age. In addition, the nature of this mutation is such that further investigation could reveal upstream regulatory elements of *Sox10*. Finally, the more severe and varied nature of the coat colour aspect of the phenotype compared to existing alleles may allow some outstanding questions about the nature of melanocyte development to be tackled.

In the case of *Col9a1*, the investigation of the **Holly** phenotype has raised as many questions as it has answered. However, it is clear that, regardless of the exact nature of the mutation, this line represents the only known model of acute closed-angle glaucoma in a genetically-well defined system, and as such, may be a useful resource for future research. In addition, given the lack of disruption to the

coding region of *Col9a1*, this mutation may also help define regulatory elements of this gene.

APPENDIX A: CHI-SQUARED ANALYSIS

The formula used to perform χ^2 analysis to determine the likelihood of linkage between the transgene and a recessive mutant trait was taken from Silver (1995). All four classes must have expected values greater than 5, permitting the use of the formula:

$$\chi^2 = \frac{n(|ad - bc| - \frac{1}{2}n)^2}{(a+b)(c+d)(b+d)(a+c)}$$

Where *a,b,c* and *d* are the four observed values in the table, *n* is the total number of animals and $|ad\text{-}bc|$ means the absolute, i.e. positive, value of the difference between *ad* and *bc*. This formula has the advantage that it contains a correction for continuity (Yates correction) without which 2 x 2 tables can give values of χ^2 which are too large (Bailey, 1981).

APPPENDIX B: CONFIDENCE LIMITS AND MEDIAN ESTIMATES OF LINKAGE DISTANCE

Confidence limits and median estimates of linkage distance in the special case of no recombinants were derived from the tables in Appendix D of Silver (1995). Additional calculation of other confidence limits and linkage distances was performed using Genelink V2.0 software (Xavier Montagutelli, 1998) which was downloaded from:
ftp://ftp.pasteur.fr/pub/GenSoft/MSWindows/linkage_and_mapping/GeneLink/

BIBLIOGRAPHY

Abdelhak, S., Kalatzis, V., Heilig, R. *et al.* (1997a). Clustering of mutations responsible for branchio-oto-renal (BOR) syndrome in the *eyes absent* homologous region (eyaHR) of EYA1. *Human Molecular Genetics* **6**: 2247-2255.

Abdelhak, S., Kalatzis, V., Heilig, R. *et al.* (1997b). A human homologue of the *Drosophila eyes absent* gene underlies Branchio-Oto-Renal (BOR) syndrome and identifies a novel gene family. *Nature Genetics* **15**: 157-164.

Abe, N., Yoshioka, H., Inoue, H. *et al.* (1994). The complete primary structure of the long form of mouse alpha-1(IX) collagen chain and its expression during limb development. *Biochimica Et Biophysica Acta - Protein Structure and Molecular Enzymology* **1204**: 61-67.

Adam, M.F., Belmouden, A., Binisti, P. *et al.* (1997). Recurrent mutations in a single exon encoding the evolutionarily conserved olfactomedin-homology domain of TIGR in familial open-angle glaucoma. *Human Molecular Genetics* **6**: 2091-2097.

Allan, I.J. and Newgreen, D.F. (1980). The origin and differentiation of enteric neurons of the intestine of the fowl embryo. *Am. J. Anat.* **157**: 137-154.

Amaya, E., Offield, M.F. and Grainger, R.M. (1998). Frog genetics: *Xenopus tropicalis* jumps into the future. *Trends in Genetics* **14**: 253-255.

Anderson, D.J. and Jan, Y.N. (1997). The determination of the neuronal phenotype. In W. M. Cowan, T. M. Jessell, & S. L. Zipursky (Eds.), Molecular and cellular approaches to neural development Oxford: Oxford University Press.

Anderson, D.R. (1972). Pathology of the glaucomas. *British Journal of Opthalmology* **56**: 146.

Andrew, A. (1974). Further evidence that enterochromaffin cells are not derived from the neural crest. *J. Embryol. Exp. Morphol.* **31**: 589-598.

Angrist, M., Bolk, S., Halushka, M. *et al.* (1996). Germline mutations in glial cell line-derived neurotrophic factor (GDNF) and RET in a Hirschsprung disease patient. *Nature Genetics* **14**: 341-4.

Aparicio, S. (1998). Exploding vertebrate genomes. *Nature Genetics* **18**: 301-303.

Asher, J.H., Harrison, R.W., Morell, R. *et al.* (1996). Effects of *Pax3* modifier genes on craniofacial morphology, pigmentation, and viability: A murine model of Waardenburg syndrome variation. *Genomics* **34**: 285-298.

Aubin-Houzelstein, G., Bernex, F., Elbaz, C. *et al.* (1998). Survival of patchwork melanoblasts is dependent upon their number in the hair follicle at the end of embryogenesis. *Developmental Biology* **198**: 266-276.

Azuma, N., Hirakiyama, A., Asaka, A. *et al.* (1999). Missense mutations of a human homologue of the Drosophila eyes absent gene (EYA1) in developmental eye anomalies. *Investigative Ophthalmology & Visual Science* **40**: 59334.

Bailey, N.T.J. (1981). Statistical Methods in Biology (2nd ed.). Hodder & Stoughton.

Baker, R.K., Haendel, M.A., Swanson, B.J. *et al.* (1997). *in vitro* preselection of gene-trapped embryonic stem cell clones for characterising novel developmentally regulated genes in the mouse. *Dev. Biol.* **185**: 201-214.

Bancroft, J.D. and Stevens, A. (1977). Theory and Practice of Histological Techniques. Edinburgh: Churchill Livingstone.

Barres, B.A. (1997). Neuron-glial interactions. In W. M. Cowan, T. M. Jessell, & S. L. Zipursky (Eds.), Molecular and cellular approaches to neural development Oxford: Oxford University Press.

Battey, J., Jordan, E., Cox, D. *et al.* (1999). An action plan for mouse genomics. *Nature Genetics* **21**: 73-75.

Baynash, A.G., Hosoda, K., Giaid, A. *et al.* (1994). Interaction of endothelin-3 with endothelin-B receptor is essential for development of epidermal melanocytes and enteric neurons. *Cell* **79**: 1277-1285.

Beddington, R.S.P., Morgernstern, J., Land, H. *et al.* (1989). An *in situ* transgenic enzyme marker for the midgestation mouse embryo and the visualization of inner cell mass clones during early organogenesis. *Development* **106**: 37.

Bermingham, J.R., Scherer, S.S., Oconnell, S. *et al.* (1996). Tst-1/Oct-6/SCIP regulates a unique step in peripheral myelination and is required for normal respiration. *Genes & Development* **10**: 1751-1762.

Bernex, F., DeSepulveda, P., Kress, C. *et al.* (1996). Spatial and temporal patterns of *c-kit* expressing cells in *W-lacZ/+* and *W-lacZ/W-lacZ* mouse embryos. *Development* **122**: 3023-3033.

Bi, W.M., Deng, J.M., Zhang, Z.P. *et al.* (1999). Sox9 is required for cartilage formation. *Nature Genetics* **22**: 85-89.

Bishop, J.O. (1996). Chromosomal insertion of foreign DNA. *Reproduction Nutrition Development* **36**: 607-618.

Boissy, R.E. and Nordlund, J.J. (1997). Molecular basis of congenital hypopigmentary disorders in humans: A review. *Pigment Cell Research* **10**: 12-24.

Bolande, R. (1975). Hirschsprung's disease, aganglionic or hypoganglionic megacolon. Animal model: aganglionic megacolon in piebald and spotted mutant mouse strains. *Am J Pathol* **79**: 189-92.

Bondurand, N., Kobetz, A., Pingault, V. *et al.* (1998). Expression of the SOX10 gene during human development. *FEBS Lett* **432**: 168-72.

Bondurand, N., Kuhlbrodt, K., Pingault, V. *et al.* (1999). A molecular analysis of the Yemenite deaf-blind hypopigmentation syndrome: SOX10 dysfunction causes different neurocristopathies. *Hum Mol Genet* **8**: 1785-1789.

Bonini, N.M., Bui, Q.T., GrayBoard, G.L. *et al.* (1997). The Drosophila eyes absent gene directs ectopic eye formation in a pathway conserved between flies and vertebrates. *Development* **124**: 4819-4826.

Bonini, N.M., Leiserson, W.M. and Benzer, S. (1998). Multiple roles of the eyes absent gene in Drosophila. *Developmental Biology* **196**: 42-57.

Borsani, G., DeGrandi, A., Brown, A. *et al.* (1998). Identification and characterization of EYA4, a novel mammalian homolog of the Drosophila melanogaster eyes absent gene. *European Journal of Human Genetics* **6**: L31.

Bradley, A., Evans, M., Kaufman, M.H. *et al.* (1984). Formation of germ-line chimeras from embryo-derived teratocarcinoma cell lines. *Nature* **309**: 255-256.

Bradley, A., Zheng, B. and Liu, P. (1998). Thirteen years of manipulating the mouse genome: a personal history. *Int. J. Dev. Biol.* **42**: 943-950.

Brann, L., Furtado, D., Migliazzo, C. *et al.* (1977). Secondary effects of aganglionosis in the piebald-lethal mouse model of Hirschsprung's disease. *Lab Anim Sci* **27**: 946-54.

Briggs, M.D., Hoffman, S.N.G., King, L.M. *et al.* (1995). Pseudoachondroplasia and multiple epiphyseal dysplasia due to mutations in the cartilage oligomeric matrix protein gene. *Nature Genet.* **10**: 330-336.

Brinster, R.L. (1974). The effect of cells transferred into the mouse blastocyst on subsequent development. *J. Exp. Med* **140**: 1049-1056.

Brinster, R.L., Chen, H.Y., Trumbauer, M.E. *et al.* (1985). Factors affecting the efficiency of introducing foreign DNA into mice by microinjecting eggs. *Proceedings Of the National Academy Of Sciences Of the United States Of America* **82**: 4438-4442.

Brunner, E., Peter, O., Schweizer, L. *et al.* (1997). Pangolin encodes a LEF-1 homologue that acts downstream of Armadillo to transduce the Wingless signal in Drosophila. *Nature* **385**: 829-833.

Bruzzone, R., White, T.W. and Paul, D.L. (1996). Connections with connexins - the molecular basis of direct intercellular signalling. *European Journal of Biochemistry* **238**: 1-27.

Burns, A.J. and LeDouarin, N.M. (1998). The sacral neural crest contributes neurons and glia to the post-umbilical gut: spatiotemporal analysis of the development of the enteric nervous system. *Development* **125**: 4335-4347.

Bush, T.G., Savidge, T.C., Freeman, T.C. *et al.* (1998). Fulminant jejuno-ileitis following ablation of enteric glia in adult transgenic mice. *Cell* **93**: 189-201.

Caniano, D., Teitelbaum, D., Qualman, S. *et al.* (1989). The piebald-lethal murine strain: investigation of the cause of early death. *J Pediatr Surg* **24**: 906-10.

Capecchi, M.R. (1989). Altering the genome by homologous recombination. *Science* **244**: 1288-1292.

Caricasole, A. and Ward, A. (1993). A luciferase reporter vector with blue-white selection for rapid subcloning and mutational analysis of eukaryotic promoters. *Gene* **124**: 139-140.

Carlson, G.A., Banks, S., Lund, D. *et al.* (1997). Failure to transmit disease from gray tremor mutant mice. *Journal Of Virology* **71**: 2342-2345.

Carninci, P., Nishiyama, Y., Westover, A. *et al.* (1998). Thermostabilization and thermoactivation of thermolabile enzymes by trehalose and its application for the synthesis of full length cDNA. *Proceedings of the National Academy of Sciences of the United States of America* **95**: 520-524.

Castrop, J., Vannorren, K. and Clevers, H. (1992). A gene family of HMG-box transcription factors with homology to TCF-1. *Nucleic Acids Research* **20**: 611.

Cavallo, R.A., Cox, R.T., Moline, M.M. *et al.* (1998). Drosophila TCF and Groucho interact to repress Wingless signalling activity. *Nature* **395**: 604-608.

Chang, B., Smith, R.S., Hawes, N.L. *et al.* (1999). Interacting loci cause severe iris atrophy and glaucom in DBA/2J mice. *Nature Genetics* **21**: 405-409.

Chen, C.M., Choo, K.B. and Cheng, W.T. (1995). Frequent deletions and sequence aberrations at the transgene junctions of transgenic mice carrying the papillomavirus regulatory and the SV40 TAg gene sequences. *Transgenic Res* **4**: 52-9.

Cheng, J., Daimaru, L., Fennie, C. *et al.* (1996). A novel protein tyrosine phosphatase expressed in lin(lo)CD34(hi)Sca(hi) hematopoietic progenitor cells. *Blood* **88**: 1156-67.

Chew, S.J. (1996). Animal models of glaucoma. In R. Ritch, M. B. Shields, & T. Krupin (Eds.), The Glaucomas (pp. 55-70). St Louis: Mosby.

Cheyette, B.N.R., Green , P.J., Martin, K. *et al.* (1994). The Drosophila *sine oculis* locus encodes a homeodomain-containing protein required for the development of the entire visual system. *Neuron* **12**: 977-996.

Chomczynski, P. and Sacchi, N. (1987). Single-step method of RNA isolation by acid guanidinium thiocyanate phenol chloroform extraction. *Analytical Biochemistry* **162**: 156-159.

Chung, E.H., Bukusoglu, G. and Zieske, J.D. (1992). Localization of corneal epithelial stem-cells in the developing rat. *Investigative Ophthalmology & Visual Science* **33**: 2199-2206.

Church, G.M. and Gilbert, W. (1984). Genomic sequencing. *Proceedings of the National Academy of Sciences of the United States of America-Biological Sciences* **81**: 1991-1995.

Churchill, A.J., Booth, A.P., Anwar, R. *et al.* (1998). PAX 6 is normal in most cases of Peters' anomaly. *Eye* **12**: 299-303.

Clozel, M. and Gray, G. (1995). Are there different ETB receptors mediating constriction and relaxation? *J Cardiovasc Pharmacol* **26 Suppl 3**: S262-4.

Collick, A., Drew, J., Penberth, J. *et al.* (1996). Instability of long inverted repeats within mouse transgenes. *EMBO J* **15**: 1163-71.

Collins, F.S., Patrinos, A., Jordan, E. *et al.* (1998). New goals for the US Human Genome Project: 1998-2003. *Science* **282**: 682-689.

Colville, D.J. and Savige, J. (1997). Alport syndrome. A review of the ocular manifestations. *Ophthalmic Genet* **18**: 161-73.

Conway, S.J., Henderson, D.J. and Copp, A.J. (1997a). *Pax3* is required for cardiac neural crest migration in the mouse: Evidence from the splotch (*Sp*(2H)) mutant. *Development* **124**: 505-514.

Conway, S.J., Henderson, D.J., Kirby, M.L. *et al.* (1997b). Development of a lethal congenital heart defect in the splotch (Pax3) mutant mouse. *Cardiovascular Research* **36**: 163-173.

Copeland, N.G., Jenkins, N.A., Gilbert, D.J. *et al.* (1993). A genetic linkage map of the mouse: current applications and future prospects. *Science* **262**: 57-66.

Copp, A.J. (1994). Genetic models of mammalian neural tube defects. *Ciba Foundation Symposia* **181**: 118-134.

Copp, A.J. (1995). Death before birth: clues from gene knockouts and mutations. *Trends in Genetics* **11**: 87-93.

Covarrubias, L., Nishida, Y. and Mintz, B. (1986). Early postimplantation embryo lethality due to DNA rearrangements in a transgenic mouse strain. *Proceedings Of the National Academy Of Sciences Of the United States Of America* **83**: 6020-6024.

Culling, C.F.A. (1974). Handbook of Histopathological and Histochemical Techniques, third edition. Butterworth & Co. (Publishers) Ltd.

Cuthbertson, R.A., Tomarev, S.I. and Piatigorsky, J. (1992). Taxon-specific recruitment of enzymes as major soluble proteins in the corneal epithelium of three mammals, chicken, and squid. *Proceedings Of The National Academy Of Sciences Of The United States Of America* **89**: 4004-8.

Dawson, W.W., Brooks, D.E., Hope, G.M. *et al.* (1993). Primary open-angle glaucoma in the rhesus monkey. *British Journal of Ophthalmology* **77**: 302-310.

Deol, M.S. (1967). The neural crest and the acoustic ganglion. *J. Embryol. Exp. Morphol.* **17**: 535-541.

Depierreux, C., Christians, E., Marchandise, J. *et al.* (1997). Characterisation of a recessive insertional mutation implying a late embryonic lethality. In A. Copp & D. A. Stephenson (Ed.), Proceedings of the 8th Mammalian Genetics and Development Workshop., *Genetical Research* **72** (pp. 64). London.

Dickens, C.J. and Hoskins, H.D. (1996). Diagnosis and treatment of congenital glaucoma. In R. Ritch, M. B. Shields, & T. Krupin (Eds.), The Glaucomas (pp. 739-749). St Louis: Mosby.

Dietrich, W., Katz, H., Lincoln, S.E. *et al.* (1992). A genetic map of the mouse suitable for typing intraspecific crosses. *Genetics* **131**: 423-447.

Dietrich, W.F., Miller, J.C., Steen, R.G. *et al.* (1994). A genetic map of the mouse with 4,006 simple sequence length polymorphisms. *Nat Genet* **7**: 220-45.

Dietrich, W.F., Miller, J., Steen, R. *et al.* (1996). A comprehensive genetic map of the mouse genome. *Nature* **380**: 149-152.

Dkhissi, O., Chanut, E., VersauxBotteri, C. *et al.* (1996). Changes in retinal dopaminergic cells and dopamine rhythmic metabolism during the development of a glaucoma-like disorder Quails. *Investigative Ophthalmology & Visual Science* **37**: 2335-2344.

Dkhissi, O., Chanut, E., VersauxBotteri, C. *et al.* (1998). Day and night dysfunction in intraretinal melatonin and related indoleamine metabolism, correlated with the development of glaucoma- like disorder in an avian model. *Journal of Neuroendocrinology* **10**: 863-869.

Dkhissi, O., Chanut, E., Wasowicz, M. *et al.* (1999). Retinal TUNEL-positive cells and high glutamate levels in vitreous humor of mutant quail with a glaucoma-like disorder. *Investigative Ophthalmology & Visual Science* **40**: 990-995.

Doray, B., Salomon, R., Amiel, J. *et al.* (1998). Mutation of the RET ligand, neurturin, supports multigenic inheritance in Hirschprung disease. *Human Molecular Genetics* **7**: 1449-1452.

Dove, W. and Cox, D. (1998). Mouse Genomics and Genetics Working Group at NIH: Priority setting for mouse genomics and genetics resources:. *http://www.nih.gov/welcome/director/reports/mgenome.htm.*

Dumas, R., Uziel, A., Baldet, P. *et al.* (1982). Glomerular lesions in the branchio-oto-renal (BOR) syndrome. *Int. J. Paed. Nephrol.* **3**: 67-70.

Duncan, M.K., Kos, L., Jenkins, N.A. *et al.* (1997). Eyes absent: A gene family found in several metazoan phyla. *Mammalian Genome* **8**: 479-485.

Dunn, K.J., Mok, J., Southard-Smith, E.M. *et al.* (1999). Analysis of SOX10 function using retroviral infection of mammalian neural crest cells. *Developmental Biology* **210**: 205.

Durbec, P.L., LarssonBlomberg, L.B., Schuchardt, A. *et al.* (1996). Common origin and developmental dependence on c-ret of subsets of enteric and sympathetic neuroblasts. *Development* **122**: 349-358.

Dvorak, A.M., Onderdonk, A.B., McLeod, R.S. *et al.* (1993). Axonal necrosis of enteric autonomic nerves in continent ileal pouches. Possible implications for pathogenesis of Crohn's disease. *Annals Of Surgery* **217**

El Shabrawi, Y., Kublin, C.L. and Cintron, C. (1998). mRNA levels of alpha 1(VI) collagen, alpha 1(XII) collagen, and beta Ig in rabbit cornea during normal development and healing. *Investigative Ophthalmology & Visual Science* **39**: 36-44.

Erickson, C.A., Duong, T.D. and Tosney, K.W. (1992). Descriptive and experimental analysis of the dispersion of neural crest cells along the dorsolateral path and their entry into ectoderm in the chick-embryo. *Developmental Biology* **151**: 251-272.

Evans, E.P. (1987). Karyotyping and sexing of gametes, embryos and fetuses and *in situ* hybridization to chromosomes. In M. Monk (Eds.), Mammalian Development: A Practical Approach (pp. 93-114). Oxford University Press.

Evans, E.P. (1994). Karyotyping mouse cells. In B. Hogan, R. Beddington, F. Costantini, & E. Lacy (Eds.), Manipulating the Mouse Embryo: a laboratory manual (pp. 311-318). Cold Spring Harbour Laboratory Press.

Evans, M.J., Carlton, M.B.L. and Russ, A.P. (1997). Gene trapping and functional genomics. *Trends in Genetics* **13**: 370-374.

Evans, M.J. and Kaufman, M.H. (1981). Establishment in culture of pluripotential cells from mouse embryos. *Nature* **292**: 154-156.

Fassler, R., Schnegelsberg, P.N.J., Dausman, J. *et al.* (1994). Mice lacking alpha(IX) collagen develop noninflammatory degenerative joint disease. *Proceedings of the National Academy of Sciences of the United States of America* **91**: 5070-5074.

Felbor, U., Gehrig, A., Sauer, C.G. *et al.* (1998). Genomic organization and chromosomal localization of the interphotoreceptor matrix proteoglycan-1 (IMPG1) gene: a candidate for 6q-linked retinopathies. *Cytogenetics and Cell Genetics* **81**: 12-17.

Ferris, S.D., Sage, R.D. and Wilson, A.C. (1982). Evidence from mtDNA sequences that common laboratory inbred strains of mice are descended from a single female. *Nature* **295**: 163-165.

Fielding, D.W. and Fryer, A.E. (1992). Recurrence of orbital cysts in the branchiooculofacial syndrome. *Journal of Medical Genetics* **29**: 430-431.

Fihn, B.M., Olsson, E. and Jodal, M. (1997). The enteric nervous system (ENS) is involved in the regulation of the epithelial permeability in the jejunum of the rat, in vivo. *Gastroenterology* **112**: A362-A362.

Fiore, C., Santoni, G., Reggiani, F.M. et al. (1985). Familial nephropathy with retinitis pigmentosa and closed-angle glaucoma. Ophthalmic Paediatr Genet 5: 39-49.

Fish, L.A., Friedman, D.I. and Sadun, A.A. (1990). Progressive cranial polyneuropathy caused by primary central nervous system melanoma. *Journal Of Clinical Neuro-Ophthalmology* **10**: 41-4.

Fitch, J., Fini, M.E., Beebe, D.C. *et al.* (1998). Collagen type IX and developmentally regulated swelling of the avian primary corneal stroma. *Developmental Dynamics* **212**: 27-37.

Flaherty, L. (1981). Congenic strains. In H. L. Foster, J. D. Small, & J. G. Fox (Eds.), The Mouse in Biomedical Research Volume I: History, genetics and wild mice. New York: Academic Press.

Flaherty, L. and Herron, B. (1998). The new kid on the block - a whole genome mouse radiation hybrid panel. *Mammalian Genome* **9**: 417-418.

Font, R.L. and Brownstein, S. (1974). A light and electron microscopic study of anterior capsular cataracts. *Am. J. Opthalmol.* **78**: 972-984.

Franke, U. and Oliver, N. (1978). Quantitative analysis of high-resolution trypsin-Giemsa bands on human prometaphase chromosomes. *Hum. Genet.* **45**: 137-165.

Freeman, T.C., A.K., D., E.A., C. *et al.* (1998). Expression Mapping of Mouse Genes. *Direct submission to Mouse Genome Database, http://www.informatics.jax.org.*

Friedrich, G. and Soriano, P. (1991). Promoter traps in embryonic stem cells - a genetic screen to identify and mutate developmental genes in mice. *Genes & Development* **5**: 1513-1523.

Fruttiger, M., Karlsson, L., Hall, A.C. *et al.* (1999). Defective oligodendrocyte development and severe hypomyelinaton in *Pdgf-A* knockout mice. *Development* **126**: 457-467.

Fujimoto, T. (1988). Natural history and pathophysiology of enterocolitis in the piebald lethal mouse model of Hirschsprung's disease. *J Pediatr Surg* **23**: 237-42.

Gaiano, N., Allende, M., Amsterdam, A. *et al.* (1996). Highly efficient germ-line transmission of proviral insertions in zebrafish. *Proc Natl Acad Sci U S A* **93**: 7777-82.

Galbraith, D.B. and Arceci, R.J. (1974). Melanocyte populations of yellow and black hair bulbs in the mouse. *J Hered* **65**: 381-2.

Gao, Y. and Spray, D. (1998). Structural changes in lenses of mice lacking the gap junction protein connexin43. *Invest Ophthalmol Vis Sci* **39**: 1198-209.

Gardner, R.L. and Brook, F.A. (1997). Reflections on the biology of embryonic stem (ES) cells. *International Journal of Developmental Biology* **41**: 235-243.

Gehrig, A., Felbor, U., Kelsell, R.E. *et al.* (1998). Assessment of the interphotoreceptor matrix proteoglycan-1 (IMPG1) gene localised to 6q13-q15 in autosomal dominant Stargardt-like disease (ADSTGD), progressive bifocal chorioretinal atrophy (PBCRA), and North Carolina macular dystrophy (MCDR1). *Journal Of Medical Genetics* **35**: 641-645.

Geissler, E.N., Ryan, M.A. and Housman, D.E. (1988). The dominant-white spotting (*w*) locus of the mouse encodes the *c-kit* proto-oncogene. *Cell* **55**: 185-192.

Gerecke, D.R., Olson, P.F., Koch, M. *et al.* (1997). Complete primary structure of two splice variants of collagen XII, and assignment of alpha1(XII) collagen (COL12A1), alpha1(IX) collagen (COL9A1) and alpha1(XIX) collagen (COL19A1) to human chromosome 6q12-q13. *Genomics* **41**: 236-242.

Gershon, M.D., Chalazonitis, A. and Rothman, T.P. (1993). From neural crest to bowel - development of the enteric nervous- system. *Journal Of Neurobiology* **24**: 199-214.

Gershon, M.D. and Rothman, T.P. (1991). Enteric glia. *Glia* **4**: 195-204.

Gershon, M.D., Teitelman, G. and Rothman, T.P. (1981). Development of enteric neurons from non-recognisable precursor cells. In K. Elliott & G. Lawrenson (Eds.), Ciba Foundation Symposium 83: Development of the autonomic nervous system (pp. 51-61). Bath: Pitman Medical.

Geyer, D.D., Church, R.L., Steele, E.C.J. *et al.* (1997). Regional mapping of the human MP70 (Cx50; connexin 50) gene by fluorescence in situ hybridization to 1q21.1. *Mol. Vis.* **3**: 13.

Giller, T., Breu, V., Valdenaire, O. *et al.* (1997). Absence of ET(B)-mediated contraction in Piebald-lethal mice. *Life Sci* **61**: 255-63.

Gong, X.H., Klier, G., Huang, Q.L. *et al.* (1997). Connexin alpha(3) gene disruption in the lens. A mouse model for nuclear cataracts. *Investigative Ophthalmology & Visual Science* **38**: 4353-4353.

Gordon, J.W., Scangos, G.A., Plotkin, D.J. *et al.* (1980). Genetic transformation of mouse embryos by micro-injection of purified DNA. *Proceedings Of the National Academy Of Sciences Of the United States Of America* **77**: 7380-7384.

Gorin, G. (1977). Clinical Glaucoma. New York: Marcel Dekker, Inc.

Gossler, A., Joyner, A.L., Rossant, J. *et al.* (1989). Mouse embryonic stem cells and reporter constructs to detect developmentally regulated genes. *Science* **244**: 463-465.

Gridley, T., Soriano, P. and Jaenisch, R. (1987). Insertional mutagenesis in mice. *Trends In Genetics* **3**: 162-166.

Hagg, R., Hedbom, E., Mollers, U. *et al.* (1997). Absence of the alpha 1(IX) chain leads to a functional knock-out of the entire collagen IX protein in mice. *Journal of Biological Chemistry* **272**: 20650-20654.

Halder, G., Callaerts, P. and Gehring, W.J. (1995). New perspectives on eye evolution. *Current Opinion in Genetics & Development* **5**: 602-609.

Hales, A.M., Chamberlain, C.G. and McAvoy, J.W. (1995). Cataract induction in lenses cultured with transforming growth factor-β. *Investigative Ophthalmology & Visual Science* **36**: 1709-1713.

Hanna, B.L., Sawin, P.B. and Sheppard, L.B. (1962). Recessive bupthalmos in the rabbit. *Genetics* **47**: 519-532.

Harper, M.E., Ullrich, A. and Saunders, G., F (1981). Localisation of the human insulin gene to the distal end of the short arm of chromosome 11. *Proceedings of the National Academy of Sciences, USA* **78**: 4458-4460.

Hatano, M., Aoki, T., Dezawa, M. *et al.* (1997). A novel pathogenesis of megacolon in Ncx/Hox11L.1 deficient mice. *Journal of Clinical Investigation* **100**: 795-801.

Hayashizaki, Y., Okazaki, Y., Kawai, J. *et al.* (1998). Full-length mouse cDNA analysis by automated fluorescent 384 capillary sequencer system (RISA: Riken Integrate Sequence Analysis system). In 12th International Mouse Genome Confererence, . Garmisch-Partenkirchen, Bavaria.

He, X. and Rosenfeld, M.G. (1991). Mechanisms of complex transcriptional regulation - implications for brain-development. *Neuron* **7**: 183-196.

Healy, C., Uwanogho, D. and Sharpe, P.T. (1999). Regulation and role of *Sox9* in cartilage formation. *Developmental Dynamics* **215**: 69-78.

Hein, H.F. and Maltzman, B. (1975). Long-standing anterior dislocation of the crystalline lens. *Annals Of Ophthalmology* **7**: 66-8.

Henderson, D.J., YbotGonzalez, P. and Copp, A.J. (1997). Over-expression of the chondroitin sulphate proteoglycan versican is associated with defective neural crest migration in the Pax3 mutant mouse (splotch). *Mechanisms of Development* **69**: 39-51.

Heng, H.H.Q., Spyropoulos, B. and Moens, P.B. (1997). FISH technology in chromosome and genome research. *Bioessays* **19**: 75-84.

Hennekam, R.C. and Gorlin, R.J. (1996). Confirmation of the Yemenite (Warburg) deaf-blind hypopigmentation syndrome. *Am. J. Hum. Genet.* **65**: 146-148.

Herbarth, B., Pingault, V., Bondurand, N. *et al.* (1998). Mutation of the *Sry*-related *Sox10* gene in Dominant megacolon, a mouse model for human Hirschsprung disease. *Proc Natl Acad Sci U S A* **95**: 5161-5.

Hicks, G.G., Shi, E., Li, X. *et al.* (1997). Functional genomics in mice by tagged sequence mutagenesis. *Nature Genetics* **16**: 338-344.

Hiraoka, Y., Ogawa, M., Sakai, Y. *et al.* (1998). The mouse Sox5 gene encodes a protein containing the leucine zipper and the Q box. *Biochimica Et Biophysica Acta-Gene Structure and Expression* **1399**: 40-46.

Hitotsumachi, S., Carpenter, D.A. and Russell, W.L. (1985). Dose-repetition increases the mutagenic effectiveness of n-ethyl-n-nitrosourea in mouse spermatogonia. *Proceedings of the National Academy of Sciences of the United States of America* **82**: 6619-6621.

Hoffman, P.M., Rohwer, R.G., Macauley, C. *et al.* (1987). Transmission in NFS/N mice of the heritable spongiform encephalopathy associated with the gray tremor mutation. *Proceedings Of the National Academy Of Sciences Of the United States Of America* **84**: 3866-3870.

Hofstra, R., Osinga, J., Tan-Sindhunata, G. *et al.* (1996). A homozygous mutation in the endothelin-3 gene associated with a combined Waardenburg type

2 and Hirschsprung phenotype (Shah-Waardenburg syndrome). *Nature Genetics* **12**: 445-7.

Hofstra, R.M.W., Valdenaire, O., Arch, E. *et al.* (1998). Loss of function mutation in the Endothelin Converting Enzyme 1 (ECE1) in a patient with Hirschsprung disease and cardiac defects. *European Journal of Human Genetics* 6: C403.

Hogan, B., Beddington, R., Costantini, F. *et al.* (1994). Manipulating the Mouse Embryo: a laboratory manual (2nd ed.). Cold Spring Harbour Laboratory Press.

Hong, H., Kohli, K., Trivedi, A. *et al.* (1996). GRIP1, a novel mouse protein that serves as a transcriptional coactivator in yeast for the hormone binding domains of steroid receptors. *Proceedings of the National Academy of Sciences of the United States of America* **93**: 4948-4952.

Hosoda, K., Hammer, R.E., Richardson, J.A. *et al.* (1994). Targeted and natural (piebald-lethal) mutations of endothelin-B receptor gene produce megacolon associated with spotted coat color in mice. *Cell* **79**: 1267-1276.

Inoguchi, K., Yoshioka, H., Khaleduzzaman, M. *et al.* (1995). The mRNA for alpha-1(XIX)-collagen chain, a new member of FACITs, contains a long unusual 3'-untranslated region and displays many unique splicing variants. *Journal of Biochemistry* **117**: 137-146.

Inoue, K., Tanabe, Y. and Lupski, J.R. (1999). Myelin deficiencies in both the central and the peripheral nervous systems associated with a SOX10 mutation. *Ann Neurol* **46**: 313-8.

Irwin, M.H. and Mayne, R. (1986). Use of monoclonal antibodies to locate the chondroitin sulfate chain(s) in type-IX collagen. *Journal Of Biological Chemistry* **261**: 6281-6283.

Jacobs-Cohen, R.J., Payette, R.F., Gershon, M.D. *et al.* (1987). Inability of neural crest cells to colonize the presumptive aganglionic bowel of *ls/ls* mutant mice: requirement for a permissive microenvironment. *Journal of Comparative Neurology* **255**: 425-438.

Jaegle, M., Mandemakers, W., Broos, L. *et al.* (1996). The POU factor Oct-6 and Schwann cell differentiation. *Science* **273**: 507-510.

Jaenisch, R. (1988). Transgenic animals. *Science* **240**: 1468-1474.

Jaenisch, R. and Mintz, B. (1974). Simian virus 40 DNA sequences in DNA of healthy adult mice derived from preimplantation blastocysts injected with viral DNA. *Proceedings Of the National Academy Of Sciences Of the United States Of America* **71**: 1250-1254.

Jeannotte, L., Ruiz, J.C. and Robertson, E.J. (1991). Low level of *Hox*1.3 gene expression does not preclude the use of promoterless vectors to generate a targeted gene disruption. *Molecular and Cellular Biology* **11**: 5578-5585.

John, S.W., Smith, R.S., Savinova, O.V. *et al.* (1998). Essential iris atrophy, pigment dispersion, and glaucoma in DBA/2J mice. *Investigative Ophthalmology And Visual Science* **39**: 951-62.

John, S.W.M., Hagaman, J.R., MacTaggart, T.E. *et al.* (1997). Intraocular pressure in inbred mouse strains. *Investigative Ophthalmology & Visual Science* **38**: 249-253.

Johnson, A.T., Alward, W.L.M., Sheffield, V.C. *et al.* (1996). Genetics and glaucoma. In R. Ritch, M. B. Shields, & T. Krupin (Eds.), The Glaucomas (pp. 39-54). St Louis: Mosby.

Johnson, K.R., Cook, S.A., Erway, L.C. *et al.* (1999). Inner ear and kidney anomalies caused by IAP insertion in an intron of the *Eya1* gene in a mouse model of BOR syndrome. *Human Molecular Genetics* **8**: 645-653.

Joyner, A.L., Kornberg, T., Coleman, K.G. *et al.* (1985). Expression during embryogenesis of a mouse gene with sequence homology to the Drosophila *engrailed* gene. *Cell* **43**: 29-37.

Joyner, A.L. and Martin, G.R. (1987). *En-1* and *En-2*, 2 mouse genes with sequence homology to the Drosophila *engrailed* gene - expression during embryogenesis. *Genes & Development* **1**: 29-38.

Kalatzis, V., Sahly, I., El-Amraoui, A. *et al.* (1998). *Eya1* expression in the developing ear and kidney: towards the understanding of the pathogenesis of branchio-oto-renal (BOR) syndrome. *Developmental Dynamics* **213**: 486-499.

Kalluri, R., Weber, M., Netzer, K.O. *et al.* (1994). COL4A5 gene deletion and production of post-transplant anti-alpha 3(IV) collagen alloantibodies in Alport syndrome. *Kidney Int* **45**: 721-6.

Kamachi, Y., Cheah, K.S.E. and Kondoh, H. (1999). Mechanism of regulatory target selection by the SOX high-mobility-group domain proteins as revealed by comparison of SOX1/2/3 and SOX9. *Molecular and Cellular Biology* **19**: 107-120.

Kanski, J.J. (1994). Clinical Opthalmology (2nd ed.). Oxford: Reed Educational and Professional Publishing.

Kapur, R.P. (1999). Early death of neural crest cells is responsible for total enteric aganglionosis in *Sox10(Dom)/Sox10(Dom)* mouse embryos. *Pediatr Dev Pathol* **2**: 559-0569.

Kapur, R.P., Livingston, R., Doggett, B. *et al.* (1996). Abnormal microenvironmental signals underlie intestinal aganglionosis in dominant megacolon mutant mice. *Developmental Biology* **174**: 360-369.

Kapur, R.P., Sweetser, D.A., Doggett, B. *et al.* (1995). Intercellular signals downstream of endothelin receptor-b mediate colonization of the large-intestine by enteric neuroblasts. *Development* **121**: 3787-3795.

Kapur, R.P., Yost, C. and Palmiter, R.D. (1992). A transgenic model for studying development of the enteric nervous system in normal and aganglionic mice. *Development* **116**: 167 et seq.

Kapur, R.P., Yost, C. and Palmiter, R.D. (1993). Aggregation chimeras demonstrate that the primary defect responsible for aganglionic megacolon in lethal-spotted mice is not neuroblast autonomous. *Development* **117**: 993-999.

Kasarskis, A., Manova, K. and Anderson, K.V. (1998). A phenotype-based screen for embryonic lethal mutations in the mouse. *Proceedings of the National Academy of Sciences of the United States of America* **95**: 7485-7490.

Kaufman, M.H. (1992). The Atlas of Mouse Development. Cambridge: University Press.

Khaleduzzaman, M., Sumiyoshi, H., Ueki, Y. *et al.* (1997). Structure of the human type XIX collagen (COL19A1) gene, which suggests it has arisen from an ancestor gene of the FACIT family. *Genomics* **45**: 304-12.

Kimura, T., Nakata, K., Tsumaki, N. *et al.* (1996). Progressive degeneration of articular cartilage and intervertebral discs. An experimental study in transgenic mice bearing a type IX collagen mutation. *Int Orthop* **20**: 177-81.

Kissane, J.M.E. (1990). Anderson's Pathology (Ninth ed.). St Louis: C.V. Mosby Company.

Koide, T., Ainscough, J., Wijgerde, M. *et al.* (1994). Comparative analysis of *Igf-2/H19* imprinted domain - identification of a highly conserved intergenic DNase I hypersensitive region. *Genomics* **24**: 1-8.

Koide, T., Moriwaki, K., Uchida, K. *et al.* (1998). A new inbred strain JF1 established from Japanese fancy mouse carrying the classic piebald allele. *Mammalian Genome* **9**: 15-19.

Kubota, Y., Petras, R.E., Ottaway, C.A. *et al.* (1992). Colonic vasoactive intestinal peptide nerves in inflammatory bowel disease. *Gastroenterology* **102**: 1242-51.

Kuhlbrodt, K., Herbarth, B., Sock, E. *et al.* (1998a). Cooperative function of POU proteins and SOX proteins in glial cells. *Journal of Biological Chemistry* **273**: 16050-16057.

Kuhlbrodt, K., Herbarth, B., Sock, E. *et al.* (1998b). Sox10, a novel transcriptional modulator in glial cells. *Journal of Neuroscience* **18**: 237-250.

Kuhlbrodt, K., Schmidt, C., Sock, E. *et al.* (1998c). Functional analysis of Sox10 mutations found in human Waardenburg- Hirschsprung patients. *Journal of Biological Chemistry* **273**: 23033-23038.

Kumar, S., Kimberling, W.J., Weston, M.D. *et al.* (1998). Identification of three novel mutations in human EYA1 protein associated with branchio-oto-renal syndrome. *Human Mutation* **11**: 443-449.

Kusafuka, T. and Puri, P. (1997). Mutations of the endothelin-B receptor and endothelin-3 genes in Hirschsprung's disease. *Pediatr Surg Int* **12**: 19-23.

Lane, P. (1966). Association of megacolon with two recessive spotting genes in the mouse. *J Hered* **57**: 29-31.

Lane, P.W. and Liu, H.M. (1984). Association of megacolon with a new dominant spotting gene (*dom*) in the mouse. *Journal of Heredity* **75**: 435-439.

Lauber, J.K. and Cheng, K.M. (1989). Heritable susceptibility to environmentally induced glaucoma in several mutants of Japanese quail. *J Hered* **80**: 268-71.

Lavitrano, M., Camaioni, A., Fazio, V.M. *et al.* (1989a). No simple solution for making transgenic mice. *Cell* **59**: 241.

Lavitrano, M., Camaioni, A., Fazio, V.M. *et al.* (1989b). Sperm cells as vectors for introducing foreign DNA into eggs - genetic transformation of mice. *Cell* **57**: 717-723.

Le Douarin, N. and Teillet, M.A. (1973). The migration of neural crest cells to the wall of the digestive tract in the avian embryo. *J. Embryol. Exp. Morph.* **30**: 31-48.

Le Douarin, N.M. (1981). Plasticity in the development of the peripheral nervous system. In K. Elliott & G. Lawrenson (Eds.), Ciba Foundation Symposium 83: Development of the autonomic nervous system (pp. 19-50). Bath: Pitman Medical.

Lefebvre, V., Li, P. and de Crombrugghe, B. (1998). A new long form of Sox5 (L-Sox5), Sox6 and Sox9 are coexpressed in chondrogenesis and cooperatively activate the type II collagen gene. *EMBO Journal* **17**: 5718-5733.

Legius, E. and Fryns, J.-P. (1992). Reply to Dr. Lin. (Letter). *Clin. Genet.* **41**: 223.

Legius, E., Fryns, J.P. and Van Den Berghe, H. (1990). Dominant branchial cleft syndrome with characteristics of both branchio-oto-renal syndrome and branchio-oculo-facial syndrome. *Clinical Genetics* **37**.

Levy, N.S. (1996). Mitochondrial extrusion hypothesis of glaucoma. *Annals of Ophthalmology-Glaucoma* **28**: 136-139.

Lewis, R. (1997). Embryonic stem cells debut amid little media attention. *Scientist* **11**: 1

Lim, A.S.M. and Constable, I.J. (1987). Colour Atlas of Opthalmology (2nd ed.). Bristol: Wright.

Lin, A.E., Doherty, R. and Lea, D. (1992). Branchio-oculo-facial and branchio-oto-renal syndromes are distinct entities (Letter). *Clin. Genet.* **41**: 221-222.

Lin, A.E., Gorlin, R.J., Lurie, I.W. *et al.* (1995a). Further delineation of the branchio-oculo-facial syndrome. *Am. J. Hum. Genet.* **56**: 42-59.

Lin, A.E., Gorlin, R.J., Lurie, I.W. *et al.* (1995b). Further delineation of the branchiooculofacial syndrome. *American Journal of Medical Genetics* **56**: 42-59.

Linsenmayer, T.F., Fitch, J.M., Gordon, M.K. *et al.* (1998). Development and roles of collagenous matrices in the embryonic avian cornea. *Progress in Retinal and Eye Research* **17**: 231-265.

Liu, C.Y., Olsen, B.R. and Kao, W.W.Y. (1993a). Developmental patterns of alpha-1(IX) collagen mRNA in mouse. *Investigative Ophthalmology & Visual Science* **34**: 1283.

Liu, C.-Y., Olsen, B.R. and Kao, W.W.-Y. (1993b). Developmental patterns of two alpha1(IX) collagen mRNA isoforms in mouse. *Developmental Dynamics* **198**: 150-157.

Liu, J., Hales, A.M., Chamberlain, C.G. *et al.* (1994). Induction of cataract-like changes in rat lens epithelial explants by transforming growth-factor-beta. *Investigative Ophthalmology & Visual Science* **35**: 388-401.

Lupas, A. (1996). Coiled coils: new structures and functions. *TIBS* **21**: 375-382.

Lupas, A., Van Dyke, M. and Stock, J. (1991). Predicting coiled coils from protein sequences. *Science* **252**: 1162-1164.

Lütjen-Drecoll, E. and Rohen, J.W. (1996). Morphology of aqueous outflow pathways in normal and glaucomatous eyes. In R. Ritch, M. B. Shields, & T. Krupin (Eds.), The Glaucomas (pp. 89-124). St Louis: Mosby.

Lyon, M.F., Rastan, S. and Brown, S.D.M. (1996). Genetic Variants and Strains of the Laboratory Mouse (3rd ed.). Oxford University Press.

Lyonnet, S., Edery, P., Mulligan, L.M. *et al.* (1994). Mutations of the ret protooncogene in Hirschsprung's disease. *Comptes Rendus De L Academie Des Sciences Serie Iii-Sciences De La Vie-Life Sciences* **317**: 358-362.

MacSween, R.N.M. and Whaley, K. (1992). Muir's textbook of pathology - 13th edition. London: Edward Arnold.

Makarova, I.V., Tarantul, V.Z. and Gazarian, K.G. (1988). Structural features of the integration site of foreign DNA in the transgenic mouse genome. *Molekulyarnaya Biologiya* **22**: 1553-61.

Mallein-Gerin, F., Ruggiero, F., Quinn, T.M. *et al.* (1995). Analysis of collagen synthesis and assembly in culture by immortalized mouse chondrocytes in the presence or absence of alpha-1(IX) collagen chains. *Experimental Cell Research* **219**: 257-265.

Mark, W.H., Signorelli, K. and Lacy, E. (1985). An insertional mutation in a transgenic mouse line results in developmental arrest at day 5 of gestation. *Cold Spring Harbor Symposia On Quantitative Biology* **50**: 453-463.

Markel, P., Shu, P., Ebeling, C. *et al.* (1997). Theoretical and empirical issues for marker-assisted breeding of congenic mouse strains. *Nat Genet* **17**: 280-4.

Marks, P.W., Bandura, J.L., Shieh, D.B. *et al.* (1999). The spontaneous coat color mutant white nose (*wn*) maps to murine Chromosome 15. *Mammalian Genome* **10**: 750-752.

Martin, G.R. (1981). Isolation of a pluripotent cell line from early mouse embryos cultured in medium conditioned by teratocarcinoma stem cells. *Proceedings Of the National Academy Of Sciences Of the United States Of America* **18**: 7634-7638.

Martucciello, G. (1996). Hirschprung's disease as a neurocristopathy. *Pediatric Surgery International* **12**: 2-10.

Matic, M., Petrov, I.N., Chen, S.H. *et al.* (1997). Stem cells of the corneal epithelium lack connexins and metabolite transfer capacity. *Differentiation* **61**: 251-260.

Mayer, T. (1965). The development of piebald spotting in mice. *Dev Biol* **11**: 319-34.

Mayer, T. (1967a). Pigment cell migration in piebald mice. *Dev Biol* **15**: 521-35.

Mayer, T. (1967b). Temporal skin factors influencing the development of melanoblasts in piebald mice. *J Exp Zool* **166**: 397-403.

Mayer, T. (1977). Enhancement of melanocyte development from piebald neural crest by a favorable tissue environment. *Dev Biol* **56**: 255-62.

Maynard, T. and Weston, J.A. (1998). Cell-cell contact increases apoptosis of a neurogenic subpopulation of avian neural crest cells. *Developmental Biology* **198**: 117.

McCarthy, L.C., Terrett, J., Davis, M.E. *et al.* (1997). A first-generation whole genome-radiation hybrid map spanning the mouse genome. *Genome Research* **7**: 1153-1161.

McCool, M. and Weaver, D.D. (1994). Branchio-oculo-facial syndrome: Broadening the spectrum. *Am. J. Med. Genet.* **49**: 414-421.

McCormick, D. and Hall, P.A. (1992). The complexities of proliferating cell nuclear antigen. *Histopathology* **21**: 591-4.

McFarlane, M. and Wilson, J.B. (1996). A model for the mechanism of precise integration of a microinjected transgene. *Transgenic Research* **5**: 171-177.

McFee, A.F., Sayer, A.M., Salomaa, S.I. *et al.* (1997). Methods for improving the yield and quality of metaphase preparations for FISH probing of human lymphocyte chromosomes. *Environmental and Molecular Mutagenesis* **29**: 98-104.

McLaren, A. and Michie, D. (1954). Are inbred mice suitable for bio-assays? *Nature* **173**: 686-688.

McMahon, A.P. and Bradley, A. (1990). The *Wnt-1* (*Int-1*) proto-oncogene is required for development of a large region of the mouse brain. *Cell* **62**: 1073-1085.

Meisler, M.H. (1992). Insertional mutation of 'classical' and novel genes in transgenic mice. *Trends in Genetics* **8**: 341-344.

Meisler, M.H., Galt, J., Weber, J. *et al.* (1997). Isolation of mutated genes from transgene insertion sites. In A. Cid & Garcia-Carranca (Eds.), Microinjection and transgenesis of cultured cells and embryos (pp. 505-520). Springer.

Melnick, M., Bixler, D., Nance, W. *et al.* (1976). Familial branchio-oto-renal dysplasia: A new addition to the branchial arch syndromes. *Clin. Genet.* **9**: 25-34.

Mercer, J.A., Seperack, P.K., Strobel, M.C. *et al.* (1991). Novel myosin heavy-chain encoded by murine dilute coat color locus. *Nature* **349**: 709-713.

Merril, C.R., Goldman, D., Sedman, A.A. *et al.* (1981). Ultrasensitive stain for proteins in polyacrylamide gels shows regional variation in cerebrospinal fluid proteins. *Science* **211**: 1437-1438.

Metallinos, D.L., Bowling, A.T. and Rine, J. (1998). A missense mutation in the endothelin-B receptor gene is associated with lethal white foal syndrome: an equine version of Hirschsprung disease. *Mammalian Genome* **9**: 426-431.

Miller, S.J. (1970). Genetics of closed-angle glaucoma. *J Med Genet* **7**: 250-2.

Mintz, B. (1967). Gene control of mammalian pigmentary differentiation. I. Clonal origin of melanocytes. *Proceedings of the National Academy of Sciences, USA* **58**: 255-262.

Mishima, N. and Tomarev, S. (1998). Chicken Eyes absent 2 gene: isolation and expression pattern during development. *International Journal of Developmental Biology* **42**: 1109-1115.

Mizuguchi, T., Nishiyama, M., Moroi, K. *et al.* (1997). Analysis of two pharmacologically predicted endothelin B receptor subtypes by using the endothelin B receptor gene knockout mouse. *Br J Pharmacol* **120**: 1427-30.

Morgan, D., Turnpenny, L., Goodship, J. *et al.* (1998). Inversin, a novel gene in the vertebrate left-right axis pathway, is partially deleted in the inv mouse [published erratum appears in Nat Genet 1998 Nov;20(3):312]. *Nat Genet* **20**: 149-56.

Morrison, J.C., Nylander, K.B., Lauer, A.K. *et al.* (1998). Glaucoma drops control intraocular pressure and protect optic nerves in a rat model of glaucoma. *Investigative Ophthalmology & Visual Science* **39**: 526-531.

Morse, D.E. and Cova, J.L. (1984). Pigmented cells in the leptomeninges of the cat. *Anatomical Record* **210**

Morse, H.C. (1981). The laboratory mouse: an historical perspective. In H. L. Foster, J. D. Small, & J. G. Fox (Eds.), The Mouse in Biomedical Research Volume I: History, genetics and wild mice. New York: Academic Press.

Mullins, L.J., Kotelevtseva, N., Boyd, A.C. *et al.* (1997). Efficient Cre-lox linearisation of BACs: Applications to physical mapping and generation of transgenic animals. *Nucleic Acids Research* **25**: 2539-2540.

Muragaki, Y., Nishimura, I., Henney, A. *et al.* (1990). The alpha-1(IX) collagen gene gives rise to 2 different transcripts in both mouse embryonic and human fetal RNA. *Proceedings of the National Academy of Sciences of the United States of America* **87**: 2400-2404.

Musio, A., Mariani, T., Frediani, C. *et al.* (1994). Longitudinal patterns similar to G-banding in untreated human- chromosomes - evidence from atomic-force microscopy. *Chromosoma* **103**: 225-229.

Myers, J.C., Li, D.Q., Bageris, A. *et al.* (1997). Biochemical and immunohistochemical characterization of human type XIX defines a novel class of basement membrane zone collagens. *American Journal of Pathology* **151**: 1729-1740.

Nadeau, J.H. and Sankoff, D. (1997). Comparable rates of gene loss and functional divergence after genome duplications early in vertebrate evolution. *Genetics* **147**: 1259-1266.

Nagahama, M., Ozaki, T. and Hama, K. (1985). A study of the myenteric plexus of the congenital aganglionosis rat (spotting lethal). *Anat Embryol (Berl)* **171**: 285-96.

Nagy, A., Rossant, J., Nagy, R. *et al.* (1993). Derivation of completely cell culture-derived mice from early-passage embryonic stem cells. *Proceedings Of the National Academy Of Sciences Of the United States Of America* **90**: 8424-8428.

Nakata, K., Ono, K., Miyazaki, J. *et al.* (1993). Osteoarthritis associated with mild chondrodysplasia in transgenic mice expressing alpha-1(IX) collagen chains with a central deletion. *Proceedings of the National Academy of Sciences of the United States of America* **90**: 2870-2874.

Natarajan, D., Grigoriou, M., Marcos-Gutierrez, C.V. *et al.* (1999). Multipotential progenitors of the mammalian enteric nervous system capable of colonising aganglionic bowel in organ culture. *Development* **126**: 157-168.

Newgreen, D. and Hartley, L. (1995). Extracellular matrix and adhesive molecules in the early development of the gut and its innervation in normal and spotting lethal rat embryos. *Acta Anat (Basel)* **154**: 243-60.

Newgreen, D.F., Southwell, B., Hartley, L. *et al.* (1996). Migration of enteric neural crest cells in relation to growth of the gut in avian embryos. *Acta Anatomica* **157**: 105-115.

Newth, D.R. (1951). Experiments on the neural crest of the lamprey embryo. *J. Exp. Biol.* **28**: 247-260.

Nguyen, T.D., Chen, P., Huang, W.D. *et al.* (1998). Gene structure and properties of TIGR, an olfactomedin-related glycoprotein cloned from glucocorticoid-induced trabecular meshwork cells. *Journal Of Biological Chemistry* **273**

Nusbaum, C., Slonim, D.K., Harris, K.L. *et al.* (1999). A YAC-based map of the mouse genome. *Nature Genetics* **22**: 388-393.

Oh, S.P., Taylor, R.W., Gerecke, D.R. *et al.* (1992). The mouse alpha 1(XII) and human alpha 1(XII)-like collagen genes are localized on mouse chromosome 9 and human chromosome 6. *Genomics* **14**: 225-231.

Oliver, G., Wehr, R., Jenkins, N.A. *et al.* (1995). Homeobox genes and connective tissue patterning. *Development* **121**: 693-705.

Opdecamp, K., Nakayama, A., Nguyen, M.T.T. *et al.* (1997). Melanocyte development in vivo and in neural crest cell cultures: Crucial dependence on the Mitf basic-helix-loop-helix-zipper transcription factor *Development* **124**: 2377-2386.

Palmiter, R.D. and Brinster, R.L. (1986). Germ-line transformation of mice. *Annual Review Of Genetics* **20**: 465-499.

Paris, D., Toyama, K., Megarbane, A. *et al.* (1996). Rapid fluorescence *in situ* hybridization on interphasic nuclei to discriminate between homozygous and heterozygous transgenic mice. *Transgenic Research* **5**: 397-403.

Pavan, W.J., Mac, S., Cheng, M. *et al.* (1995). Quantitative trait loci that modify the severity of spotting in piebald mice. *PCR - Methods and Applications* **5**: 29-41.

Payette, R., Tennyson, V., Pomeranz, H. *et al.* (1988). Accumulation of components of basal laminae: association with the failure of neural crest cells to colonize the presumptive aganglionic bowel of ls/ls mutant mice. *Dev Biol* **125**: 341-60.

Payette, R.F., Tennyson, V.M., Pham, T.D. *et al.* (1987). Origin and morphology of nerve-fibers in the aganglionic colon of the lethal spotted (ls/ls) mutant mouse. *Journal of Comparative Neurology* **257**: 237-252.

Pearse, A.G.E. (1973). Cell migration and the alimentary system: endocrine contributions of the neural crest to the gut and its derivatives. *Digestion* **8**: 372-385.

Perala, M., Savontaus, M., Metsaranta, M. *et al.* (1997). Developmental regulation of mRNA species for types II, IX and XI collagens during mouse embryogenesis. *Biochemical Journal* **324**: 209-216.

Perry, A.C.F., Wakayama, T., Kishikawa, H. *et al.* (1999). Mammalian transgenesis by intracytoplasmic sperm injection. *Science* **284**: 1180-1183.

Piatigorsky, J. (1998). Multifunctional lens crystallins and corneal enzymes - More than meets the eye. *Annals of the New York Academy of Sciences* **842**: 7-15.

Piatigorsky, J. and Wistow, G.J. (1989). Enzyme/crystallins: gene sharing as an evolutionary strategy. *Cell* **57**: 197-9.

Pierro, L.J. and Spiggle, J. (1967). Congenital eye defects in the mouse. I. Corneal opacity in C57black mice. *J Exp Zool* **166**: 25-33.

Pingault, V., Bondurand, N., Kuhlbrodt, K. *et al.* (1998). SOX10 mutations in patients with Waardenburg-Hirschsprung disease. *Nature Genetics* **18**: 171-173.

Pingault, V., Puliti, A., Prehu, M.O. *et al.* (1997). Human homology and candidate genes for the Dominant megacolon locus, a mouse model of Hirschsprung disease. *Genomics* **39**: 86-89.

Promega Corporation (1995). Technical Bulletin 220: Access RT-PCR

Puliti, A., Poirier, V., Goossens, M. *et al.* (1996). Neuronal defects in genotyped dominant megacolon (dom) mouse embryos, a model for hirschsprung disease. *Neuroreport* **7**: 489-492.

Puliti, A., Prehu, M.O., Simonchazottes, D. *et al.* (1995). A high-resolution genetic-map of mouse chromosome-15 encompassing the dominant megacolon (dom) locus. *Mammalian Genome* **6**: 763-768.

Pusch, C., Hustert, E., Pfeifer, D. *et al.* (1998). The SOX10/Sox10 gene from human and mouse: sequence, expression, and transactivation by the encoded HMG domain transcription factor. *Human Genetics* **103**: 115-123.

Raap, A.K., Vandecorput, M.P.C., Vervenne, R.A.W. *et al.* (1995). Ultra-sensitive FISH using peroxidase-mediated deposition of biotin-tyramide or fluorochrome-tyramide. *Human Molecular Genetics* **4**: 529-534.

Ramirez-Solis, R., Liu, P. and Bradley, A. (1995). Chromosome engineering in mice. *Nature* **378**: 720-724.

Read, A.P. and Newton, V.E. (1997). Waardenburg syndrome. *Journal of Medical Genetics* **34**: 656-665.

Reaume, A.G., Desousa, P.A., Kulkarni, S. *et al.* (1995). Cardiac malformation in neonatal mice lacking connexin43. *Science* **267**: 1831-1834.

Reedy, M.V., Faraco, C.D. and Erickson, C.A. (1998). The delayed entry of thoracic neural crest cells into the dorsolateral path is a consequence of the late emigration of melanogenic neural crest cells from the neural tube. *Developmental Biology* **200**: 234-246.

Reid, K., Turnley, A.M., Maxwell, G.D. *et al.* (1996). Multiple roles for endothelin in melanocyte development: regulation of progenitor number and stimulation of differentiation. *Development* **122**

Renwick, J.H. and Lawler, S.D. (1963). Probable linkage between a congenital cataract locus and the Duffy blood group locus. *Ann. Hum. Genet.* **27**: 67-84.

Rijkers, T., Peetz, A. and Ruther, U. (1994). Insertional mutagenesis in transgenic mice. *Transgenic Research* **3**: 203-215.

Robertson, K., Mason, I. and Hall, S. (1997). Hirschsprung's disease: genetic mutations in mice and men. *Gut* **41**: 436-441.

Robinson, M.L., Holmgren, A. and Dewey, M.J. (1993). Genetic control of ocular morphogenesis - defective lens development associated with ocular anomalies in C57BL/6 mice. *Experimental Eye Research* **56**: 7-16.

Robinson, M.L. and Overbeek, P.A. (1996). Differential expression of alpha A- and alpha B-crystallin during murine ocular development. *Investigative Ophthalmology & Visual Science* **37**: 2276-2284.

Ross, M.J., Reith, E.J. and Romrelli, L.J. (1989). Histology: a text and atlas (2nd ed.). Baltimore: Williams & Wilkins.

Rossant, J. (1985). Interspecific cell markers and lineage in mammals. *Philosophical Transactions Of the Royal Society Of London Series B - Biological Sciences* **312**: 91.

Ruhl, A. and Collins, S.M. (1995). Enteroglial cells (egc) are an integral-part of the neuroimmune axis in the enteric nervous-system (ens). *Gastroenterology* **108**: A 680-A 680.

Sambrook, J., Fritsch, E.F. and Maniatis, T. (1989). Molecular Cloning: A laboratory manual (2nd ed.). Cold Spring Harbour Laboratory Press.

Sanchez, M., Silos-Santiago, I., Frisen, J. *et al.* (1996). Renal agenesis and the absence of enteric neurons in mice lacking GDNF. *Nature* **382**: 70-3.

Sarfarazi, M. (1997). Recent advances in molecular genetics of glaucomas. *Human Molecular Genetics* **6**: 1667-1677.

Savontaus, M., Ihanamaki, T., Perala, M. *et al.* (1998). Expression of type II and IX collagen isoforms during normal and pathological cartilage and eye development. *Histochemistry and Cell Biology* **110**: 149-159.

Sax, C.M., Salamon, C., Kays, W.T. *et al.* (1996). Transketolase is a major protein in the mouse cornea. *Journal Of Biological Chemistry* **271**: 33568-74.

Schaible, R. (1969). Clonal distribution of melanocytes in piebald-spotted and variegated mice. *J. Exp. Zool.* **172**: 181-200.

Schauerte, H.E., vanEeden, F.J.M., Fricke, C. *et al.* (1998). Sonic hedgehog is not required for the induction of medial floor plate cells in the zebrafish. *Development* **125**: 2983-2993.

Schilham, M.W. and Clevers, H. (1998). HMG box containing transcription factors in lymphocyte differentiation. *Seminars in Immunology* **10**: 127-132.

Schilham, M.W., Oosterwegel, M.A., Moerer, P. *et al.* (1996). Defects in cardiac outflow tract formation and pro-B-lymphocyte expansion in mice lacking Sox-4. *Nature* **380**: 711-714.

Schottenstein, E.M. (1996). Peters' Anomaly. In R. Ritch, M. B. Shields, & T. Krupin (Eds.), The Glaucomas (pp. 887-897). St Louis: Mosby.

Schuchardt, A., DqAgati, V., Larsson-Blomberg, L. *et al.* (1994). Defects in the kidney and enteric nervous system of mice lacking the tyrosine kinase receptor Ret. *Nature* **367**: 380-3.

Serbedzija, G.N., Burgan, S., Fraser, S.E. *et al.* (1991). Vital dye labeling demonstrates a sacral neural crest contribution to the enteric nervous-system of chick and mouse embryos. *Development* **111**: 857-866.

Shah, N.M., Groves, A.K. and Anderson, D.J. (1996). Alternative neural crest cell fates are instructively promoted by TGFβ superfamily members. *Cell* **85**: 331-343.

Shamblott, M.J., Axelman, J., Wang, S. *et al.* (1998). Derivation of pluripotent stem cells from cultured human primordial germ cells. *Proceedings of the National Academy of Sciences, USA* **95**: 13726-13731.

Shaw, L.M. and Olsen, B.R. (1991). FACIT collagens - diverse molecular bridges in extracellular matrices. *Trends In Biochemical Sciences* **16**: 191-194.

Shi, Y.P., Huang, T.T., Carlson, E.J. *et al.* (1994). The mapping of transgenes by fluorescence in-situ hybridization on G-banded mouse chromosomes. *Mammalian Genome* **5**: 337-341.

Shields, M.B., Ritch, R. and Krupin, T. (1996). Classifications of the glaucomas. In R. Ritch, M. B. Shields, & T. Krupin (Eds.), The Glaucomas (pp. 717-725). St Louis: Mosby.

Shiels, A., Mackay, D., Ionides, A. *et al.* (1998). A missense mutation in the human connexin50 gene (GJA8) underlies autosomal dominant "zonular pulverulent" cataract, on chromosome 1q. *American Journal of Human Genetics* **62**: 526-532.

Shinohara, A. and Ogawa, T. (1995). Homologous recombination and the roles of double-strand breaks. *Trends in Biochemical Sciences* **20**: 387-391.

Sidman, R.L., Kinney, H.C. and Sweet, H.O. (1985). Transmissible spongiform encephalopathy in the gray tremor mutant mouse. *Proceedings Of the National Academy Of Sciences Of the United States Of America* **82**: 253-7.

Silver, L.M. (1995). Mouse Genetics: Concepts and Applications. New York: Oxford University Press.

Simpson, E.M., Linder, C.C., Sargent, E.E. *et al.* (1997). Genetic variation among 129 substrains and its importance for targeted mutagenesis in mice. *Nature Genetics* **16**: 19-27.

Skarnes, W.C., Auerbach, B.A. and Joyner, A.L. (1992). A gene trap approach in mouse embryonic stem cells - the *LacZ* reporter is activated by splicing, reflects endogenous gene expression, and is mutagenic in mice. *Genes & Development* **6**: 903-918.

Skarnes, W.C., Moss, J.E., Hurtley, S.M. *et al.* (1995). Capturing genes encoding membrane and secreted proteins important for mouse development. *Proceedings Of the National Academy Of Sciences Of the United States Of America* **92**: 6592-6596.

Smih, F., Rouet, P., Romanienko, P.J. *et al.* (1995). Double-strand breaks at the target locus stimulate gene targeting in embryonic stem cells. *Nucleic Acids Research* **23**: 5012-5019.

Southard-Smith, E.M., Angrist, M., Ellison, J.S. *et al.* (1999). The *Sox10^{Dom}* mouse: modeling the genetic variation of Waardenburg- Shah (WS4) syndrome. *Genome Res* **9**: 215-25.

Southard-Smith, E.M., Collins, J.E., Ellison, J.S. *et al.* (1999c). Comparative analyses of the *Dominant megacolon-SOX10* genomic interval in mouse and human. *Mammalian Genome* **10**: 744-749.

Southard-Smith, E.M., Kos, L. and Pavan, W.J. (1998). Sox10 mutation disrupts neural crest development in *Dom* Hirschsprung mouse model. *Nature Genetics* **18**: 60-64.

Sowden, J., Putt, W., Morrison, K. *et al.* (1995). The embryonic RNA helicase gene (ERH): a new member of the DEAD box family of RNA helicases. *Biochem J* **308**: 839-46.

Spring, J. (1997). Vertebrate evolution by interspecific hybridisation - are we polyploid? *FEBS Letters* **400**: 2-8.

Srinivasan, Y., Lovicu, F.J. and Overbeek, P.A. (1998). Lens-specific expression of transforming growth factor beta 1 in transgenic mice causes anterior subcapsular cataracts. *Journal of Clinical Investigation* **101**: 625-634.

Steele, E.C., Lyon, M.F., Favor, J. *et al.* (1998). A mutation in the connexin 50 (Cx50) gene is a candidate for the No2 mouse cataract. *Current Eye Research* **17**: 883-889.

Stoilova, D., Child, A., Brice, G. *et al.* (1997). Identification of a new 'TIGR' mutation in a family with juvenile- onset primary open angle glaucoma. *Ophthalmic Genetics* **18**: 109-118.

Stoilova, D., Child, A., Brice, G. *et al.* (1998). Novel TIGR/MYOC mutations in families with juvenile onset primary open angle glaucoma. *Journal of Medical Genetics* **35**: 989-992.

Stone, E.M., Fingert, J.H., Alward, W.L.M. *et al.* (1997). Identification of a gene that causes primary open angle glaucoma. *Science* **275**: 668-670.

Streeten, B.W., Robinson, M.R., Wallace, R. *et al.* (1987). Lens capsule abnormalities in Alport's syndrome. *Arch Ophthalmol* **105**: 1693-7.

Su, C.S., Ohagen, S.B. and Sullivan, T.J. (1998). Ocular anomalies in the branchio-oculo-facial syndrome. *Australian and New Zealand Journal of Ophthalmology* **26**: 43-46.

Sumiyoshi, H., Inoguchi, K., Khaleduzzaman, M. *et al.* (1997). Ubiquitous expression of the alpha1(XIX) collagen gene (Col19a1) during mouse embryogenesis becomes restricted to a few tissues in the adult organism. *Journal Of Biological Chemistry* **272**: 17104-11.

Sweet, H.O. (1981). Gray tremor (gt). *Mouse News Letter* **65**: 28.

Swiderski, R.E. and Solursh, M. (1992). Localisation of type II collagen, long form alpha1(IX) collagen and short form alpha1(IX) collagen transcripts in the developing chick notochord and axial skeleton. *Developmental Dynamics* **194**: 118-127.

Takamatsu, N., Kanda, H., Tsuchiya, I. *et al.* (1995). A gene that is related to *SRY* and is expressed in the testes encodes a leucine zipper-containing protein. *Mol. Cell. Biol.* **15**: 3759-3766.

Takatsuji, K., Sato, Y., Iizuka, S. *et al.* (1986). Animal model of closed angle glaucoma in albino mutant quails. *Invest Ophthalmol Vis Sci* **27**: 396-400.

Takatsuji, K., Tohyama, M., Sato, Y. *et al.* (1988). Selective loss of retinal ganglion cells in albino avian glaucoma. *Invest Ophthalmol Vis Sci* **29**: 901-9.

Tamm, E.R., Russell, P. and Piatigorsky, J. (1999). Development and characterization of an immortal and differentiated murine trabecular meshwork cell line. *Investigative Opthalmology & Visual Science* **40**: 1392-1403.

Tanke, H.J., Florijn, R.J., Wiegant, J. *et al.* (1995). CCD microscopy and image-analysis of cells and chromosomes stained by fluorescence in-situ hybridization. *Histochemical Journal* **27**: 4-14.

Taraviras, S., C.V., M.-G., Durbec, P. *et al.* (1999). Signalling by the RET receptor tyrosine kinase and its role in the development of the mammalian enteric nervous system. *Development* **126**: 2785-2797.

Tennyson, V.M., Gershon, M.D., Wade, P.R. *et al.* (1998). Fetal development of the enteric nervous system of transgenic mice that overexpress the Hoxa-4 gene. *Developmental Dynamics* **211**: 269-291.

Tokuda, M. (1935). An eighteenth century Japanese guide-book on mouse-breeding. *J. Heredity* **26**: 481-484.

Tomarev, S.I., Tamm, B. and Chang, B. (1998). Characterisation of the mouse *Myoc/Tigr* gene. *Biochem. and Biophys. Res. Comm.* **245**: 887-893.

Tortora, G.J. and Anagnostakos, N.P. (1990). Principles of Anatomy and Physiology (6th ed.). New York: Harper Collins.

Trachslin, J., Koch, M. and Chiquet, M. (1999). Rapid and reversible regulation of collagen XII expression by changes in tensile stress. *Experimental Cell Research* **247**: 320-328.

Tripathi, R.C. (1972). Aqueous outflow pathway in normal and glaucomatous eyes. *British Journal of Opthalmology* **56**: 157-174.

Trounson, A. and Pera, M. (1998). Potential benefits of cell cloning for human medicine. *Reproduction Fertility and Development* **10**: 121-125.

Tsuchida, T., Ensini, M., Morton, S.B. *et al.* (1994). Topographic organization of embryonic motor-neurons defined by expression of lim homeobox genes. *Cell* **79**: 957-970.

van de Wetering, M., Cavallo, R., Dooijes, D. *et al.* (1997). Armadillo coactivates transcription driven by the product of the Drosophila segment polarity gene dTCF. *Cell* **88**: 789-799.

van der Rest, M., Mayne, R., Ninomiya, Y. *et al.* (1985). The structure of type-IX collagen. *Journal Of Biological Chemistry* **260**: 220-225.

Van Etten, W.J., Steen, R.G., Nguyen, H. *et al.* (1999). Radiation hybrid map of the mouse genome. *Nature Genetics* **22**: 384-387.

van Gijlswijk, R.P.M., Wiegant, J., Vervenne, R. *et al.* (1996). Horseradish peroxidase-labelled oligonucleotides and fluorescent tyramides for rapid detection of chromosome-specific repeat sequences. *Cytogenetics and Cell Genetics* **75**: 258-262.

Vanden Hoek, T.L., Goossens, W. and Knepper, P.A. (1987). Fluorescence-labeled lectins, glycoconjugates, and the development of the mouse AOP. *Investigative Ophthalmology And Visual Science* **28**: 451-8.

Vincent, C., Kalatzis, V., Abdelhak, S. *et al.* (1997). BOR and BO syndromes are allelic defects of EYA1. *European Journal of Human Genetics* **5**: 242-246.

Voegel, J.J., Heine, M.J.S., Zechel, C. *et al.* (1996). TIF2, a 160 kDa transcriptional mediator for the ligand-dependent activation function AF-2 of nuclear receptors. *Embo Journal* **15**: 3667-3675.

Vogt, T.F., Jacksongrusby, L., Rush, J. *et al.* (1993). Formins - phosphoprotein isoforms encoded by the mouse limb deformity locus. *Proceedings Of the National Academy Of Sciences Of the United States Of America* **90**: 5554-5558.

Vogt, T.F., Jacksongrusby, L., Wynshawboris, A.J. *et al.* (1992). The same genomic region is disrupted in 2 transgene-induced limb deformity alleles. *Mammalian Genome* **3**: 431-437.

Wakamatsu, Y., Mochii, M., Vogel, K.S. *et al.* (1998). Avian neural crest-derived neurogenic precursors undergo apoptosis on the lateral migration pathway. *Development* **125**: 4205-4213.

Wakeland, E., Morel, L., Achey, K. *et al.* (1997). Speed congenics: a classic technique in the fast lane (relatively speaking). *Immunology Today* **18**: 472-477.

Wallace, M.E. (1971). Dilution-Peru. *Mouse News Letter* **44**: 18.

Wallace, M.E. and Green, P.P. (1974). Linkage for dilute-Peru (*dp*). *Mouse News Letter* **50**: 28-9.

Wang, J.C., Stafford, J.M. and Granner, D.K. (1998). SRC-1 and GRIP1 coactivate transcription with hepatocyte nuclear factor 4. *Journal of Biological Chemistry* **273**: 30847-30850.

Ward, A., Fisher, R., Richardson, L. *et al.* (1997). Genomic regions regulating imprinting and insulin-like growth factor-II promoter 3 activity in transgenics: novel enhancer and silencer elements. *Genes and Function* **1**: 25-36.

Webster, W. (1974). Aganglionic megacolon in piebald-lethal mice. *Arch Pathol* **97**: 111-7.

Wehrle-Haller, B. and Weston, J.A. (1995). Soluble and cell-bound forms of steel factor activity play distinct roles in melanocyte precursor dispersal and survival on the lateral neural crest migration pathway. *Development* **121**: 731-742.

Wehrle-Haller, B. and Weston, J.A. (1997). Receptor tyrosine kinase-dependent neural crest migration in response to differentially localised growth factors. *Bioessays* **19**: 337-345.

Werner, M.H., Ruth, J.R., Gronenborn, A.M. *et al.* (1995). Molecular-basis of human 46X,Y sex reversal revealed from the 3-dimensional solution structure of the human SRY-DNA complex. *Cell* **81**: 705-714.

Wessel, H., Anderson, S., Fite, D. *et al.* (1997). Type XII collagen contributes to diversities in human corneal and limbal extracellular matrices. *Investigative Ophthalmology & Visual Science* **38**: 2408-2422.

White, T.W., Bruzzone, R., Goodenough, D.A. *et al.* (1992). Mouse cx50, a functional member of the connexin family of gap junction proteins, is the lens fiber protein mp70. *Molecular Biology of the Cell* **3**: 711-720.

Wilkie, T.M. and Palmiter, R.D. (1987). Analysis of the integrant in Myk-103 transgenic mice in which males fail to transmit the integrant. *Molecular and Cellular Biology* **7**: 1646-1655.

Wilkinson, D.G. (1992). In Situ Hybridization: A practical approach. Oxford: OUP.

Wirtz, M.K., Acott, T.S., Samples, J.R. *et al.* (1998). Prospects for genetic intervention in primary open-angle glaucoma. *Drugs And Aging* **13**: 333-40.

Wistow, G. (1993). Identification of lens crystallins: a model system for gene recruitment. *Methods Enzymol* **224**: 563-75.

Woychik, R.P. and Alagramam, K. (1998). Insertional mutagenesis in transgenic mice generated by the pronuclear microinjection procedure. *Int. J. Dev. Biol.* **42**: 1009-1017.

Woychik, R.P., Stewart, T.A., Davis, L.G. *et al.* (1985). An inherited limb deformity created by insertional mutagenesis in a transgenic mouse. *Nature* **318**: 36-40.

Wright, E.M., Snopek, B. and Koopman, P. (1993). 7 new members of the sox gene family expressed during mouse development. *Nucleic Acids Research* **21**: 744.

Wunderle, V.M., Critcher, R., Hastie, N. *et al.* (1998). Deletion of long-range regulatory elements upstream of SOX9 causes campomelic dysplasia. *Proceedings Of the National Academy Of Sciences Of the United States Of America* **95**: 10649-10654.

Wurst, W., Rossant, J., Prideaux, V. *et al.* (1995). A large scale gene trap screen for insertional mutations in developmentally-regulated genes in mice. *Genetics* **139**: 889-899.

Xu, D., Emoto, N., Giaid, A. *et al.* (1994). Ece-1 - a membrane-bound metalloprotease that catalyzes the proteolytic activation of big endothelin-1. *Cell* **78**: 473-485.

Xu, J.M., Qiu, Y.H., DeMayo, F.J. *et al.* (1998). Partial hormone resistance in mice with disruption of the steroid receptor coactivator-1 (SRC-1) gene. *Science* **279**: 1922-1925.

Xu, P.X., Adams, J., Peters, H. *et al.* (1999). *Eya1*-deficient mice lack ears and kidneys and show abnormal apoptosis of organ primordia. *Nature Genetics* **23**: 113-117.

Xu, P.X., Cheng, J., Epstein, J.A. *et al.* (1997a). Mouse *Eya* genes are expressed during limb tendon development and encode a transcriptional activation function. *Proceedings of the National Academy of Sciences of the United States of America* **94**: 11974-11979.

Xu, P.X., Woo, I., Her, H. *et al.* (1997b). Mouse *Eya* homologues of the Drosophila *eyes absent* gene require Pax6 for expression in lens and nasal placode. *Development* **124**: 219-231.

Yada, T., Suzuki, S., Kobayashi, K. *et al.* (1990). Occurrence in chick embryo vitreous humor of a type-IX collagen proteoglycan with an extraordinarily large chondroitin sulfate chain and short alpha-1 polypeptide. *Journal Of Biological Chemistry* **265**: 6992-6999.

Yamamura, K., Oike, Y., Imaizumi, T. *et al.* (1998). Exchangeable gene trap as a tool for random mutagenesis. In 12th International Mouse Genome Conference, . Garmisch-Partenkirchen, Bavaria.

Yasuda, K., Raynor, K., Kong, H. *et al.* (1993). Cloning and functional comparison of kappa-opioid and delta-opioid receptors from mouse-brain. *Proceedings of the National Academy of Sciences of the United States of America* **90**: 6736-6740.

Yokoyama, T., Silversides, D.W., Waymire, K.G. *et al.* (1990). Conserved cysteine to serine mutation in tyrosinase is responsible for the classical albino mutation in laboratory mice. *Nucleic Acids Research* **18**: 7293-7298.

Yoles, E., Wheeler, L.A. and Schwartz, M. (1999). alpha 2-adrenoreceptor agonists are neuroprotective in a rat model of optic nerve degeneration. *Investigative Ophthalmology & Visual Science* **40**: 65-73.

Yoshioka, H., Zhang, H., Ramirez, F. *et al.* (1992). Synteny between the loci for a novel FACIT-like collagen locus (D6S228E) and alpha1(IX) collage (COL9A1) on 6q12-q14 in humans. *Genomics* **13**: 884-886.

You, Y., Bergstrom, R., Klemm, M. *et al.* (1997). Chromosomal deletion complexes in mice by radiation of embryonic stem cells. *Nature Genetics* **15**: 285-288.

Young, H.M., Hearn, C.J., Ciampoli, D. *et al.* (1998). A single rostrocaudal colonization of the rodent intestine by enteric neuron precursors is revealed by the expression of Phox2b, Ret, and p75 and by explants grown under the kidney capsule or in organ culture. *Developmental Biology* **202**: 67-84.

Zachary, I. and Rozengurt, E. (1992). Focal adhesion kinase (p125(FAK)) - a point of convergence in the action of neuropeptides, integrins and oncogenes. *Cell* **71**: 891-894.

Zambrowicz, B.P., Imamoto, A., Fiering, S. *et al.* (1997). Disruption of overlapping transcripts in the ROSA beta geo 26 gene trap strain leads to widespread expression of beta-galactosidase in mouse embryos and hematopoietic cells. *Proceedings of the National Academy of Sciences of the United States of America* **94**: 3789-3794.

Zhang, H. and Bradley, A. (1996). Mice deficient for BMP2 are non-viable and have defects in amnion/chorion and cardiac development. *Development* **122**: 2977-2986.

Zheng, B., Sage, M., Cai, W.W. *et al.* (1999). Engineering a mouse balancer chromosome. *Nature Genetics* **22**.

Zhou, X.J., Benson, K.F., Ashar, H.R. *et al.* (1995). Mutation responsible for the mouse pygmy phenotype in the developmentally-regulated factor *Hmgi-C*. *Nature* **376**: 771-774.

Zimmerman, J.E., Bui, Q.T., Steingrimsson, E. *et al.* (1997). Cloning and characterization of two vertebrate homologs of the Drosophila eyes absent gene. *Genome Research* **7**: 128-141.